# OPTIMAL PARAMETER UPDATING AND APPROPRIATE 4D SEISMIC NORMALIZATION IN SEISMIC HISORY MATCHING OF THE NELSON FIELD

**Alireza Kazemi**

Submitted for the degree of **Doctor of Philosophy**

Heriot-Watt University
Institute of Petroleum Engineering
Edinburgh – Scotland, UK
January, 2011

## Abstract

History matching of reservoirs is very important in the oil industry because the simulation model is an important tool that can help with management decisions and planning of future production strategies. Nowadays, time-lapse (4D) seismic data is very useful for better capturing the fluid displacement in the reservoir, especially between wells. It is now common to integrate 4D seismic with production data in order to constrain the simulation model to both types of data. This thesis is based on a technique for automatic production and seismic history matching of reservoirs by. This technique integrates various tools such as streamline simulation, parameterization via pilot points and Kriging and geo-body updating, a petro-elastic model and the neighborhood algorithm, all in an automatic framework.

All studies in this thesis are applied to the Nelson field but the approaches used here can be applied to any similar field. The history matching aim was to identify shale volumes and their distribution by updating three reservoir properties, net:gross, horizontal and vertical permeability. All history matching studies were performed in a six years production period, with baseline and one monitor seismic survey available, and then a forecast of the following three years was made with a second monitor for comparison.

Various challenges are addressed in this thesis. We introduce a streamline guide approach in order to efficiently select the regions in the reservoir that have a strong influence on production activity of the wells and 4D seismic signature. Updating was performed more effectively compared to an approach where parameters were changed everywhere in the vicinity of the wells. Then, three parameter updating schemes are introduced to effectively combine various reservoir parameters in order to capture correctly the flow behaviour.

The observed 4D seismic data used in this study consisted of relative pseudo-impedance with a different unit compared to synthetic impedance data. This challenge was addressed by introducing normalization. 4D predictions in the vertical well locations and full field simulation cells used in the normalization study and we observed different level of signal/noise ratio in normalized observed 4D maps at the end of study.

We include the normalized 4D maps in history matching of the field and we observed that normalization very important. We also compared the seismic and production history matching studies with a case where seismic was not included in history matching (production history matching). The results show that if 4D data is normalized appropriately, the reduction of both seismic and production misfits is better than the production only history matching case.

## Dedication

*This thesis is dedicated to my parents, my brother and my wife*

## Acknowledgements

I would like to express my endless gratitude to my parents who always supported and encourage me to do my best in my life. Also I would like to thanks my beloved wife, for her support and patience she have had these past years.

I would like to express my deepest gratitude and respect to my principal supervisor, Dr Karl D. Stephen. I have always benefited from his expertise supervision, brilliant ideas, continuous enthusiasm, rigorous attitude to science, valuable advice and extensive knowledge. His careful editing contributed enormously to the production of this thesis. I gratefully acknowledge the help and assistance of Prof. Colin Macbeth, who had trusted me from beginning to end of this project.

I also wish to thank the examiners, Prof. Bahman Tohidi from the Institute of Petroleum Engineering of Heriot Watt University and Prof. Olivier Gosselin from TOTAL S.A. / Imperial College London, for the time they invested in the reading and evaluation of this thesis.

I would also like to thank the other members of the SHM and ETLP groups specially Dr. Asghar Shams. Special thanks to Hamidreza Hamdi and Hamed Amini for their support of my work.

I would like to thank the Nelson Field partners (Premier Oil ONS Ltd., Shell UK Ltd., Total E&P UK Ltd., Idemitsu E&P UK Ltd. and Esso Exploration and Production UK Ltd.) for providing the data and permission to publish the results. BP, ConocoPhilips, Shell and StatoilHydro are thanked for funding of this work: I thank Schlumberger Geoquest for use of their software. Malcolm Sambridge is thanked for use of the Neighbourhood Algorithm.

ACADEMIC REGISTRY
# Research Thesis Submission

| | | | |
|---|---|---|---|
| Name*:* | ALIREZA KAZEMI | | |
| School/PGI: | INSTITUTE OF PETROLEUM ENGINEERING | | |
| Version: *(i.e. First, Resubmission, Final)* | FINAL | Degree Sought (Award **and** Subject area) | Ph.D<br>PETROLEUM ENGINEERING |

## Declaration

In accordance with the appropriate regulations I hereby submit my thesis and I declare that:

1) the thesis embodies the results of my own work and has been composed by myself
2) where appropriate, I have made acknowledgement of the work of others and have made reference to work carried out in collaboration with other persons
3) the thesis is the correct version of the thesis for submission and is the same version as any electronic versions submitted*.
4) my thesis for the award referred to, deposited in the Heriot-Watt University Library, should be made available for loan or photocopying and be available via the Institutional Repository, subject to such conditions as the Librarian may require
5) I understand that as a student of the University I am required to abide by the Regulations of the University and to conform to its discipline.

* *Please note that it is the responsibility of the candidate to ensure that the correct version of the thesis is submitted.*

| | | | |
|---|---|---|---|
| Signature of Candidate*:* |  | Date: | 2011/1/11 |

## zSubmission

| | |
|---|---|
| Submitted By *(name in capitals):* | ALIREZA KAZEMI |
| Signature of Individual Submitting: |  |
| Date Submitted: | 2011/1/11 |

## For Completion in Academic Registry

| | | | |
|---|---|---|---|
| Received in the Academic Registry by *(name in capitals):* | | | |
| *Method of Submission*<br>*(Handed in to Academic Registry; posted through internal/external mail):* | | | |
| *E-thesis Submitted (**mandatory for final theses from January 2009)*** | | | |
| Signature: | | Date: | |

Please note this form should bound into the submitted thesis.

Updated February 2008, November 2008, February 2009

## Publications

Part of this work is presented in the following publications:

1. Kazemi, A., Stephen, K. D. and Shams, A. (2011). "Improved normalization of time-lapse seismic data using NRMS repeatability data to improve automatic production and seismic history matching in the Nelson field." SPE 143628, SPE EUROPEC/EAGE Annual Conference and Exhibition, Vienna, Austria, 23-26 May.

2. Kazemi, A. and Stephen, K. D. (2011). "Automatic production and seismic history matching by updating locally and by geological environment in the Nelson field." SPE 143629, SPE EUROPEC/EAGE Annual Conference and Exhibition, Vienna, Austria, 23-26 May.

3. Kazemi, A., Stephen, K. D. and Shams, A. (2010). "Seismic History Matching of Nelson using Time-lapse Seismic Data: An Investigation of 4D Signature Normalization." SPE131538, SPE/EAGE EUROPEC Annual Conference and Exhibition, Barcelona, Spain, 14-17 June.

4. Kazemi, A. and Stephen, K. D. (2010). "Optimal Parameter Updating in Assisted History Matching of the Nelson field Using Streamlines as a Guide." SPE131540, SPE/EAGE EUROPEC Annual Conference and Exhibition, Barcelona, Spain, 14-17 June.

5. Kazemi, A., Stephen, K. D. and Shams, A. (2010). "Seismic History Matching of Nelson using Time-lapse Seismic Data: An Investigation of 4D Signature Normalization." Submitted to SPE reservoir evaluation and engineering journal.

6. Kazemi, A. and Stephen, K. D. (2010). "Optimal Parameter Updating in Assisted History Matching of the Nelson field Using Streamlines as a Guide." SPE131540, Submitted to SPE reservoir evaluation and engineering journal.

7. Kazemi, A. and Stephen, K. D. (2009). "Automatic Seismic and Production History Matching in Nelson Using Different Updating

Schemes." presented at the 71st EAGE Conference and Exhibition, Amsterdam, The Netherlands, 8-11 June.

8. Kazemi, A. and Stephen, K. D. (2008). "Improved Reservoir Description of the Nelson Field Via Seismic History Matching." EAGE 3942 presented at the 70th EAGE Conference and Exhibition, Rome, Italy, 9-12 June.

9. Kazemi, A., Stephen, K. D., Shams, A. and MacBeth, C. (2007). "Seismic History Matching, a North Sea application." presented in Statoil's International Student Conference (ISC), Trondheim, Norway, 9-13 October.

## Table of Contents

**1 Introduction** ..... 1

1.1 General background and definition ..... 1

1.2 A general category for history matching ..... 3

1.2.1 The choice of historical data that we want to use in history matching ..... 4

1.2.2 Manual and automatic history matching ..... 7

1.3 The history of computer aided/Automatic History Matching (AHM) ..... 9

1.3.1 Objective function ..... 12

1.3.2 Parameterization techniques ..... 13

1.3.3 Optimization tools ..... 16

1.4 History of using time-lapse seismic data for reservoir characterization ..... 22

1.5 Automatic Production and Seismic History Matching (PSHM) workflow in this thesis ..... 26

1.6 Content of thesis ..... 27

**2 Automatic history matching workflow** ..... 29

2.1 Various elements for automatic history matching workflow ..... 29

2.1.1 Generation of multiple models ..... 29

2.1.2 Simulation flow ..... 32

2.1.3 Petro-elastic model ..... 33

2.1.4 Comparison of simulated data with historical data ..... 34

2.1.5 Optimization algorithms ..... 34

2.2 Pilot points and Kriging ..... 35

2.3 Streamline simulation ..... 36

2.4 Synthetic 4D seismic data generation ..... 37

2.4.1 Effective p-Impedance for the interval ..... 40

2.4.2 Lateral downscaling (interpolation) ..... 41

2.5 Observed data ..... 43

2.6 Objective function ..... 44

2.7 Neighbourhood algorithm ..... 45

2.7.1 Approximating the misfit surface ..... 46

2.7.2 Sampling algorithm for the neighbourhood ..... 47

2.7.3 NA parameters ..... 48

2.7.4 Resampling from the posterior ..... 48

**3 Nelson field** ..... 50
3.1 Nelson field location ..... 50
3.2 History of the field ..... 51
3.3 Nelson trap ..... 52
3.4 Zonation in Nelson field ..... 52
3.5 Production scenario in Nelson ..... 60
3.6 The petro-elastic model in this study ..... 61
3.6.1 Fluid compressibility ..... 61
3.6.2 Compressibility and shear velocity measurement ..... 62
3.6.3 Petro-elastic equations ..... 63
3.7 Time-lapse seismic data ..... 65
3.7.1 Elastic impedance data in Nelson ..... 65
3.7.2 Phase shifted amplitude ..... 66
3.7.3 Time-lapse response versus reservoir activity ..... 67
3.7.4 Calculating data error of the time-lapse data ..... 72
3.8 Production data ..... 76
3.8.1 Data error of production data ..... 77
3.9 Simulation model ..... 78
3.10 Summary ..... 83

**4 Production history matching in Nelson using streamline guide approach** ..... 84
4.1 The general strategy for history matching of a reservoir ..... 84
4.2 Streamline guide concept ..... 86
4.2.1 Sensitivity of pilot point locations ..... 90
4.3 Parameter updating scheme ..... 92
4.3.1 Global single variable approach (GSV) ..... 93
4.3.1 Regional multi-variable approach (RMV) ..... 93
4.3.3 Local multi-variable approach (LMV) ..... 94
4.4 Data analysis ..... 94
4.5 Effect of changing reservoir parameters on well production ..... 95
4.6 History matching result ..... 97
4.6.1 GSV ..... 98
4.6.2 RMV ..... 105
4.6.3 LMV ..... 109
4.7 Comparison of different updating approaches ..... 112

4.8 Which updating scheme should we use? ..... 118
4.9 History matching in Nelson including more wells ..... 118
4.10 Well vicinity vs. streamline guided approach ..... 123
4.11 Discussion ..... 131

**5 Time-lapse data normalization** ..... 133
5.1 Normalization concept ..... 133
5.2 Normalization approaches ..... 135
5.2.1 Normalization procedure ..... 136
5.3 Normalization of the data ..... 140
5.4 Using reservoir section for 4D seismic normalization ..... 144
5.5 NRMS filtering ..... 146
5.6 Normalization of observed data filtered by the NRMS map ..... 148
5.7 2003-1990 4D seismic normalization ..... 151
5.8 Summary ..... 152

**6 Production and seismic history matching using streamline guide approach** ..... 153
6.1 History matching information ..... 153
6.2 History matching results ..... 154
6.3 Updated reservoir model ..... 167
6.4 Forecast accuracy ..... 171
6.5 4D seismic map prediction ..... 175
6.6 Does NRMS help the history matching process? ..... 176
6.7 Possible geological change in the reservoir after history matching ..... 178
6.8 Using automatic history matching technique for seismic normalization ..... 180
6.9 Discussion ..... 185
6.10 Summary ..... 187

**7 History matching in Nelson by updating geo-body types** ..... 189
7.1 History matching method ..... 190
7.2 Global multi-variable approach ..... 192
7.3 Production history matching result ..... 193
7.4 Production and seismic history matching ..... 202
7.5 Global updating versus local updating in history matching ..... 205
7.6 Combining geo-body type updating and the pilot point method ..... 206
7.7 Summary and discussion ..... 216

**8 Summary, conclusions and recommendations** ..... 218
8.1 Streamline guided approach and parameter updating schemes ..... 219
8.2 Normalization of 4D seismic data ..... 220
8.3 Production and seismic history matching ..... 222
8.4 History matching by updating geo-body types ..... 223
8.5 Limitations of automatic history matching method in this study ..... 224
8.6 Conclusions ..... 227

**Appendix A** ..... 229
A.1 Simple Kriging ..... 229
A.2 Streamline simulation ..... 231

**Appendix B** ..... 235
B.1 Streamline density number (SLD) ..... 235
B.2 The pressure calculation time steps ..... 240

**References** ..... 244

## List of Figures

Figure 1.1: Location of various time-lapse projects carried out all over the world by BP for past 25 years until end of 2007 (Foster 2008). There have been 74 seismic surveys in the North Sea. Each colour inside the circle indicates the geological location and the area of each is relative to highest number of surveys in North Sea. ..... 3

Figure 1.2: The spectrum of 4D seismic application from qualitative to quantitative use (O'Donovan et al. 2000)..... 5

Figure 1.3: The differences of post and pre-stack amplitude for real data (a) and synthetic data (b) for a sector of Schiehallion field (Hatchell et al. 2002).. .. 6

Figure 1.4: The various domains for comparison of measured and predicted seismic data (red circle identify the domain that we use in this work) (MacBeth 2007).. . 7

Figure 1.5: The similarity and differences between manual and automatic history matching runs. ..... 9

Figure 1.6: A two dimensional view of a streamline pattern for a reservoir. The different colors identify the well drainages regions (Agarwal and Blunt 2004)..... 10

Figure 1.7: A general procedure for automatic history matching (modified from Roggero et al. 2007). ..... 12

Figure 1.8: Exploration versus exploitation strength of optimization algorithms (Sambridge and Mosegaard 2002). ..... 20

Figure 1.9: Seismic and production history matching workflow (Stephen 2006) as used in this work (the red box highlight the role of optimization algorithm in this workflow). ..... 23

Figure 2.1: Various methods that can be used for parameterization of a reservoir model through history matching... ..... 30

Figure 2.2: The role of petro-elastic model for generation of synthetic seismic in amplitude versus impedance domain. ..... 34

Figure 2.3: A synthetic models as an example of the location of pilot points where we make change (pink dots) versus black dots where no change is enforced (Stephen 2007). ..... 36

Figure 2.4: Comparison of the coarse and fine grids used in our study. Thick grey lines indicate the coarse cells while large circles show the location at which the impedances are predicted. Equation 2.25 is used to interpolate the impedances to obtain values at the small black circles, i.e. where the observed seismic would normally be measured. Broken and solid arrows indicate the principal directions of the coarse (simulation) and fine (seismic) grids respectively (Stephen 2007). ..... 42

Figure 2.5: Quasi-uniform random points and Voronoi cells for a) 10 points, b) the Voronoi cells of 100 points generated by the neighbourhood approximation, c) as b but for 1000 points and d) contours of the test objective function

(Sambridge 1999). The black dots in Figure belong to the misfit value of different models..... 46

Figure 2.6: A uniform random walk restricted to a Voronoi cell (Sambridge 1999)..... 47

Figure 3.1: Location of Nelson field in the North Sea in relation to Forties-Montrose trend (Kunka et al. 2003)..... 50

Figure 3.2: Nelson platform and sub-sea facility (Kunka et al. 2003). ..... 51

Figure 3.3: Fault location in Nelson field. Blue is water and yellow is oil..... 52

Figure 3.4: Nelson lithostratigraphy of Sele Unit S1 (Kunka et al. 2003). ..... 53

Figure 3.5: Nelson field structural cross-sections (Kunka et al. 2003). ..... 55

Figure 3.6: Zone 4 net:gross (from simulation model supplied by field operator). ..... 55

Figure 3.7: The channelized structure in Nelson in different reservoir producing intervals, a) top (T75) and b) bottom (T70). ..... 56

Figure 3.8: Two hydraulic flow units that exist because of the shale baffle (Shepherd and Gill 2009)..... 57

Figure 3.9: Top view of Nelson field showing transmissibility of the reservoir. ..... 57

Figure 3.10: Log porosity distribution for all sample of Forties Sandstone (Kunka et al. 2003)..... 58

Figure 3.11: A schematic of geology of the reservoir before and after history matching. Black lines are representative of shale layers and between shales there are sands. The shale predominantly deposited as flatbeds between turbidity events but may be eroded as shown with red. This erosion controls the vertical permeability. The curvature results from shale drapes in channels affecting horizontal permeability. ..... 59

Figure 3.12: The location of water injector wells (black) compared to the rest of wells in the reservoir. ..... 60

Figure 3.13: A West-East cross section of the reservoir which shows the location of initial oil-water contact ( Shepherd and Gill 2009). ..... 61

Figure 3.14: Schematic for definition of effective pressure.(MacBeth 2007) ..... 62

Figure 3.15: The horizons in Nelson (left) which were used to generate the 2 dimensional maps of differences of elastic impedance for reservoir intervals.. ..... 63

Figure 3.15: The maps of differences of phase shifted amplitude for top reservoir interval (T75) in two different time differences, a) 1990-2000 and b) 1990-2003. ..... 66

Figure 3.16: a) Zero-phase Riker seismic model, and b) ninety-degree Riker seismic model (coloured inversion) (Hongliu and Backus 2005).. ..... 67

Figure 3.17: The maps of differences of phase shifted amplitude (similar to coloured inversion) for top reservoir interval (T75) in two different time differences, a) 1990-2000 and b) 1990-2003... ..... 68

Figure 3.18: Variation of compressional velocity as a function of formation fluid pressure and fluid substitution because of different production scenarios at different initial pressure; vertical arrows indicate fluid displacement and along curve arrows indicate pore pressure change (Johnston 1997). ..... 70

Figure 3.19: Average reservoir pressure during production period (monthly time steps) ..... 70

Figure 3.20: A 2D (an arithmetic averaging performed vertically) of reservoir pressure differences during production period (1994-2000). ..... 71

Figure 3.21: Effect of production on rock parameters on 1000 psia pressure depletion (typical sand with 23% porosity, 10% shale volume) ..... 71

Figure 3.22: Effect of water saturation and reservoir pressure change on p-wave impedance. Note that the black line represent the pressure effect when Eq 3.6 did not consider. ..... 72

Figure 3.23: A synthetic example shows the effect of geology, strips and noise in a seismic survey. ..... 74

Figure 3.24: The 2D map of a) original 4D map (Well+base map defined in Chapter 5, Figure 5.7c), b) original map filtered by 4D signals, c) local average performed on b, and d) the residuals for subtracting c from b.. ..... 74

Figure 3.25: 2D semi-variogram map of the a) original survey (Figure 3.23a) and b) calculated local average attribute (Figure 3.24b). ..... 75

Figure 3.26: 2D semi-variogram map for the residual map presented in Figure 3.24d. . 75

Figure 3.27: Mono-variogram in NW-SE direction (the direction of the elongated structures) for residual map (Figure 3.24d).Symbols indicate the value of semi-variogram at each separation distance. ..... 76

Figure 3.28: The water cut in each production well (red colour in each circle) across the geological regions. The area of each circle shows the relative total production rate for the well up to 2003 (Shepherd and Gill 2009). ..... 77

Figure 3.29: The distribution of different reservoir properties, a) porosity, b) net:gross, c) horizontal permeability and d) vertical permeability. ..... 78

Figure 3.30: Distribution of reservoir properties in the first reservoir interval (T75) for Channel Axis, a) net:gross, b) horizontal permeability and c) vertical permeability and Interchannel area d) net:gross, e) horizontal permeability and f) vertical permeability.. ..... 79

Figure 3.31: Distribution of reservoir properties in second reservoir interval (T70) for Channel Axis, a) net:gross, b) horizontal permeability and c) vertical permeability. ..... 79

Figure 3.32: Average reservoir properties for first (a) and second (b) reservoir interval.. ..... 80

Figure 3.33: Distribution of reservoir properties in third reservoir interval (T65), a) net:gross, b) horizontal permeability and c) vertical permeability..... 81

Figure 3.34: Field oil and water production volumes for historical and simulated data... ..... 81

Figure 3.35: Oil and water production rates for each individual wells for a) first 13 wells with highest misfit and b) the rest 14 wells. Well numbering is based on geographical locations from left to right and top to bottom..... 82

Figure 4.1: The place of parameter updating schemes in the automatic history matching workflow. ..... 85

Figure 4.2: Streamline pattern for one production well in Nelson showing a cluster changing at different times a) July 98, b) Oct 98 and c) Jan 99. Only a fraction of streamlines are shown, evenly sampled for better visualization. 87

Figure 4.3: Location of wells selected for history matching along with the other production and injection wells in the reservoir. The black dots show master pilot points for 6 wells..... 88

Figure 4.4: The normalized misfit value for an example well as it varies over time. A threshold of 25% of the maximum is used as a threshold for investigating streamline distributions. ..... 88

Figure 4.5: An example location of the master pilot point near a well chosen by streamlines..... 89

Figure 4.6: Wells and associated regions in the reservoir chosen for a sensitivity study of the streamline guided approach. Black boxes indicate regions suggested for updating by streamlines while A, B and C regions are alternatives considered for each of the three wells. ..... 90

Figure 4.7: Reduction of production misfit value using the alternative location of master pilot point compared to the original case using streamline guide approach for 3 regions a) 1, b) 2 and c) 3. The colour coding is consistent with the colours of A-C in Figure 4.6. ..... 92

Figure 4.8: Various outcomes for each parameter chosen for history matching, a) parameter converged to a specific value, b) parameter could not converge to a specific value, c) multiple minima, d) parameter reached one limit and e) probability distribution of each parameter type in parameter interval range during history matching. ..... 96

Figure 4.9: The effect of each parameter on the well production misfit value in each region. The scale on y axis in not the same for all cases because the magnitude of the water production misfit varies considerably. The misfit value for each well was normalized by the base model value. ..... 97

Figure 4.10: Sum of misfits of oil and water rates for the targeted wells versus model index for automatic history matching (AHM) results changing one variable at a time. The normalized misfit value of base model by dividing over the number of observed data is 1100..... 99

Figure 4.11: Sum of misfits of the oil and water rates for the targeted wells versus model index for AHM result of changing one parameter type at a time. The

normalized misfit value of base model by dividing over the number of observed data is 1100. ..... 100

Figure 4.12: Probability of different parameters in parameter range during history matching for two different regions a and b chose for history matching study. ..... 101

Figure 4.13: The procedure for generating 10 final simulation models..... 102

Figure 4.14: Sum of misfits of the oil and water rates for the targeted wells in the history and forecasting periods for the 10 generated models. The normalized misfit value of the base model by divided by the number of observed data is 1100. Note that indices in this figure are just based on sorting misfits and it is not related to history matching indices mentioned above (the same things happened for the rest of figures).. ..... 104

Figure 4.15: Sum of misfits of the oil and water rates for the targeted wells in the history and forecasting periods for the best 10 history matched models (NTG, $K_h$, $K_z$) and also final generated 10 models..... 104

Figure 4.16: Various regions in the reservoir..... 105

Figure 4.17: Sum of misfits of the oil and water rates for the targeted wells in each region versus models ran during history matching in Edge and Centre of reservoir, the star shows the misfit value of base model. The normalized misfit value of the base model, obtained by dividing by the number of observed data, is 1100 for Centre and 1200 for Edge.. ..... 106

Figure 4.18: Total field oil production rate for the best model for the history matching and the forecasting period (for well by well analysis see Figure 4.28)..... 107

Figure 4.19: Sum of misfits of the oil and water for the targeted wells used in history matching up to year 2000 and from 2000 to 2003 for different models. The normalized misfit value of base model by dividing over the number of observed data is 1100. ..... 108

Figure 4.20: Sum of misfits of the oil and water rates for the targeted wells in the history and forecasting periods for the best 10 history matched models (CENTRE and EDGE, Eq. 4.3) and also final generated 10 models.. ..... 109

Figure 4.21: Well water production misfit versus model index for 6 wells in different part of reservoir, the blue star shows the misfit value of base model. ..... 110

Figure 4.22: Sum of misfits of the oil and water for the targeted wells for different models in history and forecasting periods. The normalized misfit value of base model by dividing over the number of observed data is 1100. ..... 111

Figure 4.23: Sum of misfits of the oil and water rates for targeted wells, comparing the model generated by combination of parameter in each locality ($LMV_{Final1}$) with sum of misfits value for each locality(Eq. 4.5) . ..... 112

Figure 4.24: Sum of misfits of the oil and water for the targeted wells for the best 10 models of each case. The normalized misfit value of base model by dividing over the number of observed data is 1100..... 114

Figure 4.25: Forecasting misfit reduction versus matching for the best 10 models of each case. 115

Figure 4.26: Oil production misfit in forecasting period versus history period for different schemes. 115

Figure 4.27: Best parameter multipliers applied to update the base model in various cases for a) net:gross, b) horizontal permeability and c) vertical permeability. 116

Figure 4.28: Oil and water rate for best history matched model for 4 different wells. 118

Figure 4.29: (a) Total field oil production rates (b) and water cut for the best model compared to historical data and the base case model (for well by well analysis see Figure 4.33). 120

Figure 4.30: Multipliers of parameter for the best reservoir model over the base model for a) net:gross, b) horizontal permeability and c) vertical permeability. 120

Figure 4.31: Cross section of water movement near a well for the base model (a to c) and one of best models after history matching (d to f) in different time steps. The arrow shows the water discplacement from the aquifer toward the well. Because this is a 3D view so that the water oil contact does not look horizontal. 121

Figure 4.32: Sum of misfits of the oil and water for the targeted wells for best 10 models in history and forecast period. The normalized misfit value of base model by dividing over the number of observed data is 860 122

Figure 4.33: Oil rate and water cut of 4 different wells in history and forecast (light blue) period. 122

Figure 4.34: Location of master pilot points in black box in the vicinity of each well. 123

Figure 4.35: Well production misfit through history matching for well vicinity and streamline case in different locations in the reservoir. 124

Figure 4.36: Sum of misfits of the oil and water for the targeted wells in (a) history matching in matching period and (b) forecast period. The normalized misfit value of base model by dividing over the number of observed data is 860 in history matching period and 380 in forecasting period. 125

Figure 4.37: Oil and water production rates for the best model from well vicinity updating and the streamline case in various location of the reservoir for history matching and forecasting (light blue shading). 125

Figure 4.38: Cross plot of misfit reduction in matching and forecast period for best 10 models of well vicinity and streamline based cases. 126

Figure 4.39: Multipliers of parameter for the best reservoir model over the base model for a) net:gross, b) horizontal permeability. and c) vertical permeability. 127

Figure 4.40: Grid cell properties for those cells where increases were applied as a result of history matching showing a) net:gross, b) horizontal permeability and c) vertical permeability for the base case model and d) net:gross, e) horizontal permeability and f) vertical permeability for the best history matched model

using streamlines. The black line indicates the boundary of the oil filled rock. ..... 129

Figure 4.41: Grid cell properties for those cells where increases were applied as a result of history matching showing a) net:gross, b) horizontal permeability and c) vertical permeability for the base case model and d) net:gross, e) horizontal permeability and f) vertical permeability for the best history matched model locating pilot points in the well vicinity ..... 130

Figure 5.1: Production and seismic history matching workflow. The red box is the area of study in this chapter. ..... 134

Figure 5.2: Schematic of 4D seismic normalization. a) observed 4D seismic before normalization, b) synthetic 4D seismic, c) comparison of observed versus synthetic for the cross line shows in black colour in the maps and d) observed 4D seismic after normalization.. ..... 135

Figure 5.3: Qualitative analysis of observed 4D seismic data by comparing a) observed data and b) synthetic data from the base model. The black lines indicate the main reservoir that is seismically active in this interval. All production and injection wells were also identified in the map as black points.. ..... 136

Figure 5.4: Schematic of the location of a vertical well in a) seismic scale and b) reservoir scale. The red box shows the boundary of seismic bins which are at the same location of the simulation cell in b. Arithmetic averaging was used to calculate one value of real seismic in the red box and Backus (1962) averaging was used to get one value of synthetic seismic at the location of the well. ..... 137

Figure 5.5: Cross-plot of a) well water cut for history versus model and b) observed versus synthetic 4D seismic. The error bars in b are representative of standard deviation of observed seismic data for the bins at the location of each well. ..... 138

Figure 5.6: Cross-plot of observed and synthetic 4D impedances for a) full set of simulation cells of the base model (Map+base), b) full set of simulation cells of the best model (Map+best), c) cells of vertical wells in the base model (Well+base) and d) cells of vertical wells in the best model (Well+best) (red line is obtained by ignoring two wells indicated by red symbols). ..... 141

Figure 5.7: Normalized observed 4D seismic obtained by using the regression equation of a) Map+base model, b) Map+best model, c) Well+base model, d) Well+best model, e) Well+best model with ignoring two wells and f) synthetic 4D seismic for base reservoir model (The sum of square of the differences between real and synthetic seismic of base reservoir model was calculated in each case). ..... 142

Figure 5.8: Raw data observed 4D map before normalization. A coloured threshold of 1100 shows the 4D signals in the map... ..... 144

Figure 5.9: Cross-plot of observed and synthetic 4D impedances for a) set of simulation cells in reservoir section only of the base model and b) set of simulation cells in reservoir section only of the best history matched model.. ..... 145

Figure 5.10: Normalized observed 4D seismic obtained by using the regression equation of a) set of simulation cells in reservoir section of base model and b) set of simulation cells in reservoir section of best history matched model ..... 145

Figure 5.11: The NRMS map for the 2000-1990 time-lapse data and for the first reservoir interval. ..... 147

Figure 5.12: Cross-plot of observed and synthetic 4D impedances for a) full set of simulation cells of the base model (Map+base+NRMS), b) full set of simulation cells of the best model (Map+best+NRMS), c) cells of vertical wells in the base model (Well+base+NRMS) and d) cells of vertical wells in the best model (Well+best+NRMS) (a part of data filtered by using NRMS equals to 30%).. ..... 149

Figure 5.13: Normalized observed 4D seismic obtained by using the regression equation of a) Map+base+NRMS model, b) Map+best+NRMS model, c) Well+base+NRMS model, d) Well+best+NRMS model from Figure 5.17 and e) the synthetic seismic data for base reservoir model. .Black circles show the location of 15 production wells that under predict water rate for the base reservoir mo..... 150

Figure 5.14: Cross-plot of observed and synthetic 4D impedances for a) full set of simulation cells of the base model (Map+base), b) cells of vertical wells in the base model (Well+base), c) full set of simulation cells of the best model (Map+best). ..... 152

Figure 5.15: Normalized 4D seismic map in 2003-1990 periods based on a) Map+base, b) Well+base and c)Map+best. ..... 152

Figure 6.1: Misfit reduction for seismic and liquid production rate for each well for 3 different areas of the reservoir. ..... 155

Figure 6.2: Sum of misfits of the oil and water rates for all wells, comparing the model generated by combination of parameter in each locality ($LMVPSHM_{Final1}$) with sum of misfits value for each locality (Eq. 6.2) for a)Map+base, b)Map+best, c)Well+base, d)Well+best, e)Well+best with ignoring two wells, f)Map+base+NRMS, g)Map+best+NRMS, h)Well+base+NRMS and i)Well+best+NRMS. ..... 157

Figure 6.3: Reduction of misfits of production and 4D seismic data for the best reservoir model from each history matching case. Reductions are compared to the base case model except for green bars which is a comparison to the best PHM model..... 158

Figure 6.4: Reduction of misfits of production and 4D seismic data for the best reservoir model. Using the 4D seismic normalized map filtered by NRMS..... 161

Figure 6.5: Reduction of seismic, production and total misfit value through the 4D seismic history matching process (for Well+base case) for different wells

(well names are based on Figure 3.35). Black stars show the misfit value for base simulation model. ..... 163

Figure 6.6: Cross plot of seismic and production misfits for wells presented in Figure 6.5. Black stars show the misfit value for base simulation model. ..... 164

Figure 6.7: Reduction of seismic, production and total misfit value through PHM. Note that seismic and total misfit were calculated after history matching process (for seismic misfit calculation Well+base map used) (well names are based on Figure 3.35). Black stars show the misfit value for base simulation model.. ..... 165

Figure 6.8: Cross plot of seismic and production misfits for wells presented in Figure 6.7. Black star shows the misfit value of production and seismic for base simulation model.. ..... 165

Figure 6.9: The best synthetic 4D impedance maps after history matching where raw date was normalized using a) Map+base, b) Map+best, c) Well+base, d) Well+best, e) Well+best by ignoring two wells and finally f)the PHM model with no seismic.. ..... 166

Figure 6.10: The best synthetic 4D data after history matching for a) Map+base+NRMS, b) Map+best+NRMS, c) Well+base+NRMS, d) Well+base+NRMS, and e) PHM model... ..... 167

Figure 6.11: Multipliers of properties changed in the base model via history matching for a) net:gross, b) horizontal permeability and c) vertical permeability in log scale. Note that actual changes to net:gross were limited so that unity was not exceeded and this is not reflected in the above plot..... 169

Figure 6.12: Multipliers of properties changed in the base model via history matching for a) net:gross, b) horizontal permeability and c) vertical permeability in log scale. Note that actual changes to net:gross were limited so that unity was not exceeded and this is not reflected in the above plot..... 170

Figure 6.13: Misfit reduction by percentage for the best history matched model of each case by considering all production wells. This is only for the cases where NRMS filtering was not used ..... 171

Figure 6.14: Reduction of total production misfit in forecasting versus matching periods for different history matching studies ..... 172

Figure 6.15: Reduction of total production misfit in forecasting versus matching periods for different history matching studies.. ..... 173

Figure 6.16: Sum of misfits of the oil and water rates for all wells from 1994 to 2003(history plus forecasting period) versus the same property but for 1994 to 2000 (history period only ) Showing history matching cases in a) Figure 6.3 and b) Figure 6.4. Note that the misfit value of base reservoir model is 300,000 and 430,000 for the history and history plus forecasting periods respectively..... 174

Figure 6.17: Oil and water production rates in matched and forecast periods (light blue) for the best history matched model using production data only (blue) and for

the best model using both production and seismic data (Map+best+NRMS) (green).. ..... 175

Figure 6.18: The 4D seismic data for (a) the base reservoir model, (b) PHM model, (c), the normalized observed data (Map+best) and (d) and the best seismic and production history matched model Well+base (Figure 6.3)..... 176

Figure 6.19: Multipliers of best reservoir model for two different cases over the base model for a) net:gross, b) horizontal permeability and c) vertical permeability in log scale. ..... 178

Figure 6.20: Average reservoir properties in first reservoir interval for different history matching studies. (a) net:gross, (b) horizontal permeability and (c) vertical permeability..... 179

Figure 6.21: Areas chose for normalization study close to well N6 and A1.. ..... 181

Figure 6.22: Magnification of two areas chosen for normalization in a) the simulation model b) synthetic seismic time-lapse data for base model and c) observed time-lapse seismic. Top row is A1, bottom row is N6. ..... 182

Figure 6.23: Cross-plot of observed and synthetic 4D impedances for a) set of simulation cells in area belong to A1 in Figure 6.20 and for the base model, b) set of simulation cells in area belong to A1 and after history matching and c) same as (b) but ignoring the poorly matching region..... 183

Figure 6.24: Cross-plot of observed and synthetic 4D impedances for a) set of simulation cells in area belong to N6 in Figure 6.21 and for the base model, b) set of simulation cells in area belong to N6 and after history matching and c) same as (b) but ignoring the data with high error..... 184

Figure 6.25: Normalized observed 4D seismic obtained by using the regression equation of a) study based on A1 and equation in Figure 6.23c and b) study based on N6 and equation in Figure 6.24c... ..... 185

Figure 7.1: History matching workflow based on updating reservoir properties in geo-body types. ..... 191

Figure 7.2: Main history matching studies performed to globally update reservoir properties in geo-body types. ..... 193

Figure 7.3: Reduction of sum of misfits of the oil and water rates for the all wells for each 3D history matching problem (top plots) and the convergence of various reservoir parameters to the final result (lower plots). Different 3D history matching were for updating properties in a) aquifer, b) Channel Margin, c) Interchannel and d) Channel Axis. The red lines in the top plots are representative of the misfit value of the base reservoir model. Also, as an example, the boundary for the initialisation models ($n_i$) is shown as a vertical red line in the NTG for (a) following by red arrows which is the number of iterations to repeat generating $n_s$ models. ..... 195

Figure 7.4: Reduction of total production misfit in forecasting versus matching periods for different history matching studies. ..... 196

Figure 7.5: Sum of misfits of the oil and water rates for all wells from 1994 to 2003 (history plus forecasting period) versus the same misfits for the history period from 1994 to 2000. Note that the misfit value of the base reservoir model is 300,000 and 430,000 for the history period and history plus forecasting period respectively..... 197

Figure 7.6: The multipliers of various reservoir parameters; a) net:gross, b) horizontal permeability and c) vertical permeability for the best history matched models. Note that in 6D and 9D problems only one Channel Axis and Interchannel geo-body type was altered for the both reservoir intervals therefore the multiplier of parameters is same for each geo-body type in 1st and 2nd interval as shown in the this figure. Three black lines in the bars show the average value of multiplier for the best 10 history matched model. ..... 198

Figure 7.7: Average reservoir properties in first reservoir interval for different history matching studies. (a) net:gross, (b) horizontal permeability and (c) vertical permeability..... 200

Figure 7.8: Average reservoir properties in second reservoir interval for different history matching studies. (a) net:gross, (b) horizontal permeability and (c) vertical permeability..... 201

Figure 7.9: Reduction of total production misfit in forecasting versus matching periods for different history matching studies.. ..... 202

Figure 7.10: Synthetic 4D seismic map (2000-1994) for base reservoir model (a), observed map (b) and best history matched model (c)..... 203

Figure 7.11: Average reservoir properties in the first reservoir interval, comparing the PHM and PSHM studies.. ..... 204

Figure 7.12: Average reservoir properties in second reservoir interval, comparing PHM and PSHM study. ..... 205

Figure 7.13: Reduction of total production misfit in forecasting versus matching periods for different history matching studies. ..... 206

Figure 7.14: Well water production misfit for the base model (black) and best history matched model after geo-body type updating (red) from 1994 to 2000 .... 207

Figure 7.15: Well water production rates for the worst matched wells. The well number is based on the number in Figure 7.14 ..... 209

Figure 7.16: Sum of misfits of the oil and water rates for all wells, comparing the model generated by combination of parameter in each locality ($LMV_{Final1}$) with sum of misfit value for localities (Eq. 6.2) ..... 210

Figure 7.17: Reduction of total production misfit in forecasting versus matching periods for different history matching studies.. ..... 211

Figure 7.18: Individual well water production misfits for the base model (black) and best history matched model after geo-body type updating (red) from 1994 to 2000..... 212

Figure 7.19: Well water production rate for individual well, comparing the best history matched model after geo-body type updating and then further reservoir improvement via pilot point application.. ..... 213

Figure 7.20: Average reservoir properties of the best history matched model in a) first and b) second intervals. The numbers indicates the location of the well that study. The properties of base model were presented in Figures 7.11 and 7.12. ..... 214

Figure 7.21: Average reservoir properties of the best history matched model using production data only and pilot point as parameterization (Chapter 4) in a) first and b) second intervals. The numbers indicates the location of the well that study. The properties of base model were presented in Figures 7.11 and 7.12. ..... 216

Figure A1.1: Simple Kriging in 3D (Doyen 2007).. ..... 229

Figure A1.2: Definition of simple Kriging system (Doyen 2007). ..... 231

Figure A2.1: Streamline tracing through grid, showing points and segments between the points (Schlumberger Geoqueat Manual, 2007). ..... 232

Figure A2.2: Algorithm for streamline simulation. ..... 233

Figure B.1: The density of streamlines in the reservoir for different value of SLD, a) 1, b) 0.5, c) 0.1, d) 0.05 and e) 0.005.Note that for better visualisation this figure shows a fraction of streamlines (10% for all cases)... ..... 236

Figure B.2: The sum of misfit of the oil and water for all wells versus CPT time. The number in the line shows the SLD belongs to each case.. ..... 237

Figure B.3: Field oil production rate for different streamline cases with changing the SLD number. Note that the field production rate for SLD=1, 0.5, 0.1 and 0.05 are almost the same.... ..... 237

Figure B.4: Field oil production rate for streamline and Eclipse cases... ..... 238

Figure B.5: Well water production misfit for Eclipse and streamline base model.... ... 238

Figure B.6: The differences of oil saturation at the end of production period between Eclipse and streamline case (averaged vertically) for, a) SLD=1.0, b) SLD=0.5, c) SLD=0.1, d) SLD=0.05 and e) SLD=0.005..... ..... 239

Figure B.7: The differences of oil saturation at the end of production period between high density streamline case (SLD=1.0) and different streamline cases with lower SLD, a) SLD=0.5, b) SLD=0.1, c) SLD=0.05, d) SLD=0.005.(for all maps vertical arithmetic averaging performed).... ..... 240

Figure B.8: 2D maps for the differences of reservoir pressure between two following biannual time steps, modelling by Eclipse simulator.... ..... 241

Figure B.9: The sum of misfit of the oil and water for the whole wells versus CPT time. The misfit value normalized in each case by the number of time steps.... 242

Figure B.10: The differences of oil saturation at the end of production period between streamline with biannual time step and, a) streamline with monthly time step

and, b) streamline case with quarterly time steps (the arithmetic averaging performed for both maps)..... 243

Figure B.11: The average of pressure difference at the end of production period between streamline with biannual time step and, a) streamline with monthly time step and, b) streamline case with quarterly time steps..... 243

## List of Tables

Table 3.1: Summarized the key biostratigraphic events in the reservoir.. ..... 54

Table 3.2: Nelson field, pressure effect on acoustic properties. From dry frame SCAL measurements (Boyd-Gorst and Garnham 1999)..... 64

Table 4.1: Main elements for the history matching runs.. ..... 98

Table 4.2: Summary of number of models used in history matching, total CPU time using 1 processor and total CPU time using cluster. *In this study CPU time to simulate each reservoir model using streamline simulator is around 8 minutes on an 3.4 GHz processor..... 113

Table 4.3: Number of each type of parameters model in each scheme..... 113

Table 5.1: Assumptions and disadvantages of different 4D seismic normalization strategies, for modifying the base reservoir model through seismic and production history matching..... 139

Table 6.1: History matching parameters.. ..... 154

Table 7.1: Main elements for history matching runs... ..... 194

Table 7.2: Reduction (%) of production and seismic misfit in history matching period for different studies... ..... 207

Table 7.3: Main information for different history matching studies..... 209

## Nomenclature

| | |
|---|---|
| $K_h$ | Horizontal permeability, $mD$ |
| $K_z$ | Vertical permeability, $mD$ |
| $O$ | Objective function |
| $\vec{d}$ | Data vector |
| $\vec{\alpha}$ | Parameter model vector |
| $C_d$ | Covariance matrices of data |
| $C_\alpha$ | Covariance matrices of prior parameter |
| $W$ | Weighting matrix |
| $O_T$ | Total objective function |
| $O_p$ | Production objective function |
| $O_s$ | Seismic objective function |
| $\beta$ | Weighting factor between production and seismic objective function |
| $X$ | Reservoir property |
| $m(u)$ | The expected mean value of variable $X$ |
| $n$ | The number of data points |
| $w_i$ | The weighting function between the points |
| $Var$ | Variance |
| $\sigma_E^2(u)$ | The variance of the estimator |
| $R(u)$ | Residual |
| $Cov$ | Covariance |
| $C_R$ | Covariance of residuals |
| $Q_i$ | Total flow rate into segment $i$ |
| $dTOF$ | Time of flight in the segment $i$ |
| $P$ | Pore pressure, $Psia$ |
| $K_w$ | Water bulk modulus, $Pa$ |
| $K_o$ | Oil bulk modulus, $Pa$ |
| $K_g$ | Gas bulk modulus, $Pa$ |
| $K$ | Saturated bulk modulus, $Pa$ |
| $\mu_{wet}$ | Saturated shear modulus, $Pa$ |
| $\rho$ | Effective bulk density of the sand-shale fluid system, $Kg/m^3$ |
| $\rho_{sand}$ | Dry sand density, $Kg/m^3$ |
| $V_{sh}$ | Shale volume fraction, $m^3/m^3$ |

$\rho_{sh}$ Dry shale density, $Kg/m^3$

$\rho_w$ Water density, $Kg/m^3$

$\rho_o$ Hydrocarbon density, $Kg/m^3$

$\varphi$ Effective porosity

$S_w$ Water saturation

$S_o$ Oil saturation

$S_g$ Gas saturation

$K_m$ Bulk modulus of sand and shale grains, $Pa$

$\mu_d$ Shear modulus of dry rock frame, $Pa$

$K_d$ Bulk modulus of dry rock frame, $Pa$

$K_f$ Bulk modulus of the oil water mixture, $Pa$

$V_s$ Shear velocity, $Km/s$

$V_p$ Compressional velocity, $Km/s$

$I_P$ Compressional acoustic impedance, $Kgm^{-2}S^{-1}$

$I_{pAve}$ Average value of p-impedance for a column of simulation cells, $Kgm^{-2}S^{-1}$

$M$ Bulk and shear modulus of sand and shale in a simulation cell, $Pa$

$M^{sand}$ Bulk and shear modulus of sand in a simulation cell, $Pa$

$M^{sh}$ Bulk and shear modulus of shale in a simulation cell, $Pa$

$\langle\ \rangle$ Vertical volume weighted average over the reservoir interval

$I_{ij}^{interp}$ Interpreted value of p impedance for the location of bins i and j between the simulation cells

$w_{ijIJ}$ Interpolated factor

$\underline{r}$ Position vector for the centre of cells

$\underline{X_i}$ Seismic and production data for the $i^{th}$ variable

$I$ Impedance, $Kgm^{-2}S^{-1}$

$\varepsilon$ Error in observed impedance data

$I^{obs}$ Observed seismic impedance

$I^{cal}$ Calculated seismic impedance

$Q^{obs}$ Observed production data

$Q^{cal}$ Calculated production data

$\sigma_I^2$ Variance of observed impedance data

$\sigma_Q^2$ Variance of observed production data

$d$ Dimension of parameter space

| | |
|---|---|
| $n_i$ | The initial sample NA needs for its initialisation |
| $n_s$ | Total number of models NA generate for each new step |
| $n_r$ | Best model chosed after each step of NA for generation of Voronei cells |

**Abbreviation**

| | |
|---|---|
| WOR | Water/oil ratio |
| GOR | Gas/oil ratios |
| WGR | Water/gas ratios |
| BHFP | Bottom hole flowing pressure |
| TOF | Time Of Flight |
| $PV$ | Pore volume |
| TVD | True vertical depth |
| $NTG$ | net:gross |

**Subscript**

| | |
|---|---|
| $obs$ | Observed |
| $calc$ | Calculated |
| $prior$ | Prior information |
| $i$ | Refers to a particular location in the reservoir |
| $sand$ | Sand |
| $sh$ | Shale |
| $I$ and $J$ | Grid cells in simulation model |
| $i$ and $j$ | Seismic bins |

# Chapter 1: INTRODUCTION

**Overview:**

In this first chapter of the thesis we present a general view of the area of work and some main definitions. Then we summarize the main steps of the process of automatic production and seismic history matching. As a literature review we look at various studies to see the history behind this study. Finally there is a short introduction for each chapter of the thesis.

## 1.1 General background and definition

One of the most important strategies in an oil or gas company is optimization of production scenarios in order to maximise the final profit. Generation of accurate and reliable reservoir models via characterisation can be an important tool in order to achieve the field operators's aims. To build a reservoir model we usually need to have integration across several disciplines including geology, geophysics and reservoir engineering.

The general focus of this work is history matching where the primary objective is to modify a prior model (this model consists of various parameters with uncertainties) such that the updated model reflects the available production data and the uncertainties in production forecasts are reduced. Usually the flowing steps are performed to perform history matching successfully:

- Identify variables in the reservoir model that have influence on history matching and perform appropriate parameterization
- Defining a suitable objective function for optimization
- Reduce the objective function to a minimum value by selecting or designing a suitable optimisation algorithm which is efficient in terms of computational cost

The historical data used in history matching are usually production data such as oil, water and gas rates or bottom hole pressure. These measured data usually reflect behaviour in a small part of a reservoir such as the drainage region of the wells and but also the connected volume. One of the real challenges here is that not enough information is obtained about the behaviour of the reservoir far from the wells. More precisely for a given volume the further that a sub-volume is from a well, the less

influence it will have on that particular well. Time-lapse seismic is very useful for measuring reservoir activity areally, especially between the wells where production information is weak. The strength of 4D seismic data is that it makes reflects dynamic activity which varies across the reservoir. The dynamic activity that we observed in 4D seismic data are not necessarily related to the specific location 4D data has been taken, however. In a many cases, what we observe as 4D signal in a given location depends on all connected regions. Therefore experience and care is needed in order to analyse and relate 4D signals to relevant production activity in the reservoir.

3D seismic imaging and interpretation is a tool that can be used to understand the reservoir volumetrically. This 3D information is very helpful to complete a more accurate image of the subsurface and enhances the ability of the reservoir description team to interpret the reservoir and make meaningful decisions successfully. Although these data offer very useful information to build the static reservoir model, 3D seismic data does not give a picture of the dynamic processes in a reservoir. On the other hand, the repeated acquisition of 3D seismic data over calendar time (known as 4D seismic data) enables monitoring of fluid movement in the reservoir (because of pressure change, compaction, saturation change etc). Monitoring can capture various processes such as reservoir depletion from primary through tertiary oil recovery that happens more in mature fields. In primary production we will see the effect of changing pore pressure due to compaction (which happens mainly in fields that are geomechanicaly active), pressure reduction and gas evolution. In secondary recovery, water saturation and pore pressure changes can be detected by using time-lapse seismic. Tertiary recovery often results in thermal and saturation changes due to steam injection, in-situ combustion, hot water injection etc. All these changes in pore pressure, pore volume and fluid saturation have an impact on geophysical properties such as rock and fluid compressibility, shear modulus and bulk modulus that ultimately can be observed in 4D seismic data.

To understand better the importance of time-lapse seismic application for the oil industry we can see from Figure 1.1 which shows the spread of time-lapse projects all over the world for BP who used this important tool for better field management.

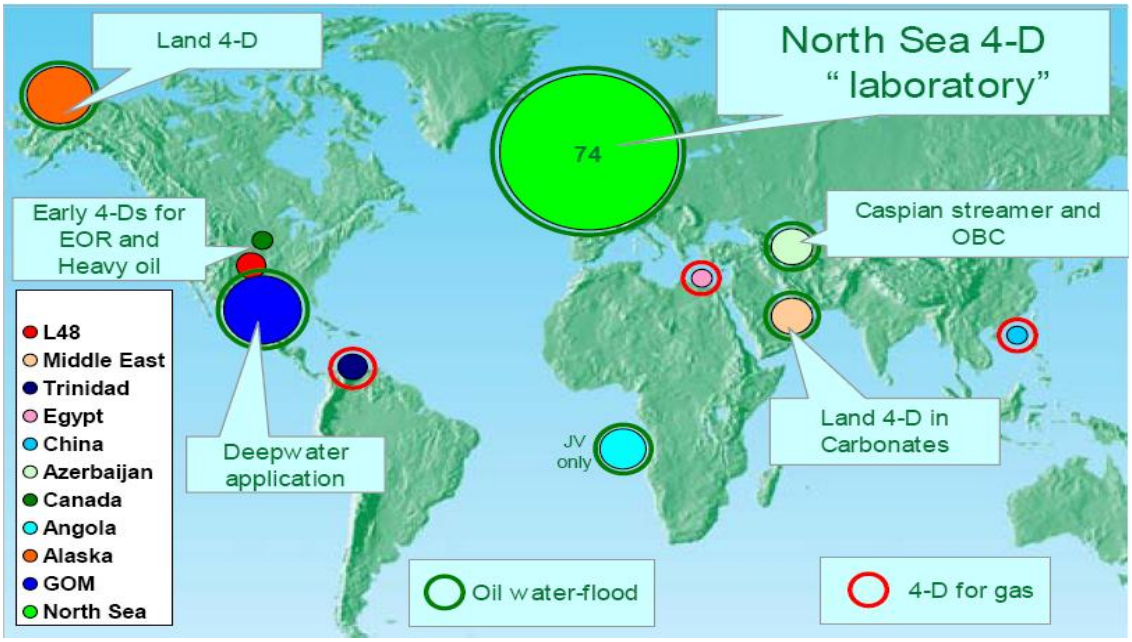


*Figure 1.1: Location of various time-lapse projects carried out all over the world by BP for past 25 years until end of 2007 (Foster 2008). There have been 74 seismic surveys in the North Sea. Each colour inside the circle indicates the geographical location and the area of each is relative to highest number of surveys in North Sea.*

A major challenge of this thesis is proper assimilation of the valuable information obtained from time-lapse seismic data into reservoir history matching in order to better represent fluid flow movement in the reservoir. This study is categorized as an integration study between geophysics and reservoir engineering.

## 1.2 A general category for history matching

History matching can be divided into two aspects:

1. The choice of historical data that we want to use in history matching.
    - Production history matching
    - Seismic history matching
    - Seismic and production history matching
2. Solution of history matching problem
    - Manual history matching
    - Automatic history matching

### *1.2.1 The choice of historical data that we want to use in history matching*

In general the production data that are matched during history matching are oil/water/gas production rates, water/oil ratio (WOR's), gas/oil ratios (GOR's), water/gas ratios (WGR's), water and gas arrival times and fluid saturations from core data. Well bottom hole pressure , RFT's and bottom hole flowing pressure (BHFP's) can be used for history matching as well (Mattax and Dalton 1990). The data mentioned above is called dynamic data because they are related to dynamic fluid displacement in the reservoir due to production activity.

The above dynamic production data will contrast with other types of reservoir properties called static data that includes well logs, core photographs and plug data along with well testing. These data give accurate details about the reservoir at the wells, between well information relies on seismic measurements however. These static data are commonly used to generate fine scale geological models.

Another type of dynamic data is time-lapse (4D) seismic. The effect of pressure and saturation changes can be obtained in time-lapse seismic data providing two dimensional maps or three dimensional volumes of the missing information. Time-lapse seismic can convey very good information about fluid movement and stress changes during production and helps potentially in history matching.

The time-lapse seismic data can be used in the workflow in varying degrees from the qualitative (Parr et al. 2000; Aggio and Burns 2001) to quantitative (Landa and Horne 1997; Huang et al. 1997; Guerin et al. 2000; O' Donovan et al. 2000; Van Ditzhuijzen et al. 2001; Gosselin et al. 2001; Fagervik et al. (a) 2001; Aarenas et al. (a) 2001; Waggoner et al. 2002; Lygren et al. 2002; Gosselin et al. 2003; Aanonsen et al. 2003; Mezghani et al. 2004; Falcone et al. 2004; Roggero et al. 2007). Figure 1.2 shows the range of possibilities from qualitative to quantitative usage of time-lapse seismic. Qualitative use of time-lapse data is more useful for late life of a field in order to use data for identifying the upswept part of the reservoir independently from simulation models. A first quantitative application of data would be visual comparison of the output of simulation (pressure and saturation) with seismic data. In this case it is possible to better identify compartmentalization in the field as well as better develop the in-fill well targets. In a semi-quantitative time-lapse seismic study, synthetic 4D seismic will be derived from reservoir simulations and then compared to real data in

order to obtain an areal/volume match in the model as part of history matching. In full quantitative studies, the synthetic 4D seismic can be calibrated based on real data. In such a case, at some well locations the impedance data will be calculated from sonic log and then a rock-physic model will be inverted through an iterative adjustment of inversion properties (which is case dependent and could be fluid properties as one example) by minimizing a misfit function until agreement between real impedance (from log) and synthetic impedance from forward rock-physic modelling observed (Falcone et al. 2004). Another value of quantitative 4D history matching would be identifying the reservoir properties heterogeneities in the model by a full volume match in the reservoir, further increasing value. Greater quantitative application increases the value of this data to connect better the reservoir properties and the location of infill wells.

We can see in Figure 1.3 an example of qualitative use of time-lapse seismic data in the Schiehallion field in order to distinguish pressure and saturation effects in the reservoir. This analysis is very important in order to map out the pressure compartments and connectivity issues in the reservoir (Hatchell et al. 2002).

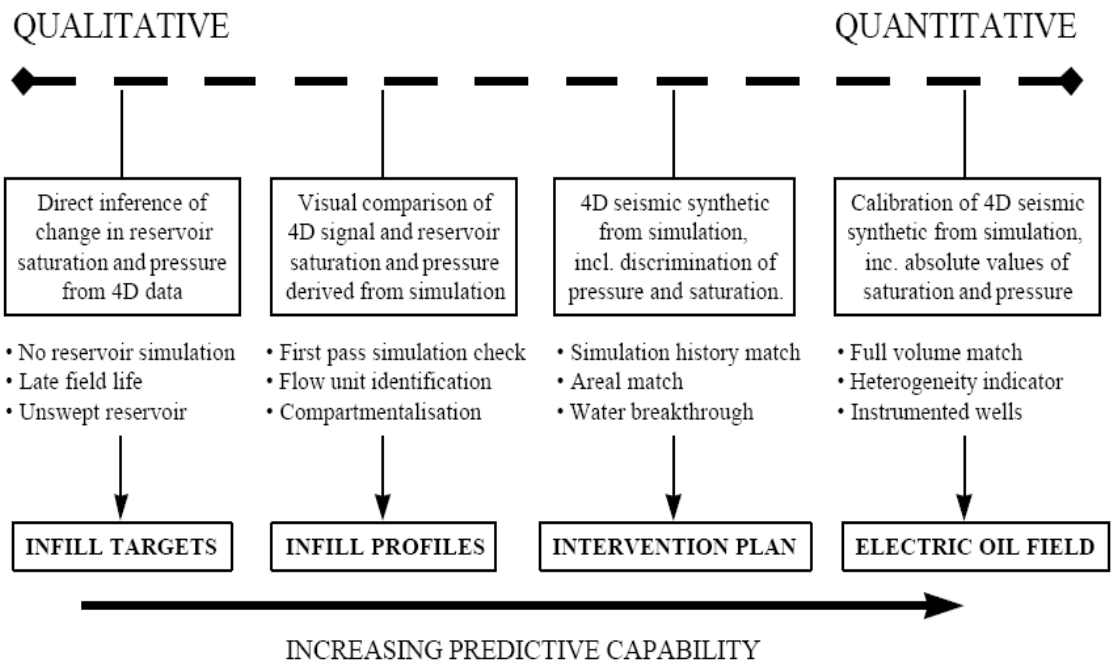


*Figure 1.2: The spectrum of 4D seismic application from qualitative to quantitative use (O'Donovan et al. 2000).*

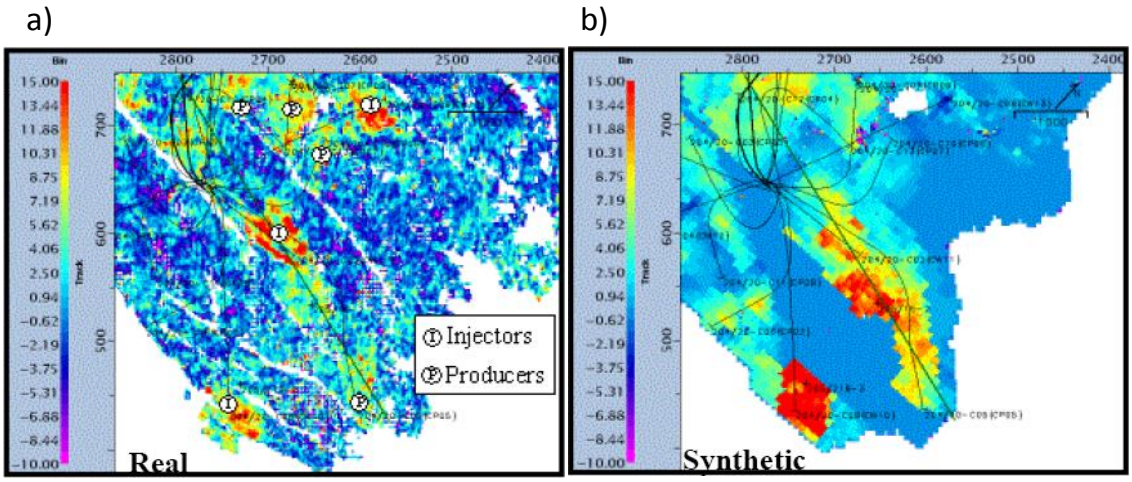


*Figure 1.3: The differences of post and pre-stack amplitude for (a) real data and (b) synthetic data for a sector of Schiehallion field (Hatchell et al. 2002).*

In quantitative applications of time-lapse seismic data in the history matching process, there are various domains in which we can compare real and predicted data including seismic, impedance (or pseudo impedance) and pressure/saturation domains (Figure 1.4). There are various uncertainties and difficulties in each domain. If we start from the simulation model and generate synthetic seismic traces, there are two main sources of uncertainties which come from the petro-elastic model and seismic modelling. The latter is moderately CPU intensive for convolution methods (equivalent to simulation time, roughly) but too time consuming using full wave simulation. On the other hand starting from measured seismic data to invert for pressure and saturation, there are two important uncertainties which come from the seismic inversion process used to calculate attributes and also either from the petro-elastic model again or else from calibration issues via empirical inversion (Floricich et al. 2004). The optimum domain for the seismic comparison is still a topic of research and in this work, to reach a balance between time and accuracy we considered the impedance domain as the best place for comparing real and synthetic data (Stephen et al. 2006).

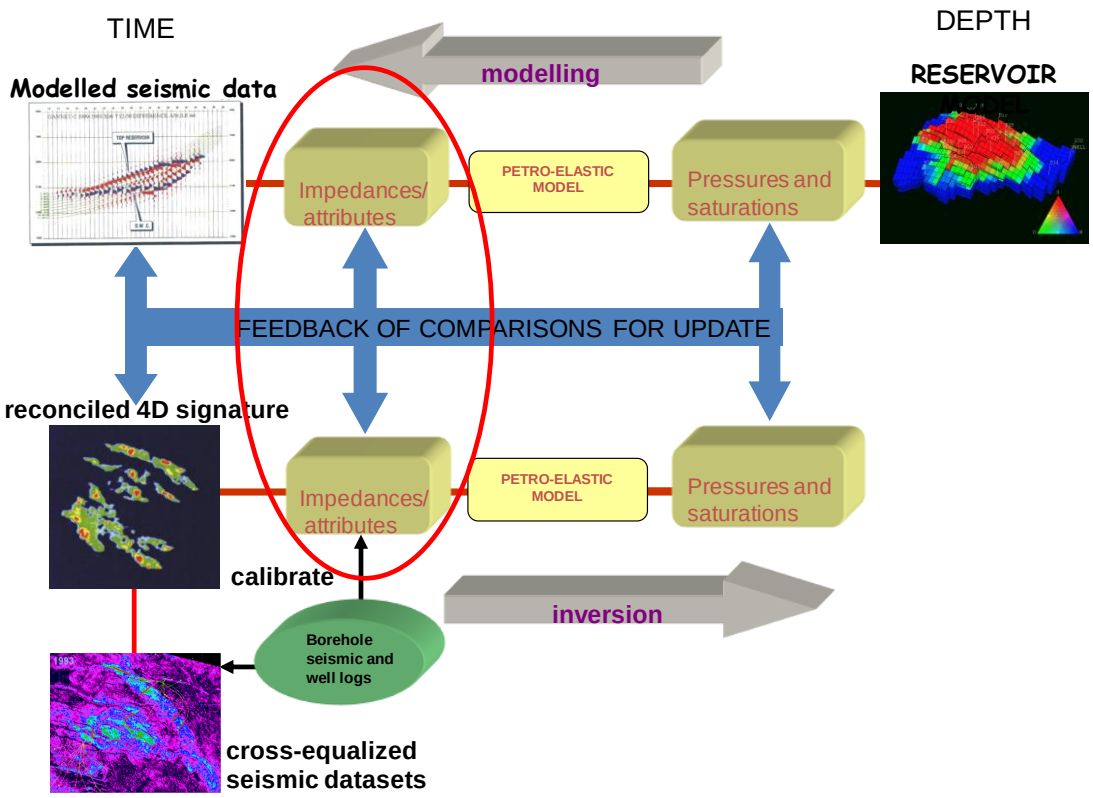


*Figure 1.4: The various domains for comparison of measured and predicted seismic data (red circle identify the domain that we use in this work) (MacBeth 2007).*

In this study, we sought to avoid forward modelling to generate synthetic seismic traces and attributes for comparison with the observed data (in the seismic domain). We therefore required observed impedance data or an equivalent attribute. We first used inverted elastic impedance data to derive observed 4D signatures (Stephen et al. 2007; Kazemi and Stephen 2008). Subsequently, the operator provided better processed amplitude data with lower uncertainties. We switched to using this new data and all results in this thesis are based it. Following advice and information provided by the operator, phase shifted amplitude data were obtained from which Root Mean Square (RMS) attributes yield pseudo-impedance data. These were compared to predicted impedances. More information about phase shifted amplitude data will be given in Chapter 3, Section 3.7.2. The concept of normalization is also introduced in chapter 5 in order to make the real pseudo impedance and synthetic impedance data in the same units.

### *1.2.2 Manual and automatic history matching*

In traditional history matching the reservoir engineer usually identifies the uncertain and the important parameters in the reservoir according to his/her experience. As an

example the parameters that can be changed are (1) aquifer transmissibility, (2) aquifer storage, (3) reservoir thickness (4) reservoir permeability and (5) relative-permeability and capillary pressure functions (Mattax and Dalton 1990). Also some other parameters such as (6) reservoir porosity and thickness, (7) structural definition, (8) rock compressibility, (9) reservoir oil and gas properties, (10) water/oil contact and gas/oil contact and (11) water properties may be changed during history matching as well. However, there are various degrees of uncertainty in these data. For example for the cases where data are measured in the lab such as fluid properties, rock compressibility and relative permeability the uncertainty would be lower than other data though there are issues of representatively.

Given the number of possible unknowns, therefore, manual history matching will be very time consuming and an expert engineer is needed who knows the reservoir very well. Even so a lot of work must still be done to find a well matched reservoir model. However, in automatic history matching it is possible to modify some parameters automatically in the reservoir.

Figure 1.5 shows a simple comparison between manual and automatic history matching. In Figure 1.5 we can see that many parts of history matching are the same for both cases. First we need to define the scope of history matching followed by identification of the reservoir variables that require modification including where and how these variables need to be updated in the reservoir. However there are other similarities. For example in both cases the same parameter selection should be performed (following sensitivity analysis), the same data analysis (uncertainty consideration of observed data, calculating estimating data errors) and pre-processing are also necessary. Then if we choose to manually update the reservoir, with the exception of the flow simulation part, the rest is dealt with by the reservoir engineer to check the result and select various values of parameters. Therefore the workflow consists of many trial and error choices of updates followed by data management and analysis. In contrast, in the automatic approach, the part of selecting parameter values is under the control of an optimization algorithm. Ultimately, similar to the manual technique, we still need to check the result to make sure that we are improving the reservoir correctly.

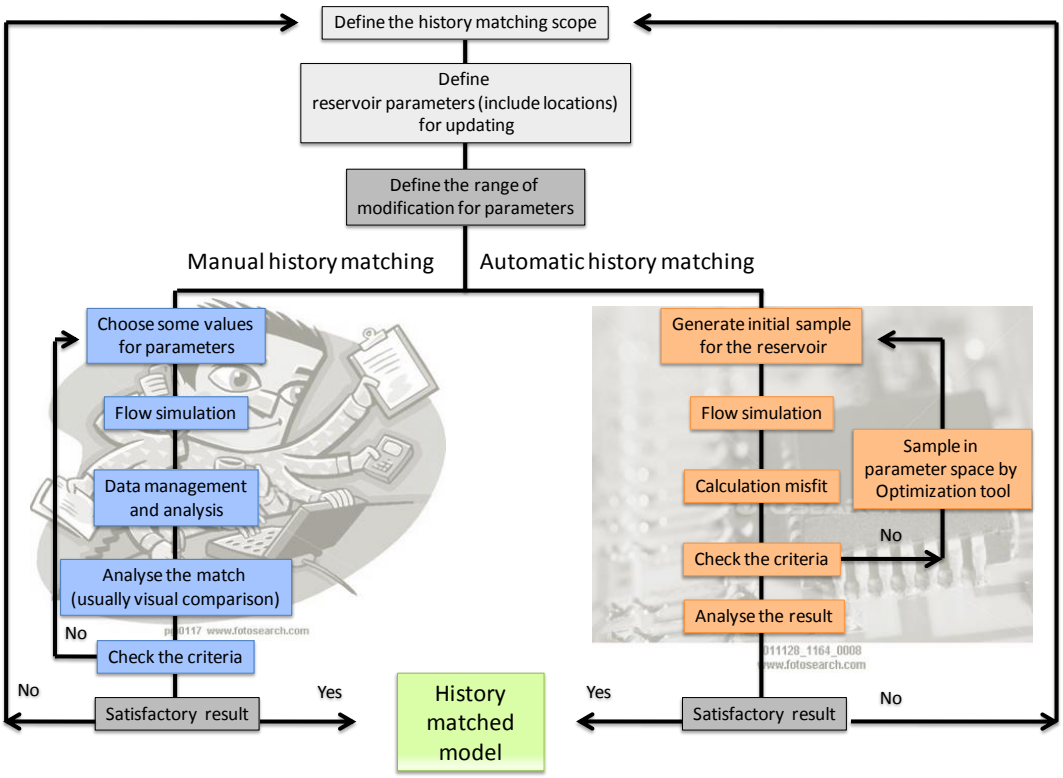


*Figure 1.5: The similarity and differences between manual and automatic history matching runs.*

### 1.3 The history of computer aided/Automatic History Matching (AHM)

Computer aided (assisted) history matching is an important topic that has been under research for more than 4 decades. A part of this process is usually called automatic history matching. The general purpose for both approaches is to find a better representation of the reservoir, firstly constrained by geological information of the reservoir and secondly to honour the production observations and in some cases 4D seismic data. For assisted history matching the idea is to help the reservoir engineer to history match the reservoir, by applying some mathematical tools such as the Gauss-Newton algorithm, Jacobian matrix, etc (MacMillan et al. 1999; Cheng et al. 2005**)** to identify more sensitive reservoir parameters for updating. Another common example of assisted history matching in the literature uses a streamline simulator in order to find the region in the reservoir affecting flow (Emanuel and Milliken 1998; Milliken et al. 2000; Lolomari et al. 2000; Baker 2001; Maschio and Schiozer 2005; Agarwal and Blunt 2004) as shown in Figure 1.6. Here the streamline was very useful in order to show the drainage region close to different wells.

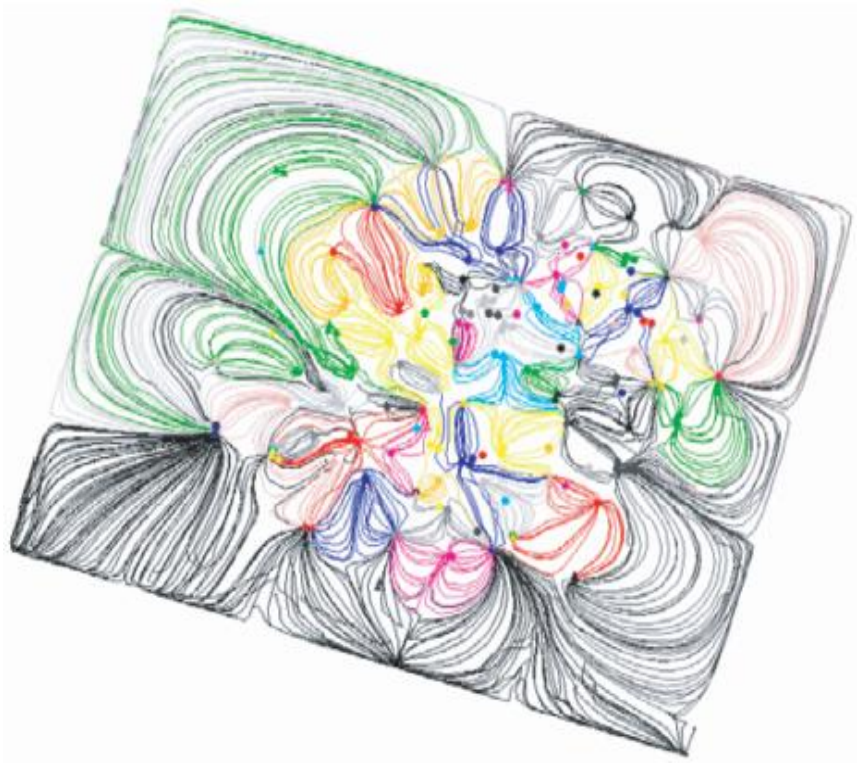

*Figure 1.6: A two dimensional view of a streamline pattern for a reservoir. The different colors identify the well drainages regions (Agarwal and Blunt 2004).*

The general idea behind all those assisted studies is the assumption that the best result will be achieved by choice made by humans and they have developed a set of tools to assist engineer.

However, automatic history matching can be consider as a part of computer aided techniques and specifically it refers to the algorithm where an optimization method is used to control the majority of the history matching process by changing the values of selected parameters, running the simulation model, calculating the misfit value and updating the parameters. This loop is continued until a defined misfit threshold is reached. Usually in all proposed AHM methods, there are still some parts of the process that need to be defined manually such as the choice of variables to update, the regions to update in the reservoir, the best history matching result etc. It is worth mentioning that the reservoir engineer experience is still crucial for any computer aided/automatic techniques. The big advantages of using these techniques, is the gain of time which can be used for a better analysis of data and results.

In the literature, some people prefer to refer to all assisted and automatic history matching methods as Computer Aided History Matching (CAHM) because this term is

more general. In this work we prefer to call the history matching loop as AHM because we specifically use one optimisation algorithm for automatically updating the parameters. Later on in this thesis, in the AHM loop for the cases where production data were used, the Production History Matching (PHM) term was used and when both production and 4D seismic data were used, we called that Production and Seismic History Matching (PSHM).

Figure 1.7 shows a general workflow for history matching of a reservoir under control of an optimization tool where both production and seismic data are used. AHM starts from a reasonable realization of a geo-model conditioned to static data such as core, log, 1D, 2D or 3D seismic. The model is upscaled to a reservoir model to save CPU time. Then from simulation we obtain flow rates at the wells and also pressure and saturation for each individual cell. The pressure and saturation are the input of a petro-elastic model that is used to generate synthetic impedance data of the scale of the reservoir model. The synthetic impedance can be downscaled from the reservoir model scale to the seismic acquisition grid scale if desired. Through an appropriate objective function we can then compare, quantitatively, our measured data with observed data. Using an appropriate parameterization method we need to generate new representatives of the reservoir by updating certain reservoir parameters. The whole loop of generating new reservoir models, calculating the mismatch between observed and measured data and updating reservoir parameters can be controlled automatically by using an optimization algorithm in order to converge to a minimum misfit value. The violet boxes in Figure 1.7 are representative of the main elements for the workflow and we will discuss various approaches we can use in Chapter 2, section 2.1.

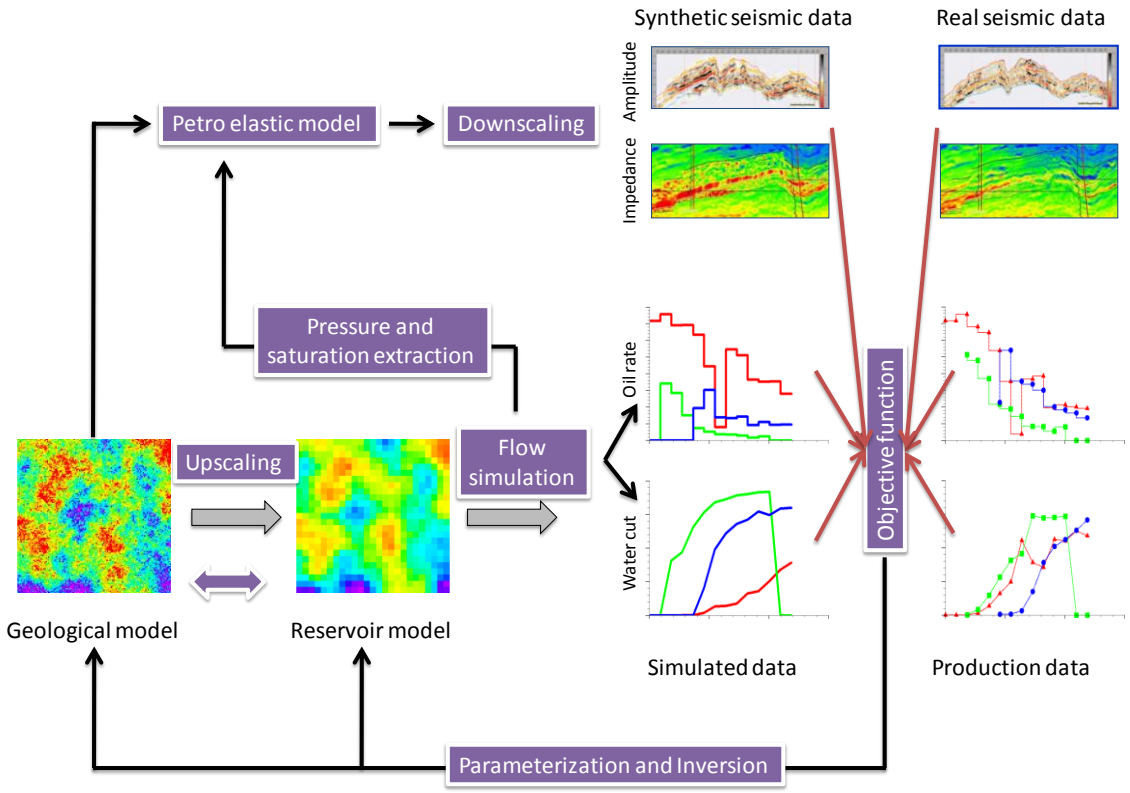


*Figure 1.7: A general procedure for automatic history matching (modified from Roggero et al. 2007).*

### *1.3.1 Objective function*

Assuming Gaussian distributions for both model and measurement errors the objective function is presented as Eq. 1.1 (also called L2 norm and was developed from theory of probability (Tarantola 1987).

$$O_p(\theta) = \left[\left(p(\theta) - d_p\right)^T C_p^{-1}\left(p(\theta) - d_p\right)\right] \quad (1.1)$$

Where the vector $\theta$ is the set of model parameters that need to be estimated, $d_p$ is the vector of production data, $p(\theta)$ is corresponding calculated production data from the simulation and $C_p$ is the covariance matrix representing the data and model error.

In the case of integrating both production and seismic data in the objective function, there is another term for seismic. We can consider a weighting factor as indicated in Eq. 1.2 to bias towards data with higher accuracy.

$$O_T = \beta * O_p + (1 - \beta) * O_s \quad (1.2)$$

where:

$$O_s(\theta) = [(s(\theta) - d_s)^T C_s^{-1}(s(\theta) - d_s)] \quad (1.3)$$

$O_p$ and $O_s$ are production and seismic objective function respectively, $\beta$ is the weighting factor between production and seismic objective functions, $d_s$ is the vector of seismic data, $s(\theta)$ is the corresponding simulated data to match and $C_s$ is the covariance matrix including data and model errors. Choosing the appropriate value for the weighting factor could be a challenging decision in any history matching study. This factor should be a function of accuracy for production and seismic data. For example, Waggoner et al. (2002) considered a least squares formulation for $O_p$, and for $O_s$ . He used a function of normalised cross correlation between the predicted and the observed impedance. In this thesis $\beta = 1/2$.

However, in time-lapse seismic data there are various levels of uncertainties that could appear in the data during the data acquisition, processing, etc. Because of technological development in this area the time-lapse seismic data can be used reasonably confidently but still there are some issues for estimating noise and other uncertainties.

### *1.3.2 Parameterization techniques*

Much of the work reported in the literature has been directed at developing and improving the parameterization with a view to reducing the number of simulation runs for big history matching problems by reducing the number of unknowns. De Marsily et al. (1984), Roggero and Hu (1998) and Le Ravalec-Dupin and Noetinger (2002) were more concerned about the geostatistical constraint on reservoir models updating during automatic history matching algorithms. For example, in 1997, Bissell et al. (1997) used the pilot point method (De Marsily et al. 1984) as a geostatistical tool. The pilot points are a means of selecting some locations in the reservoir where the parameters are going to be updated. Bissell et al. (1997) fixed the porosity at the wells assuming it was known exactly. By dedicating the variogram of porosity this properly could be distributed around the well using Kriging (for details see Chapter 2, Section 2.2 and Appendix A.1). They combined this approach of reservoir updating with the gradient based Gauss-Newton/Steepest-Descent optimization method.

The Gradual Deformation Algorithm (GDA) generates a set of realizations that are merged smoothly while preserving the overall statistical characterization of the reservoir. A gradient based optimization algorithm is used for history matching of the model in some studies (Roggero and Hu 1998; Le Ravalec-Dupin and Noetinger 2001). The value of GDA is that instead of choosing the reservoir parameters (such as porosity) in all simulation cells as unknowns, during the history matching some limited number of parameters will be tuned. In this method a Gaussian distribution is considered for the parameter in the reservoir. Then, the principle is that a new realization is a linear combination of two previous realizations. A mixing coefficient can be considered as the parameter that is updated during the inversion process. Caers (2003) developed a method called Probability Perturbation for honouring the geological information through history matching. His method did not require gradual deformation of the reservoir model. This method is based on perturbation for the underlying probability distribution which is used to create the 3D geological model rather than properties directly. Therefore, the geological continuity of the model is always honoured. The drawback for this method is that a similar amount of perturbation is imposed everywhere in the model. Therefore, this method is limited to geologically simple or small models with a small number of cells. Because of that limitation Hoffman and Caers (2005) introduced another method called Regional Probability Perturbation that allows perturbation of the geological realization of a model differently in different regions. Therefore, with this method it is possible to only focus on the wells with poor match to production and keep the other wells unchanged.

Emanuel and Milliken (1998) used a very simple method to retain the geostatistical characterization of the reservoir by keeping the relationship between porosity and permeability fixed during automatic history matching of the reservoir. Therefore by changing one property in the reservoir the others will be changed accordingly by using the defined correlation between the parameters.

**Experimental design (ED)**

Experimental design was first developed in the 1920's for agricultural purposes and nowadays it is widely used in the petroleum industry. Experimental design is the planning of experiments to maximise the amount of information. The basic idea is that several parameters are varied simultaneously based on a predefined pattern and then the results are connected by means of a mathematical model. This model may then be used

for interpretation, prediction, and optimization. Alternatively, as in history matching, it may be used to simplify the problem by removing unimportant variables or parameters. ED can be applied to history matching studies as part of sensitivity analysis and parameter interaction estimation. For the response surface we can consider the production behaviour of the reservoir or its misfit. In a specific type of ED, the experiment can be designed in such a way that for each explanatory variable we have three levels: the base case, middle or most likely case and two extremes, which can be coded numerically as 0, -1 and +1 respectively. This design plays an important role in more complicated design problems, because in addition to the main effect and interaction this design can be used to determine the second order non-linear effects. A disadvantage of the ED is that the number of experimental combinations increases rapidly as the number of variables increase.

In this thesis we used something similar to ED for understanding the sensitivity of parameters in reservoir performance. In our study, one parameter at a time sensitivity analysis was performed (Chapter 4, Section 4.5) in order to investigate the sensitivity of each parameter. However the optimization algorithm that we used (Chapter 2, Section 2.7) considers random combinations of the parameters in the exploration phase with more than the two or three levels associated with experimental design. This means more exploration in the parameter space but potentially less efficiency.

In addition to the above points we can add that, in this thesis the aim was updating the reservoir parameters in order to improve both production and seismic misfits. Therefore, we should consider both types of data in order to have an efficient ED study. However the observed seismic data was pseudo impedance and some techniques need to be applied in order to prepare this data for use in the history matching loop (it was not ready before history matching study started). A part of that seismic preparation was including normalized of the seismic attributes (for details see Chapter 5). Therefore, technically 4D data was not available for ED study and by ignoring seismic data; there was high risk of eliminating some parameters which may have influence on seismic if we do not include that in the ED study.

In this section we had an overview about developing parameterization techniques, however in Section 1.4 we discussed about developing seismic history matching techniques and as a part of that development we observed the important role of

integrating parameterization techniques. Therefore, in Section 1.4 we had a small discussion to shows the importance of parameterization in seismic history matching studies.

### *1.3.3 Optimization tools*

Having defined the parameterization scheme it is necessary to guide the choice of making update using optimization algorithms. To date, research in automatic history matching has been based on generation of optimization tools that are robust and efficient. By robust we mean that the algorithm should converge to a minimum for any reasonable initial guess for reservoir parameters and by efficient we mean that it must obtain the minimum value of the objective function with a reasonable amount of computational effort. By reasonable we mean that we need to manage the time spent for the study based on the dimension of the reservoir model and the facilities available to simulate each model.

At the beginning of research in this area in 1970, the main application was for simple geological fields. The focus was on mathematical minimisation of the objective function without considering how it would work with complex reservoirs with a lot of unknowns.

Coats et al. (1970) defined a nonlinear objective function that was based on a linear relation between reservoir parameters and the error of observation and measurements. This approach requires a large number of simulation runs, at least equivalent to the number of parameters controlling changes in the model. Reduction of the number of simulations has been the goal of researchers such as Solorzano et al. (1973) who used a linear distribution of parameters around each production well to reduce the number of unknowns. The gradient based method is one well known category for minimization of the objective function that is mainly based on Gauss-Newton (Fletcher 1987). In these methods the derivatives of the objective function are calculated with respect to the parameters such that a lot of models are needed in order to incrementally change each parameter and to reach convergence. However the analytical gradient methods, provided these may be calculated, are much less time consuming and more accurate compared to the previously mentioned numerical gradient approaches. The approach is sometimes combined with other techniques such as Marquardt's modification of the Gauss-Newton method (Watson and Lee 1986) or combined with optimal control theory

via the Adjoint Method (Chen et al. 1974; Chavent et al. 1975) which can efficiently evaluate the gradient of the objective function regardless of the dimensionality of the problem (Yang and Watson 1988). In the Adjoint Method instead of performing a lot of simulations to estimate gradients, the calculation is based on the output of one simulation model. Then an adjoint formulation needs to be solved that ultimately gives us the sensitivity of production data with respect to the different parameters though it does not need the sensitivity coefficient matrix. The drawback for the adjoint method is that we need to obtain the derivative equation of production data such as pressure or saturation with respect to the all parameters such as porosity, permeability, etc. Also programming these derivative equations could be time consuming. Simulation software developers could code a generic set of sensitivities however.

Yang and Watson (1988) applied their method on a two-phase one-dimensional reservoir and showed that their method was more efficient than other first derivative methods such as steepest-descent and conjugate-gradient.

Another gradient based method is Limited Memory Boyden-Fletcher-Goldfarb-Shanno method (LMBFGS) (Zhang and Reynolds 2002; Zhang et al. 2005; Wang et al. 2005). This method is suitable when the number of measurements of conditioning production data varies from a few hundred to several hundreds and the number of reservoir variables ranges from several hundred to tens of thousands. The advantage of this algorithm is that instead of calculating, directly, the inversion of the Hessian matrix (which comes from the calculation of the second derivative of objective function) it approximates the Hessian in an iterative formula. The term of 'Limited memory' arose because high dimensional problems require large amounts of memory to store the Hessian matrix. This can be reduced in this method by using a smaller number of gradient values in the Hessian matrix. They applied this method on various cases including 3D single-phase flow, 2D three-phase flow and 3D three-phase flow and they compared the efficiency of this optimization method with other gradient based methods. Liu and Oliver (2004) used the same algorithm for history matching by adjusting the facies boundaries.

The general drawback for gradient based method is the limitation for calculation of the inversion for the Hessian matrix especially for high dimensional problems. On the other hand at the end of the inversion process, these methods only provide one model to

give the minimum misfit of the objective function, which maybe a local minimum of the function. As a result these algorithms are also called local optimizer algorithms.

Another category of inversion algorithm includes stochastic search methods. In this category there are Simulated Annealing (SA), Genetic Algorithm (GA) and Neighbourhood Algorithm (NA) (for details see Chapter 2, Section 2.7). These inversion algorithms are also called derivative free algorithms because they do not try to solve the derivative of objective function versus parameters. The objective function in these algorithms is used only to calculate misfit values of various models in the parameters space according to the guide from the algorithm. Compared to gradient based methods, the CPU intensive mathematical part reduces significantly while on the other hand more models need to be generated. As a summary the advantage of these algorithms is that we will find multiple matching models instead of a single model.

**Simulated annealing**

SA originates from the thermodynamic process of freezing liquids that causes crystallization. At the time that a pure crystal is formed the atoms have minimum energy and nature is able to find this minimum state when the system is cooled slowly (Metropolos et al. 1953). The SA works by generating samples equally distributed in the model space. The algorithm will stop either because the objective function reaches a predetermined value or because an iteration limit was reached. The convergence of SA is very slow compared to the gradient methods but it is better at finding the global minima of the objective function rather than local minima. One recent application of SA for seismic history matching can be found in Jin et al. (2009).

**Genetic algorithm**

Holland in 1970 developed this algorithm. The principle of GA is based on reproduction of the biological principles of evolution. An initial ensemble of models is generated randomly in the parameter space. Then a number of models are chosen as parents that are paired up for breeding. The parametric element is randomly combined to generate new models by a cross-over process. To avoid trapping in local minima the 'Mutation' (random perturbation of one of the parameter) process is used in some cases. This process is repeated by adding new models to the population and continuing the procedure. Similar to SA, this algorithm is also slower than gradient based method to

converge to the local minima but it is better for finding global minima of the objective function.

There are a lot of applications of stochastic algorithms and, for example, Quenes et al. in 1993 used simulated annealing for history matching of a gas reservoir using the well pressure as observation. Portellaand and Paris (1999) used simulated annealing with the pilot point method for history matching of a 3D synthetic model. Some other examples for SA are in Huang (2001), Fagervik et al. (2001), Lygren et al. (2003) and Jin et al. (2007). GA also used in different studies as optimization algorithm such as in Top–Down Reservoir Modelling proposed by BP (Williams et al. 2004; Walker et al. 2006). In 2002 Christie et al. (2002) used NA for history matching and uncertainty analysis of the 10'th SPE comparative solution project. NA also has been used as an optimization algorithm for a number of seismic and production history matching studies (Stephen et al. 2006, Kazemi and Stephen 2009, Kazemi et al. 2010)

Figure 1.8 shows the balance between exploration (how wide we explore in the parameter space) and exploitation (how much we use the information from previous models) strength of various optimization algorithms. The deterministic algorithms are very strong in exploitation and they try to converge to the minimum of the misfit very fast. On the other hand, the stochastic algorithms are less exploitative but they are stronger at exploring the parameter space. Exploration is usually a very important issue for history matching of the reservoir because multiple various models get similar result which ultimately defines various production scenarios in the reservoir. There should be a broad search in the reasonable range of various parameters in order to choose the most optimum combination of parameters that gives us a reliable reservoir model.

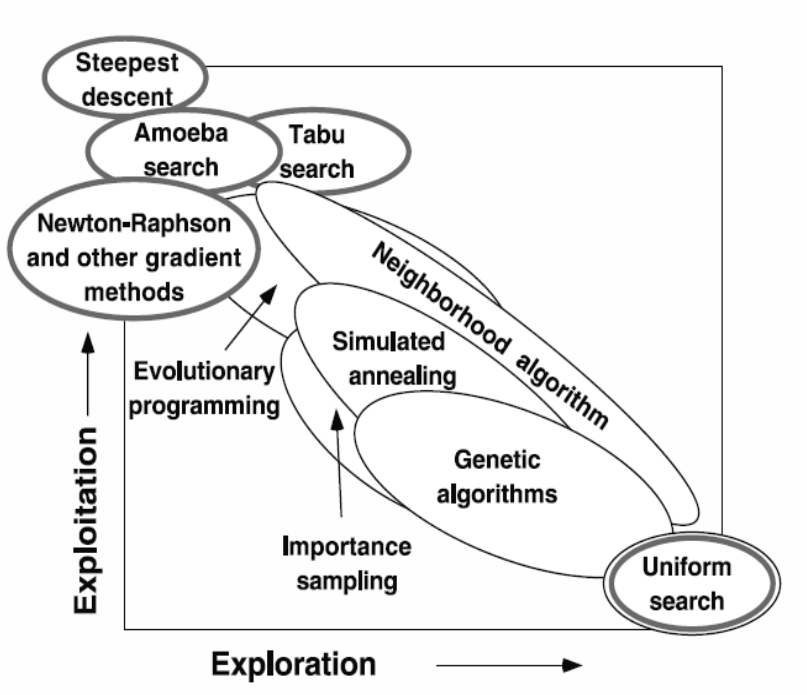


*Figure 1.8: Exploration versus exploitation strength of optimization algorithms (Sambridge and Mosegaard 2002).*

The third type of inversion algorithm is probabilistic methods. Two famous algorithms in this category are Monte Carlo and Ensemble Kalman Filter algorithms.

**Monte Carlo (MC)**

MC is a purely probabilistic framework for solving inverse problems. MC methods consist of two parts, the sampling method and the optimization method (Mosegaard and Sambridge 2002). In the sampling part, MC produces pseudo-random numbers which is a series of numbers that appears random if tested with any reasonable statistical test. The random numbers will be generated from a specific probability distribution. Hundreds or thousands of possible outcomes of models will be generated then. Usually the optimization part of MC is based on random walks. By this it means that the algorithm will move around a marker in multi-dimensional space in order to find the lower misfit.

**Ensemble Kalman Filter (EnKF)**

Evensen in 1994 originally introduced the Ensemble Kalman Filter (EnKF) which is a Monte Carlo sequential Bayesian inversion algorithm. This algorithm provides an approximate solution for the combined parameters and state-estimation problem. The output of EnKF is an approximation of posterior probability density for the model input

parameter such as porosity and permeability, state variables (pressure and saturation) and other input data (well production history). The method works by conditioning the problem to measured dynamic data which is sequentially assimilated. The EnKF does not require the adjoint equations and the programming is independent of reservoir simulators. The main value of this algorithm is sequential updating of the reservoir simulation model. This algorithm starts with a generation of an ensemble of initial models (typically 40-100) that are consistent with prior information of the initial state of the reservoir and its probability distributions. A forward reservoir simulation is performed for each model up to the time of the next period of observation of dynamic data. Then, in the data assimilation process the models are updated by correcting the variables describing the model in order to honour the observation. Property distributions are updated via Bayes theorem and these are sampled using the so called Kalman gain to modify the flow variables (such as permeability, net:gross, etc) but also state variables (such as saturation and pressure). This process is then continued for the next period of history.

This algorithm is more suitable for the cases with a small number of observed data which is not the case where time-lapse seismic data are included in history matching problems (Aanonsen et al. 2009). In these cases it would be difficult to update reservoir variables in order to honour seismic data in all grid cells. On the other hand in time-lapse studies we are dealing with some observed data that are generated based on the state of the reservoir in two different time steps. In the case that there is a weak match between prediction and observed data, the problem could be because of the state of the reservoir at the current time or from the time of first survey. When using the EnKF algorithm, it is not straightforward to go back in time in order to improve the reservoir model in the time of earlier seismic surveys (so called Kalman smoothing).

**Evolutionary Algorithms**

Another type of optimization algorithm is based on Evolutionary Algorithms (Back 1996, Goldberg 1989). In artificial intelligence, Evolutionary Algorithm (EA) is the umbrella term for all computational models that are inspired by evolutionary mechanisms: reproduction, mutation, recombination, and selection. Although the particular representations can heavily differ from each other they all share basic principles. The most popular type of EA is Genetic Algorithm. However there are other types of algorithms such as Genetic programming, Evolutionary programming,

Evolution strategy and Neuroevolution which all categorize in EA types algorithms. Every algorithm organizes a population of individuals. These algorithms only use the objective function value to determine new search steps and they do not require any gradient information from the optimization problem. Therefore they can be used in cases where gradient information is not available or when other algorithms fail because of significant non-linearity or discontinuities in the search space. The main concept in Evolutionary Algorithms is the use of ensembles in generating parent-to-child sequences. This ensemble can lead to parallel computing in optimization procedure.

**Tunnelling method**

This method will be categorized as a global optimization technique (Levy and Montalvo 1985). Tunnelling is an essentially deterministic method that makes use of gradient information. The method is seeks to find a series of minima with a sequentially decreasing objective value and the lowest value in the series will be the global minimum. The attraction of this method is that the low computational cost.

The basic idea of the method is to tunnel from one valley of the objective function to another in order to find a sequence of local minima with decreasing function values. An important feature of this algorithm is that it can ignore all the local minima with larger objective function value than the ones already found. This feature makes this algorithm fast and efficient. Starting from an initial point this method has two phases of local minimization and tunnelling that are repeated alternately until convergence is achieved. In the minimization phase any algorithm designed to solve local optimization problems can be used. Once the local minimum has been found, the tunnelling phase uses gradient-based methods. A pole is placed at the minima and tunnelling begins from a point in the neighbourhood.

## 1.4 History of using time-lapse seismic data for reservoir characterization

In this study we describe an automatic Production and Seismic History Matching (PSHM) method and apply that on a producing field. Figure 1.9 shows schematically the various parts of the method that were used and here we discus each part of this loop very briefly. Later on, in chapter 2, we will discuss the various parts in more detail.

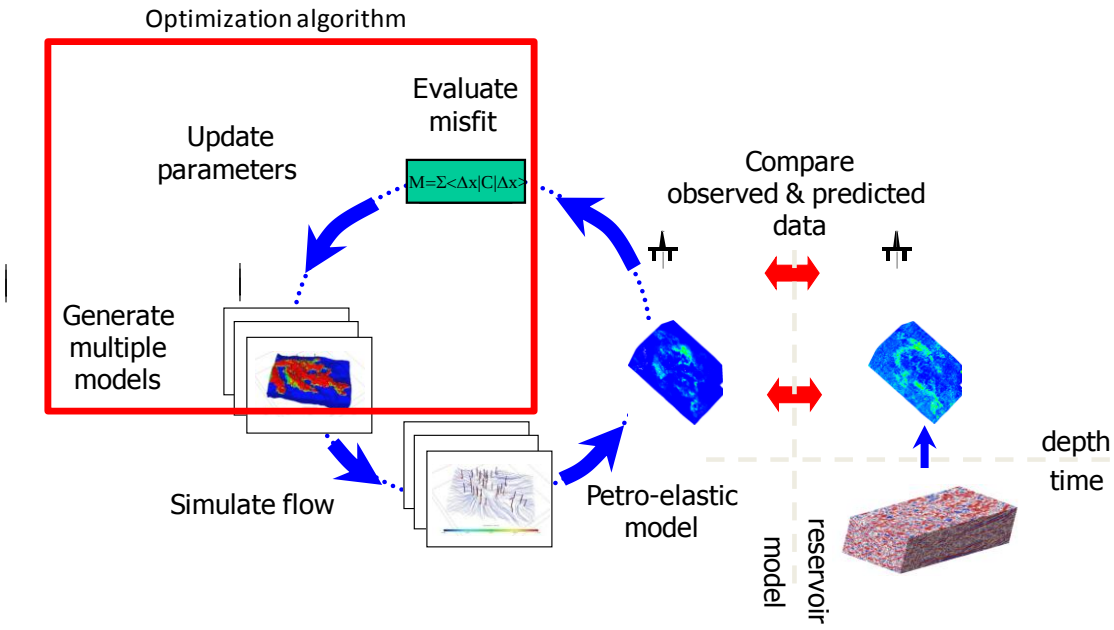


*Figure 1.9: Seismic and production history matching workflow (Stephen 2006) as used in this work (the red box highlight the role of optimization algorithm in this workflow).*

There are a lot of examples for the application of time-lapse seismic data for reservoir characterization and history matching. As some examples, a range of various reservoir properties and flow condition have been examined by using time-lapse seismic data as a constraint for reservoir updating (Huang et al. 1997; Huang et al. 1998; Guerillot and Pianelo 2000; Guerin et al. 2000; Arenas et al. b 2001; Hatchel et al. 2002; Vasco et al. 2003; Portella and Emerick 2005; Dong and Oliver 2005; Dadashpour et al. 2007), monitoring reservoir production processes such as gas out of solution, water injection or water sweep from the aquifer (Parr et al. 2000; O' Donovan et al. 2000; Lygren et al. 2002), identifying reservoir continuity and segmentation (O' Donovan et al. 2000; Waggoner et al. 2002), fault transmissibility estimation (Fagervik et al. (a) 2001; Fagervik et al. (b) 2001; Lygren et al. 2003), managing properly the location of infill wells (Clifford et al. 2003; Huang and Lin 2006).

Because of the important challenges we may face in reservoirs, we categorize the history of application of 4D seismic into real cases and application to synthetic reservoirs. In the synthetic studies it was possible to investigate the effect of 4D seismic signal/noise ratio in the final history matching result and generally know the degree of success. Additionally the size of simulation model was small in all cases making it easier to parameterize the reservoir.

Application of 4D seismic in real field has been applied in two main regions, Gulf of Mexico and the North Sea. In 1997 Huang et al. (1997) presented a new approach to reservoir characterization by integrating time-lapse seismic and production data. They used simulated annealing as an optimization tool to automatically reduce the misfit. The observed seismic that they used was acoustic impedance. They used the relation between porosity and permeability as a parameterization constraint. They tested various combinations of production and seismic data and they found that by using both data with similar weighting in the misfit function a better history matching result was obtained.

The above example covers many challenges that we may encounter during integration of 4D seismic data in history matching. Some questions remain regarding how we can retain the geological features (such as channel, shale bodies, shale barriers) by identifying a more reliable parameterisation (more information for development of parameterization techniques is in Section 1.3.2).

There are several studies where people tried to honour the geological information of the reservoir by implementation of some parameterisation method such as Gradzone (Gosselin et al. 2001; Aanonsen et al. 2003; Gosselin et al. 2003), pilot points (Arenas et al. a 2001), gradual deformation (Kretz et al. 2002; Mezghani et al. 2004; Roggero et al. 2007) and wavelet transforms (Jin et al. 2007).

The History-Matching Using Time-lapse Seismic (HUTS) project (Gosselin et al. 2003; Aanonsen et al. 2003), proposed a quantitative use of 4D data in history matching. The HUTS approach used an iterative, gradient-based optimisation method to adjust the initial reservoir parameters. In various field studies such as Gosselin et al. (2001 and 2003), they found that the Gradzone analysis technique can easily be used when dealing with production data only but more experience is needed when using 4D seismic data. However, in their studies, the parameter selection was based on the objective function sensitivity and, therefore, the parameters that needed to be updated were different for production data compared to 4D seismic data. They concluded that this technique would be less easy to apply for real cases (including 4D) and more research was needed in order to find a better parameterization technique. Arenas (2001) found that when pilot points were located in the heterogeneities areas there was a better chance to

capture them by using automatic history matching algorithm. Application of the Gradual Deformation Method (GDM) to updating the facies realization of the Girassol field during the history matching process was presented by Roggero et al. (2007). Another application for GDM was by Mezghani et al. (2004) that successfully updated the initial reservoir porosity by considering a porosity/permeability correlation in order to compute the field permeability.

One of the important questions in seismic history matching is the suitable seismic domain for comparing real and synthetic data (Figure 1.4). Some of the researchers chose the seismic domain (Huang et al. 1997; Huang et al. 1999; Parr et al. 2000; Aggio and Burns 2001; Dadashpour et al. 2007), seismic attribute domain (Fagervik et al. a 2001; Fagervik et al. b 2001; Lygren et al. 2002; Lygren et al. 2003) some people chose the seismic impedance domain (Bentley 1998; Guerillot and Pianelo 2000; Guerin et al. 2000; Gosselin et al. 2001; Waggoner et al. 2002; Gosselin et al. 2003; Mezghani et al. 2004; Portella and Emerick 2005; Dong and Oliver 2005; Emerick et al. 2007; Skjervheim et al. 2007; Roggero et al. 2007) or the saturation and pressure domain to compare seismic data (De Souza et al. 2010).

However there are studies where pseudo impedance seismic data were integrated into the history matching loop such as Stephen et al. 2005; Stephen 2006; Stephen and Macbeth 2006; Stephen et al. 2007 and Stephen and Macbeth 2008. In all of the above studies (except Stephen et al. 2007 who derived pseudo impedance from elastic impedance data of Nelson field), coloured inversion was used to get pseudo impedance for 4D seismic history matching of Schiehallion field. More recently some work published on Nelson field where phase shifted amplitude (pseudo impedance) data integrated into seismic history matching loop (Kazemi et al. 2010; Kazemi et al. 2011, in press, and Kazemi and Stephen 2011, in press). In all of these studies, pseudo impedance seismic data was compared with synthetic impedance data, therefore these studies also categorized in seismic impedance domain.

These domain studies were very challenging in the cases that real observed time-lapse seismic data is available. On the other hand for synthetic cases the only differences between domains are the equation that will be used to calculate seismic attribute, seismic impedance or saturation in simulation cells. The main reason that some researchers preferred the impedance domain because it is reasonably straightforward for

calculation of impedance and this process is not too time consuming. However the seismic impedance domain has been chosen for the study in this thesis.

## 1.5 Automatic Production and Seismic History Matching (PSHM) workflow in this thesis

The term "automatic history matching" comes from adding an optimization tool to the history matching loop in order to automatically guide the search in the parameter space and choose the best combination of variables to find a better representation of the reservoir.

It is becoming more and more common to use assisted or automatic history matching methods to find various combinations of reservoir simulation models that agree with available production and time-lapse seismic data. Even with the aid of an optimization tool in reservoir history matching still there is a major challenge that models with a large number of cells contain millions of unknown parameters and selecting the correct values can be difficult. In practice not all are important but finding which parts of the reservoir require updating and how to parameterise the variables can be difficult. However, integrating time-lapse seismic data appropriately with production data is also another big challenge particularly for automatic methods.

We summarize the history matching approach as follows to put this thesis in a general context. The history matching method used in this thesis combines assisted and automatic history matching based on control by a global optimization algorithm. In our workflow we start with a base model supplied by the operator of the field and we distribute new models around this model. The operator's model was made with standard geo-modelling tools. At the beginning of the loop we need to generate some initial models that are various representations of the reservoir in order to search in the parameter space. These were generated by using the pilot point method by randomly selecting values for different parameters and then Kriging was used for interpolation of parameters between the pilot points. More information about Kriging is given in Appendix A1 and for the specific field in this study some information about pilot points and Kriging can be found in Chapter 4, Section 4.2 and Table 4.1. To update each model, suitable locations of the reservoir have been chosen in order to apply changes to the properties. We run each model by a streamline simulator (Schlumberger Geoquest

Manual, 2007). Then we use an objective function in order to quantify the differences between predicted production and seismic data, and corresponding observed data, and a global optimization algorithm is used to minimize this function.

In this work some important issues for developing the automatic history matching loop include:

1) Investigating various ways to optimally identify the areas in the reservoir where we want to update the parameters;

2) Studying the proper combination of the parameters in order to reduce the dimension of the problem efficiently;

3) Normalizing observed time-lapse seismic data (with associated uncertainty) to be prepared for using in history matching;

4) Filtering of time-lapse seismic data with repeatability maps;

5) Updating the model based on improving the properties in geological environments.

## 1.6 Content of thesis

The work in this thesis is divided into following:

Appropriate choice of regions to update in the reservoir, normalization time-lapse seismic data for preparation for integration with production data, calibration of time-lapse with a repeatability map by using the combination of the different parts of our automatic history matching loop and applying these to Nelson. The thesis is divided into the following chapters.

Chapter 2 presents the workflow that we used in this study in order to automatically update reservoir parameters during history matching. We explain and discuss in detail different parts of the work flow and we show the techniques used. In this chapter we describe the pilot point method and Kriging, streamline simulator, petro-elastic model, misfit function and neighbourhood algorithm in details.

Chapter 3 describes the Nelson field; its geology and geophysics, reservoir, production history and 4D seismic data. Also we discuss the petro-elastic model used for the Nelson field.

Chapter 4 describes the application of history matching to Nelson. This chapter describes how streamlines were used to guide the choice region to be updated in the reservoir and compare various schemes.

In Chapter 5 we describe how we analysed 4D seismic data in Nelson and shows how we used that in the history matching work flow. In this chapter we show the development of various methods of normalizing observed 4D seismic data demonstrating difficulties that arose. We also used the repeatability concept in order to initiate observed time-lapse seismic data in order to eliminate the data in seismic bins with low repeatability.

In Chapter 6 we describe how we used the normalized 4D seismic data to help history matching in Nelson. We compare the result with previous results in Chapter 4 where we only use production data.

In Chapter 7 we show how we performed various updating of reservoir with help of geological features. We can see various geological elements such as Channel Axis, Interchannel in the reservoir and how updating of reservoir properties within these geological elements helped us to better update the reservoir model. In this chapter we use both production and 4D seismic data in the history matching loop and we compare the result. We also compared the result with the previous study (Chapter 4) where we used the streamline guide to choose the regions to be updated in the reservoir in addition to pilot point and Kriging as parameterization for history matching.

Finally we discuss conclusions and recommendation of future work at the end of this study in Chapter 8.

# Chapter 2: AUTOMATIC HISTORY MATCHING WORKFLOW

**Overview:**

The aim of this chapter is to describe the technical methods and concepts that have been used in this work through the history matching loop (Figure 1.9). Chapter 1 introduced this workflow but now we go into more details.

The structure of this chapter is such that we:

- Introduce the pilot point method and Kriging which is the first part of the loop to generate different models.
- Describe the streamline simulation concept as this is the method we used to simulate each model.
- Explain the petro-elastic model which converted reservoir properties to equivalent synthetic 4D data.
- Present the misfit function which was used to compare observation and production of each model;
- Summarize the Neighbourhood algorithm which we used as an optimization tool to find the best reservoir model that better predicted history of the well and 4D data.

In this chapter we first introduced different parts of automatic history matching loop in Section 2.1 and then from Section 2.2 afterwards we specifically focused on different tools that we used in this thesis.

## 2.1 Various elements of the automatic history matching workflow

In this section there is a short introduction of various elements of the history matching loop that we used in this study. This history matching loop consists of several components and a part of the loop acts under control of an optimization method (red box in Figure 1.9). There are various methods for each part of the loop as seen in the literature.

### *2.1.1 Generation of multiple models*

In the PSHM method used here, we sought to parameterize the model with various combinations of parameters in the reservoir to generate multiple models. At the

beginning, the general questions in any history matching study is what variables do we need to update, where is the best place to update those variables and how can we update them.

There are various methods for parameterization as shown in Figure 2.1 and we categorize them in two options based on small and large number of unknowns.

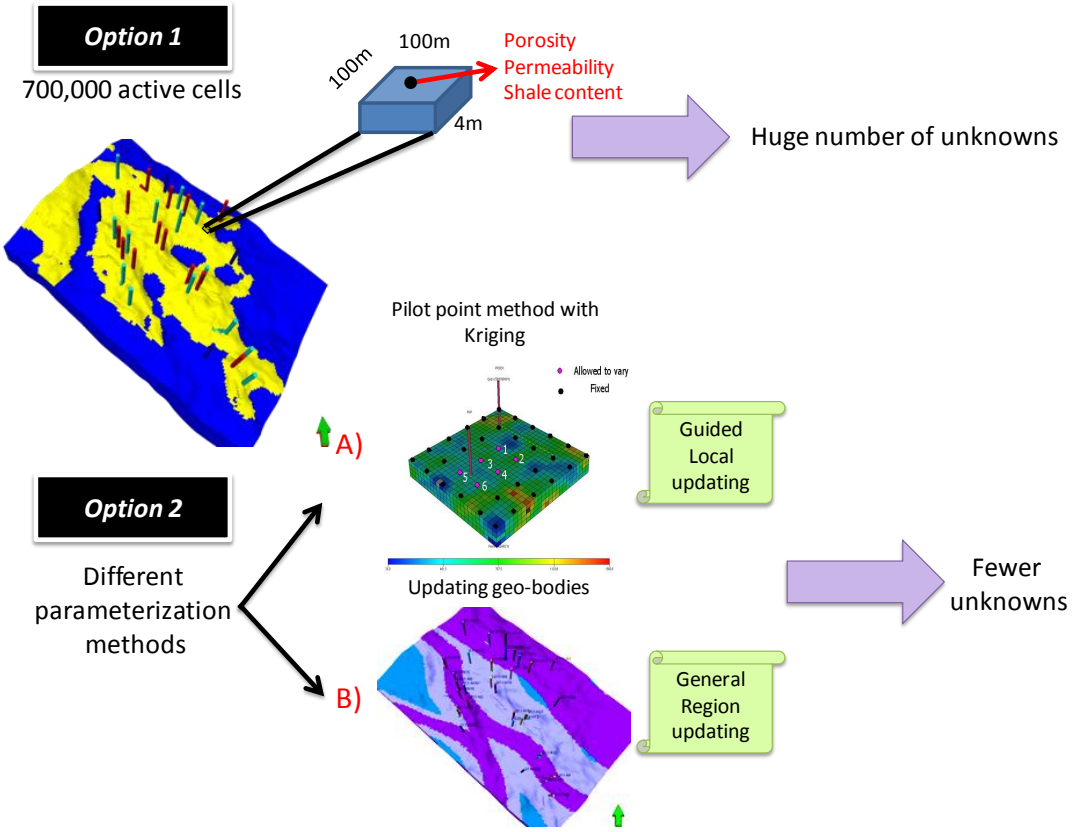


*Figure 2.1: Various methods that can be used for parameterization of a reservoir model through history matching.*

*Option 1: Grid block method*

In this method (Option 1 in Figure 2.1) all grid block values have been considered as independent parameters. In this approach, no preconceived idea about the geology of the reservoir is considered during history matching. The main problems with this approach are the large number of unknowns and the lack of spatial continuity in the reservoir model (Floris et al. 2001). A recent application of this method can be found in a synthetic study by Dadashpour et al. (2007). However this method is not suitable for real cases in oil industry.

*Option 2.A: Pilot points*

By geostatistical methods the dimensionality of the parameter space will be reduced such that the model depends on global statistic describing spatial distributions of the parameters and how they are inter-related. Pilot point (Option 2, case A) is a geostatistical method that is used to parameterize the parameter space spatially in the reservoir (De Marsily et al. 1984).

*Option 2.B: Regions*

This method (Option 2, case B) is a way to reduce the number of unknowns by using homogeneous regions of modification. Regions can be based on geological layers or genetic units within layers or they can be used to characterize drainage areas around the wells. With regions, the unknown parameters for history matching will be reduced but the assumption of homogeneity of update within the geo-body type may not be justified and can lead to abrupt changes across the boundaries (Floris et al. 2001). Floris et al. (2001) found that by considering a homogenous region as a parameterization method, satisfactory history matching results in the PUNQ field were not found. A large spread of production data was observed in the forecasting period. They also tried the pilot point method, which gave more reasonable results compared to the previous study.

Another parameterization method is called Global Parameters (Floris et al. 2001). These parameters are those that cannot be linked to a particular spatial location. Stochastic parameters such as mean values, standard deviation, correlation lengths or geobody parameters such as channel width and length are examples of global parameters.

In this study the pilot point method with Kriging was used for parameterization of the reservoir as well as a geo-body updating scheme. The former method was very useful for updating reservoir parameters smoothly during history matching. This is more realistic compared to geo-body updating where all changes of parameters will take place in a wide area in the reservoir. Therefore we used Pilot point and Kriging as our parameterization method in Chapter 4 and 6 and finally in Chapter 7 the history matching was performed by using a more geographically global parameterization method.

### *2.1.2 Simulation of flow*

Flow simulation is an important part of the history matching loop. There are various numerical simulation methods and we chose the appropriate one for history matching based on our requirement for speed and accuracy on reservoir field of study. Here we want to introduce briefly the finite difference and streamline method for history matching.

The streamline concept is based on the streamtube idea to solve the pressure and saturation through the tube instead of grid cells (Bratvedt et al. 1996; King and Datta-Gupta 1998). First, the pressure is solved with an implicit numerical method in each cell and then the saturation equation is solved using an explicit method. The pressure equations are solved based on rock properties, current fluid distribution and boundary conditions whereas the rock properties include initial static information such as permeabilities, porosities, net:gross etc that are defined at the centre of grid cells. The boundary conditions can be open wells, aquifer models, pressure boundaries and flux boundaries that can be defined by the user. The pressure is used to compute the streamlines and also to compute a velocity field that is then used to capture the saturation front. The saturation equation is solved on the streamline using front tracking (is similar to Buckley-Leveret equation) as a 1D problem and numerical methods (Frontsim technical description, 2007; Bratvedt et al. 1992; Bratvedt et al. 1993).

With streamline methods a single pressure calculation is made and held constant for a longer time step (e.g. months). By contrast, the finite difference method descretises time and space and moves pressure and saturation forward together in small steps (e.g. hours to a few days). By reducing the number of pressure calculations the streamline method offers a considerable speed up but it may introduce some errors as well. The errors depend on the number of streamlines used in the simulation, number of time steps for recalculation of the pressure equation and gravity segregation in the model. These errors are considerable in the cases where there are three phases in the reservoir. It is also recommended that the targets of the wells are always adjusted as reservoir rate instead of phase rate. The reason is that if the phase rates are changing considerably during the time steps, the streamline simulator might have difficulties to honor a target exactly for the rates. This is something common for the whole IMPES type simulators. Some recent application of streamline for production and seismic history matching can be found in Trani et al. (2009), Kazemi and Stephen (2009) and Kazemi et al. (2010).

Stephen et al. in 2009 investigate the model error issue of using streamline for history matching study.

In this study we carried out history matching on the Nelson field with a reservoir pressure maintained above bubble point that therefore simulation by a streamline simulator is suitable. We will discuss this simulator further in Section 2.3.

### *2.1.3 Petro-elastic model*

A Petro-Elastic Model (PEM) can be used to convert changes in fluid saturations and pressures from the simulation into predicted impedance or other elastic properties for each simulation cell. Figure 2.2 shows, schematically, the role of the PEM in order to generate the synthetic seismic data. A PEM is derived based on some laboratory work on core data, and ultimately it may be tested and calibrated by using petrophysical data from the logs. The output of the petro-elastic model will be elastic properties of the reservoir which will be used to generate the seismic data in the impedance domain or in the amplitude domain. Working in the amplitude domain requires some additional steps such as grid regularisation (refinement of the reservoir model grid in order to be in the same scale as observed seismic data) in order to match the output of PEM in reservoir model scale to seismic scale. The domain of comparison in this thesis is the impedance domain.

The petro-elastic model is usually generated from various empirical equations derived for particular fields and some equations for fluid substitution such as the Gassmann (1951) equation are commonly used. We will discuss more about the PEM equations used in this study in Section 2.4 and Chapter 3, Section 3.6.

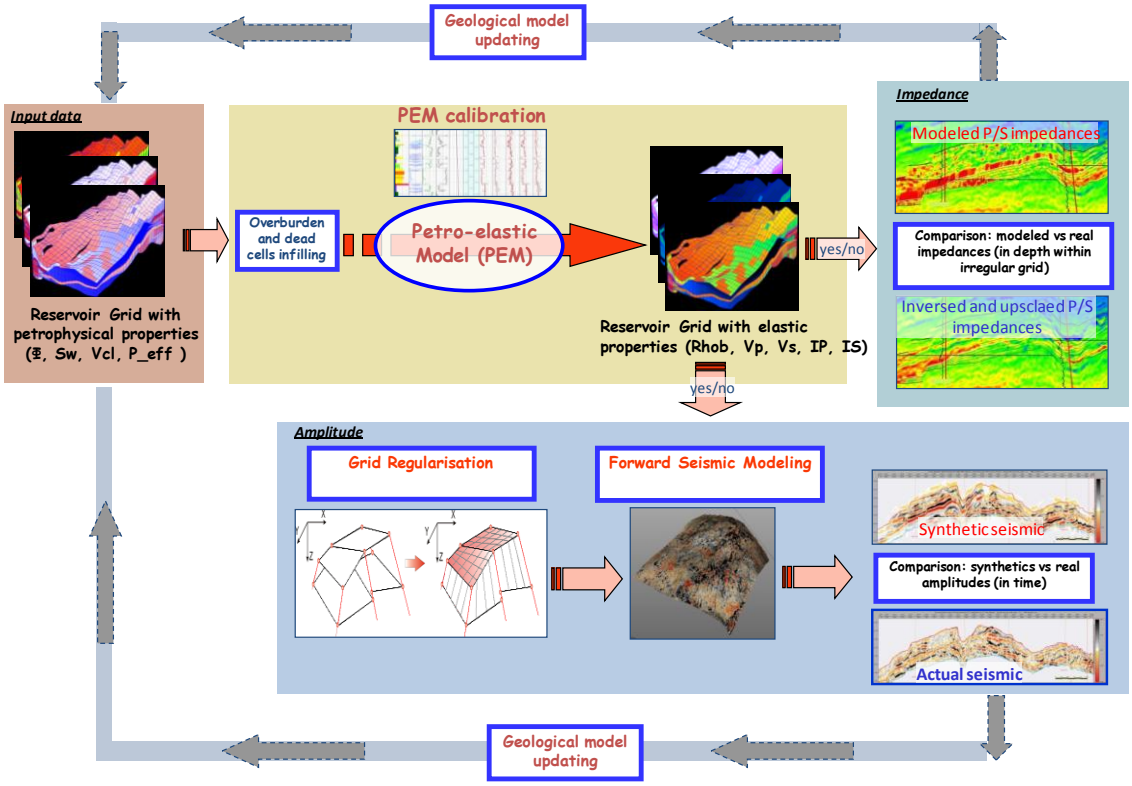


*Figure 2.2: The role of petro-elastic model for generation of synthetic seismic in amplitude versus impedance domain.*

### *2.1.4 Comparison of simulated data with historical data*

In the next stage of PSHM we want to compare well data and/or seismic output with historical observed data. In order to measure the validity of a reservoir model that is conditioned to the available history data, a function must be defined to quantify the mismatch between the simulated response of the reservoir and the history data. This comparison is performed through the objective function which was introduced in Section 1.3.1. The specific objective function for this thesis is introduced in Section 2.6.

### *2.1.5 Optimization algorithms*

The most mathematical component of PSHM loop is the optimization algorithm and its effects on the speed of the history matching process as well as the ability to find a good combination of parameters to obtain a better representation of the field. Previously in Chapter 1, Section 1.3.3 we introduced different type of optimization algorithms. In this thesis the Neighbourhood Algorithm (NA) (Sambridge, 1999) was used because as discussed previously compared to other inversion methods because it is better at searching the parameter space to find to minimum misfit.

## 2.2 Pilot points and Kriging

After choosing the appropriate variables to update at a suitable location in the reservoir, we need to use a method for parameterization. In parameterization the selected variables will be modified in such a way that the geological features and reservoir properties do not change drastically or unrealistically. In this work the pilot point method and Kriging was used for updating the reservoir (De Marsily et al. 1984).

Pilot points are used to directly control where changes are made to properties such as permeability and net:gross. The change at the pilot point becomes the parameter of the inversion scheme. In this work a multiplier vector was used for each variable with specific limits and one specific value is chosen in this range. These changes are interpolated laterally using Kriging. The changes are applied uniformly in the vertical direction within intervals. In order to further reduce the number of unknowns and to spread changes more smoothly, a set of pilot points may be grouped so that changes are applied all in the same way. This approach is often called the master pilot point approach (Roggero 1997). Modifications at the pilot points are initially chosen randomly and a number of new models are generated. Figure 2.3 shows the location of pilot points (in a simple synthetic model) where the parameters will be changed (pink dots) compared to the rest of the reservoir where the reservoir kept unchanged as the base model that we start with (black dots). The decision about the location of pink or black dotes is a real challenge because practically the whole reservoir is uncertain. In this study streamline were used in order to make a reasonable selection (Chapter 4).

A benefit of the pilot point method is that we can change the reservoir smoothly while honouring the geostatistical prior information. The Kriging–based techniques are well known for interpolating reservoir properties within the reservoir and were first developed by Matheron in 1971. There are different kinds of Kriging such as simple, universal, co-Kriging and factorial Kriging. In our work we use the simple Kriging for interpolating properties multipliers between the pilot points. More information about Kriging is presented in Appendix A1.

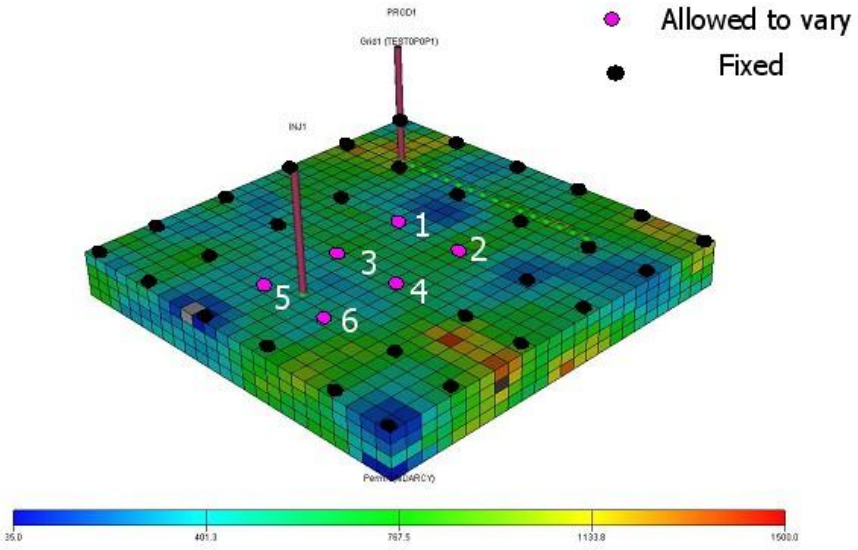


*Figure 2.3: A synthetic models as an example of the location of pilot points where we make change (pink dots) versus black dots where no change is enforced (Stephen 2007).*

## 2.3 Streamline simulation

Large reservoirs with a hundred thousand grid blocks and a complex production activity can be easily simulated with a streamline approach very quickly and with a reasonable accuracy. Historically (Schlumberger Geoquest Manual, 2007) there have been on important criteria that, for maximising the benefit of streamline simulation there should be no gas in the model so that the model is two phase flow. More recently software has been able to include gas phase in the simulation model (Schlumberger Geoquest Manual, 2009-1). On the other hand another criteria for using streamline is that, the pressure cannot change drastically between the time steps because during the fluid flow calculations, pressure is constant in each time steps. Large and rapid variation of pressure therefore makes a big error in calculations. More information about streamline simulation is in Appendix A2. For this thesis the variation of pressure in the Nelson field is negligible during the production period as shown in Figure 3.19 (and Appendix B, Figure B.8) therefore this field is suitable for streamline simulation based on the criteria mentioned above.

The number of streamlines that are needed to capture the fluid flow precisely in the reservoir is a function of the number of grid cells, the number of wells and the magnitude of flow. In Frontsim (Schlumberger Frontsim simulation, 2007) simulations

(which we use in our work) the default for this number is approximately 10% of the number of active cells plus the number of active wells and there is an option in the simulator in order to reduce the number of streamlines for speeding up the simulation, referred as StreamLine Density factor (SLD). We can also control the number of time steps the simulator needs to recalculate the pressure in the reservoir which is equal to the report steps by default. Appendix B describes the impact of adjusting SLD and time steps for the Nelson field.

### 2.4 Synthetic 4D seismic data generation

The concept for generation of synthetic 4D seismic data is based on a Petro-Elastic Model (PEM). Petro-elastic models are widely used in the geosciences for different reasons: 1) modelling of the logs of elastic properties (velocities, impedances) to provide different fluid scenarios; 2) quantitative lithoseismic interpretation and supervised seismic facies classifications; 3) 3D and 4D seismic history matching loops. In Section 1.4 there are some references of application of PEM for 4D seismic history matching purposes.

The objective of a petro-elastic model is to set up mathematical equations which link the petrophysical parameters of a rock, such as porosity, water saturation, effective pressure and shale volume to its elastic properties such as P impedance , S impedance and Poisson's ratio.

A lot of variables can have influence on the elastic behaviour of the rock such as effective pressure, temperature, diagenesis of the rock, porosity, size and shape of the grains, clay content, etc. Many of them could be known at wells but it is almost impossible to obtain all of those properties in a 3D reservoir. Usually the PEM represents a combination of equations and different parameters consisting of two parts: one representing the shaly part of the reservoir and the other one representing the sandy part.

The acoustic impedance for compressional and shear waves are defined as:

$$I_P = \rho V_P \tag{2.1}$$

$$I_s = \rho V_s \tag{2.2}$$

Where $\rho$ is the density of representative volume and was defined in Eq 3.3 in Chapter 3. The effective modulus can be used to determine the shear and compressional velocities using the following equations:

$$V_s = \sqrt{\frac{\mu_d}{\rho}} \tag{2.3}$$

$$V_p = \sqrt{\frac{(K+\frac{4}{3}\mu_d)}{\rho}} \tag{2.4}$$

Where $V_s$ and $V_p$ are shear and compressional velocities respectively. The observed seismic data used in this study was based on near angle stacking therefore data provided by company was equivalent to compressional acoustic impedance ($I_s$ was not available). Therefore, we only used the synthetic compressional acoustic impedance to compare to observed data which is defined with Eq 2.1 for a simulation cell.

Finally the Gassmann fluid substitution has been used to calculate the bulk modulus for the saturated frame:

$$K = K_d + \frac{(1-\frac{K_d}{K_m})^2}{\frac{\phi}{K_f}+\frac{(1-\phi)}{K_m}-\frac{K_d}{K_m^2}} \tag{2.5}$$

Where $K_f$ is the bulk modulus of the oil water mixture and is calculated based on the saturation weighted harmonic average of the individual phase bulk modulus:

$$\frac{1}{K_f} = \frac{S_w}{K_w} + \frac{S_o}{K_o} + \frac{S_g}{K_g} \tag{2.6}$$

There are various empirical formulas for calculation of dry bulk and shear modulus and for the Nelson field we used equation introduced in Chapter 3, Section 3.6.3. However there is contact theory which is used to calculate the effective elastic properties of

unconsolidated sediments or cemented sediments. Here, rocks are assumed to be collections of separate grains. Hertz-Mindlin (Mindlin 1949) theory used for the majority of contact models. The bulk ($K_d$) and shear ($\mu_d$) modulus of dry unconsolidated sand mixture can be defined with:

$$K_d = \left[\frac{\varphi/\varphi_c}{K_{HM}+4\mu_{HM}/3} + \frac{1-\varphi/\varphi_c}{K_s+4\mu_{HM}/3}\right]^{-1} - \frac{4}{3}\mu_{HM} \tag{2.7}$$

$$\mu_d = \left[\frac{\varphi/\varphi_c}{\mu_{HM}+z} + \frac{1-\varphi/\varphi_c}{\mu_{HM}+z}\right]^{-1} - z \tag{2.8}$$

Where:

$$K_{HM} = \left[\frac{n^2(1-\varphi_c)^2 {G_s}^2}{18\pi(1-v)^2} P_{eff}\right]^{\frac{1}{3}} \tag{2.9}$$

$$\mu_{HM} = \frac{5-4v}{5(2-v)}\left[\frac{3n^2(1-\varphi_c)^2 {G_s}^2}{2\pi^2(1-v)^2} P_{eff}\right]^{\frac{1}{3}} \tag{2.10}$$

$$z = \frac{\mu_{HM}}{6}\left(\frac{9K_{HM}+8\mu_{HM}}{K_{HM}+2\mu_{HM}}\right) \tag{2.11}$$

In these equations, $\varphi_c$ is critical porosity, $\varphi$ is porosity, $K_{HM}$ and $\mu_{HM}$ are dry rock bulk and shear modulus at critical porosity, $P_{eff}$ is the effective pressure, $G_s$ and $v$ are shear modulus and Poisson's ratio of solid phase and $n$ is the coordination number (the average number of contacts per grain).

However, there are potential uncertainties in this method based on the basic assumptions considered in this model. For example in this method grains are modelled as identical spheres with a random packing. Several other assumptions are made within this model. First, in solving for the normal and tangential stiffnesses, Mindlin (1949) assumes that the compressional force is applied, followed by a subsequent tangential force. Again, for simplicity, Mindlin (1949) assumes that there is no slip along the contact surface between the grains. For the sake of estimating the effective bulk moduli error is negligible. Direct measurements from laboratory data avoid any errors from

these assumptions and so we prefer to use more empirical relationships where necessary.

### *2.4.1 Effective p-Impedance for the interval*

The calculated p-wave impedance is on a scale of the reservoir simulation model which is about 75m x 75m x 4m. We therefore need to implement vertical upscaling and horizontal downscaling so that impedance predictions represent the same volumes as the observed seismic data which is usually acquired in 12.5m x 12.5m x 25m bins.

Backus averaging (Backus 1962) is used to calculate the average value of p-impedance for a column of simulation cells. This approach is valid (MacBeth 1995) for reservoir beds that are less than one tenth of the seismic wavelength thick and reservoirs of around one quarter seismic wavelength thick (a typical wavelength is 50 to 100m) or greater.

$$I_{pAve} = \sqrt{\langle \rho \rangle \langle \frac{1}{M} \rangle^{-1}} \tag{2.12}$$

$$\frac{1}{M} = \frac{(1-V_{sh})}{M^{sand}} + \frac{V_{sh}}{M^{sh}} \tag{2.13}$$

$$M^{sand} = K + \frac{4}{3}\mu_d \tag{2.14}$$

$$M^{sh} = K_d + \frac{4}{3}\mu_d \tag{2.15}$$

Where $\rho$ is the arithmetic average of effective bulk density of the sand-shale fluid system over the reservoir interval, $\langle\ \rangle$ indicates a vertical volume weighted average over the reservoir interval. $M$, $M^{sand}$ and $M^{sh}$ are p-wave modulus for sand-shale mixture, sand and shale respectively. From the lab report the value of $K_d$ and $\mu_d$ for shale were considered as 11.7 and 2.51 GPa respectively (Boyd-Gorst and Garnham 1999).

### *2.4.2 Lateral downscaling (interpolation)*

In the objective function we need to have the same resolution for synthetic and observed seismic impedance data. We categorized all possibilities as follows:

1. We may choose to build the simulation model in the seismic scale and compare real and synthetic seismic impedance in this scale. The drawback for this option is that first of all the geologists do not usually build their models based on the seismic grid and scale and secondly even if we have a model in this scale it would be very slow in terms of flow simulation. We are not aware of this being done in practice.
2. Simulation on the geo-model scale is an option. In this case the simulation would still be very slow despite some speed up compared to a seismic scale geo-model. On the other hand there is a high degree of uncertainty introduced when mapping synthetic seismic from the geo-model scale to seismic scale for misfit calculation. We are not aware of this being done in practice.
3. Simulating in the simulation scale and downscaling properties to seismic impedance scale can be considered. In this case various properties can be downscaled and also various methods can be used for downscaling. Therefore it is possible to sub-categorize this option as:

   3.1 Downscaling saturation and pressure to the seismic impedance scale. The problem here is that there is not a straight forward way for downscaling of these properties. This is a simulator based inversion problem which has been tried (Castro 2007). The advantage is that fine scale modelling of the static properties is carried out.

   3.2 Interpolation of saturation and pressure in order to generate maps from simulation scale to seismic impedance scale. The fluid properties are not properly conditioned to the flow as well as the previous approach but in some cases may be no less accurate.

   3.3 Downscaling of synthetic impedance data to scale of observed data. This is what we do as described below. The model ignores the fine scale altogether but avoids introduction of model errors also. Also, if predictions are made on the seismic scale (e.g. Roggero et al. 2007), fine scale updating and upscaling is required which can further introduce uncertainties.

An option for downscaling of synthetic seismic is to use the Kriging method. However this is complex because by Kriging we need to define some relationships between the unknown locations and some known data nearby. In reality we do not know these relationships. On the other hand it may be hard to solve the covariance matrix we have in the Kriging system for this case.

In this work, the fine scale reservoir model was not available for the study. The gridding system for observed data is obtained as a set of points defined by the acquisition inline and crossline coordinates. In Figure 2.4 we can see the location of the centre of the bins compared to the centre of simulation cells schematically. The simulation grid is parallel to the seismic inline discretized to simulation cells with a dimension of 75m x 75m whereas for seismic bins the dimension is 12.5m x 12.5m.

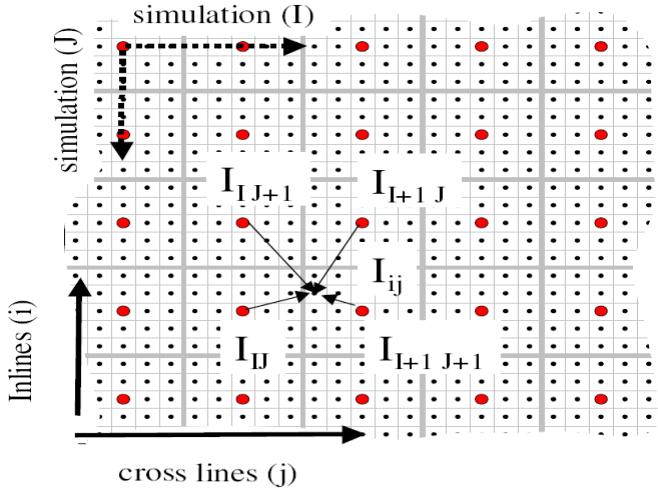


*Figure 2.4: Comparison of the coarse and fine grids used in our study. Thick grey lines indicate the coarse cells while large circles show the location at which the impedances are predicted. Equation 2.16 was used to interpolate the impedances to obtain values at the small black circles, i.e. where the observed seismic would normally be measured. Broken and solid arrows indicate the principal directions of the coarse (simulation) and fine (seismic) grids respectively (Stephen 2007).*

The interpolated impedance is obtained from:

$$I_{ij}^{interp} = \frac{\sum_{IJ} w_{ijIJ} I_{IJ}}{\sum_{IJ} w_{ijIJ}} \tag{2.16}$$

where

$$w_{ijIJ} = (\exp(-\beta|\underline{r}_{IJ} - \underline{r}_{ij}|) \quad (2.17)$$

Where indices $I$ and $J$ indicate grid cells in simulation model and $i$ and $j$ indicate seismic bins, $\underline{r}$ is position vector for the centre of cells. It was found previously (Stephen et al. 2006) that $\beta = 0.05\, m^{-1}$gives the best results, minimising the representivity error.

In contrast to downscaling of synthetic impedance we can also think about upscaling of observed data. Here the issue is that we do not know what to do to upscale at this stage. For flow upscaling, for example, we would look at the fine scale behavior and derive equations that give the same behavior on the coarse scale (i.e. same pressure drop and flow rate for the average and the fine scale permeability). It is not clear what an upscaled trace looks like. "Binning" is where signals from the 12.5 m cube are grouped and we could consider something like using a larger 100 m bins but there are other issues with that. Simple averages are a first approximation but only that. The upscaling issue requires a good knowledge of seismic processing and it is beyond the scope of this thesis.

As an alternative approach it is possible to use seismic inversion methods to get a fine scale representation (i.e. a value per cell) of impedance. This would enable estimation of impedance at a fine scale vertically and is often performed nowadays. The process can be applied before trying to history match but, due to non-uniqueness, it is likely end up with the wrong distribution at that point as we have not included any constraints from flow.

## 2.5 Observed data

Two kinds of observed seismic data were made available; one was near angle elastic impedance and the other was phase shifted amplitude data. The former was used early in the study. The latter was provided more recently and is considered to be of better quality and was used in work presented here. It is worth mentioning that phase shifted amplitude was produced through a pseudo inversion procedure and it considered as pseudo impedance data in the industry (Lancaster and Whitcombe 2000, Hongliu and Backus 2005) (more information in Section 3.7.2). However there is an inconsistency

between the units of measurement of synthetic impedance and pseudo impedance data, which is a relative measure. Therefore, we used normalization which will be described in Chapter 5. This will rescale the data so that they can then be directly differenced. For production data we were provided monthly oil and water volumes of the wells. More information about the data is available in Chapter 3, Sections 3.7 and 3.8.

## 2.6 Objective function

In order to make quantitative comparisons of new reservoir models to the base model, we need to define a misfit function. This misfit function can give us the accuracy of each model by comparing the measured data with the observed data. In this work the objective function was based on the L2 norm formula (Tarantola 1987) which is already defined in Chapter 1 (Section 1.3.1 Eq 1.1 to1.3).

In Eq. 1.1 we assumed that there is a Gaussian distribution of the errors in the observed data and this error is additive to each datum. e.g for seismic data.

$$d_s = d_s{}^{truth} + \varepsilon \tag{2.18}$$

where $\varepsilon$ is data error in observed impedance data ($d_s$).

In this study we assume that the observed data errors are uncorrelated therefore we use a diagonal matrix with variance which is the square root of standard deviation of data error. In this thesis the production data that was used in history matching, such as well oil and water flow rates are estimated for total monthly volume. In this case the uncorrelated assumption for observe data is valid. For seismic data we usually deal with a lot of data because the bin size is small and there are many bins. Therefore it is very important to determine whether or not the data errors are correlated. If they are correlated it is important to include the inverse of the covariance matrix. However, it is not easy to calculate that matrix and including that matrix in the objective function can make a big different in terms of CPU time (Aanonsen et al. 2003; Gosselin et al. 2003). In this study in Chapter 3 (Section 3.7.4) we discussed the data error estimation of 4D seismic in Nelson field. Considering uncorrelated data errors, Eq. 1.1 changes to Eq. 2.19:

$$O_T = \sum \frac{(d_s - s(\theta))^2}{\sigma_s^2} + \sum \frac{(d_p - p(\theta))^2}{\sigma_p^2} \quad (2.19)$$

where $d_s$ is represents acoustic impedance, $\sigma$ is the standard deviation of the observed data error which will be calculated differently for seismic and production data, $d_p$ is the well production data such as oil rate, water rate, etc. In Chapter 3 (Section 3.7.4) we provide more information about the calculation of standard deviation for production and seismic data.

## 2.7 Neighbourhood algorithm

The Neighbourhood Algorithm (NA) (Sambridge 1999) is a derivative-free search engine for finding models with acceptable data fit in a multidimensional parameter space. The benefit of using this algorithm is that we can generate an ensemble of models that preferentially sample the good data-fitting regions of parameter space compared to other algorithms which seek a single optimal model. This behaviour is very useful in reservoir history matching.

Comparing this algorithm with gradient methods we can say that because this method is derivative-free we do not have the problem of calculating the partial derivative of data with respect to model parameters which sometimes has a very limited range of applicability. On the other hand compared to the algorithms in the same class (stochastic methods) such as simulated annealing (Kirkpatrick et al. 1983) or Genetic Algorithms (GA) (Goldberg 1989) this algorithm is powerful in finding the global minima of the problem with a self-adaptive behaviour in searching the parameter space.

One important motivation for using the NA is the idea behind this algorithm to appropriately use information from previous models, for which the forward problem has been solved in order to guide the search for minima of the problem. Other stochastic search methods such as uniform Monte Carlo (MC) (Hammersley and Handscomb 1964) or simulated annealing make no use of previous samples and the GA make use of previous samples but in a complex way. A simple generalized algorithm for searching a parameter space would be:

1- For previous $n_p$ models where the forward problem has been solved we need to construct the approximate misfit surface

2- by using the approximation with a search algorithm we can generate new $n_s$ models

3- add $n_s$ to $n_p$ and go back to (1)

### *2.7.1 Approximating the misfit surface*

In NA after sampling $n_p$ models in the model space and subsequent calculation of the misfit function, the geometrical construct known as Voronoi diagram (Voronoi 1908) is implemented. The Voronoi cell is a unique way of dividing the d-dimensional model space into $n_p$ regions. Each cell is chosen as a nearest neighbour region about one of the previous samples. Figure 2.5 shows a set of Voronoi cells which was calculated by NA for 10, 100 and 1000 irregularly distributed points in a 2D example.

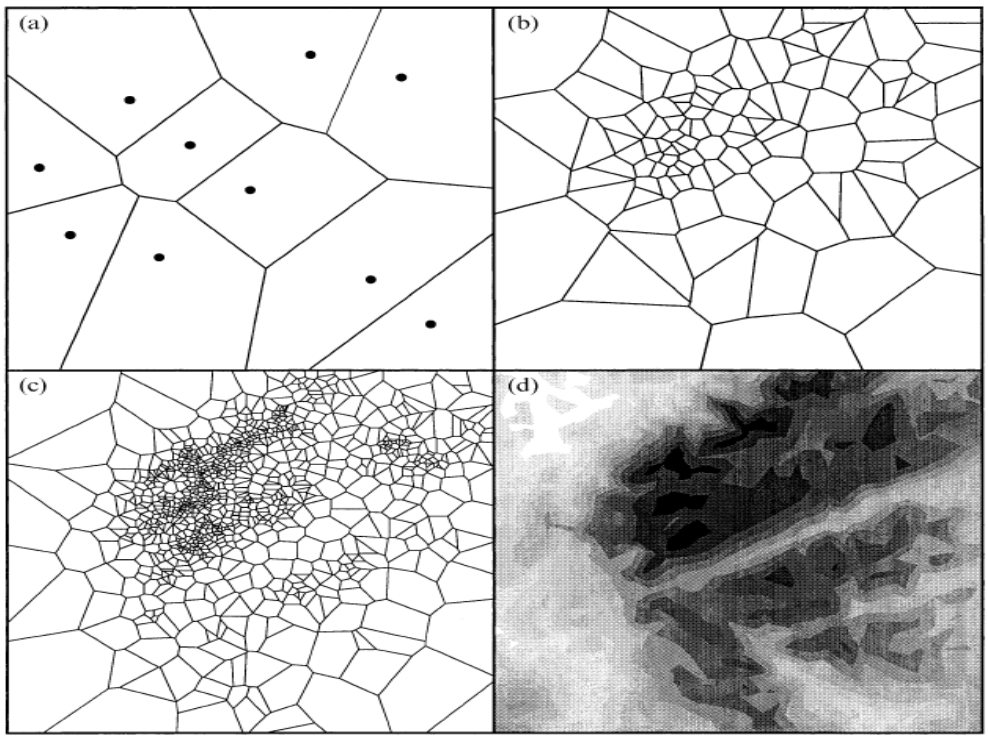


*Figure 2.5: Quasi-uniform random points and Voronoi cells for a) 10 points, b) the Voronoi cells of 100 points generated by the neighbourhood approximation, c) as b but for 1000 points and d) contours of the test objective function (Sambridge 1999). The black dots in Figure belong to the misfit value of different models.*

Knowing the misfit values for all previous samples, inside each Voronoi cell a constant value of misfit will be considered. Therefore to evaluate the approximate misfit value for a new model we only need to know the previous samples it is closest to. For any distribution and density of samples the structure of Voronoi cells would be unique and

the space filling and size of the cells are inversely proportional to the sampling density (Figure 2.5).

### *2.7.2 Sampling algorithm for the neighbourhood*

The NA uses a direct search method by using the spatial properties of Voronoi cells to guide the sampling of the parameter space. The key point is that NA generates new samples by resampling within chosen Voronoi cells with a locally uniform density probability. The NA algorithm can be summarized in the following steps:

1- Generate an initial set of $n_i$ models randomly distributed in parameter space;
2- Calculate the misfit value for the models and rank them based on the lowest misfit to choose the best $n_r$ models;
3- Generate new $n_s$ models by performing a uniform random walk in the Voronoi cells of each of the $n_r$ chosen models; ($n_s/n_r$ samples in each cell)
4- Go to step 2 to calculate misfit value for new models;

The Gibbs sampler used for generation of a uniform walk within a chosen Voronoi cell as shown in Figure 2.6.

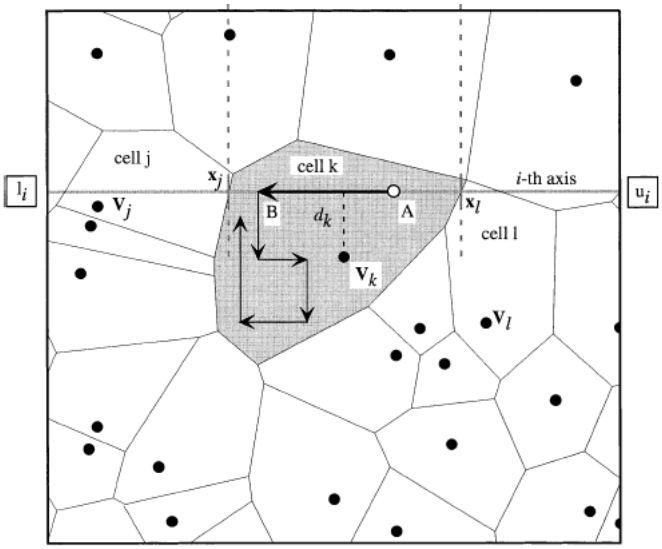


*Figure 2.6: A uniform random walk restricted to a Voronoi cell (Sambridge 1999).*

At each step the $i^{th}$ component of the current model, $x_A$ is replaced with a uniform random walk restricted to a specific boundary for the current Voronoi cell. From the assumption that the misfit value is uniformly constant in each Voronoi cell at each iteration new samples are concentrated in the cells with better data-fitting models.

Similar to Experimental Design (ED, see Section 1.3.2) a large number of models are generated initially. However instead of selecting parameter values deterministically from a limited number of extrema and perhaps mid points, to initialize NA we select values between extrema stochastically. In addition, NA automatically selects the best combinations of parameters in its exploration phase and searches around the value of those parameters in order to find the best result.

### *2.7.3 NA parameters*

The number of dimensions for a history matching problem is equal to the number of model unknowns and this affects the topology of Voronoi cells. According to Sambridge (2001) the numbers of corners of a Voronoi cell,$n$, is equal to:

$$n = 2^d \tag{2.20}$$

where $d$ is the dimension of the parameter space. We can take this as a measure for the number of initial models we need to generate at the beginning of the search in parameter space ($n_i$). Therefore large numbers of initial models need to be generated for a high dimension parameter space in order to reasonably fill the space.

Two other parameters of NA are $n_s$ and $n_r$ which control the exploration and exploitation behaviour of the algorithm. As $n_r$ increases the algorithm tends to search more of the parameter space which means that we increase the explorative behaviour of the NA. By increasing the $n_s/n_r$ the selected Voronoi cells will be visited more frequently and it means that the exploitative behaviour of the algorithm increases to find the global minimum.

### *2.7.4 Resampling from the posterior*

After generating an ensemble of models by NA it is useful to qualify the degree of uncertainty of the model parameters by calculating the posterior probability distribution (PPD) because the prior sampling from NA is a proper sample of the posterior density function (PDF). However the quality and accuracy of uncertainty qualification will depend on how representative the ensemble distribution of the true PDF is. In this thesis NA-Bayesian (NAB) algorithm is used to calculate an approximation of the PPD via a Gibbs sampler were used (Geman and Geman 1984). In this algorithm (Sambridge 1995) the Voronoi cells used by NA as the representative of parameter

space and the PPD of unknowns will be interpolated by using these cells. In the interpolation it was assumed that the known PPD of each model is constant inside each Voronoi cell. During the posterior sampling NAB does not need to perform any forward modelling during the interpolation procedure.

In this chapter different parts of the automatic history matched loop were introduced. This loop was implemented years before in SHM project and was applied to another field. However there are some differences between this study and previous applications in terms of the workflow. First of all the simulation was used in this study is streamline and secondly the petro-elastic model was used for the Nelson field is derived based on the specific data for the field. In particular the petro-elastic models in Nelson is porosity dependent and no stress sensitivity was considered for dry and shear bulk modulus. In Nelson, fluid compressibilities were calculated based on empirical equations whereas in previous application Batzle and Wang (1992) was used.

# Chapter 3: NELSON FIELD

**Overview:**

All applications of the history matching workflow and the various studies performed in this thesis were applied to the Nelson field. In this chapter this field is introduced in order to present information such as the geological description of the reservoir, the simulation model specifications, production and time-lapse seismic data and the main uncertainty issues in the field. Such information is very useful in order to have a suitable understanding of the reservoir and to make reasonable decisions for reservoir updating through history matching.

## 3.1 Nelson field location

The Nelson field is located in blocks 22/11, 22/6a, 22/7 and 22/12a in the UK sector of the North Sea 180 Km East of Aberdeen and it is in 275 ft of water. This field is in a series of Palaeocenne oil accumulations and it is situated on the Forties-Montrose High as shown in Figure 3.1 (Kunka et al. 2003).

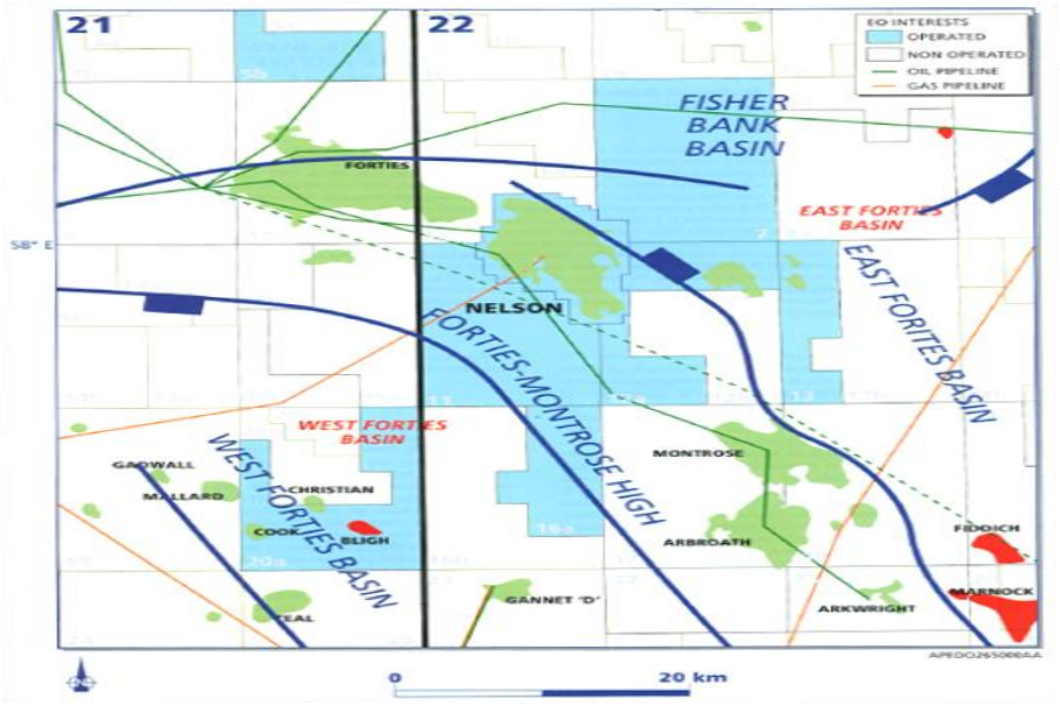


*Figure 3.1: Location of Nelson field in the North Sea in relation to Forties-Montrose trend (Kunka et al. 2003).*

The reservoir consists of channelized turbedite sandstone of the Palaeocene Forties sandstone member which is subdivided into five zones, numbered 1 to 5, and there are three channel complexes aligned in the NW-SE direction across the structure. The field is connected to a regionally extensive aquifer of the Forties field in the north and the Montrose and Arbroath fields to the south (Kunka et al. 2003).

### 3.2 History of the field

In 1967 the first exploration well, 22/11-1, was drilled with unsuccessful production result and the well was abandoned. In 1985, 3D seismic data was acquired over block 22/11 and 22/6a which was followed by the drilling of two field discovery wells in 1987 and another 13 wells afterward (Kunka et al. 2003).

In order to have a better plan for developing the field a second 3D seismic survey was acquired in 1990. The development concept was a 36 slot minimum facilities platform as shown in Figure 3.2. The capacity of production facilities was a daily rate of 25,000 cubic meters of oil and 1.84 million cubic meters of gas. Production of the field started on 18 February 1994 from ten development wells comprising eight platform and two sub-sea producers. Between 1994 to 1999, 19 platform producers, four platform water injectors and four sub-sea producers were brought on stream for further development of the field. Additional 3D seismic surveys were acquired in 1997, 2000 and 2003.

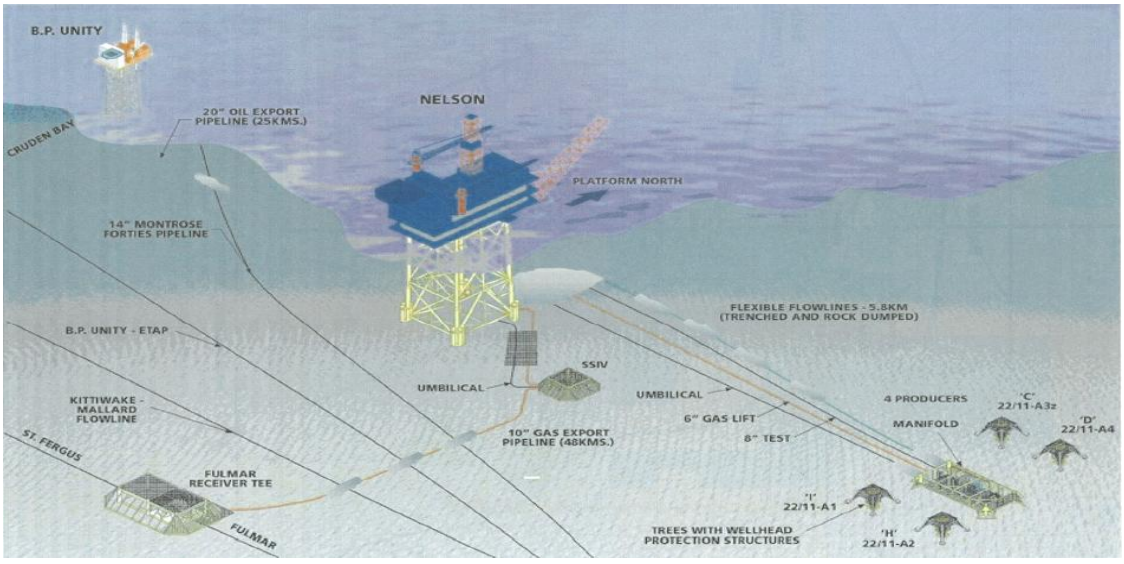


*Figure 3.2: Nelson platform and sub-sea facility (Kunka et al. 2003).*

The original oil in place was estimated at 126 million cubic metres and up to end of 2000, 46 million cubic metres had been produced from the field (UK DTI, 2009)

### 3.3 Nelson trap

The maximum oil column in Nelson is around 278 ft thick which traps between a crestal depth of 7192 ft TVDss and an average oil-water contact at 7470 ft TVDss. As a result of pressure depletion of the Forties field there is a tilted oil-water contact which ranges from 7449 ft TVDss in the south of Nelson to 7501 ft TVDss in the northwest and this is the water contact of the main Nelson accumulation. There are few major faults in Nelson and the production data shows little influence of fault seal with a confirmation from well test pressure build-up data (Kunka et al. 2003). Figure 3.3 shows the location of all faults in Nelson.

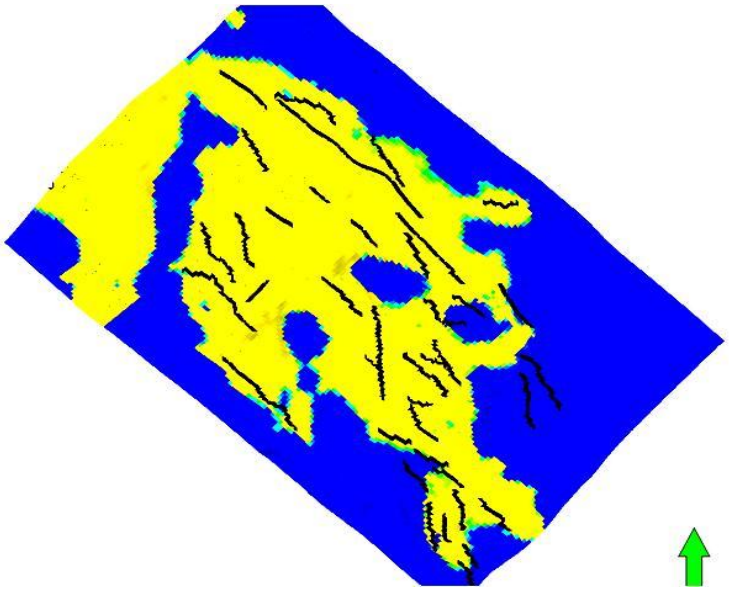

*Figure 3.3: Fault location in Nelson field. Blue is water and yellow is oil.*

### 3.4 Zonation in Nelson field

The mapping of different reservoir properties such as net:gross ratio, porosity and permeability is based on a reservoir zonation scheme. These reservoir properties are used in the construction of the simulation blocks of the reservoir model which is used to manage the reservoir, predict the future performance and also locate the best place for infill wells. Figure 3.4 shows an example well with the different zones.

The Upper Forties reservoir consists of the Top Forties zone and a unit seen as a deeper seismic event coinciding with the top of the lower Forties unit.

The basis for zonal mapping in Nelson is identification of bio-events (biostratigraphic) where repeat over the field such as well-documented regional event or sub-regional events. From the zonal scheme channel abandonment events are identical and are characterized by thin bedded turbidites and occasionally muddy debris flows (Kunka et al. 2003).

Zone 1 is characterized by channel activity with little evidence of shale. Zone 2 represents the boundary between the upper and lower unites of Forties Sandstone Member in the Nelson field. Along the north-south axis of the Central Channel complex there is Zone 3a (Table 3.1). Figure 3.5 shows a cross section of the reservoir in two directions in order to illustrate the consistency of Zone 3 in a north-south direction along the central channel complex.

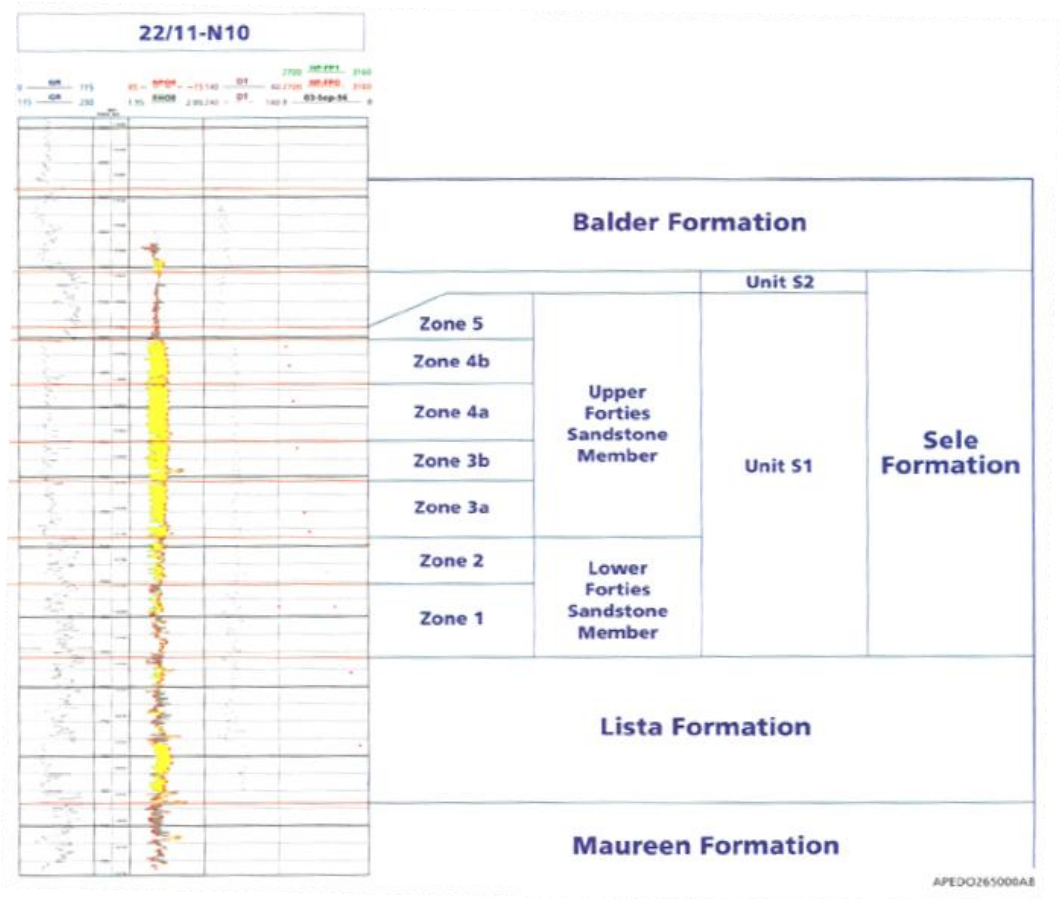


*Figure 3.4: Nelson lithostratigraphy of Sele Unit S1 (Kunka et al. 2003).*

| Reservoir zones | Depositional setting |
|---|---|
| Zone 5 | Abandonment of the Forties Fan, submarine channel deposition in the eastern channel complex |
| Zone 4b | Western and eastern channel complex dominant |
| Zone 4a | Western and eastern channel complex dominant |
| Zone 3b | Central channel complex dominant |
| Zone 3a | Central channel complex dominant |
| Zone 2a | Regional slump event |
| Zone 2b<br>Zone 1 | Channelized facies dominant in the centre of the field |
| Lista Formation | |

*Table 3.1: Summarized the key biostratigraphic events in the reservoir.*

Figure 3.6 shows the net:gross map of Zone 4. In the east and west of the reservoir high net:gross can be seen which means more sand in the channel facies.

From analysis of log and seismic data there are two main hydrocarbon reservoir intervals in the Forties Sandstone member (Upper section in Figure 3.4) which are known as T75, T70 and T65. The last is containing the reservoir aquifer and is called lower Forties Sandstone member in Figure 3.4. The two main channel complexes (Western and Eastern) are located in T75 (Figure 3.7) and the Central channel complex is in the T70 interval.

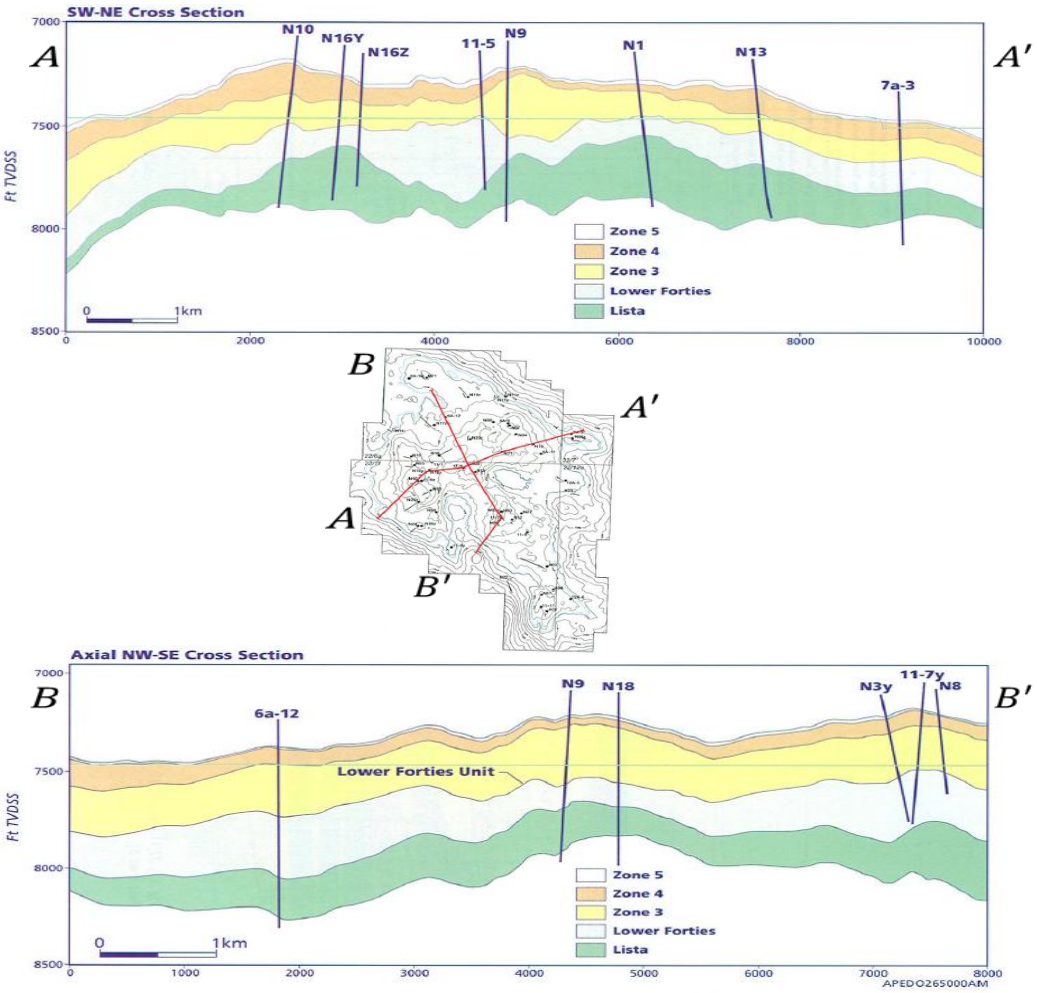


*Figure 3.5: Nelson field structural cross-sections (Kunka et al. 2003).*

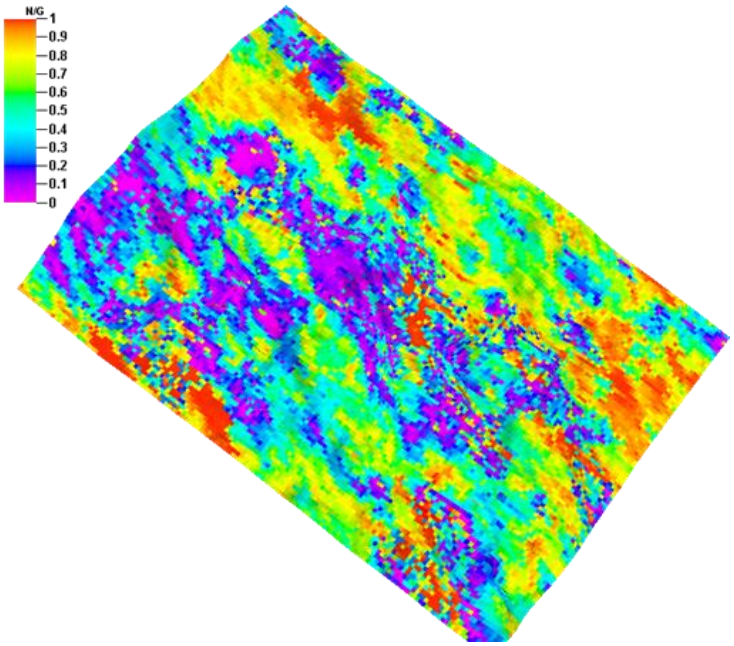


*Figure 3.6: Zone 4 net:gross (from simulation model supplied by field operator.*

According to the operator's information there are three geological environments in Nelson named Channel Axis, Channel Margin and Interchannel as shown in Figure 3.7. The channel complexes (Channel Axis) are spread throughout the reservoir in both intervals and Channel Margin geo-bodies lie between Channel Axis and Interchannel. The main differences between these geo-bodies is the distribution of different facies within each system and, simply, it can be said that in the Channel Axis there are larger proportions of sands compared to the other two geological environments. Channel Margin deposits are partitioned by even lower net:gross Interchannel regions. From Figure 3.7 it can be seen that the principal areas of oil production are the Western, Central and Eastern Channels.

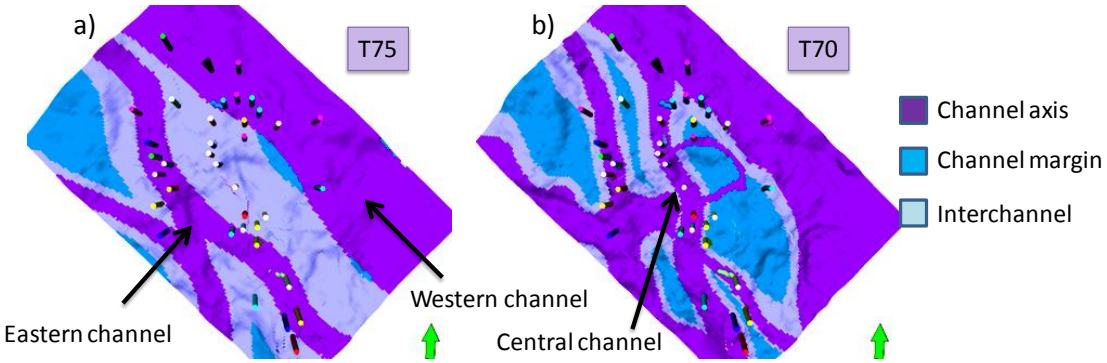


*Figure 3.7: The channelized structure in Nelson in different reservoir producing intervals, a) top (T75) and b) bottom (T70).*

There is a major barrier to vertical flow in the T75 interval which separates Nelson into two hydraulic unites as shown in Figure 3.8. As an example, the distribution of pure shale bodies in the top of the reservoir is shown in Figure 3.9 for the regions where transmissibility is almost zero. This separate hydraulic flow behaviour is crucial for appropriate updating of the reservoir.

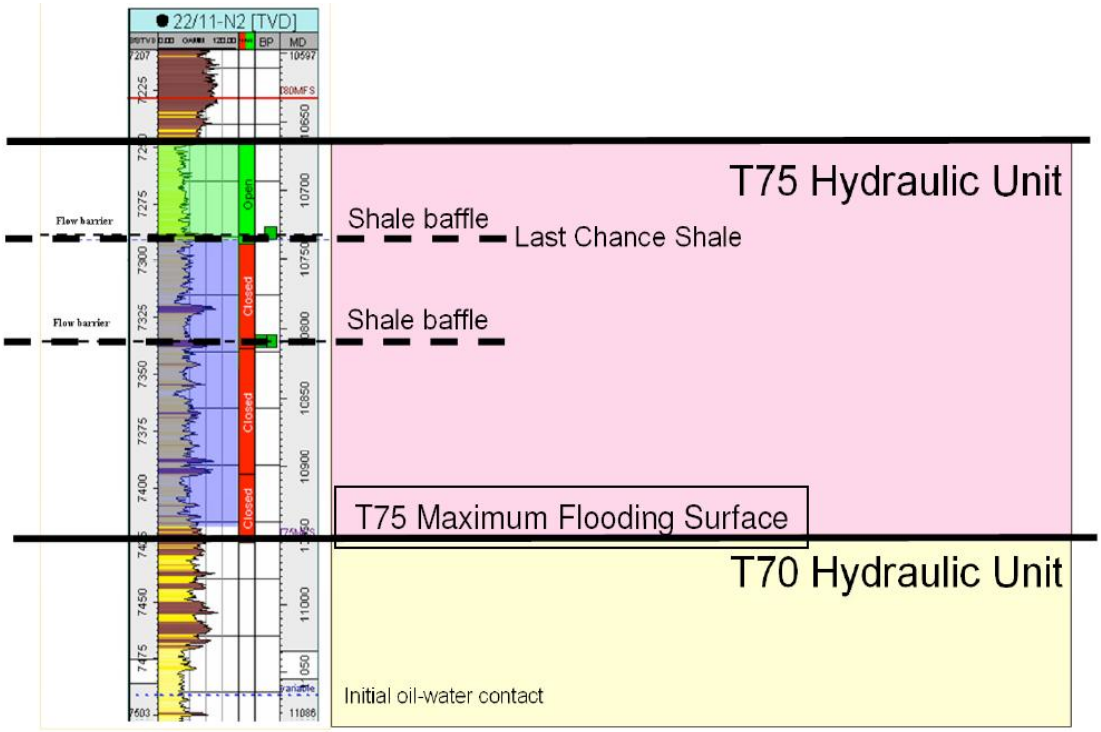


*Figure 3.8: Two hydraulic flow units that exist because of the shale baffle (Shepherd and Gill 2009).*

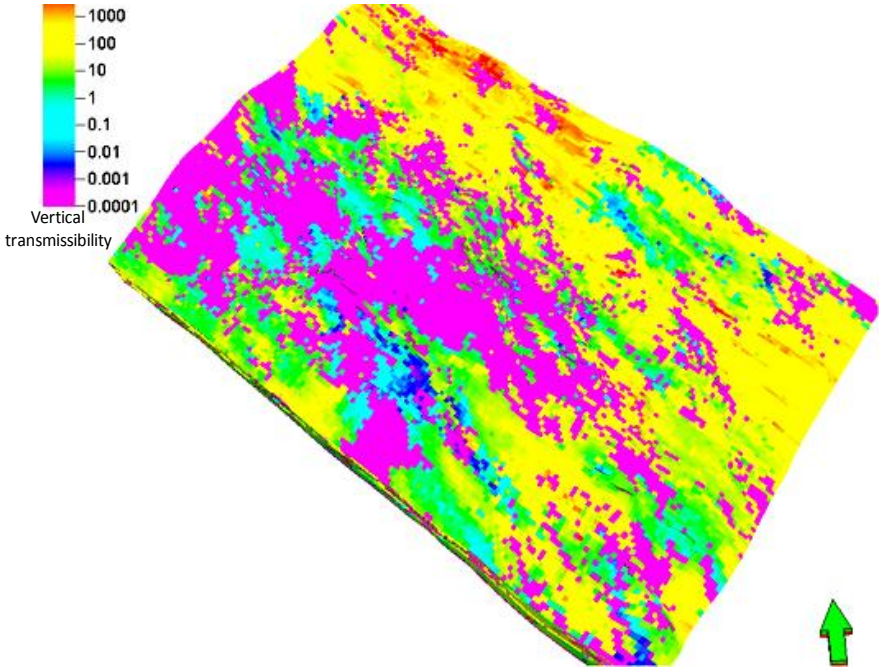


*Figure 3.9: Top view of Nelson field showing transmissibility of the reservoir.*

According to the different facies presented in the geo-bodies there are different values for reservoir properties. For example, for sandy facies the cells have high porosity and permeability whereas for shale facies the permeability is lower. The porosity of the

reservoir is independent of grain size but permeability is strongly correlated with grain size. Figure 3.10 shows the frequency distribution of porosity for all zones as described from petrophysical analysis. It can be seen that there is a normal distribution of porosity with a mean of 22%.

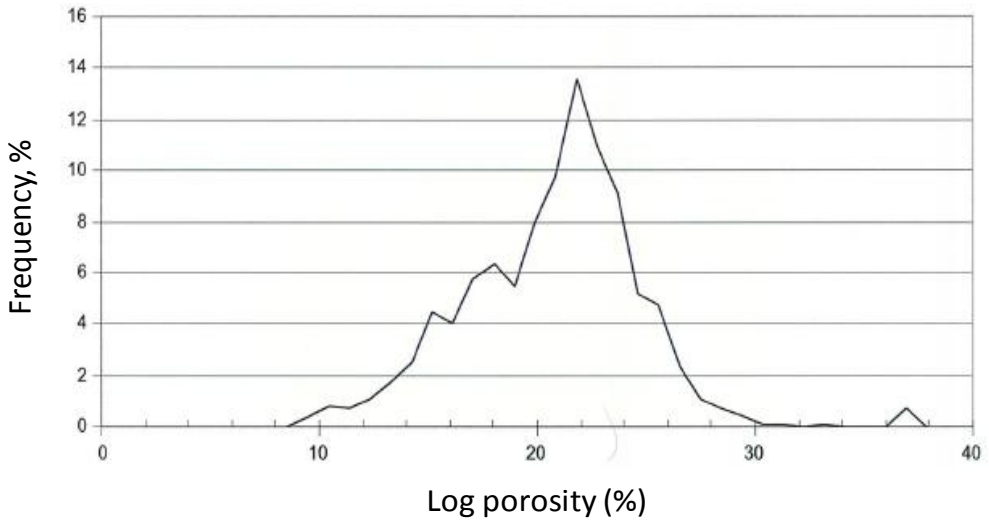


*Figure 3.10: Log porosity distribution for all samples of Forties Sandstone (Kunka et al. 2003).*

The most permeable reservoir facies is located in the units called Channel Axis and the values exceed 1000 mD in some regions (1700 mD is the maximum). "*Reservoir rocks with clay contents in excess of 20% possess permeabilities of less than 100 mD*" (Kunka et al. 2003). The net reservoir cut-off in Nelson is where the porosity is less than 15% which is approximately equal to permeabilities of 1 mD.

A long time before there were big channel complexes in Nelson that gradually filled with sands through turbidity events. Then because of erosions we may have some smaller channels and there is a high chance in order to have shale between these smaller channels (Stephen et al. 2009). Shale content is considered to be a major uncertainty in Nelson and its volume and distribution affect net:gross and horizontal and vertical permeabilities. We therefore update these variables but first we must assess what various combinations of change might mean. Figure 3.11 shows the various combinations of possible changes. There are 8 combinations presented where the parameters are increased or decreased and based on that, it is possible to understand what each means geologically. As an example for the case that all variables are increased after history matching this is possible if the base reservoir is very shaly (large

number of black lines in Figure 3.11) also both horizontal and vertical permeabilities are low because the shale layers are curved therefore it would be harder for flow to pass in the sands between the shales and the erosions in the shale layer (red symboles in Figure 3.11) is very low. Therefore, there is a very poor connection vertically between sands. By increasing all variables there are fewer shale layers in the reservoir that illustrated with lower number of black lines. The sands are very well connected horizontally because of straight lines shown in the Figure 3.11 and finally there is a good vertical connection between the sands having more red lines in Figure 3.11.

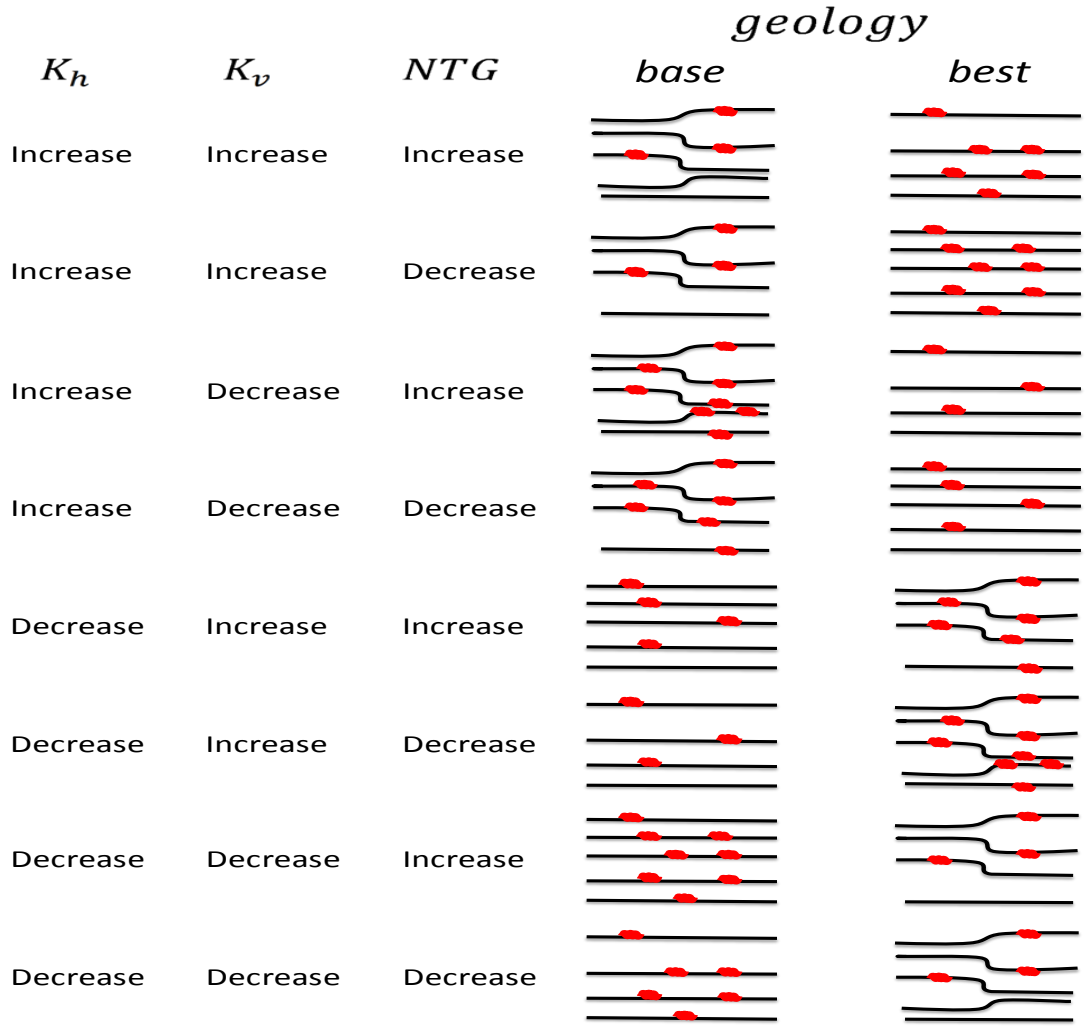


*Figure 3.11: A schematic of geology of the reservoir before and after history matching. Black lines are representative of shale layers and between shales there are sands. The shale predominantly deposited as flatbeds between turbidity events but may be eroded as shown with red. This erosion controls the vertical permeability. The curvature results from shale drapes in channels affecting horizontal permeability.*

### 3.5 Production scenario in Nelson

The displacement of oil in Nelson is by water from two different sources; injectors and aquifers. The four injectors are located at the edges of the reservoir as shown in Figure 3.12.

There is also good aquifer support for the Nelson field. There is both bottom and edge drive from the aquifer in different locations. In the Channel Axis there is mainly bottom drive support while in the Interchannel regions, edge drive occurs due to differences in vertical permeability. Figure 3.13 shows, as an example, the original oil water contact below the Channel Axis and Interchannel regions in an East-West cross section of Nelson.

Because of the good pressure support from injectors and the aquifer the pressure of the field is maintained above bubble point and the model has been simulated with two phase flow therefore.

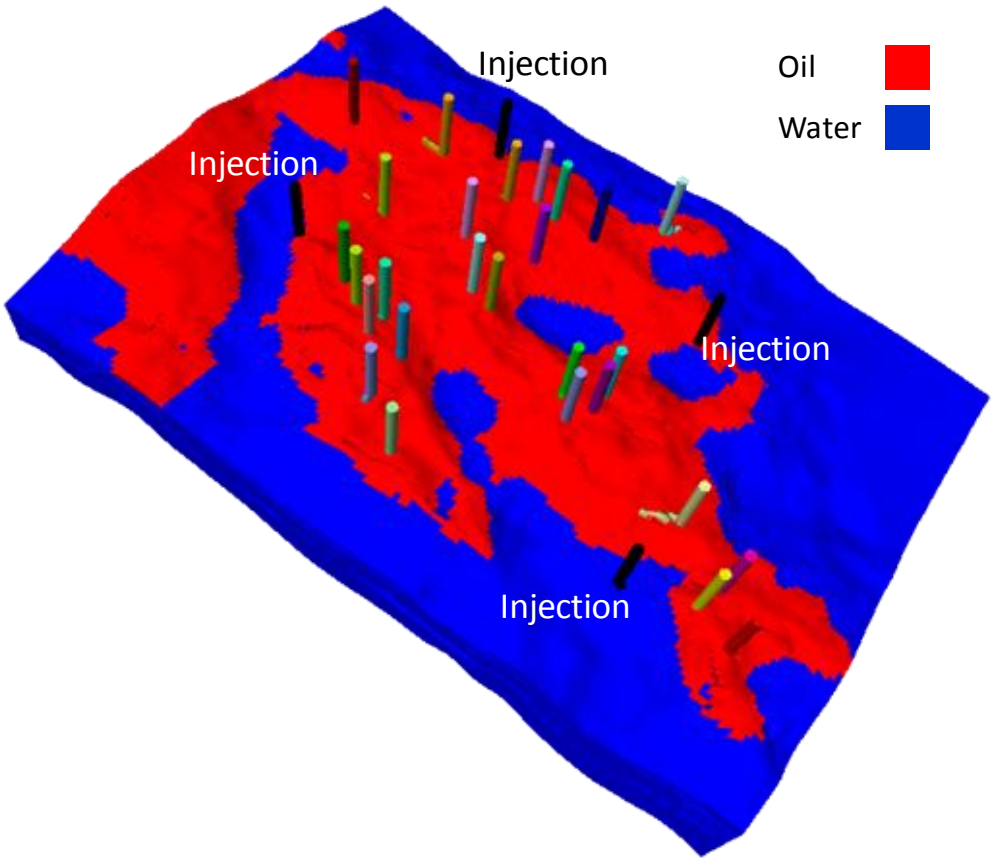


*Figure 3.12: The location of water injector wells (black) compared to the rest of wells in the reservoir.*

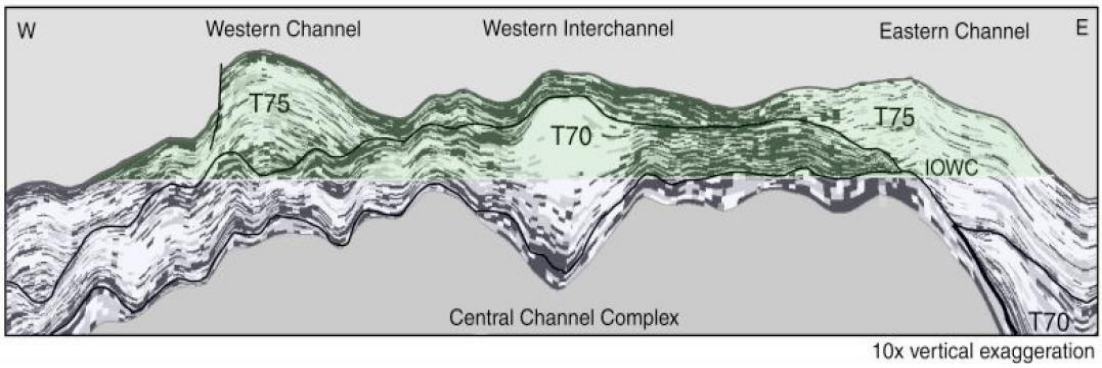


*Figure 3.13: A West-East cross section of the reservoir which shows the location of Initial Oil-Water Contact (IOWC) (Shepherd and Gill 2009).*

## 3.6 The petro-elastic model in this study

The PEM which we are going to use in this study is representative for Sele shale and Forties sandstone based on the data from the Nelson field wells in the North Sea and the special core analysis study (UKCS North Sea rock physics analysis 1997). To derive the PEM for a particular field we need to have some measurements for compressibility of fluids in the reservoir (such as formation water, oil, gas, drilling mud) and compressibility and shear velocity measurements for the dry and wet frames. From those measurements we can set the relationships between fluid compressibility and acoustic properties of rock with pressure. The data and equations that we used here were supplied by a former operator of Nelson (Boyd-Gorst and Garnham 1999).

### *3.6.1 Fluid compressibility*

The fluid compressibility for Nelson formation water shows a well defined linear increase of bulk modulus with pressure which is also consistent with the trends established by Batzle and Wang (1992). At a reservoir temperature of 225 Fahrenheit the relationship is:

$$K_w = 7e^{-5}.P + 2.4359 \quad (3.1)$$

Where $P$ is the pore pressure in psia.

For a pore pressure reduction of 1000 psia (from an initial pressure of 3250 psia) the $K_w$ varies between 2.66-2.59 GPa which indicates less than 3% change. For the oil phase,

the bulk modulus is equal to 0.534 GPa for initial reservoir pressure and 0.464 GPa at 2250 psia which means 13% drop in bulk modulus. The relationship for the oil is:

$$K_o = 7e^{-5}.P + 0.306 \quad (3.2)$$

### *3.6.2 Compressibility and shear velocity measurement*

In Nelson, a total of 30 plug samples in 17 depth positions from a well were used in this study. Most of these samples are from the oil leg. The compressibility study was performed in a range of effective pressure from 3800 to 5300 psia. The effective pressure is defined as the overburden pressure (the pressure imposed to rock by the weight of overlying material) minus the pore pressure. Figure 3.14 shows the definition of different pressures we are dealing with here.

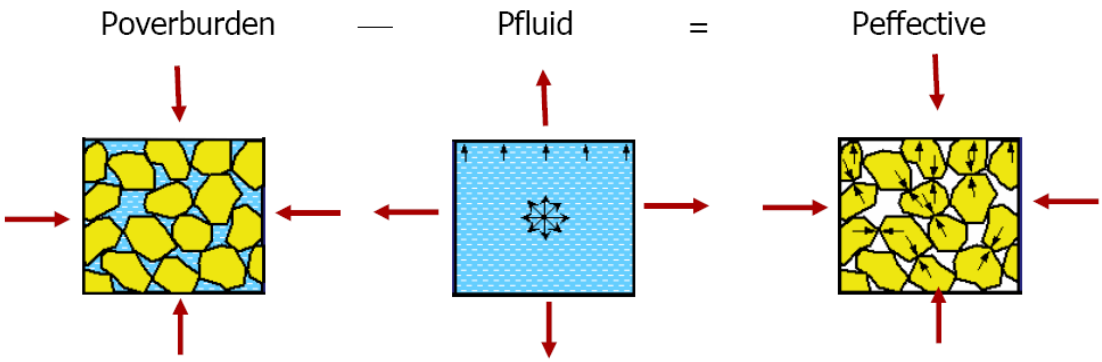


*Figure 3.14: Schematic for definition of effective pressure (MacBeth 2007).*

Assuming a 1psi/ft pressure gradient in the reservoir the overburden pressure is 7300 psia. Taking into account the initial reservoir pressure of 3250 psia the initial effective pressure would be 4050 psia. Therefore the specific range of effective pressures used in this study was defined in order to span the initial effective pressure.

The measurements shows that there is a significant change in the saturated bulk modulus ($K$) and shear modulus ($\mu$) due to pressure change. $K$ increases by 27-34% for a corresponding 1500 psia increase in effective pressure and $\mu$ increases by 9-13% for the same pressure change (Boyd-Gorst and Garnham 1999).

The result for dry bulk modulus shows a strong relationship of modulus with porosity and clay volume. Comparing the measured result with empirical Murphy's relationship

(Murphy et al. 1993) we can see overestimation of dry modulus. By using the Eberhart-Phillips relationship (Eberhart-Phillips et al. 1989) to predict compressional and shear velocities we generally overestimate compressional and underestimate shear velocities. Therefore the experimental result were used in order to drive the petro-elastic model.

### *3.6.3 Petro-elastic equations*

The modelling concept for PEM in this field was based on the theoretical formulation originally developed by Kuster and Toksoz (Kuster and Toksoz 1974). This model was used to calculate the elastic properties of the dry frame rock (rock matrix and inclusions). Finally Gassmann fluid substitution (Gassmann 1951) was used to calculate the wet bulk modulus.

#### *Matrix properties*

*Bulk density:* the Eq. 3.3 used to calculate the bulk density of a cell:

$$\rho = \rho_{sand}(1 - V_{sh})(1 - \varphi) + \rho_{sh}V_{sh} + \varphi.[\rho_w S_w + \rho_o(1 - S_w)](1 - V_{sh}) \qquad (3.3)$$

Where $\rho$, $\rho_{sand}$, $\rho_{sh}$, $\rho_w$ and $\rho_{hc}$ are the effective bulk density of the sand-shale fluid system, dry sand density, dry shale density, water density and hydrocarbon density respectively. $\varphi$ is the effective porosity of the sand , $S_w$ is water saturation and $V_{sh}$ is shale volume fraction. The shale volume used in this study was assumed to be (1-net:gross) and this was considered reasonable by operator.

*Bulk modulus:* According to Simmons and Wang (Simmons and Wang 1971) a bulk modulus of 37 GPa considered for sand grains ($K_m$) with a density of 2.2 g/cc at atmospheric conditions.

#### *Dry frame modulus*

*Dry frame modulus:* The effective shear modulus of dry rock frame can be calculated using the empirical equation obtained from cores:

$$\mu_d = 30.2 * (1 - 4.67 * \varphi + 7.162 * \varphi^2) \qquad (3.4)$$

and the dry bulk modulus is calculated using the relationship:

$$K_d = 32 * (1 - 2.07 * \varphi - 2.384 * \varphi^2) \quad (3.5)$$

Based on observed pressure depletion from field data (around 1000 psi maximum at the wells) and synthetic seismic difference modelling from the operator (Boyd-Gorst and Garnham 1999), the effect of fluid (where the water saturation increases from 0.1 to 0.9) is approximately 1.4 times larger than the pressure effect. More importantly the corresponding change in dry frame Poisson's ratio due to water influx is around 3.1 times larger than the typical pressure response. Based on this information and the spread of pressure drawdown laterally, in our study we are expecting to see 4D seismic signal in the reservoir from saturation change only.

***Potential Pressure effect***

In the report on petro-physical measurements made by the Nelson field operator (Boyd-Gorst and Garnham 1999), the importance of the pressure effect on the dry rock frame was determined according to Table 3.2. Typically, for 1000 psia formation pressure depletion ($P_f$ increases) there is a corresponding + 0.33 km/s*g/cc change in $I_P$ (Eq. 2.1). Changes in fluid compressibility have also been incorporated using the relationships defined in Section 3.6.1.

| $\Delta P_f$, psia | 500 | 1000 | 1500 |
|---|---|---|---|
| $\Delta I_P$, km/s*g/cc | 0.19 | 0.33 | 0.5 |

*Table 3.2: Nelson field, pressure effect on acoustic properties. From dry frame SCAL measurements (Boyd-Gorst and Garnham 1999).*

Based on Table 3.2 and considering a zero change of impedance for zero pressure difference, we fitted a polynomial equation between pressure depletion and impedance change;

$$\Delta I_P = -3\mathrm{E}-8 \times (\Delta P_{eff})^2 + 0.0004 \times \Delta P_{eff} + 0.0046 \quad (3.6)$$

According to this equation still for zero change pressure differences there is a small change of $I_P$. Based on the fact that, reservoir pressure change was negligible in Nelson

(Figure 3.19 and 3.20) and also the advice of the field operator we did not include Eq. 3.6 in calculation of synthetic impedance data in Nelson.

## 3.7 Time-lapse seismic data

For better understanding of the available observed data three different categories of time-lapse seismic data have been considered: cubes of seismic amplitude, cubes of elastic impedance, and cubes of phase shifted amplitude (equivalent to coloured inversion). However, the last two types of data were derived from the seismic amplitude data. In Nelson, the amplitude data that was phase shifted was reprocessed and was of better quality compared to the data used to derive elastic impedance cubes. The elastic impedance and phase shifted data are layer based while amplitudes are interface based. For this reason only the elastic impedance data and the phase rotated amplitude data were used to generate 4D signatures. As previously discussed in Chapter 1 (Section 1.2.1) the choice of comparison of 4D data in this thesis was the impedance domain. Therefore, the observed data had to be transformed from the time domain using attributes of pseudo-impedance to be comparable with the synthetic data. There are three intervals in the reservoir identified by picked horizons and the names of the top of each interval is T80-MFS, T75-MFS, T70-MFS and T65-MFS from top to the bottom respectively. For EI and phase shifted amplitudes, attributes were obtained for the seismic signal between the horizons of each interval.

### *3.7.1 Elastic impedance data in Nelson*

In the Nelson field all three of the above seismic data were available. Elastic impedance cubes were available as differences of observed near angle stack elastic impedance. A maximum amplitude attribute of the change in EI was used within each interval to generate a 4D signature attribute. Therefore, the maps of 1990-2000 for the first (T80-MFS - T75-MFS) and second (T75-MFS - T70-MFS) intervals have been generated and also the maps of 2000-2003 for the same intervals as well (Figure 3.15).

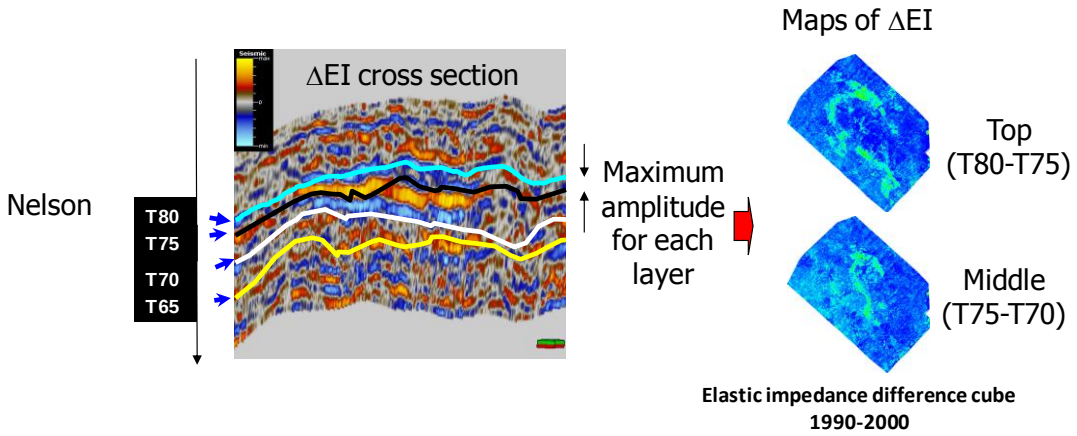


*Figure 3.15: The horizons in Nelson (left) which were used to generate the 2 dimensional maps of differences of elastic impedance for reservoir intervals.*

These generated elastic impedance data used in previous studies such as Stephen et al. 2007 and Kazemi and Stephen 2008, but based on the quality of inversion process the field operator advice to ignore this data for this study.

### *3.7.2 Phase shifted amplitude data*

As previously mentioned we had another data set in Nelson which consisted of phase shifted amplitudes (similar to coloured inversion). This dataset is different from the previously discussed dataset because the full inversion process is not performed. However phase shifted amplitudes can be used to obtain pseudo impedance because there is zero crossing of the trace at the interface in both types of data. In each reservoir interval the value of phase shifted amplitude could be equivalent to the impedance value.

According to Francis and Syed (2001) coloured inversion is the most cost-effective, impedance product that derived. Some advantages of coloured inversion are, ease of interpretation and, as a seismic attribute, it avoids artefacts which may be introduced by models used to constrain deterministic inversions. As Lancaster and Whitcombe (2000) discussed, in the coloured inversion process, a single convolutional inversion operator is derived in order to optimally invert the data and honour available well data in a global sense. Inherently there is stability in the above process and there is consistency with known acoustic impedance behavior. The construction of the inversion operator is a simple process and implementation can be readily performed on most interpretation workstations. On the other hand the coloured inversion process does not require any

explicit wavelet other than testing for a residual constant phase rotation as the last step. This removes an inherently weak-link that more sophisticated processes rely on (Lancaster and Whitcombe 2000). Figure 3.16 shows, simply, the outcome after coloured inversion. The seismic wavelet has been shifted from layer interface to the layer and therefore it provides information of the layer's characteristics (similar to seismic impedance).

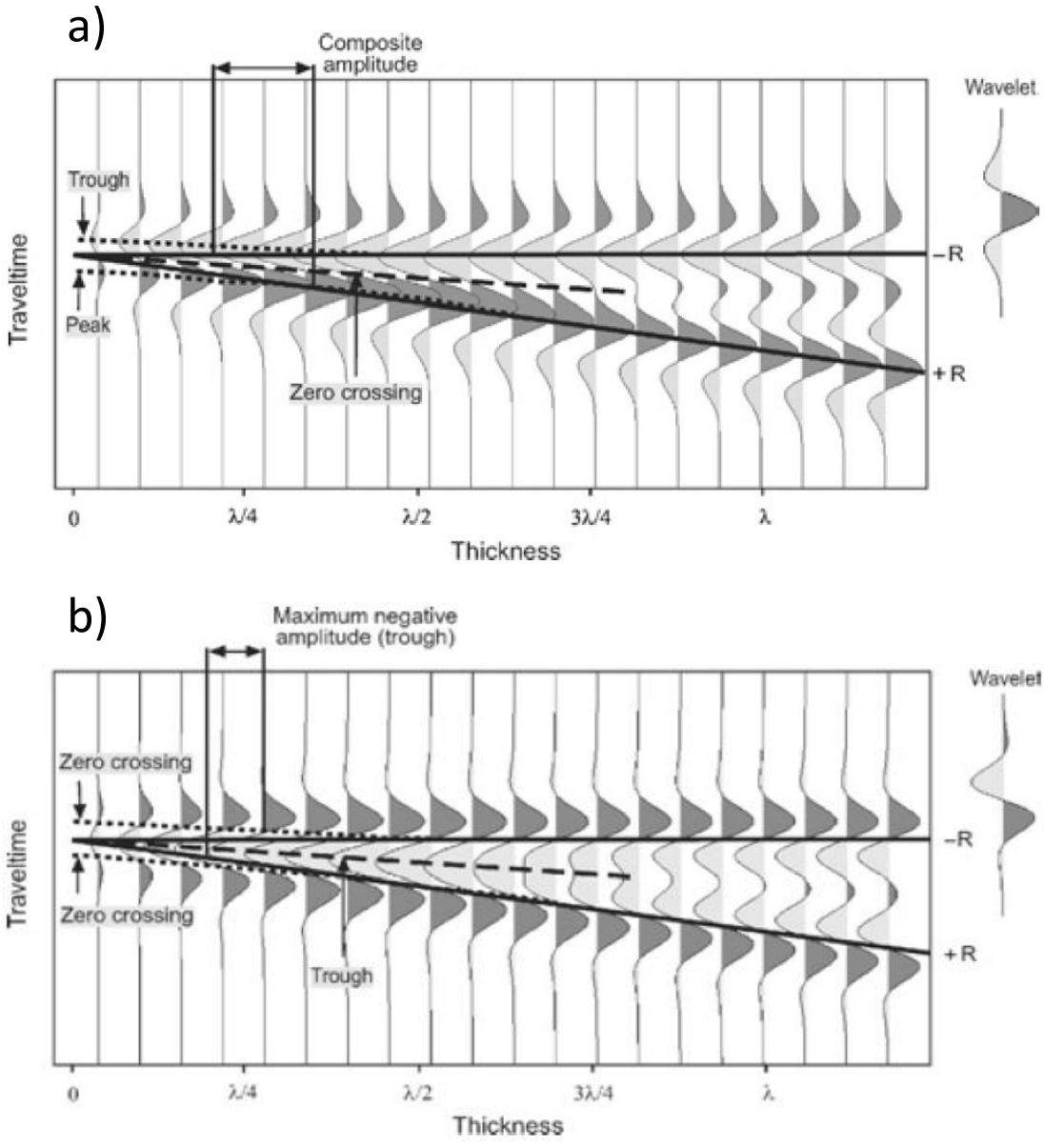


*Figure 3.16: a) Zero-phase Riker seismic model and b) ninety-degree Riker seismic model (coloured inversion) (Hongliu and Backus 2005).*

Although the outcome of coloured inversion is equivalent to impedance however, the unit of this data depends on how the original amplitude and this data is calibrated. In order to enable quantitative integration of coloured inversion data , or equivalent data as used here, into the history matching loop we need some kind of calibration and/or normalization in order to data in the same units equivalent to the unit of synthetic acoustic impedance data (as discussed in Chapter 5).

Root Mean Square of the phase shifted amplitudes were used to derive relative pseudo impedance and then maps were derived from differences of the attribute. These maps were compared to equivalent predictions of changes in acoustic impedance. Figure 3.17 shows as an example two time differences maps for the top reservoir interval.

Following the strategy used in this study, reservoir properties were updated in the model in order to get a better match to production data from 1990 to 2000. Then the quality of the history matching result was checked by looking at the available data from 2000 to 2003.

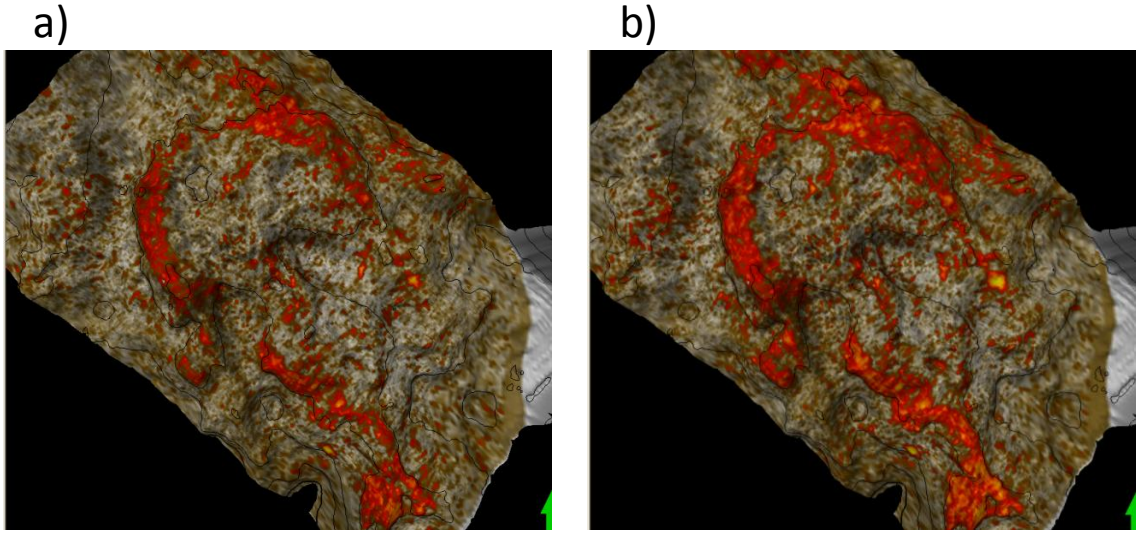


*Figure 3.17: The maps of differences of phase shifted amplitude (similar to coloured inversion) for top reservoir interval (T75) in two different time differences, a) 1990-2000 and b) 1990-2003.*

### *3.7.3 Time-lapse response versus reservoir activity*

Between two different time steps for which there are seismic surveys, we need to consider what reservoir changes are expected. For example the reservoir may be under

primary depletion or there may be an important influence from the aquifer influx or gas and water injections, etc. These reservoir activities can mainly induce saturation change effects as well as pressure.

The fluid displacement occurs in the reservoir because of production activity which changes the compressibility of rock and pore fluids and ultimately changes the bulk velocity and strength of reflectors. For example in water flooding, because of fluid displacement, the compressibility of the fluid decreases which causes increase of compressional velocity (Eq. 2.3 to 2.6). On the other hand an increase in pore pressure reduces $V_p$. Figure 3.18 shows a summary of different production activities in reservoirs. For the gas out of solution case, there is a large decrease in velocity but as pore pressure decreases too velocity increase a little. For the gas production, because of pressure depletion there is an increase in velocity and by fluid substitution the velocity is increased drastically. In gas injection processes the oil will be displaced by gas which causes reduction in velocity but by increasing the pore pressure further reduction of velocity is observed. We see that near well pressure and fluid movement usually result in opposing effects.

From Figure 3.19 and 3.20 according to production activity in Nelson (Section 3.5) there is a good pressure support from the aquifer and four injectors. It has been considered therefore, that reservoir pressure does not reduce drastically. Also the pressure profile of the base reservoir model delivered by the operator confirms that average reservoir pressure changes a little during 6 years production of the reservoir as shown in Figure 3.19. On the other hand there is a good transmissibility of the faults in the reservoir (Figure 3.3) therefore it was not expected that regional pressure build up or drawdown would be seen.

Based on the laboratory report (Boyd-Gorst and Garnham 1999) of generating the petro-elastic model from the literature (supplied by operator) a 1000 psia pressure depletion in the reservoir has 0.7 of the effect of water saturation change (up to 80%) as shown in Figure 3.21. According to this figure the maximum change in water saturation of 80% makes 0.457 km/s*g/cc increase in the p-wave impedance whereas 1000 psia change of pressure makes 0.38 km/s*g/cc change in impedance value. Based on the above analysis and observations it was expected that the time-lapse signal in the reservoir should show water/oil saturation change.

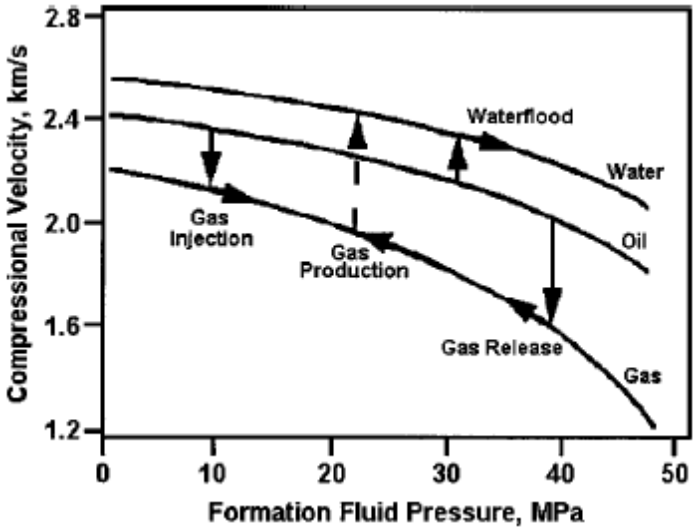


*Figurer 3.18: Variation of compressional velocity as a function of formation fluid pressure and fluid substitution because of different production scenarios at different initial pressure; vertical arrows indicate fluid displacement and along curve arrows indicate pore pressure change (Johnston 1997).*

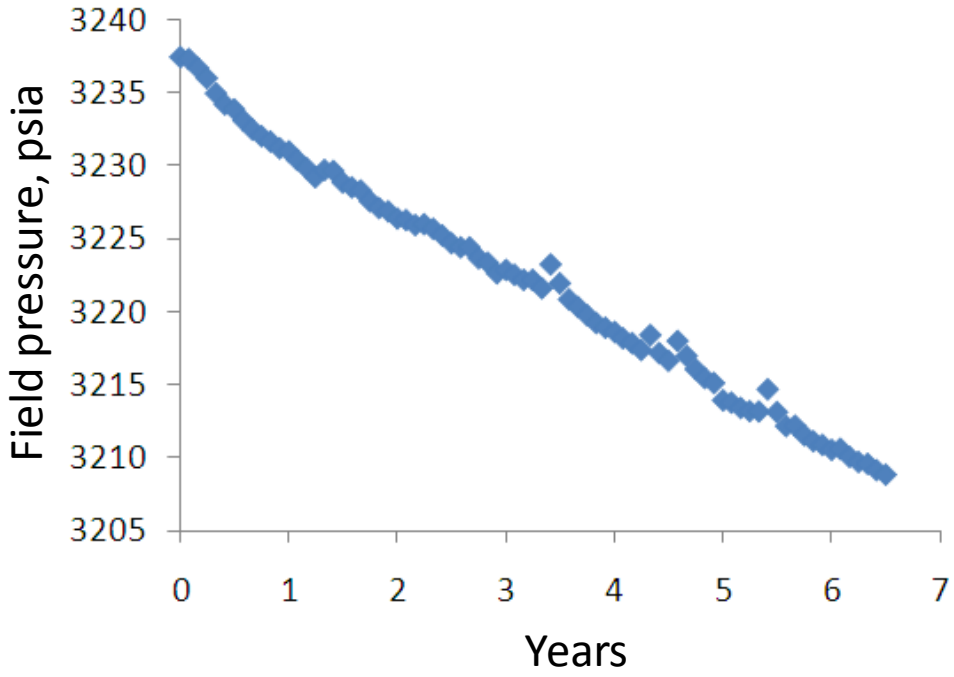


*Figure 3.19: Average reservoir pressure during production period (monthly time steps).*

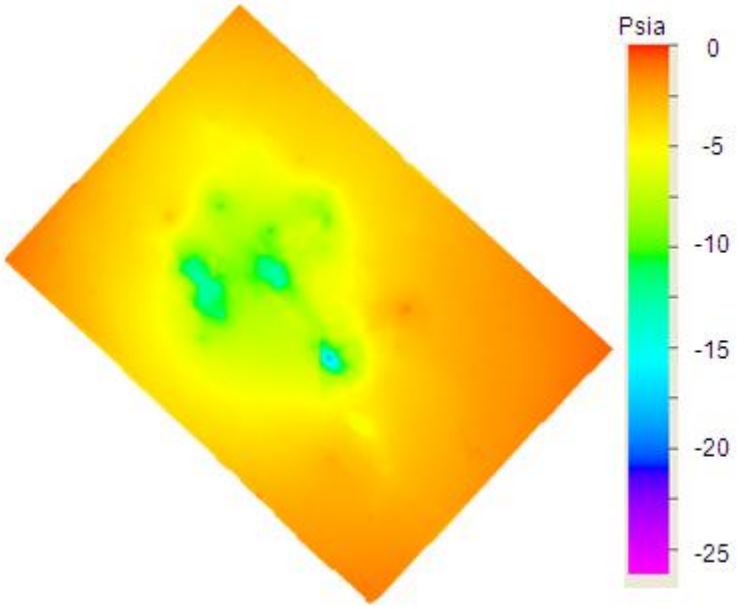


*Figure 3.20: A 2D (an arithmetic averaging performed vertically) of reservoir pressure differences during production period (1994-2000).*

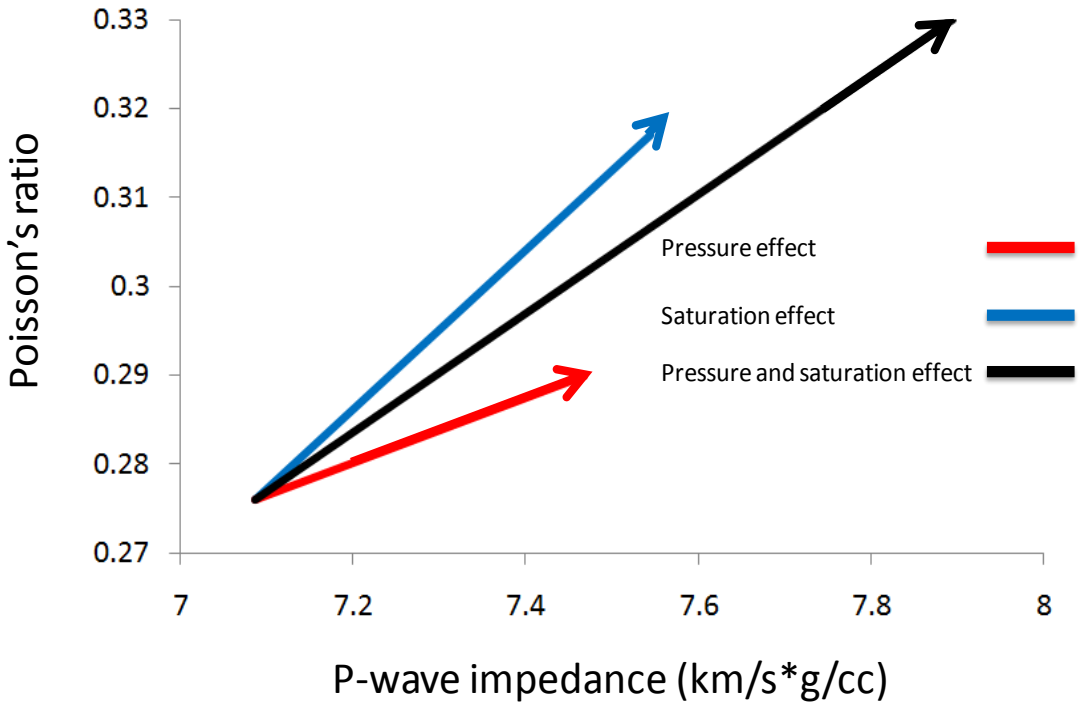


*Figure 3.21: Effect of production on rock parameters on 1000 psia pressure depletion (typical sand with 23% porosity, 10% shale volume).*

Considering the PEM equation for the Nelson field (Section 3.6) and the effect of pressure on the dry rock frame (Eq. 3.6), it is possible to calculate the sensitivity of the P-wave impedance by changing water saturation and reservoir pressure as shown in Figure 3.22. According to this figure the synthetic seismic impedance data is sensitive to water saturation and the same effect observed for pressure effect whe considering Eq. 3.6.

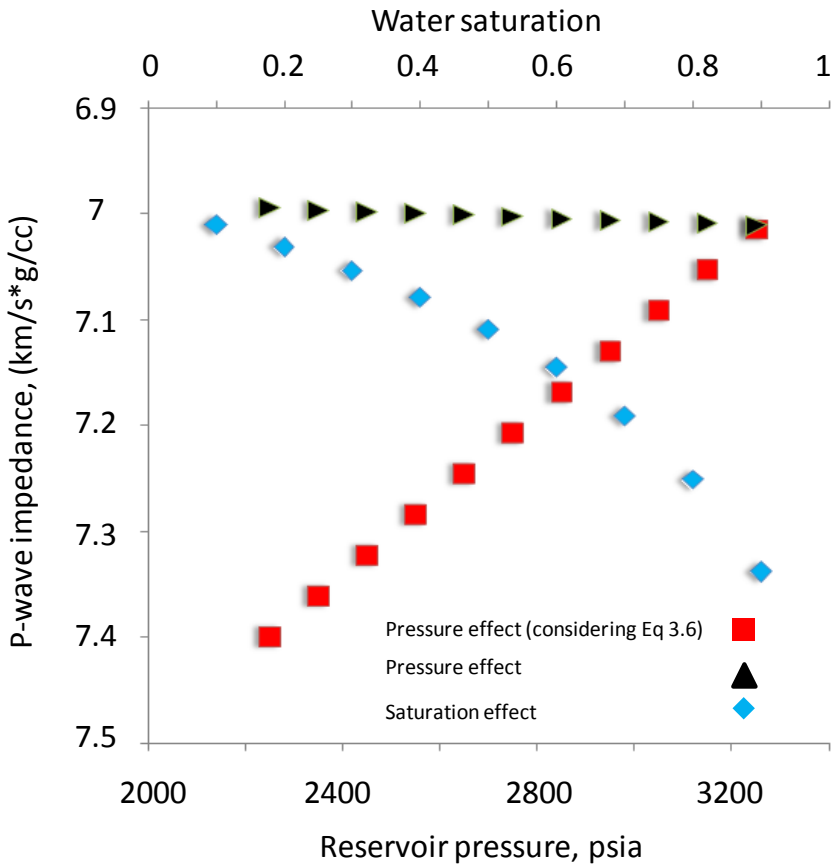


*Figure 3.22: Effect of water saturation and reservoir pressure change on p-wave impedance. Note that the black line represent the pressure effect when Eq. 3.6 did not consider.*

### *3.7.4 Calculating data error of the time-lapse data*

When time-lapse seismic data is analysed properly it should also be prepared for input into the objective function (Eq. 2.19). At this stage, the data error for the noise should be calculated based on the understanding of the signal and noise.

The survey noise estimation requires some special techniques such as factorial Kriging (Kriging with measured error). This is an interpretative process based on the covariance

analysis and is justified when nested structures are observed (Doyen 2007). Figure 3.23 shows that a survey image is actually a multi-phenomena response in which the signal is superimposed on a background of noise, geology and acquisition footprints. Although the noise could be of complex origins, its random-like nature can be justified though existence of some apparently random structures with short scale spatial variability. The 2D semi-variogram map could be a used as a guideline in recognizing the random noise through evaluating the nugget effect. The nugget effect corresponds to either random noise or to variability at a scale smaller than the sampling interval (Doyen 2007). Toward this aim, we first filtered the original 4D survey (Figure 3.24a) by removing data we assumed as signals by considering threshold of 0.05 in Figure 3.24a (the filtered 4D map is Figure 3.24b). For each cell we can take a window of 1000m by 1000m with the cell in the middle, and calculate the arithmetic average. This gives a locally averaged map (Figure 3.24c) and will capture trends. It is worth mentioning that in order to save computational time of the semi-variogram map, (semi-variogram map was calculated by Petrel) the original seismic map was upscaled by the grid size of 100m by 100m, and the following calculation (local averaging) was performed on the newly gridded seismic map. We then compared the semi-variogram map of the Figure 3.24b with its calculated local average attribute (Figure 3.24c). The angle tolerance of 25 degree was used in the calculation of semi-variogram map. The number of lag distance was chosen to be 30 by 30 in x and y directions. Figure 3.25a and b show that the nugget effect has been significantly reduced (from 0.68 to 0.22) and the small scale structures have been smoothed out of the map. In addition, we can subtract the local average map from the original filtered map to construct a so-called "residual map" (Figure 3.24d) which is an indicator of the dominant background trends (e.g high spatial frequency noise). The 2D variogram map of the residuals (Figure 3.26) shows a small correlation length compared to the original filtered studied map that could be interpreted as random noise. The calculated mono-variogram in NW-SE direction (the direction of the elongated structures) corroborates the 2D variogram map as well (Figure 3.27).

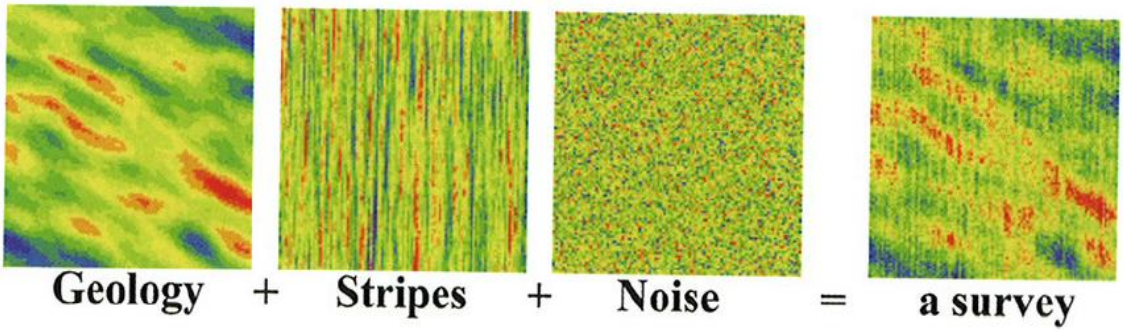


*Figure 3.23: A synthetic example shows the effect of geology, strips and noise in a seismic survey.*

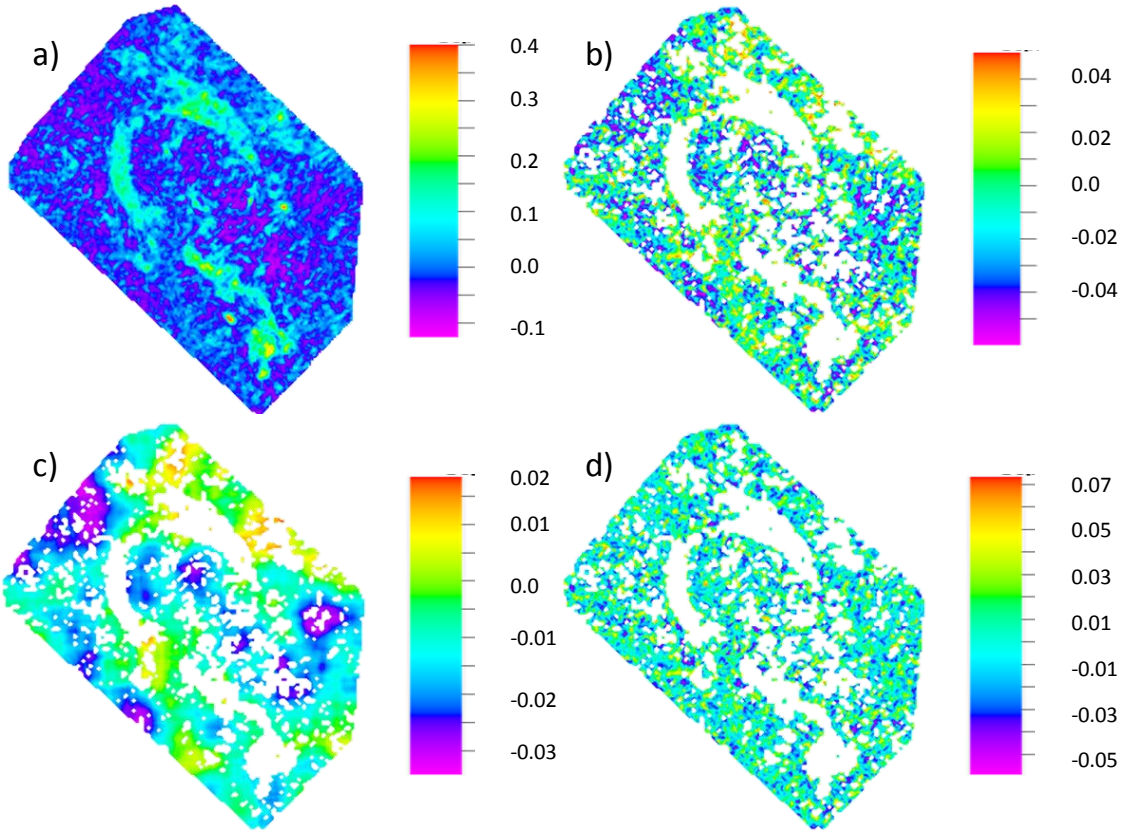


*Figure 3.24: The 2D map of a) original 4D map (Well+base map defined in Chapter 5, Figure 5.7c), b) original map filtered by 4D signals, c) local average performed on b, and d) the residuals for subtracting c from b.*

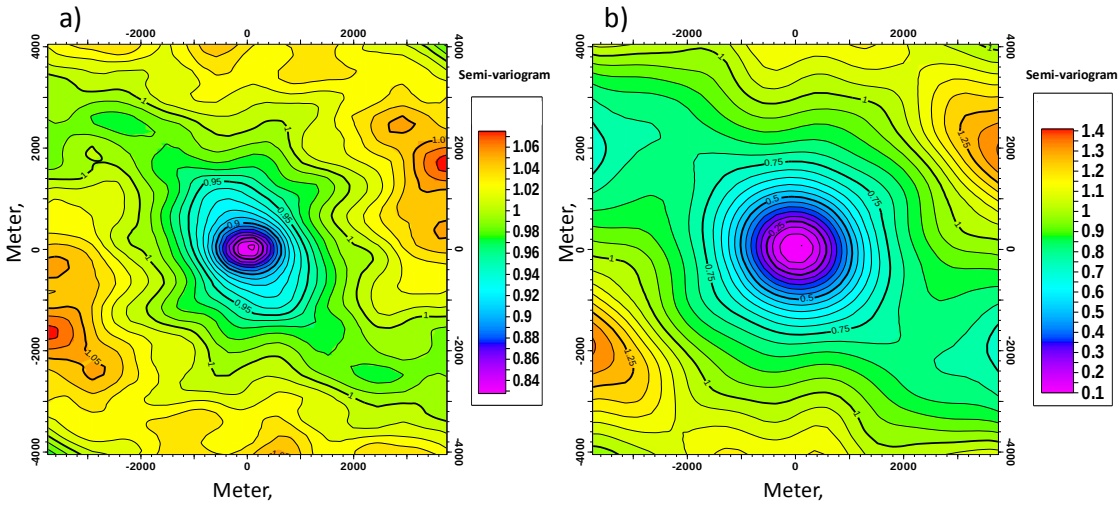


*Figure 3.25: 2D semi-variogram map of the a) original survey (Figure 3.24a) and b) calculated local average attribute (Figure 3.24b).*

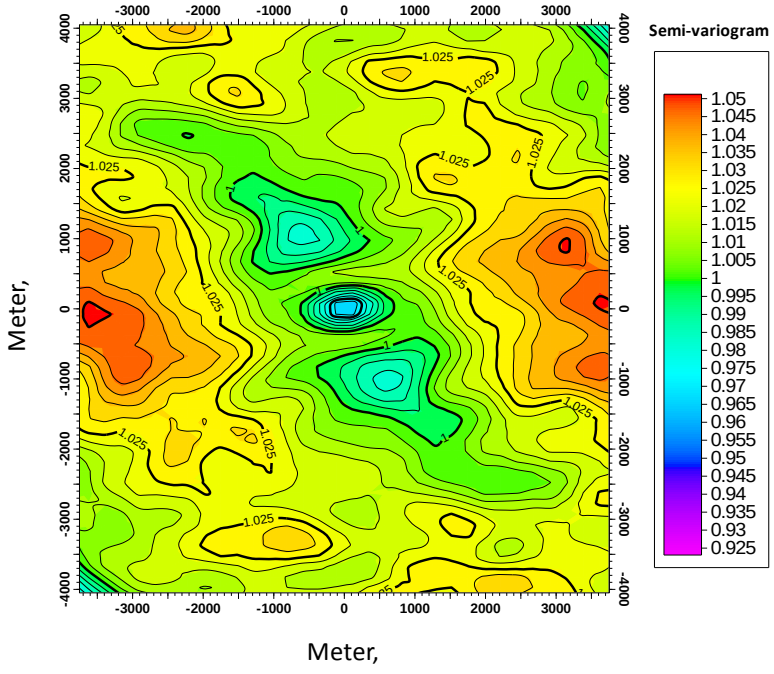


*Figure 3.26: 2D semi-variogram map for the residual map presented in Figure 3.24d.*

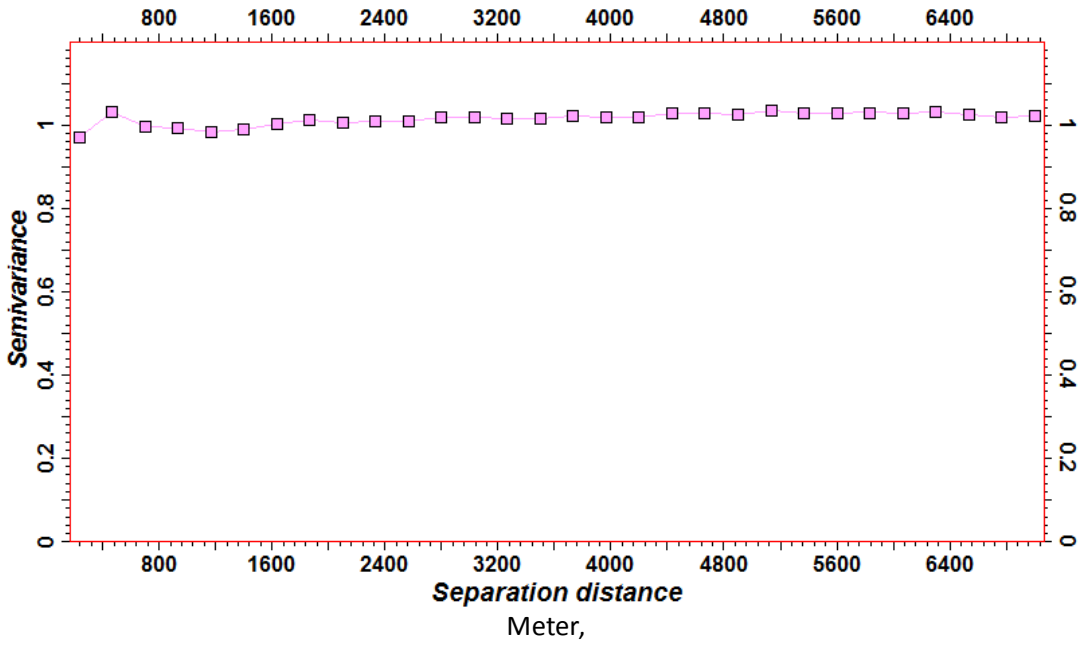


*Figure 3.27: Mono-variogram in NW-SE direction (the direction of the elongated structures) for residual map (Figure 3.24d).Symbols indicate the value of semi-variogram at each separation distance.*

Based on the fact that noise is not correlated in our data we tried to calculate the standard deviation of noise. For Figure 3.24b we calculate standard deviation using Eq. 3.7 below.

$$\sigma = \sqrt{\frac{1}{N-1}\sum_{i=1}^{N}(x_i - \bar{x})^2} \tag{3.7}$$

Where $\{x_1, x_2, \dots, x_N\}$ are the observed values and $\bar{x}$ is the mean value of these observations.

### 3.8 Production data

For Nelson we were provided history of monthly oil and water production volumes for the wells from 1994 to the end of 2003. These were converted to give average monthly, quarterly and biannual rates. Depending on the location of the wells in the reservoir there are generally two types of the wells. A high water production was observed for the wells that are located in the Channel Axis sands and for the wells in the Interchannel sands there is a low water cut as shown in Figure 3.28.

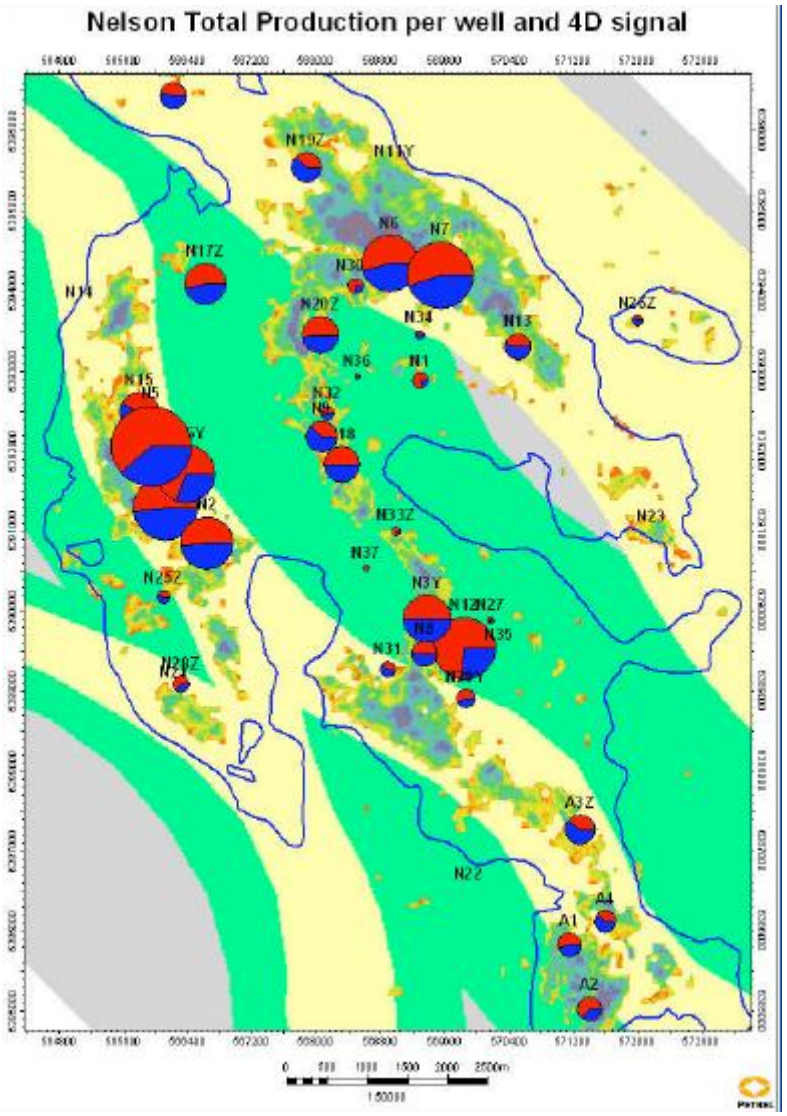


*Figure 3.28: The water cut in each production well (red colour in each circle) across the geological regions. The area of each circle shows the relative total production rate for the well up to 2003 (Shepherd and Gill 2009).*

### *3.8.1 Data error of production data*

As discussed previously, in Chapter 2, the standard deviation of production data should be identified for input into the misfit function (Eq. 2.19). Based on the information from the operator, a 10% error in oil and water production rates at the wells was used while 1% was used for field total rates. Also, a normal distribution of production rates and two standard deviation covers 95% of data. The average values for water and oil rate for the whole wells are 2800 and 6000 STB/day respectively. Therefore the standard deviation for each rate is obtained from:

$$1.1 \times mean = mean + 1.96 \times standard\ deviation \tag{3.8}$$

This gives the standard deviation of 142 and 306 STB/day for water and oil rates respectively.

### 3.9 Simulation model

This history matching study is based on a simulation model which was generated by the operator of the field. The model has more than 500,000 thousand active cells and the size of each cell is approximately 75 X 75 X 8 m. There are several faults in the reservoir with good fault transmissibility and therefore, they do not affect the flow behaviour. Figure 3.29 shows the histogram of different reservoir properties for the simulation model.

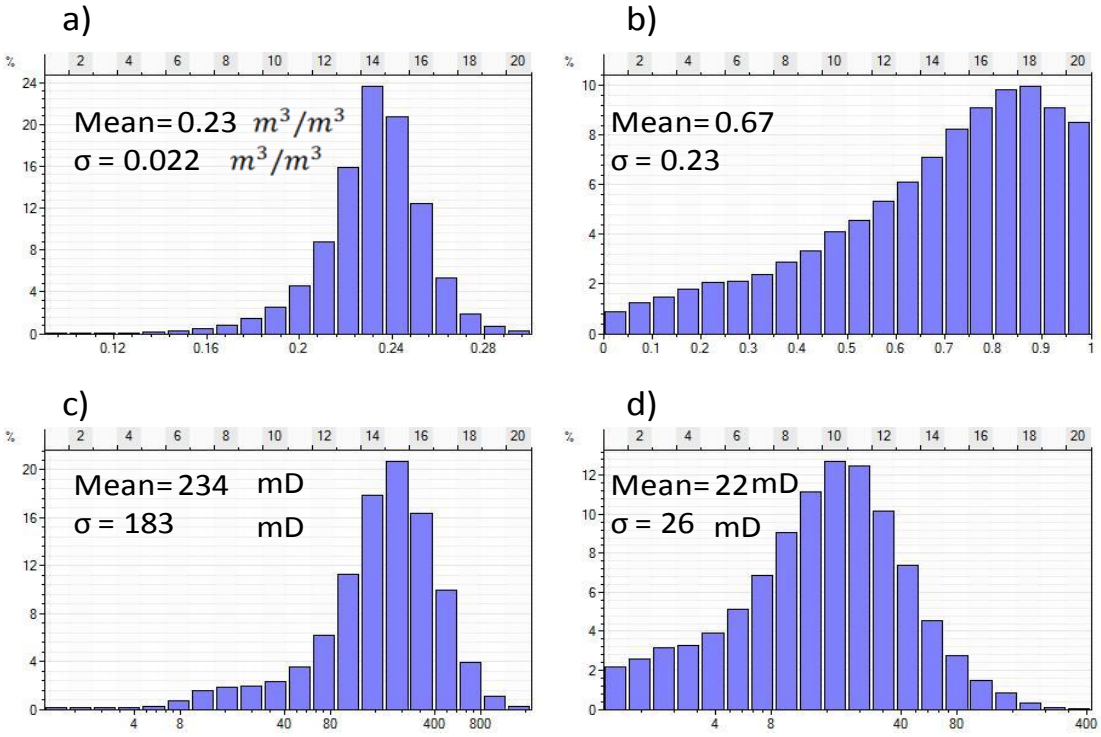


*Figure 3.29: The distribution of different reservoir properties, a) porosity, b) net:gross, c) horizontal permeability and d) vertical permeability.*

Figure 3.29a shows the same trend of porosity as Figure 3.10. The mean value for net:gross, horizontal and vertical permeability in the model are 0.67, 234 mD and 22 mD respectively. The reservoir properties in the Channel Axis and Interchannel sands for the top reservoir interval (T75) in Nelson was compared. In Figure 3.30 we can see that from the Channel Axis to Interchannel sands there is a shift in the histogram to the left side which means a reduction of the properties because of shalier characteristics of

the Interchannel sands. The mean value of net:gross changes from 0.73 to 0.6, horizontal permeability from 321 to 122 mD and vertical permeability from 33 to 11 mD. From the top reservoir interval (T75) to bottom reservoir interval (T70) there is also a reduction in reservoir properties. For example in the Channel Axis, the net:gross reduces from 0.73 to 0.66, horizontal permeability from 321 to 230 mD and vertical permeability from 33 to 23 mD (Figure 3.31).

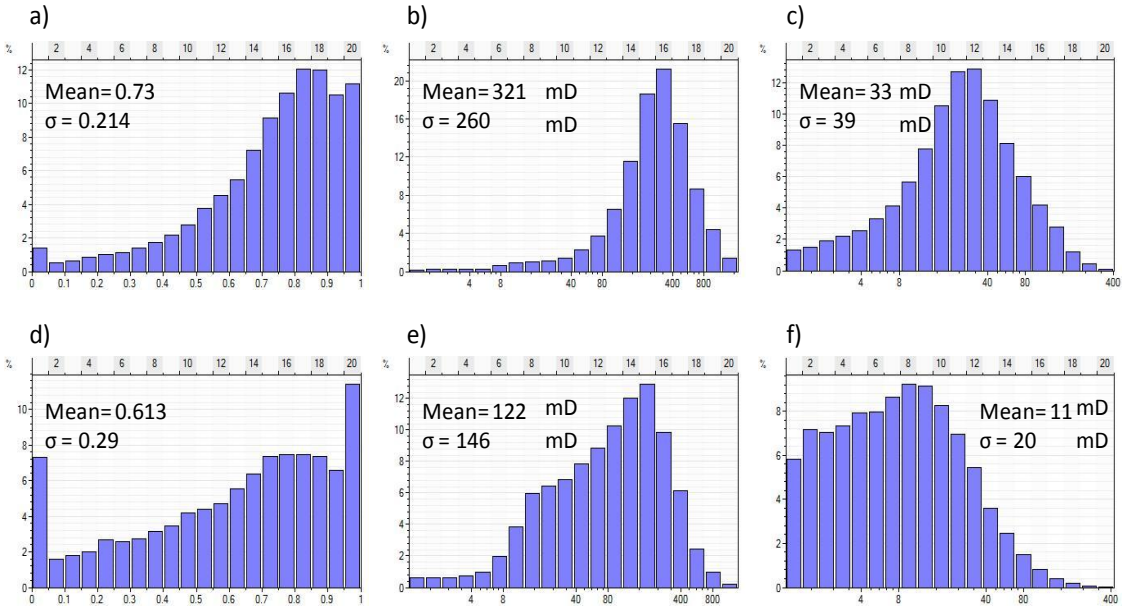


*Figure 3.30: Distribution of reservoir properties in the first reservoir interval (T75) for Channel Axis, a) net:gross, b) horizontal permeability and c) vertical permeability and Interchannel area d) net:gross, e) horizontal permeability and f) vertical permeability.*

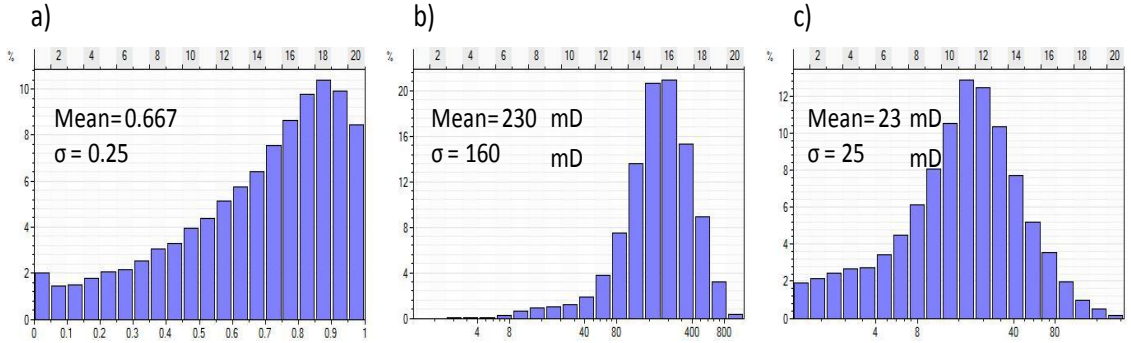


*Figure 3.31: Distribution of reservoir properties in second reservoir interval (T70) for Channel Axis, a) net:gross, b) horizontal permeability and c) vertical permeability.*

Figure 3.32 shows the average value of various reservoir properties for the first and second reservoir intervals respectively. All reservoir properties are quite high in the

Channel Axis in the first and second interval which is consistent with the histogram of properties presented previously. In Interchannel and Channel Margin regions the reservoir is more shaly reflected by low value for net:gross and permeabilities.

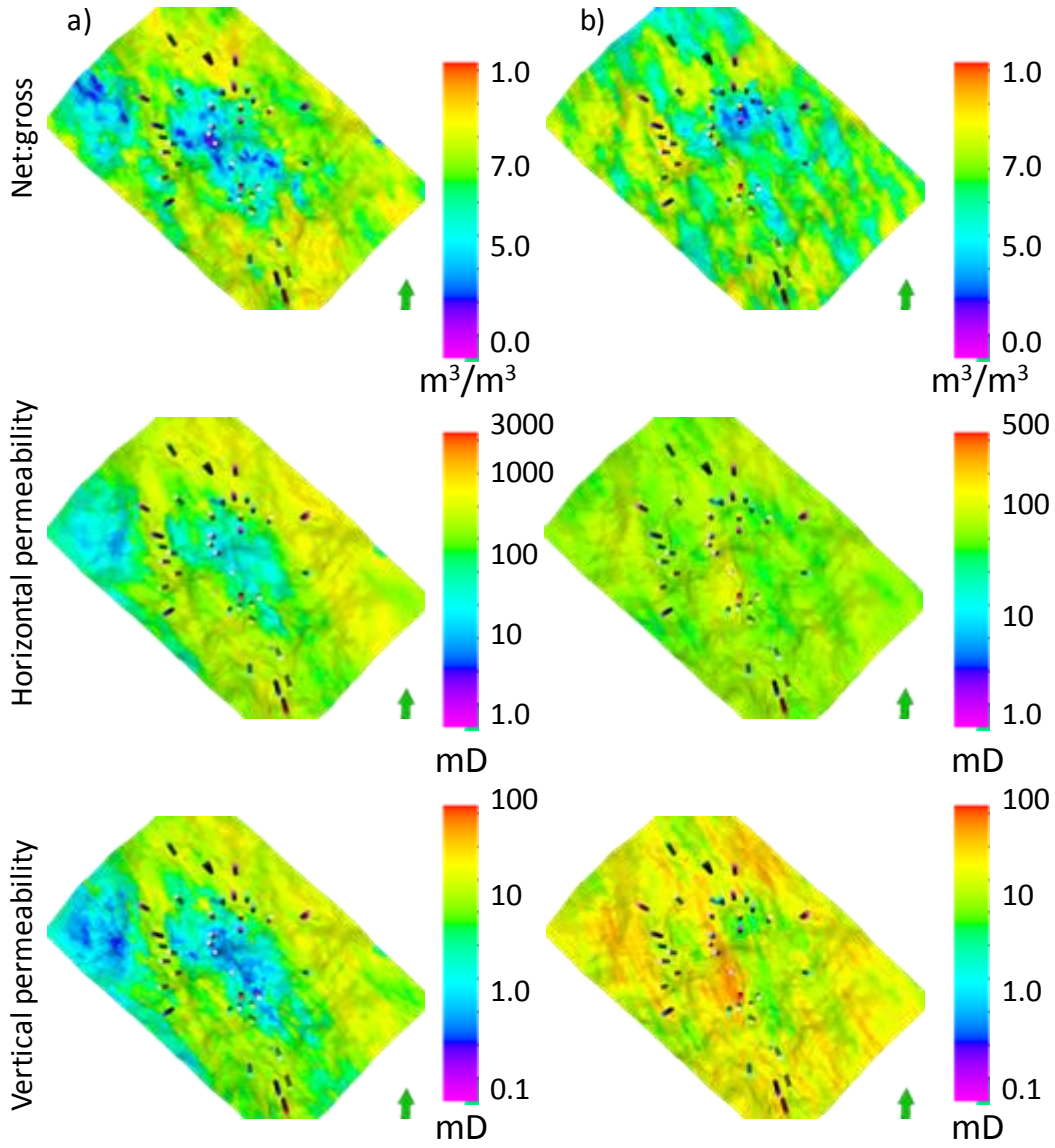


*Figure 3.32: Average reservoir properties for first (a) and second (b) reservoir interval.*

Figure 3.33 shows the properties of the reservoir in the third interval (T65, Section 3.4) which is also the location of bottom aquifer. The histograms show that the properties in this part of the model are quite high and more like those of sand.

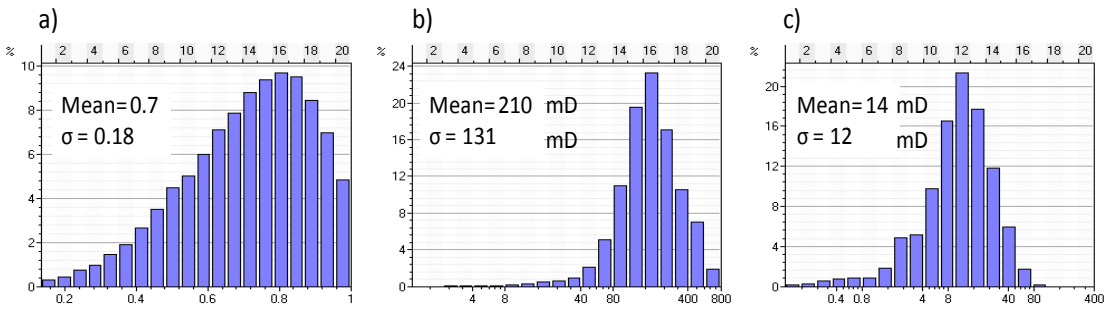


*Figure 3.33: Distribution of reservoir properties in third reservoir interval (T65), a) net:gross, b) horizontal permeability and c) vertical permeability.*

The calculated water and oil production rates from the base simulation model shows that from 1994 to 2000 the base model generally produces more water compared to reality and less oil. The total production volume of water for all wells is around 18% greater than observed and for oil it is 6% less (Figure 3.34). Therefore the goal of history matching would be to update the reservoir model in order to produce less water and more oil compared to the base simulation model.

Oil and water production rate for each individual well are plotted in Figure 3.35.

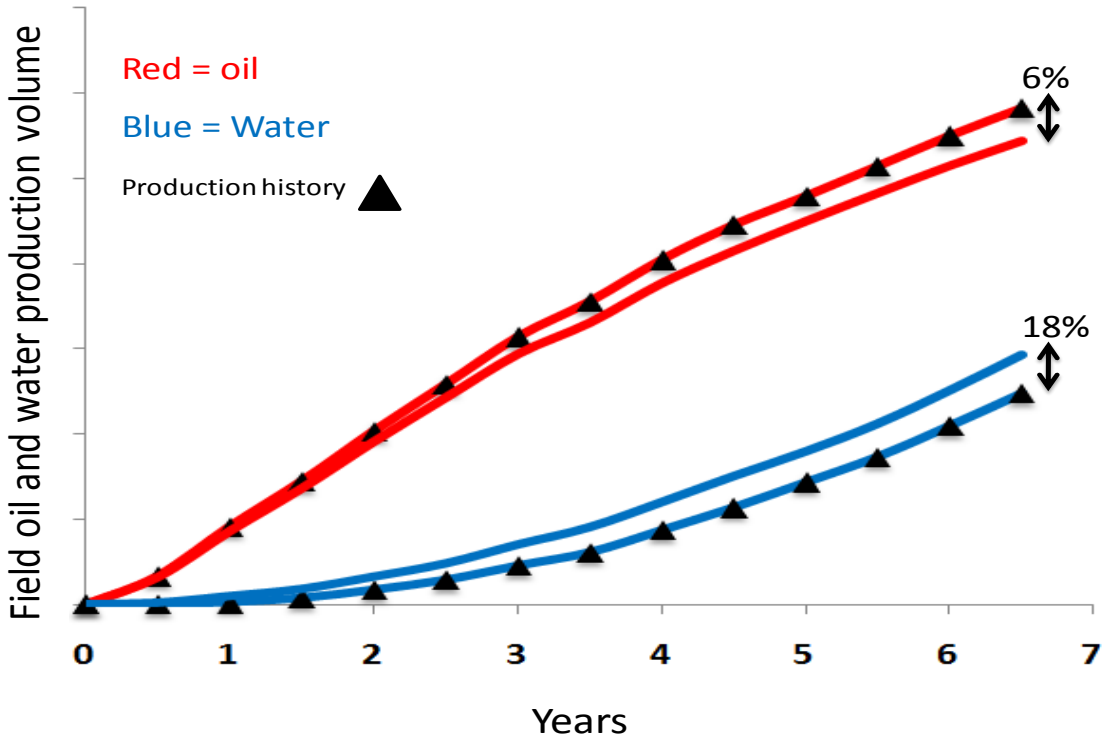


*Figure 3.34: Field oil and water production volumes for historical and simulated data.*

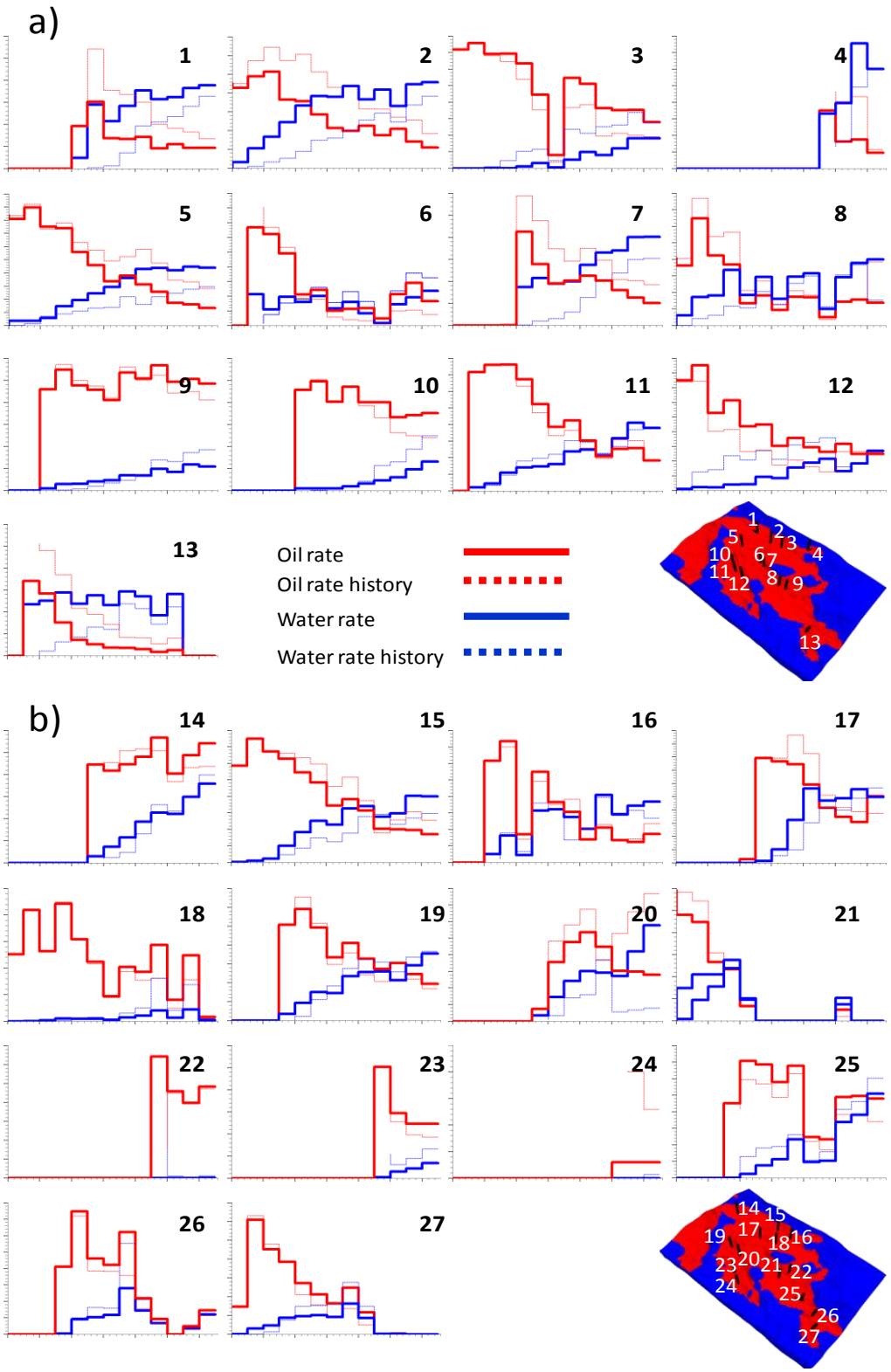


*Figure 3.35: Oil and water production rates for each individual wells for a) first 13 wells with highest misfit and b) the rest 14 wells. Well numbering is based on geographical locations from left to right and top to bottom.*

### 3.10 Summary

In this chapter a summary of important information has been presented for the Nelson field. The important points, which are the basis for the rest of the thesis, are summarized as below:

1- The Nelson field is a channelized reservoir which consists of (in order of increasing shale content) Channel Axis, Channel Margin and Interchannel sands.
2- Three reservoir properties, net:gross ($NTG$), horizontal ($K_h$) and vertical ($K_z$) permeability control the effect of the shale proportion and continuity on flow (Section 3.4).
3- The production process in Nelson is water displacement from injectors along with aquifer support. Bottom drive is expected in the Channel Axis sands and edge drive in Channel Margin sands. The same reservoir properties as an item 2 can control the water displacement in the reservoir.
4- The production rates from the base model shows that the simulation model needs to be updated in order to have less produced water and more oil.
5- Based on the above for the rest of this work the goal is updating net:gross, horizontal and vertical permeability in appropriate parts of the reservoir in order to first, modify the shale volumes and distributions and second, to control better water displacement in the reservoir.
6- The reservoir consists of two different intervals, separated by a shale barrier, which creates two separate hydraulic flow unites. In this study, therefore the reservoir has been updated to takes into account the separation between the two intervals.
7- There are 9 years of production history of the wells (1994 to 2003) and 4 seismic surveys (1990, 1997, 2000 and 2003). In this study the 6 years production and the seismic data from 1994 to 2000 has been used as a history matching period and three further years of data from 2000 to 2003 were used to check the accuracy of new models in order to forecast the production behaviour.
8- It has been concluded that there is a similarity between water saturation change of the reservoir and the observed seismic data.

# Chapter 4: PRODUCTION HISTORY MATCHING IN NELSON USING STREAMLINE GUIDE APPROACH

**Overview:**

In this chapter we report that history matching of the Nelson field began by appropriately finding the right locations to modify the model. Also, reasonable combinations of the parameters that needed to be changed were identified. These included petrophysical properties such as net:gross and permeabilities in specific parts of the reservoir individually or across second region simultaneously. For this chapter production data only was used in the history matching.

## 4.1 The general strategy for history matching of a reservoir

In order to have success in solving the history matching inverse problem, an appropriate strategy needs to be considered. This strategy involves understanding and analysing available data such as geological information or fluid flow patterns in the reservoir, studying the sensitivity of the effect of selected parameters on fluid movement, combining different variables in the history matching study in order to keep the geological features and to control the fluid displacement, and finally analysing the output of simulation and deciding to accept or reject the new reservoir models. Figure 4.1 shows a complete workflow of history matching of a reservoir from the beginning (which involves choosing the regions to update in the model) to the end.

The first stage in a history matching strategy is likely to be selection of reservoir variables that require modification. Also we need to know where and how these variables need to be updated in the reservoir (Stage 1 in Figure 4.1). Generally for any history matching study, the reservoir parameters which include, their location where modifications are made, must then be chosen using the available knowledge for the uncertainty of various data in the reservoir, the geological understanding of the reservoir and also change to the fluid movement that can be expected. In this study the guide for choosing the reservoir properties initially is mainly based on the geology of the reservoir and different fluid flow behaviours that were discussed in Chapter 3 (Section 3.4). As a reminder, the challenge in Nelson was to update shale volumes, their distributions and effect on flow by updating three variables net:gross, horizontal and

vertical permeability. Multipliers are used to change those variables and a reasonable range needed to be chosen based on prior information. We considered these to be the most important variables with respect to the history match and only changed those.

For selecting the updating regions in the reservoir, the idea in this study is that by using streamlines. Streamlines represent the path of fluid displacement in the reservoir, therefore appropriate selection of regions to update can be made. This idea would be suitable for the any active region of the reservoir.

For appropriate updating of the reservoir, various parameter updating schemes are introduced (Stage 2 in Figure 4.1). This is the main focus on this work, where we sought the most efficient ways to combine the parameters in order to reduce the number of simulations significantly and make Automatic History Matching (AHM) workable. It is worth mentioning that the aim in this chapter is to introduce various updating schemes that should be suitable for any field. However, certainly there are some limitations and drawbacks for each scheme that also will be discussed in this chapter. In the study, because of the limitations for running a huge number of simulation models for high dimensional problems, it was considered that the maximum number of models should be 4000 for a given history matching run. Various runs are then compared.

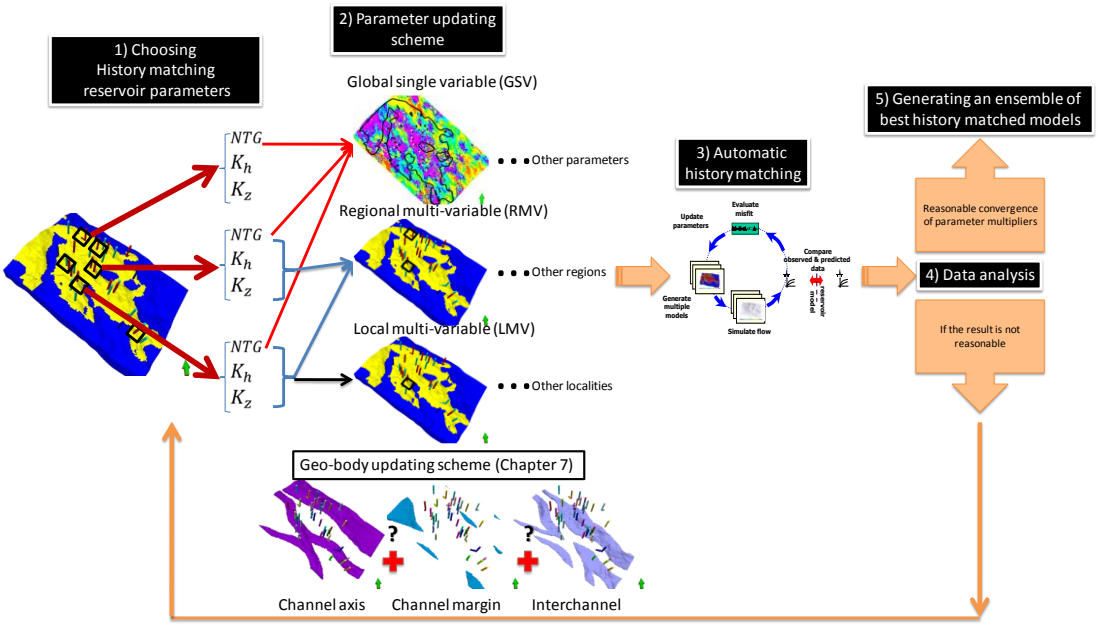


*Figure 4.1: The place of the parameter updating schemes in the automatic history matching workflow.*

As an alternative to the various parameter updating schemes shown in Figure 4.1 (and discussed later in Section 4.3) we also introduce another approach for updating the reservoir which is based on geo-bodies in the reservoir. In this scheme history matching parameters were modified in a geographically broader scheme in various geo-bodies. This approach was tested and discussed further in Chapter 7 (Figure 7.1 shows more information for this updating scheme).

As part of using an AHM workflow (Stage 3 in Figure 4.1) the aim was to reduce the mismatch between observed and modelled data by updating the parameters in the reservoir and applying data analysis (Stage 4 in Figure 4.1). After analyzing the parameters, and also the reduction of misfit, there were two options. If the results were satisfactory and the parameters converged to a specific value, we went to the final steps of the process (Figure 4.1 step 5) and by combining the best results; an ensemble of best reservoir models was obtained. Otherwise, the process returned to the beginning of the loop and chose another region for reservoir updating, changing the parameters or modifying the range of the parameters for sampling. In the following sections there is more discussion about the different parts of Figure 4.1.

## 4.2 Streamline guide concept

In heterogeneous reservoir models, the effect of preferential flow paths can often be seen in simulators using streamlines. These will appear to be more densely distributed in regions of high flow rate (Figure 4.2). Since these regions channel most of the flow, it is reasonable, therefore, that we should focus on them first to improve the prediction from models. This flow channel could be, for example, a body of sands with high permeability. The flow is then more likely to pass through that region. The breakthrough time and the growth of early water cut for a well are probably controlled by the flow properties in these regions. It may be that the permeability of such conduits is greater in comparison to the surrounding region or the width of such regions may be incorrect in the model in these considerations. The initial modifications were applied to the model on these regions. The assumption is that the base case simulation model contains a reasonable representation of the dominant flow pathways and for the purpose of this work, they will not change with additional realizations or changes to the geological model. This is reasonable in many cases where the model is constrained to seismic data at the larger scale. Figure 4.2 also shows that there was a change in the

streamline density over time. If this changed too much then it was not possible to focus on one region. On the other hand, the aim was to use the most representative distribution to identify the region targeted for updating.

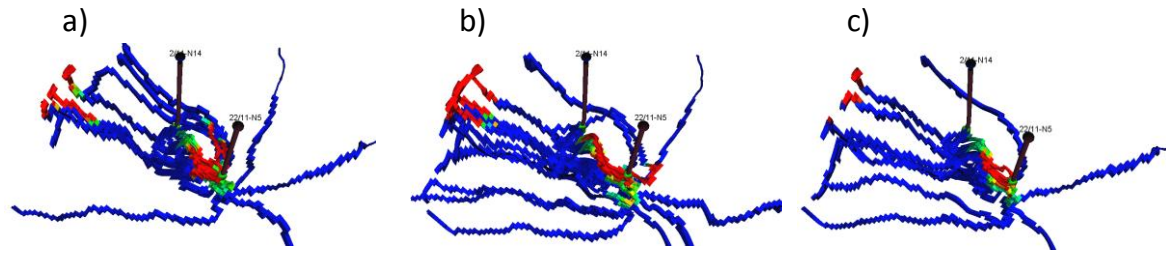


*Figure 4.2: Streamline pattern for one production well in Nelson showing a cluster changing at different times a) July 98, b) Oct 98 and c) Jan 99. Only a fraction of streamlines are shown, evenly sampled for better visualization.*

In Nelson, the monthly volumes of water and oil produced were used to generate either monthly or biannual rates of production. The former were used for fixing pressures in the streamline simulation approach where streamlines were used as a guide. On the other hand the streamline simulator was also used for each new model during the history matching study and for that the biannual rates were used in the data set to reduce the CPU time. The data for the first six years of production were used as a history matching constraint. To reduce the size of the problem, the 6 wells with the largest misfit were targeted initially. Figure 4.3 shows the location of the wells in Nelson. Around each well there are regions occupied by a master pilot point and history matching variables are going to change there. There was almost no interaction between these wells and the various locations of pilot points. The misfit for each well varies over time (e.g. Figure 4.4) and the focus was on those time steps with the biggest misfits. For each well, we used streamline distributions for the steps within an arbitrary 25% of the maximum time step misfit for that well. This range of misfit was chosen for each of the 6 wells and covers different volumes of total water production over the 6 years. The time window represented 30% for well 6 compared to 78% for well 2.

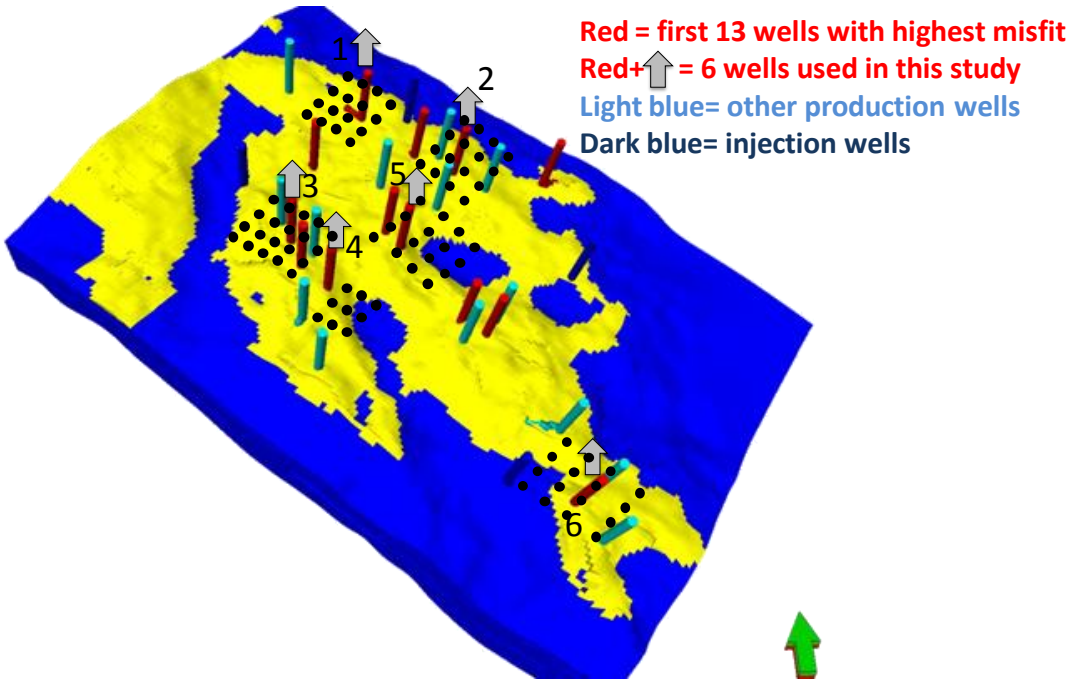


*Figure 4.3: Location of wells selected for history matching along with the other production and injection wells in the reservoir. The black dots show master pilot points for 6 wells.*

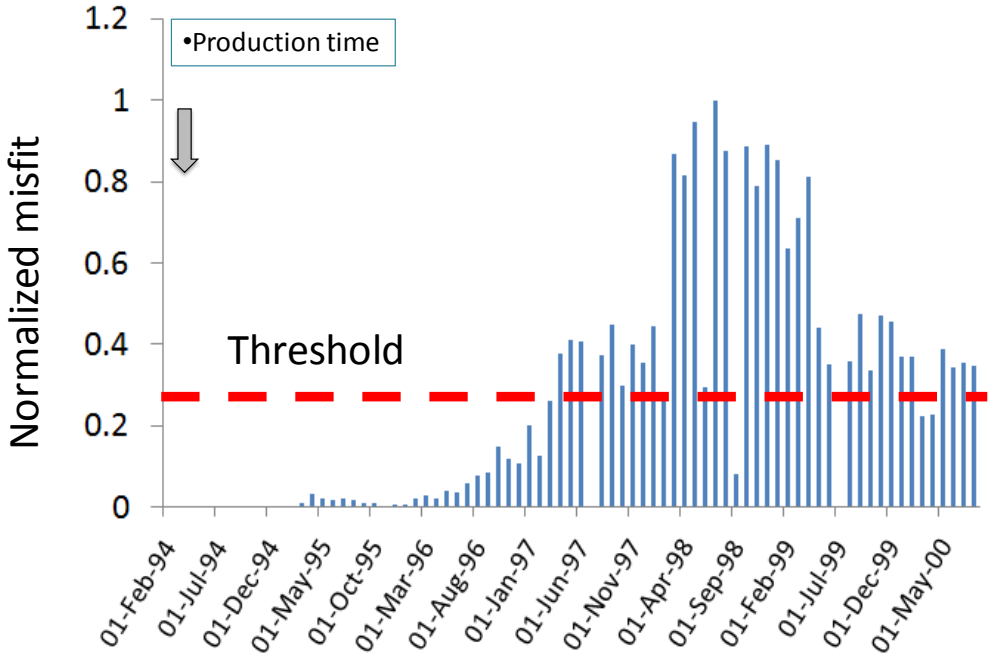


*Figure 4.4: The normalized misfit value for an example well as it varies over time. A threshold of 25% of the maximum is used as a threshold for investigating streamline distributions.*

In previous studies (Cheng et al. 2005, Arroyo-Negrete et al. 2008), the impact of streamline sensitivity from changes to individual cells was considered. In this study a

wider volume was considered through which a cluster of streamlines passes. The aim is to generate a more qualitative understanding, therefore. This also allows us to set up a master pilot point such that groups of pilot points are used and properties at each individual location are changed by the same change within the group. Figure 4.5 shows the well in Figure 4.4, and specifies the region that was finally chosen for the location of master pilot points in this case. This region covered most of the streamlines around this well.

The same procedure was applied to choose pilot point locations needed for other wells. For a larger number of targeted wells, the number of pilot points needed to be increased and master pilot points eventually overlapped. The separation between pilot points was 5 simulation cells (~500m) in this study and for the cells around the pilot points, Kriging with a variogram range of 15 cells (~1500m). Depending on the size of the region that was updated, the number of pilot points varied between 9 and 25 per master pilot point. As an example the Figure 4.3 shows the pilot point locations for all targeted wells.

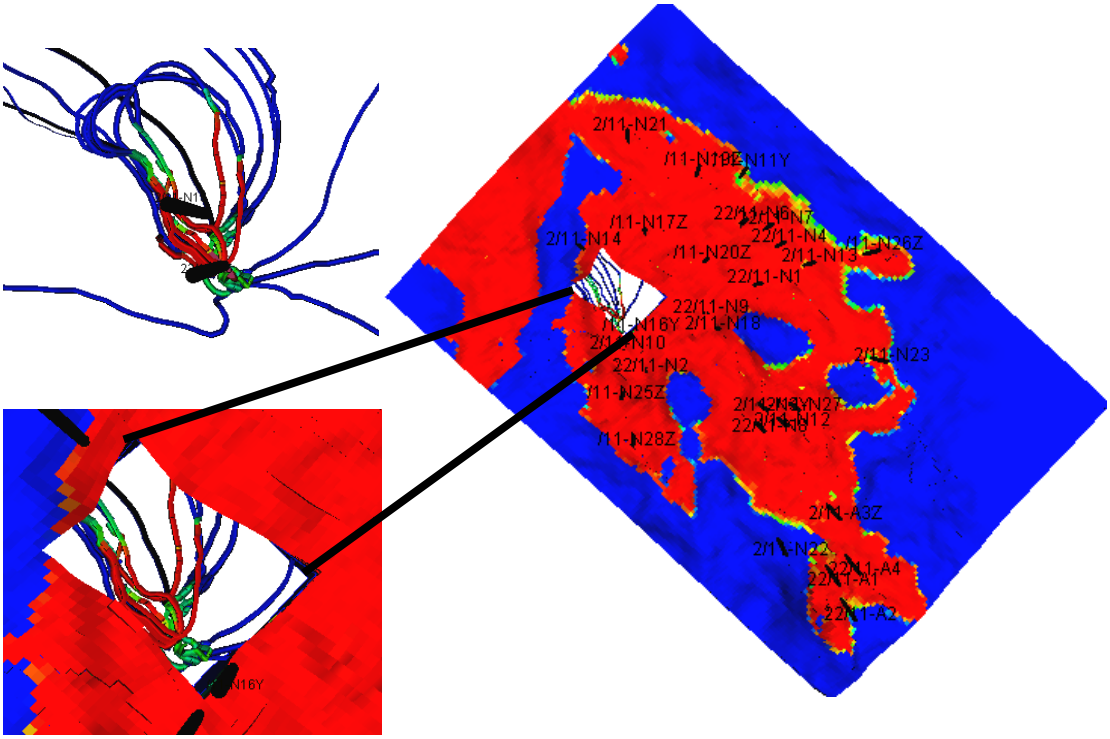


*Figure 4.5: An example location of the master pilot point near a well chosen by streamlines.*

### *4.2.1 Sensitivity of pilot point locations*

In order to understand better the importance of using streamlines to guide the choice of pilot point locations, a sensitivity analysis was performed. For each well, the streamline approach was used to identify a preferential location of the master pilot point and the modified region is offset from the well. This means that roughly three-quarters of the region around the each well was unchanged. In this study, the relative impact of changing those other three quarters was considered. Each quarter was treated as a pilot point region, separately or together with the streamline guided region. The streamline guided regions was identified in Figure 4.6 as the black box and the other three regions using the coloured arrows with labels A-C. These new pilot point locations were treated in the same way as the streamline guided region such that the dimensionality of the sub-problem was the same.

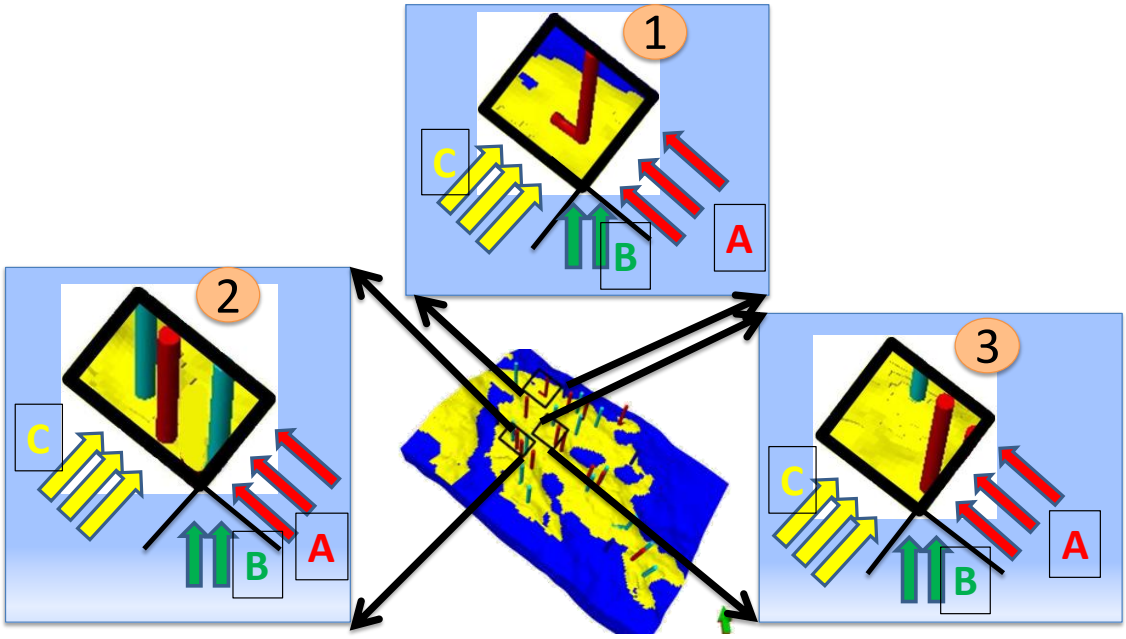


*Figure 4.6: Wells and associated regions in the reservoir chosen for a sensitivity study of the streamline guided approach. Black boxes indicate regions suggested for updating by streamlines while A, B and C regions are alternatives considered for each of the three wells.*

The three wells were chosen in Figure 4.6 due to their respective fluid behavior which results from connectivity between wells and the aquifer. For Well 1, regions 1B and 1C were located between Well 1 and another well and changes there affected the water displacement from the aquifer. The streamline guided region for Well 2 was also

situated towards the edge of the reservoir with an injector nearby. There were two other producers very close and within the box. Although particular wells were targeted to improve the match, we did not want to degrade the match of other wells in the process. Region 3 was located at the centre of the reservoir and there was no injector close to this well. In contrast to Wells 1 and 2, this well was completed in both geological intervals whose different properties add complexity. Three regions for pilot points were chosen in both intervals around this well and each could be control of different water displacement toward this producer.

Wells 1 and 2 history matching cases were three dimensional for the original streamline guided region and so for A, B and C the same dimensionality was considered for each well. Each of A, B and C properties were changed on their own and also history matching was performed for modifying them with the region identified from streamlines so that there were six dimensional problems. The reason for combining two regions (or sets of pilot points) was to investigate whether or not there was a local interaction or if changes were spread more widely around the well. For Region 3, however, the pilot point locations were in two intervals and the problem was 6 dimensional. Therefore history matching only run individually in 3A, 3B and 3C as 6D to avoid 12D problems.

Figure 4.7 compares the misfit change when updating the alternative regions A, B or C on their own compared to the streamline guided case. The streamline guided result was clearly the best option in all cases. There was some improvement to the target wells when changing the properties in the other regions. In fact, different results were observed with less change in the streamline guided region when combined with A, B or C. However, it was found that the misfit of non-targeted wells deteriorated. If these were included in the misfit then very little change to the alternative regions occurred. This sensitivity study for the three wells showed that regardless of the complexity of the history matching problem (in terms of the combination of well location and interaction with other parts of reservoir) the optimum location of pilot points around these wells were found using the streamline guided approach.

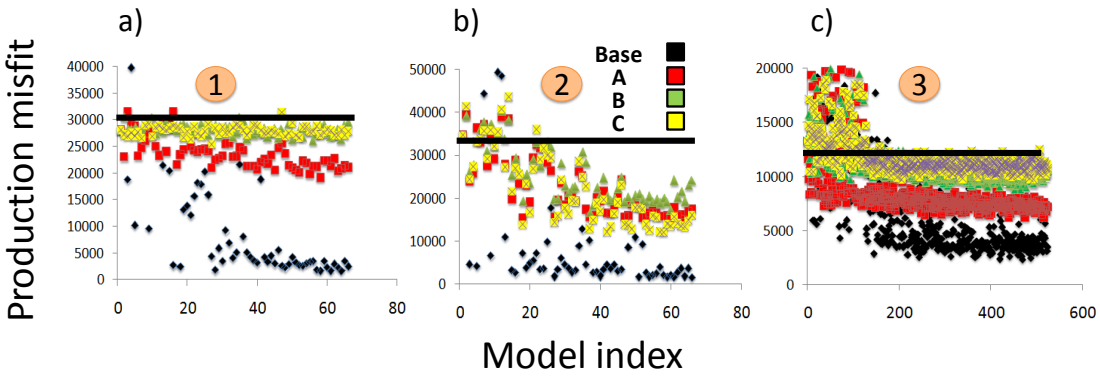


*Figure 4.7: Reduction of production misfit value using the alternative location of master pilot point compared to the original case using streamline guide approach for 3 regions a) 1, b) 2 and c) 3. The colour coding is consistent with the colours of A-C in Figure 4.6.*

### 4.3 Parameter updating scheme

All history matching methods require a scheme to search the parameter space using information about misfits from existing models. In general it may have to be assumed that each parameter that changes interacts with the others when considering their effect on the misfit. In large dimensional problems, this assumption can require that a prohibitively large number of simulations be carried out. The number of simulations grows exponentially with the dimension of the problem.

The main reason for introducing various parameter updating schemes, in this study, was because of the lack of computing power to perform the inversion of a high dimensional inverse problem on the one hand. On the other, the aim was to retain the geological features of the reservoir by updating the right parameters in the right locations. In the updating approaches that were used in this study, different variables were combined in the model during the AHM process. This was done globally for the all updated regions in the reservoir or locally for each individual region. The global term here means that parameters were modified for all the selected regions in the reservoir (we may have other definitions for global such as geographically, where we change the reservoir model in every cell, which is not the case here). Then within each updated regions, an appropriate geostatistical method was used to smoothly propagate the updated parameters in the reservoir. This geostatistical approach was the pilot point with Kriging which was introduced previously in Chapter 2 (Section 2.2).

### *4.3.1 Global single variable approach (GSV)*

In this approach, just one variable was changed at a time. This scheme is suitable for those cases where history matching parameters do not have interactions such that they are independent. As an example, if the history matching problem is solved by first matching reservoir pressure and then flow rates (as is often done manually) we can focus on separate parameters. For example by updating aquifer properties (as a single variable) or field average permeability through history matching we can first match the reservoir pressure response. Then by updating appropriate reservoir parameter such as permeability variations or relative permeability we can match liquid production (usually water cut) from the reservoir.

In this study the GSV method was applied to properties such as Net:Gross which was changed at all locations selected for updating in the reservoir while permeabilities are fixed to capture some of the regional parameter interactions (follow red arrows in Figure 4.1 to net:gross map). The same procedure was then repeated for other variables (fixed variables were set as the base reservoir model). For this study we are dealing with three reservoir variables. Updating net:gross alone can have an important influence on history matching by increasing the amount of pore volume in the reservoir and hence STOIIP. Horizontal permeability updating alone can have an influence of lateral water displacement in the reservoir which can be important to match the well performance and vertical permeability has a reasonable effect on water displacement from the bottom of the reservoir to the producers. However, there is often some relationship between various petrophysical properties of the reservoir and changing one parameter may require updating the other parameters too. Therefore, there is a small probability that this scheme will work for the Nelson field.

### *4.3.2 Regional multi-variable approach (RMV)*

This updating scheme is suitable for a field where there are dependencies between selected parameters (such as in the Nelson field) but we can also separate the reservoir into different regions with a low dependency and therefore history matching can performed in different regions. Here, regions were identified within which parameter interactions might occur. Various bases can be used to choose the regions in the model such as separating the reservoir based on different geological intervals, separating by reservoir and non-reservoir sections or using geological bodies such as channels to distinguish between the regions. In Nelson two separate regions were identified with

the help of streamlines. A search was performed for all parameters within a region simultaneously and one region was searched at a time (follow blue arrows in Figure 4.1).

### *4.3.3 Local multi-variable approach (LMV)*

The name of LMV comes from the fact that history matching parameters will be updated locally (i.e. over a few tens of grid cells) in the reservoir. This updating approach can be applied in cases where multiple history matching parameters affect the misfit locally but where there are many small regions that are independent. In this approach the parameters at every locality will be modified simultaneously in order to capture local interactions only. The difference between this approach and RMV is that, here, the selected regions for updating are much smaller and specifically relate to the drainage area of a well. Very precise locations were needed to make sure that there was negligible interaction. All parameters at each locality were updated and one locality is modified at a time (follow black arrows in Figure 4.1) though with a suitable algorithm, all localities could be updated simultaneously.

## 4.4 Data analysis

27 parameters (Figure 4.3) were identified and used with each of the three updating approaches. These parameters were selected based on the well completion intervals. For the wells that were completed in first interval (layer T75 according to definition in Chapter 3, Section 3.4) the master pilot points was located in the region defined by the streamline guide approach (Section 4.2) and then the history matching parameters were set as the multipliers of net:gross, horizontal permeability and vertical permeability in the location of pilot points. The number of pilot points in each master pilot point was varied from 9 to 25 depending on how big the selected region was. For the wells that were completed in both intervals (T75 and T70 of Nelson, Chapter 3, Section 3.4) two separate master pilot point were defined for each interval. Then the multiplier of three parameters were allowed to change separately in each interval in the pilot point locations. 6 parameters were updated during the history matching process for these wells, therefore.

Figure 4.8 shows four typical outcomes of the history matching process and the figure is used to illustrate the results. In Outcome 1 the parameter converges to a specific value

leading to the lowest misfit and we would hope for this every time. Outcome 2 shows that the parameter did not converge to any particular value because in the sampled range, there is no influence on the misfit. This may be because the combination of this parameter with other parameters does not produce a model with lower misfit; therefore technically this parameter does not have an important influence on reduction of misfit value. We might find influence if we also change other parameters in a different range. Outcome 3 means that more than one value of this parameter leads a minimum value. This kind of behaviour makes the analysis of history matching more difficult in the choice of models. In Outcome 4 the parameter approaches the limits that were set at the start of AHM. In this case, in order to make sure that the conceptual geological model is honoured, there is a need to revisit the geological description of the reservoir. If increasing the limit of change for the parameters makes a big change in the reservoir that is not valid, geologically, we should not change the range. Otherwise it is possible to make the range bigger and perform the history matching again to get a better result. In the middle of Figure 4.8e there is the probability curve. The trend for a probability distribution curve is compatible with each outcome. For example when there is an outcome as in Figure 4.8a a probability distribution curve also shows one peak. This corresponds to the most likely parameter value observed during the history matching process to give the minimum misfit.

## 4.5 Effect of changing reservoir parameters on well production

Before starting history matching it is often useful to check the effect of changing each parameter one at a time in each region selected for updating to see the importance of that parameter. For the Nelson field, the information from the operator allowed modification of the selected reservoir net:gross, horizontal and vertical permeability in a range of multipliers from -1 to 1 on a $log_{10}$ scale and for net:gross, particularly there is an upper limit of 1.

Figure 4.9 shows the effect of changing each parameter over a fixed multiplier range in each updated region on the water production misfit of the corresponding well. The misfit for each well was normalized based on the base case water production misfit value of that well in order to make the comparison easier.

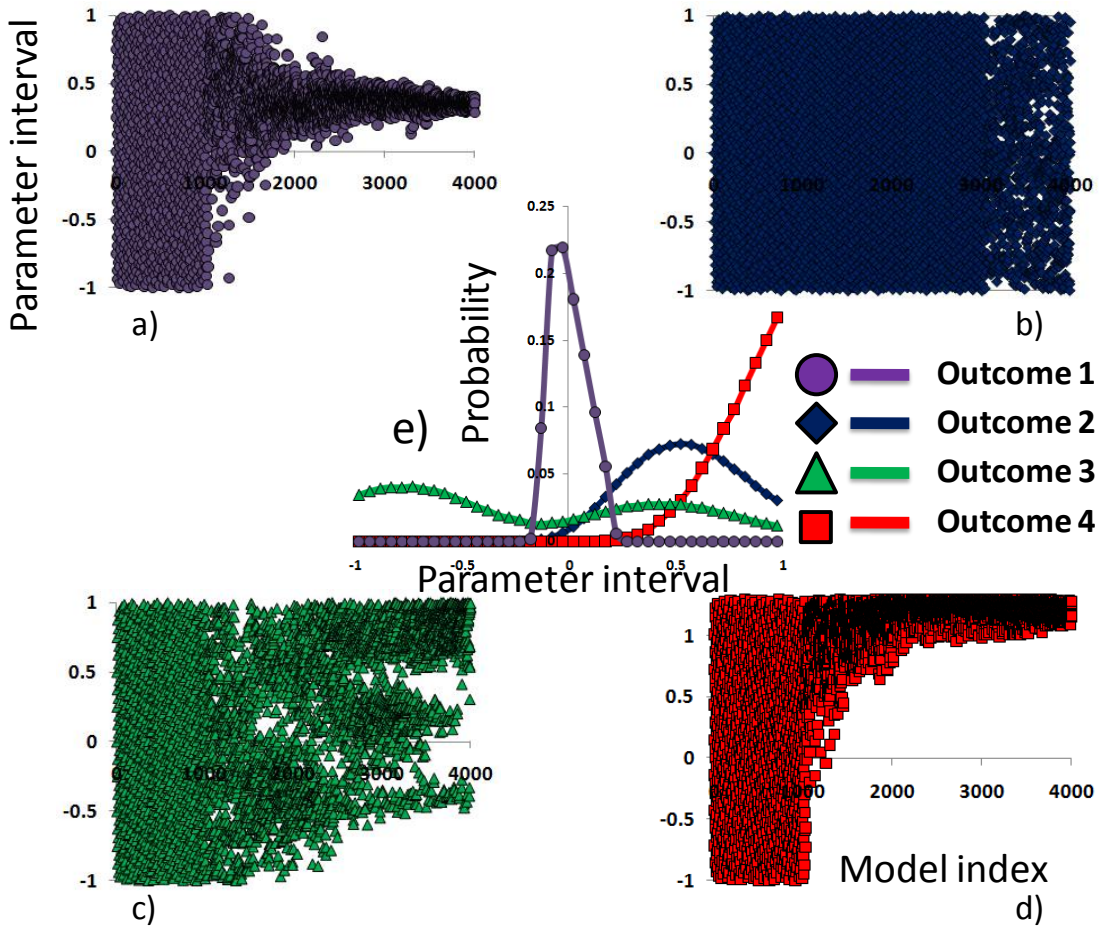


*Figure 4.8: Various outcomes for each parameter chosen for history matching, a) parameter converged to a specific value, b) parameter could not converge to a specific value, c) multiple minima, d) parameter reached one limit and e) probability distribution of each parameter type in parameter interval range during history matching.*

From the analysis of the misfit trend for the wells (Figure 4.9) it can be seen that by changing the multiplier of various parameters, the misfit value is reduced by around 50% of the base case which is quite reasonable except for some cases such as Well 2 in Interval 2, Well 4, Interval 2 and Well 5, Interval 1. The explanation for those exceptions is that because shaly facies exist between the two reservoir intervals (T75 and T70), and the change in the parameter is in one interval only, the fluid displacement in the other is not affected. On the other hand this sensitivity study does not show the effect of updating several parameters at a time which is important in many cases. Therefore the general conclusion of this part of the study is that history matching of this field is needed so that the water displacement in both intervals is captured and predicted more accurately by considering changing all variables in various combinations.

Generally, for analysing the sensitivity parameters of history matching, we can perform Experimental Design (ED) analysis (Chapter 1, Section 1.3.2). In this study a similar approach was used. One parameter was varied at a time and this confirmed that almost all of the selected parameter have significant influence on well production performance. This approach was more straightforward than ED where more models are required.

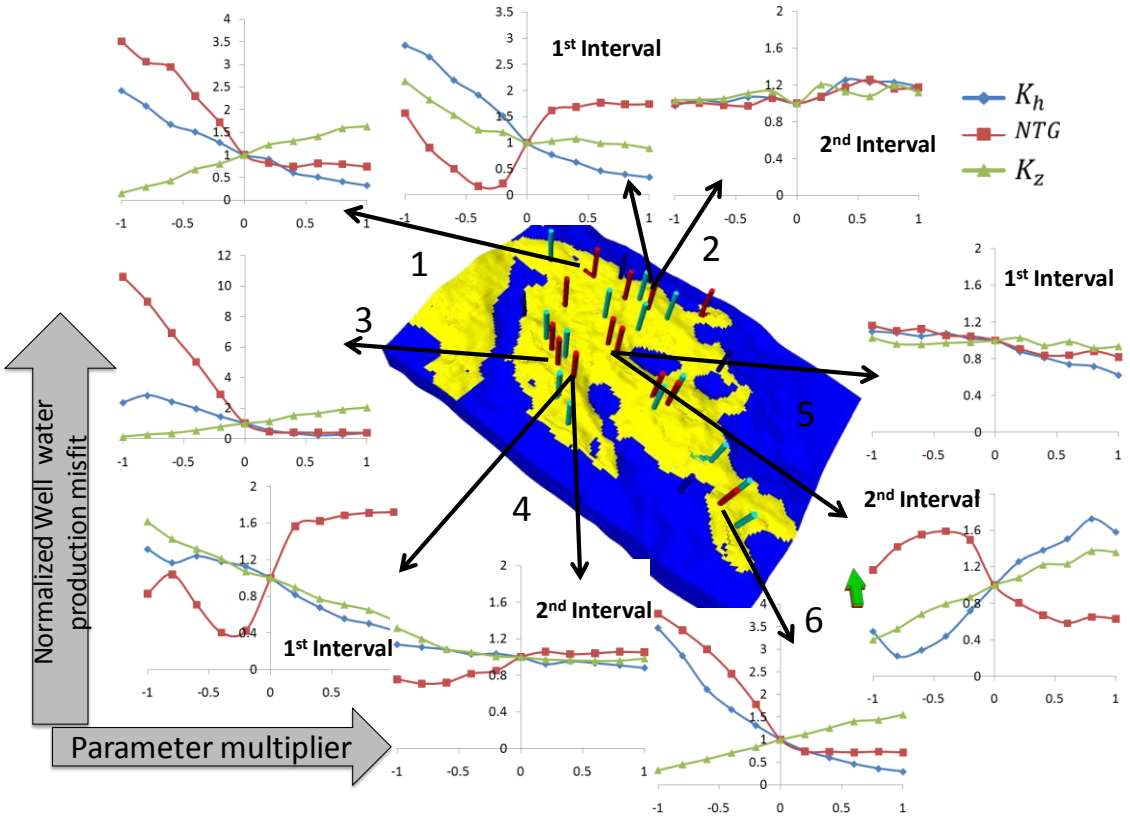


*Figure 4.9: The effect of each parameter on the well production misfit value in each region. The scale on y axis in not the same for all cases because the magnitude of the water production misfit varies considerably. The misfit value for each well was normalized by the base model value.*

### 4.6 History matching result

Table 4.1 shows a summary of important information for the following history matching studies. At the end of each study various history matching results were obtained for each updating scheme. However there were different types of output for history matching including reduction in misfits and the probability density function for each parameter changed during history matching. These results helped us to determine how each approach performs. Also, we can find out the variation of each parameter during the process to make a decision whether or not to modify the range of parameters or not.

The degree of change to each of the reservoir properties (such as net:gross and permeabilities) was also analysed close to each well by the degree of improvement in well production misfit. Finally the ability of the new reservoir models to forecast future liquid production was examined. As discussed in Chapter 2 we used $2^n$ ($n$ is the number of variables) number of models initially.

| | | | | | |
|---|---|---|---|---|---|
| Regions chosen for history matching | 9 regions based on streamline guide:<br>3 in 1st interval only and 3 in both intervals | | | | |
| Reservoir variables updated | $K_h$, $K_z$ and $NTG$ | | | | |
| Dimension | For GSV:<br>9D for each variable<br><br>For RMV:<br>12D for one region<br>15D for another region<br><br>For LMV:<br>3D for 6 regions in first interval only<br>6D for 7 regions in both intervals | | | | |
| NA parameters | | **3D** | **6D** | **9D** | **12D** | **15D** |
| | $\mathbf{n_i}$ | 16 | 128 | 1024 | 2000 | 3058 |
| | $\mathbf{n_s}$ | 10 | 18 | 28 | 36 | 46 |
| | $\mathbf{n_r}$ | 5 | 9 | 14 | 18 | 23 |
| | **total** | 66 | 524 | 4104 | 2720 | 4070 |
| Production well data chosen | Oil and water rates for 6 wells | | | | | |
| Pilot point information | Pilot points separation: ~500m<br>Kriging variogram range: ~1500m<br>The number of pilot points per master: 9 - 25 | | | | | |

*Table 4.1: Main elements for the history matching runs.*

### *4.6.1 GSV*

In this approach the goal was to improve one variable, (such as horizontal permeability) at a time using the history matching workflow. In this study there were just 9 regions making the problem 9 dimensional as summarized in Table 4.1. The history matching was performed to update this reservoir property. Then the same procedure was repeated for the other two variables (vertical permeability and net:gross) and the results were analysed.

The result of history matching for each variable is that the sum of misfits of the oil and water for the targeted wells decreased (Figure 4.10). Horizontal and vertical permeability had more effect on the misfit value compared to net:gross. From this

figure it can be concluded that net:gross modification will reduce the misfit value by around 50%. Also changing vertical and horizontal permeability has reduced the misfit by 70% and 75%.

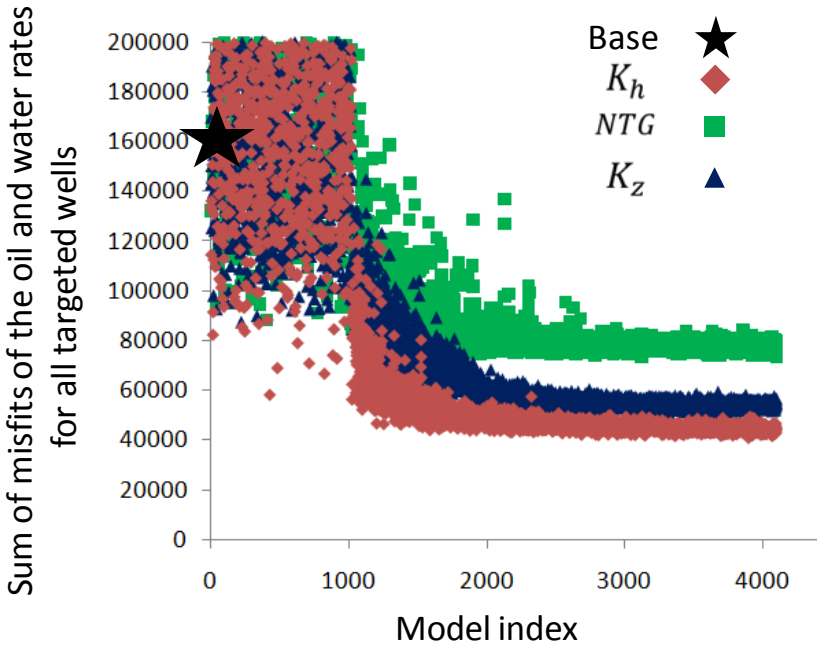


*Figure 4.10: Sum of misfits of oil and water rates for the targeted wells versus model index for automatic history matching (AHM) results changing one variable at a time. The normalized misfit value of base model by dividing over the number of observed data is 1100.*

Of the 27 parameters 13 approached the upper limit and 5 the lower limit. It was decided that for those reaching the upper limit, the limit should be increased to 1.3 (which is equal to a factor 20 multiplier on a linear scale) and a lower limit to -2 for those parameters that approached the lower limits. Increasing the upper limit to more than 1.3 was not geologically valid because the increase in permeability was too large which would alter the geology of reservoir model. For the new repeated history matching study (after updating range of multipliers), as long as the number of master pilot points and the parameters in each reservoir location did not change, the number of initial reservoir models ($n_i$) and number of search ($n_s$) and iteration (NA parameters) were also the same as previous history matching run.

Figure 4.11 shows the reduction of the sum of production misfits for the 6 wells after modification of each variable range. From this figure there was now 50%, 80% and

75% reduction in the sum of misfits of the oil and water for net:gross, $K_h$and $K_v$ respectively. Comparing with the first step of history matching there is only 10% further reduction in the misfit by extending the range of $K_h$ limits.

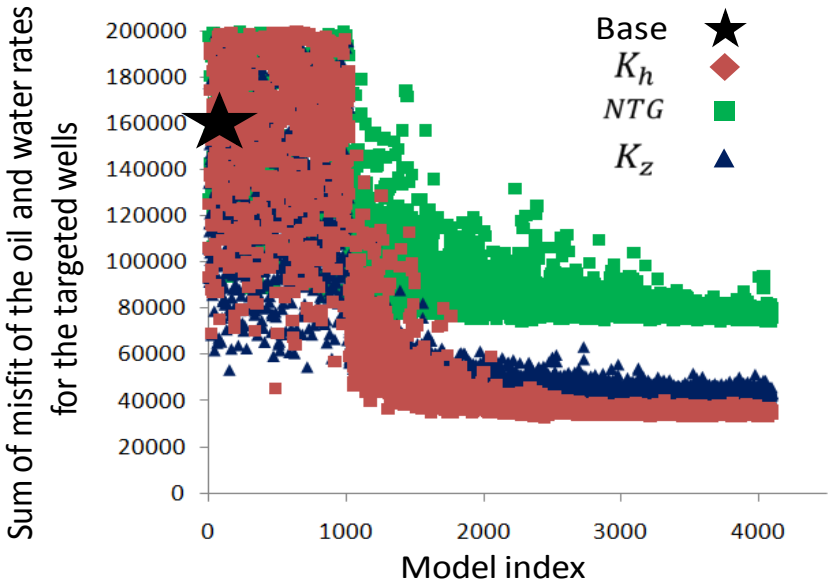


*Figure 4.11: Sum of misfits of the oil and water rates for the targeted wells versus model index for AHM result of changing one parameter type at a time. The normalized misfit value of base model by dividing over the number of observed data is 1100.*

Another analysis which aids in the understanding of the results is the probability distribution of each parameter obtained after applying history matching process. Figure 4.12 shows as an example the probability of three variables for two different regions of the reservoir which was calculated by NAB as discussed previously in Chapter 2 (Section 2.7.4). There are different trends of probability curves. For example the $K_h$ line in Figure 4.12a shows that the highest probability of parameter is at the maximum value. This kind of trend is consistent with Figure 4.8d.

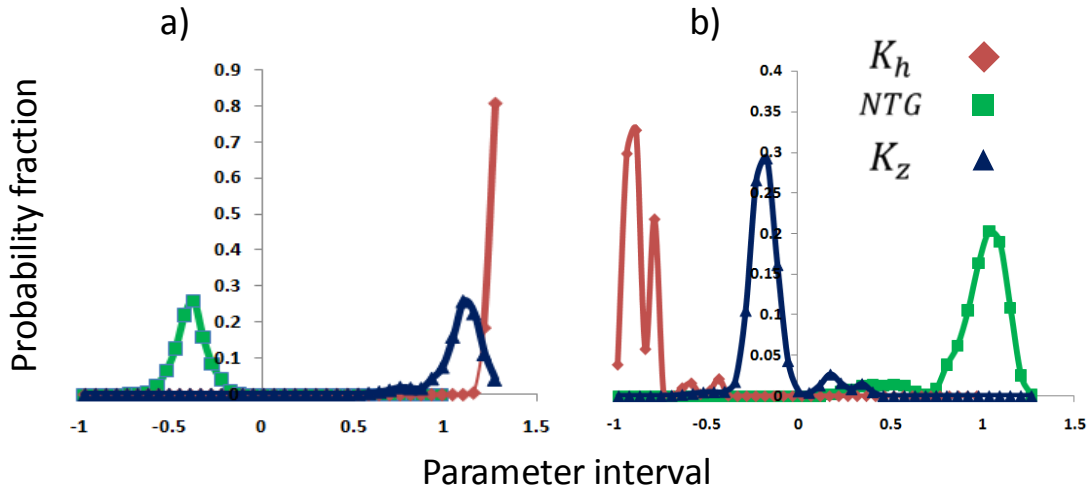


*Figure 4.12: Probability of different parameters in parameter range during history matching for two different regions a and b chosen for history matching study.*

The net:gross and $K_z$ lines in Figure 4.12a show a wide bell shaped probability distribution. This trend is consistent with Figure 4.8b. The trend for $K_z$ in Figure 4.12b shows a narrow probability curve for this parameter which means that a specific value of this parameter was selected repeatedly during generation of reservoir models and this behaviour is similar to the Figure 4.8a. The $K_h$ trend in Figure 4.12b has two peaks in the probability distribution indicating two possible solutions for this parameter. One of the solutions could be a local minimum in the misfit. Such a result indicates the problem of non-uniqueness in history matching more clearly. In this study it can be seen that even after widening the limits there was a high probability of obtaining a parameter value near the new limits of the interval ($K_h$ in Figure 4.12a). As discussed previously this parameter interval could not be made bigger because it changes the conceptual geological model too much. It may be concluded also that the selected parameters that were changed for that specific region were not sufficient and others should be found.

At the end of each history matching study we require a model (or a set of models) including the most appropriate changes that were made to the reservoir parameters. On the other hand as previously discussed in Section 4.3.1, for the field in this study, the updated reservoir parameters may be inter-dependent and the history matching results need to be analysed after combining the resulting parameters. For this purpose all models were sorted for the history matching runs by each variable based on the decrease of the sum of misfits of the oil and water rates for the targeted wells. Then, the

parameters of the 10 models with lowest misfits were chosen and combined to get one reservoir model with updated permeabilities and net:gross for each rank (i.e. best NTG combined with best permeability, 2nd best NTG with second best permeability and so on) (Figure 4.13).

The functions $NTG_i(u)$, $KH_i$ (u) and $KZ_i$ (u) represent the updated reservoir variables net:gross, horizontal permeability and vertical permeability respectively (as a function of location vector, $u$) after history matching and $i = 1,2,3,..10$ to denote the order of misfit from best to worst (lowest is for $i = 1$) . Thus, the final simulation models were generated by combining the updated reservoir parameter (as shown in Figure 4.13) such that:

$$GSV_{Final1} = f\left(NTG_1(u), KH_1(u), KZ_1(u)\right) \tag{4.1}$$

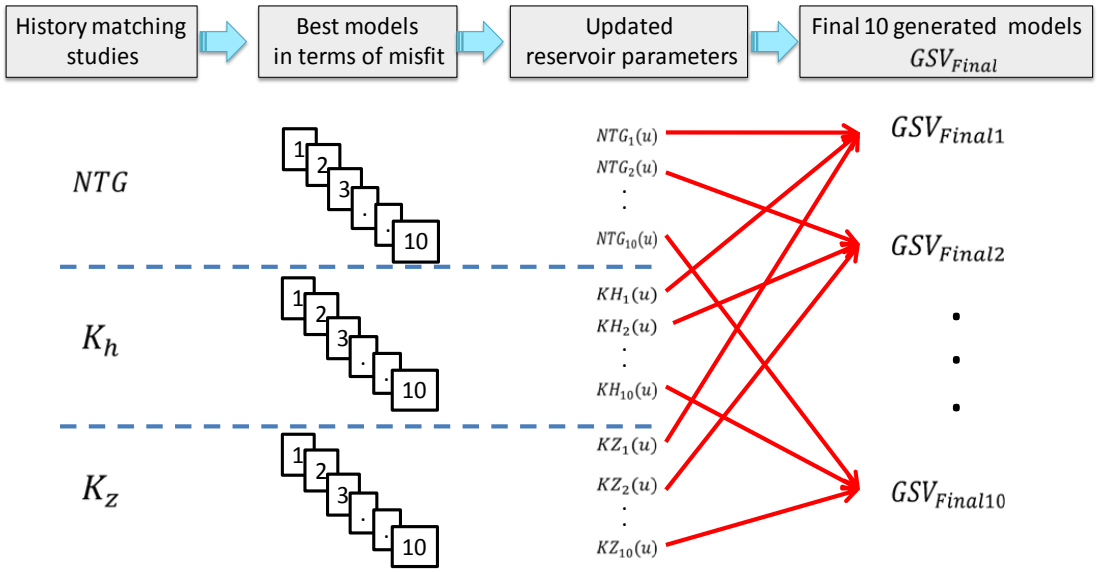


*Figure 4.13: The procedure for generating 10 final simulation models.*

To compare between these final models, the sum of misfits of the oil and water rates for the targeted wells can be seen in Figure 4.14 for the history matching period, and for forecasting. All models were sorted by misfit and then they were compared with the base case model. It can be observed that the combination of the best values for each parameter after history matching did not improve the well misfit that much and in forecasting was even worse as the misfit value was higher than the base model. This result shows the importance of considering different combinations of parameters while history matching.

In order to better compare the newly generated 10 models and previous history matching result of the GSV approach ($NTG$, $K_h$ and $K_z$ history matching results in Figure 4.11), we selected the 10 best history matched models for each case. Then we plotted the production misfit of the selected models as shown in Figure 4.15. The result shows that because the selected history matching parameters are dependent one variable at a time history matching does not improve the misfit value enough. Therefore the two alternative updating schemes described below may be more suitable for this field.

The Nelson field is complex and the way we updated properties could change the fluid flow representation. For example a region near the aquifer with a very low vertical permeability and net:gross was shaly and the shales were very well connected and acted as a barrier. If we only increased net:gross we effectively added more sand but if vertical permeability stayed low the remaining shale was well connected. This introduced the edge drive from the aquifer. If we increased net:gross and vertical permeability together we ended up with a sandy region which was very well connected vertically and then the aquifer supported bottom drive. Also decreased horizontal permeability strengthened bottom drive compared to edge drive.

However there are still some general advantages for the GSV approach. For example for some history matching cases this approach can be use for investigating the effect of different type of variables for updating the reservoir. Then by ignoring the less important variables and combining all variables together in a large history matching study, it is possible to efficiently modify the reservoir. On the other hand another application of this approach would be for the cases where parameters are independent. For example if in a case, the fault transmissibilities and aquifer properties are updated then with the GSV approach, we can modify the aquifer properties and then fault transmissibility.

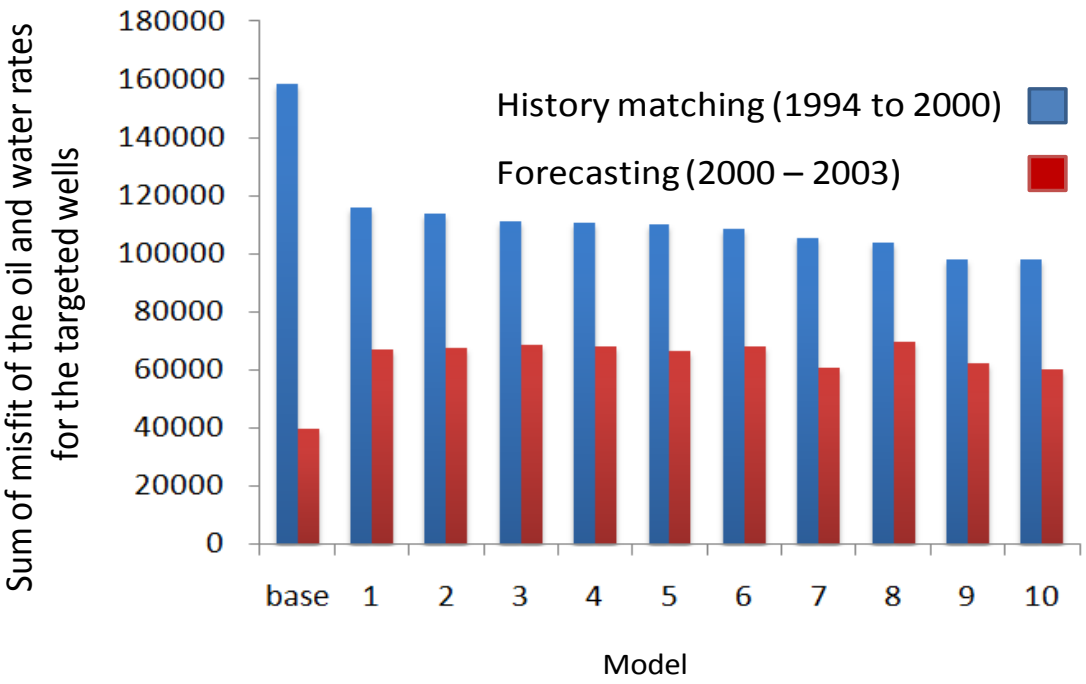


*Figure 4.14: Sum of misfits of the oil and water rates for the targeted wells in the history and forecasting periods for the 10 generated models. The normalized misfit value of the base model by divided by the number of observed data is 1100. Note that indices in this figure are just based on sorting misfits and it is not related to history matching indices mentioned above (the same things happened for the rest of figures).*

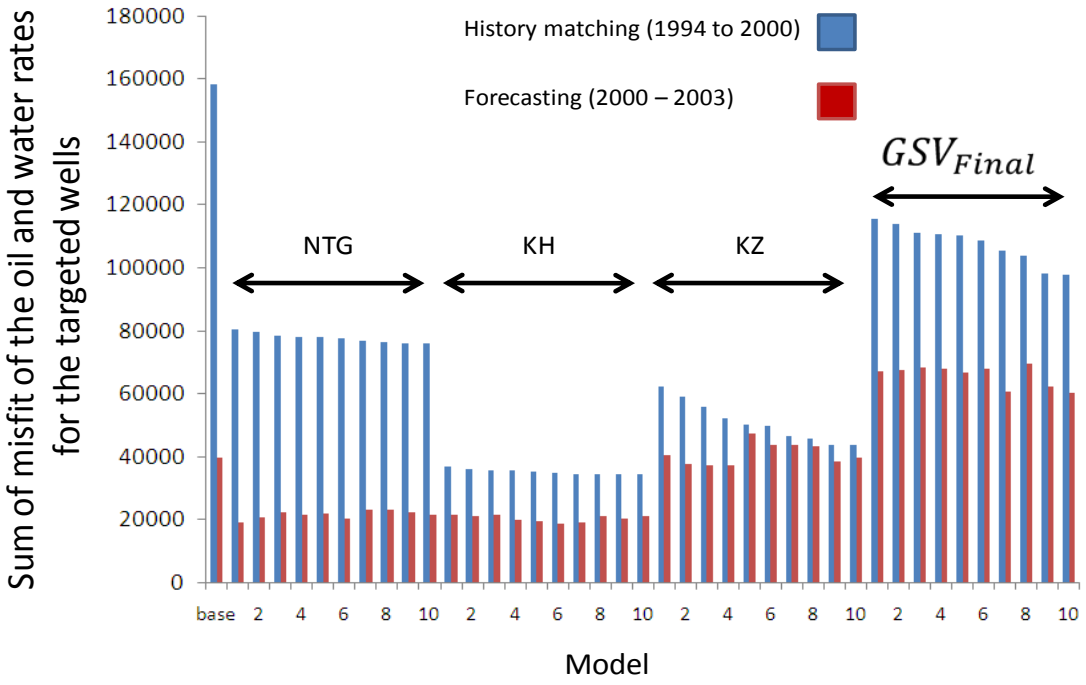


*Figure 4.15: Sum of misfits of the oil and water rates for the targeted wells in the history and forecasting periods for the best 10 history matched models (NTG, KH and KZ) and also final generated 10 models.*

### *4.6.2 RMV*

In this approach, the reservoir was divided into two parts with the idea that there was a very low interaction between reservoir parameters between these two regions. There are three wells in the *Edge* of the reservoir (Figure 4.16) which has 4 locations for updating; for three in the first interval and one in the second interval. Also there are three wells in the *Centre* of the reservoir consisting of 5 locations of pilot points; three in the first interval and two in the second interval. Based on this division we create 12 parameters in the *Edge* section and 15 parameters in the *Centre* section (Table 4.1).

However according to the model number limitation rule of thumb that we set ourselves (Chapter 2, section 2.7.3), for *Edge* study 2700 models were used and for *Centre* study 4000 (Table 4.1). Obviously in the *Centre* case more models were used because it is a 15 dimensional problem. Figure 4.17 shows the reduction of the sum of misfits of the oil and water for the targeted wells during history matching workflow. In this work for the *Edge* case, three wells were included in the edge of the reservoir for calculation of the misfit and for the *Centre* case three wells in the centre of the reservoir included. According to Figure 4.17 the misfit value decreases by 85% for wells located in the edge and the centre region.

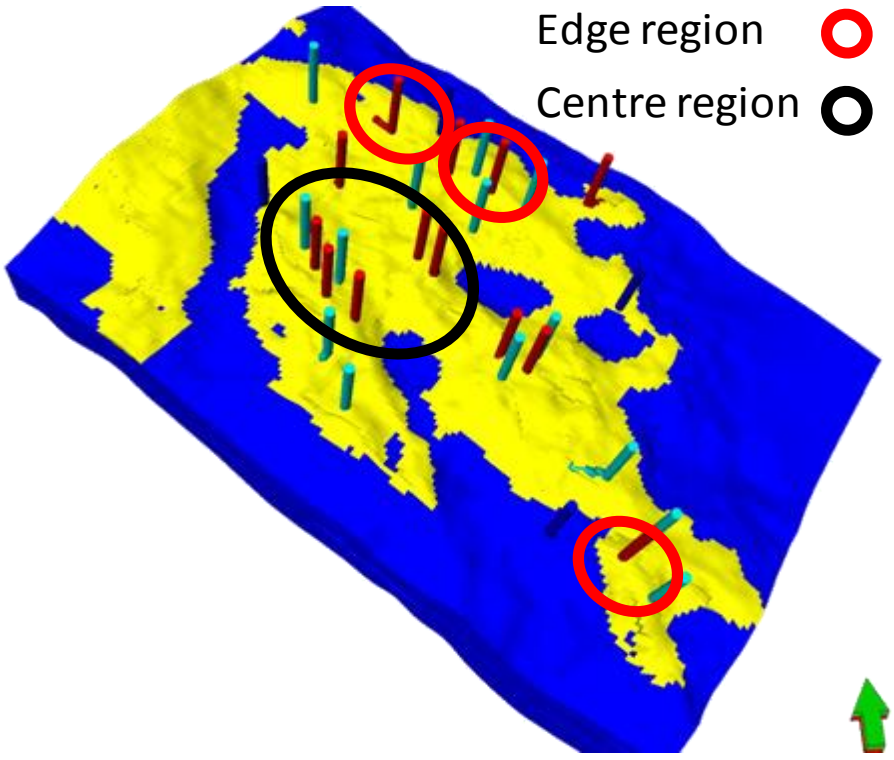


*Figure 4.16: Various regions in the reservoir.*

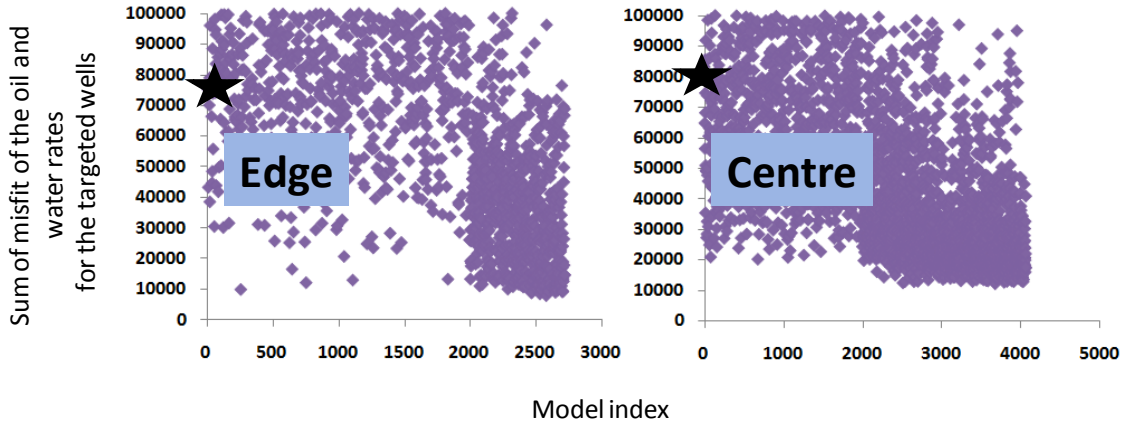


*Figure 4.17: Sum of misfits of the oil and water rates for the targeted wells in each region versus models ran during history matching in Edge and Centre of reservoir, the star shows the misfit value of base model. The normalized misfit value of the base model, obtained by dividing by the number of observed data, is 1100 for Centre and 1200 for Edge.*

The parameters were changed as in Figure 4.8b mainly because of the dimension of problem. We did not generate enough reservoir models using this updating scheme such that insufficient searching was carried out to find a global minimum. Convergence was not observed therefore.

Again in this scheme, reservoir parameters will be updated in different regions and we need to consider all changes in the performance of a reservoir model. Therefore similar to GSV, for this scheme also we generated 10 models by using updated reservoir parameters of Centre and Edge history matching study. In this case all reservoir parameters were updated at the same time (but in different regions) therefore we used abbreviation CENTRE and EDGE for history matching result of Centre and Edge cases respectively. Then the final models sere generated by combining the updated reservoir parameter such that:

$$RMV_{Final1} = f((NTG_1(u), KH_1(u), KZ_1(u))_{CENTRE}, (NTG_1(u), KH_1(u), KZ_1(u))_{EDGE},) \quad (4.2)$$

Figure 4.18 shows field total production rate for the history matching and the forecasting periods for the best of 10 generated models ($RMV_{Final1}$). From this figure it can be seen that at the field scale the best history matched model is between the base and the history of the field in matching period but during forecasting the base and the

best models have similar responses. Since only 6 wells were included in history matching out of 27. Therefore, getting less improvement would be acceptable.

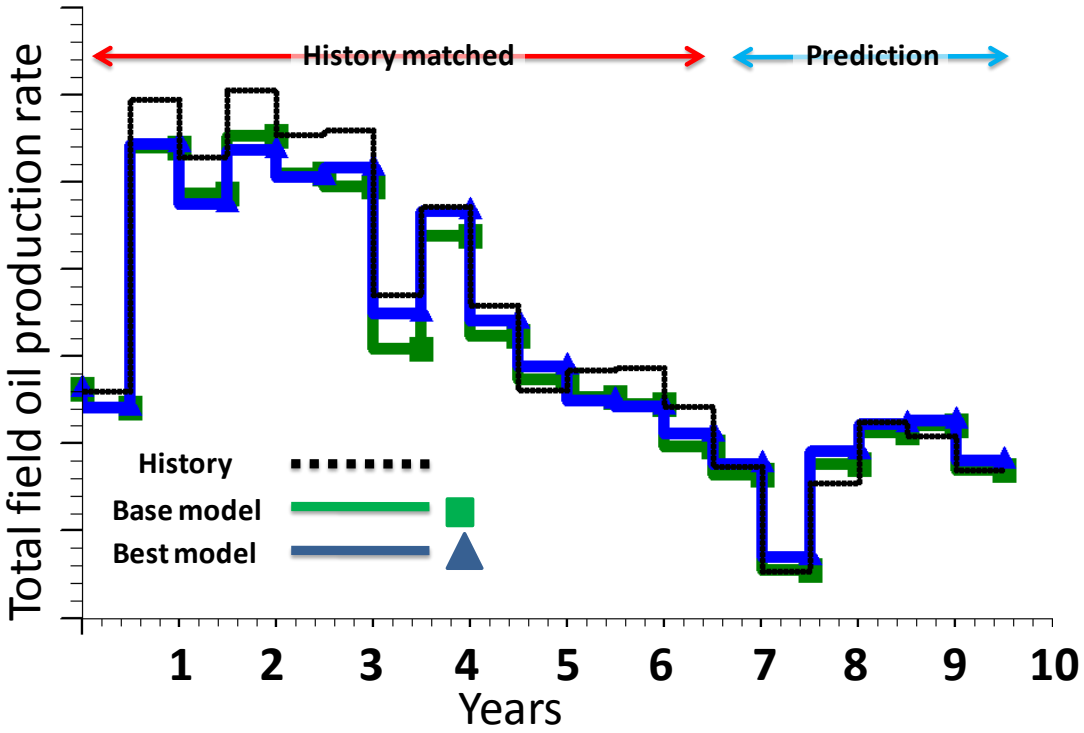


*Figure 4.18: Total field oil production rate for the best model for the history matching and the forecasting period (for well by well analysis see Figure 4.28).*

Figure 4.19 shows the base model and the ten final models ($RMV_{Final}$) for the history matching period (up to 2000) and the misfits comparing differences between 2003 and 2000 indicating the degree of improvement in the forecasting period. A very good reduction in the misfits was observed for the best models and also, in the forecasting period, the misfits decreased. Model 10 (in Figure 4.19) is the best model for both history matching and forecasting periods. Similar to the GSV scheme, we also compared the misfit value of the 10 final models with history matching result of individual RMV cases (CENTRE and EDGE) as shown in Figure 4.20. The result shows that after combination of history matched reservoir parameters, the final generated model matches production data reasonably well with a lower misfit value. Moreover, the act of combining best models actually improves the history match and also the forecast slightly. We need to mention that in each individual RMV case there are 3 wells; 3 wells for CENTRE and 3 wells for EDGE region for which the misfit is reduced. Then the misfit for CENTRE+EDGE in Figure 4.20 calculated based on equation below:

$$misfit_{(CENTRE+EDGE)_i} = misfit_{CENTRE_i} + misfit_{EDGE_i} \quad (4.3)$$

Where $i = 1,2,..10$ represented the best history matched models.

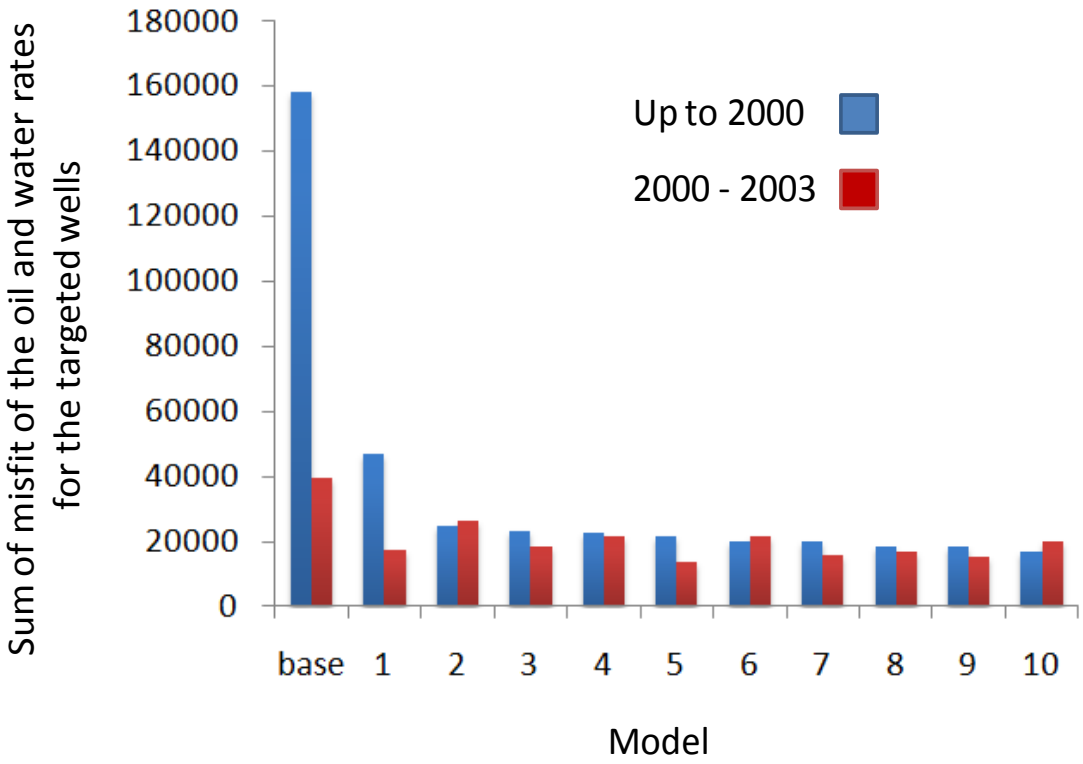


*Figure 4.19: Sum of misfits of the oil and water rates for the targeted wells used in history matching up to year 2000 and from 2000 to 2003 for the best 10 models. The normalized misfit value of base model by dividing over the number of observed data is 1100.*

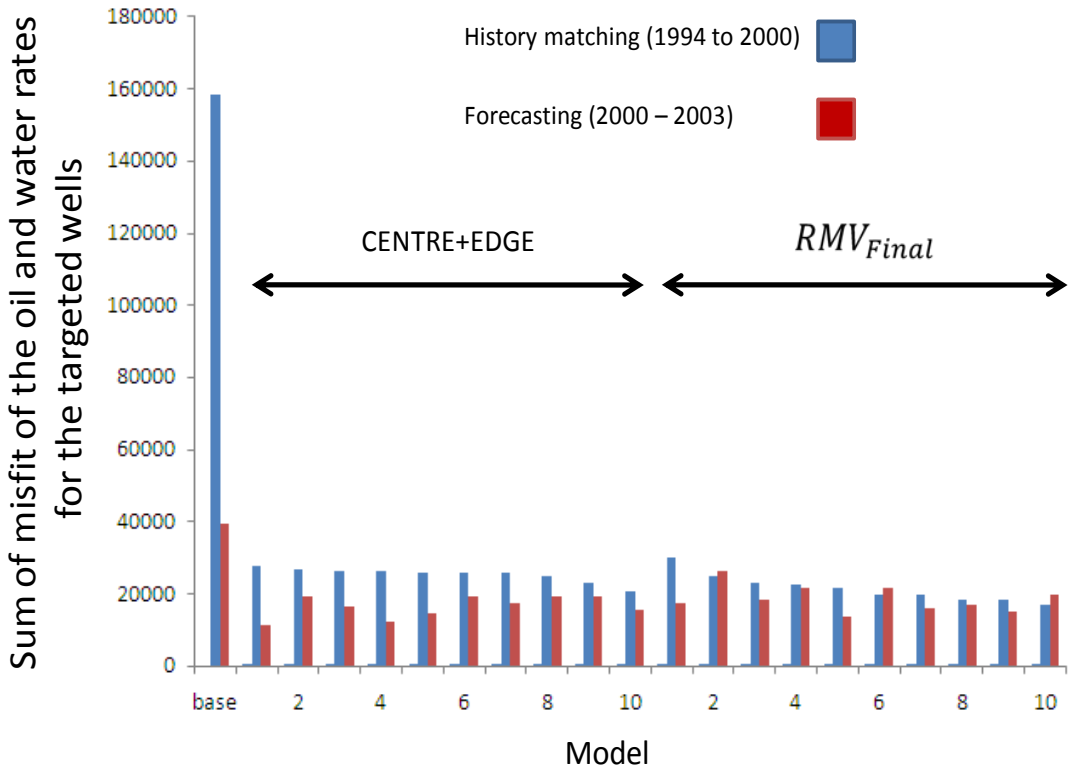


*Figure 4.20: Sum of misfits of the oil and water rates for the targeted wells in the history and forecasting periods for the best 10 history matched models (CENTRE and EDGE, Eq. 4.3) and also final generated 10 models.*

### *4.6.3 LMV*

In this approach, the aim was to update the reservoir model in 6 different regions near the wells, one by one, by changing all of three variables. Three of the updated regions were in the first interval such that the problem is 3 dimensional in these three cases. The others were in both intervals and the problem is 6 dimensional. The prior range of parameters was identified similar to previous schemes. Because in the LMV case, each locality that was selected for history matching was specific for a well, only that well's misfit was calculated. This means that in each history matching run there was only one well used in the misfit calculation. For the first observation, the reduction of the well production misfit through history matching for each well is analysed in Figure 4.21. From this figure it can be seen that the reduction of water production misfit for each individual well ranged from 82% to 95%, which was very good. All parameters converged as in Figure 4.8a. The reason for this could be the low dimension of the inverse problem such that the NA performed a deeper search of the parameter space. The parameter multiplier range did not need to be modified in this case and the result of history matching was used in final stage of history matching (stage 5 in Figure 4.1).

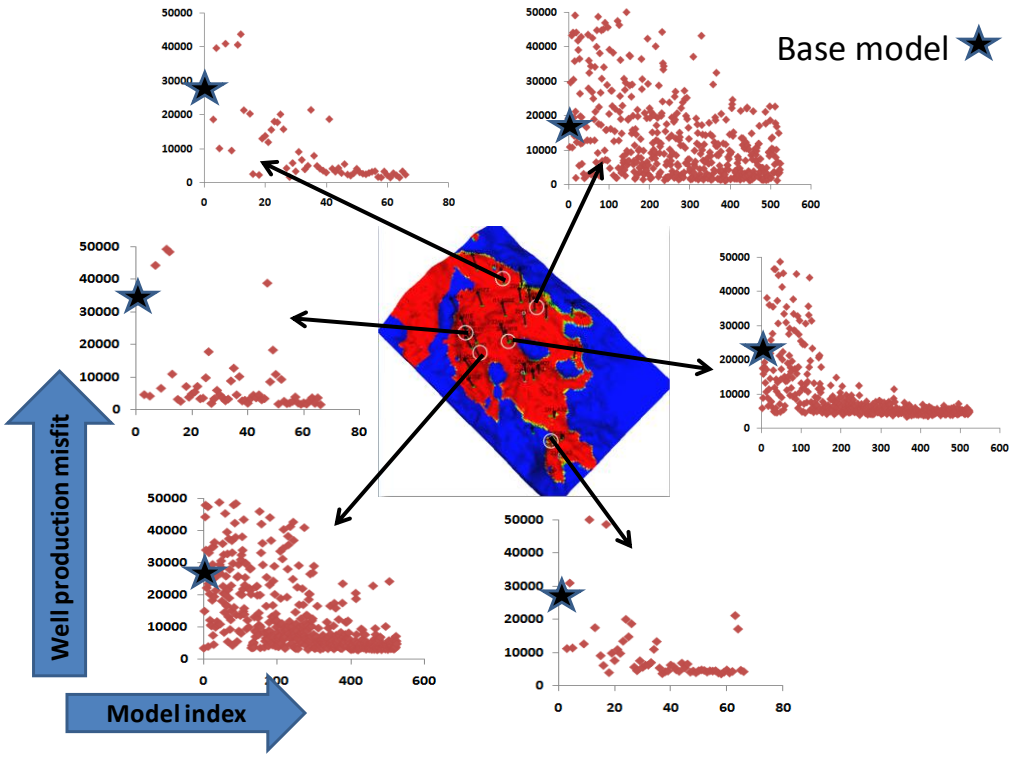


*Figure 4.21: Well water production misfit versus model index for 6 wells in different part of reservoir, the blue star shows the misfit value of base model.*

Similar to GSV and RMV for this scheme also we generated 10 models by using updated reservoir parameters of each local history matching study. Then the final models were generated by combining the updated reservoir parameter such that:

$$LMV_{Final1} = f\left((NTG_1(u), KH_1(u), KZ_1(u))_{Locality_1}, \ldots\ldots, (NTG_1(u), KH_1(u), KZ_1(u))_{Locality_6}\right) \quad (4.4)$$

As in the previous studies the misfit of the 10 final models ($LMV_{Final}$) was again selected. Figure 4.22 shows the sum of misfits of the oil and water for the targeted wells for each model in the matching and the forecasting periods. Between these models, $LMV_{Final1}$ was the best reservoir model because of the low misfit value. For this study, we also made a comparison between misfit values when reservoir parameters were combined ($LMV_{Final1}$) with individual history matching studies ($Locality_j$ where j indicates the j'th locality) as shown in Figure 4.23. Each locality was updated independently with one misfit per well per locality. Afterwards, the individual misfits for each locality were summed according to:

$$misfit_{locality} = misfit_{Locality_1} + .. + misfit_{Locality_6} \quad (4.5)$$

These misfits are shown in Figure 4.22.

To avoid repetition of the same figure for each scheme, a general comparison was made between the different schemes to determine which one gives a more accurate result and which required fewer models.

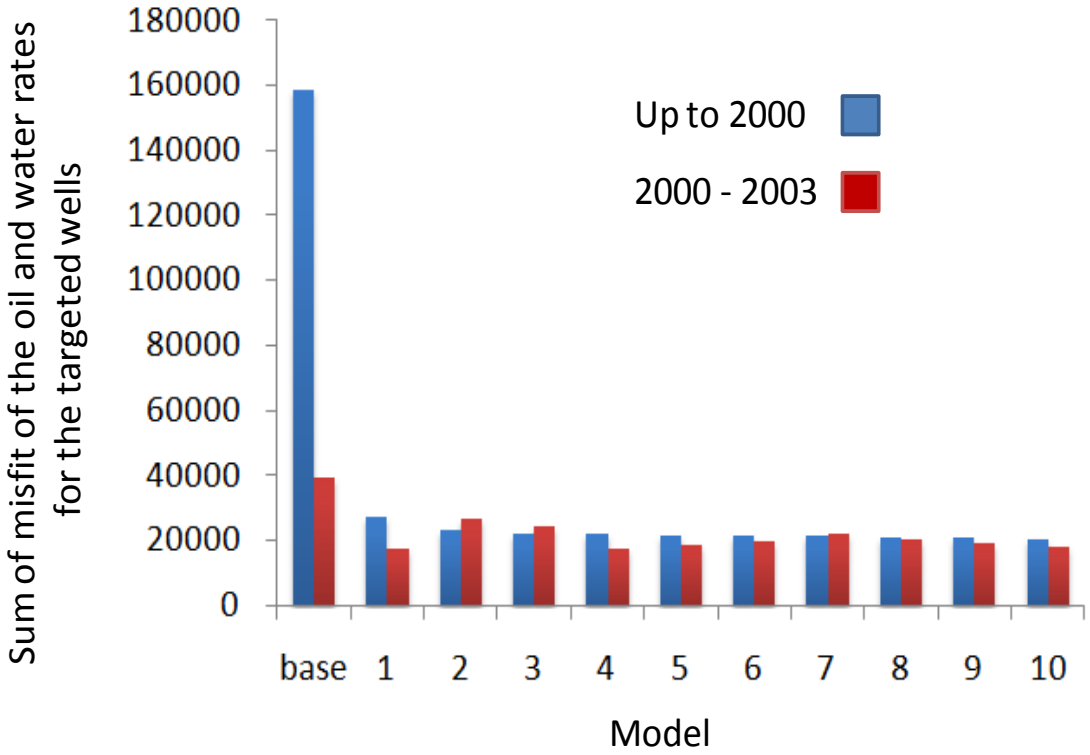


*Figure 4.22: Sum of misfits of the oil and water rates for the targeted wells for different models in history and forecasting periods. The normalized misfit value of base model by dividing over the number of observed data is 1100.*

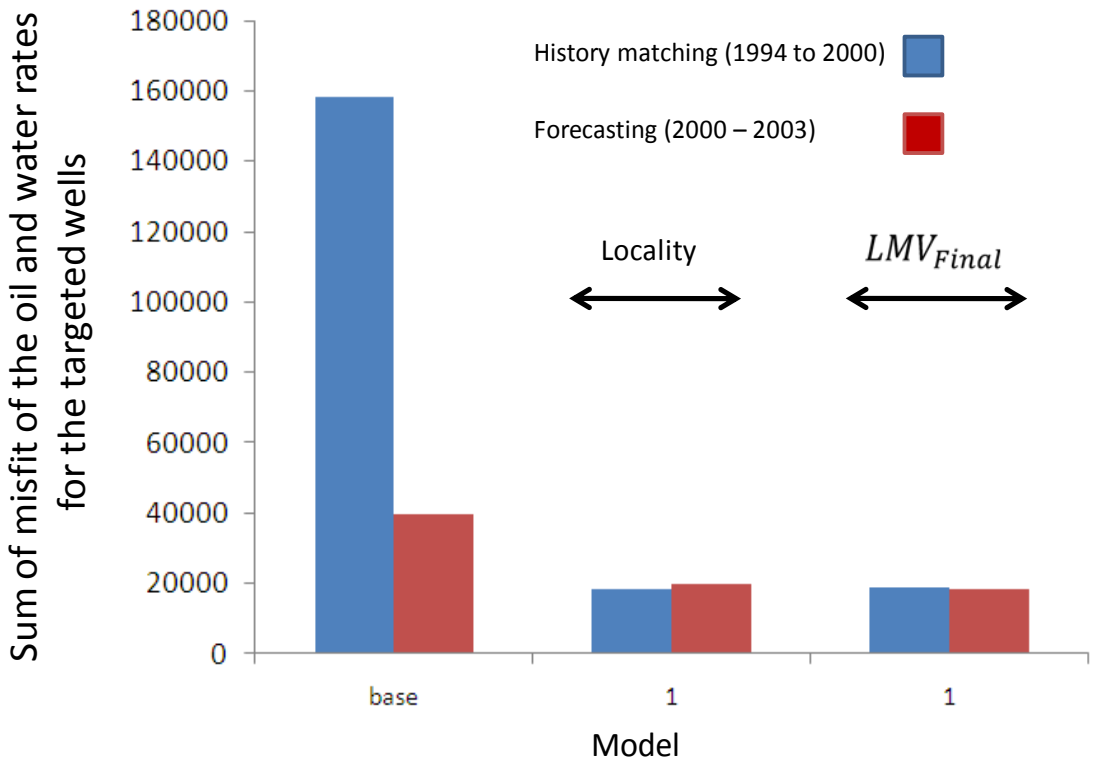


*Figure 4.23: Sum of misfits of the oil and water rates for targeted wells, comparing the model generated by combination of parameter in each locality ($LMV_{Final1}$) with sum of misfits value for each locality (Eq. 4.5).*

### 4.7 Comparison of different updating approaches

This part of the study was important because it was the basis for choosing one of the updating schemes for application later.

There are 4 basic metrics for these comparisons:

1. the CPU time used to get a reasonable result;
2. the ease of analysis and the understanding of the result from each scheme;
3. the scheme that gives us better representation of the reservoir in terms of reduced misfit and also least change in geology of reservoir;
4. the ability of updated model to have a best forecast.

Table 4.2 shows the number of history matching steps and models needed in each case. Looking at the CPU time column, using one processor, we need at least 137 days to using the global single variable scheme compared to 10 days for the local scheme. Further generating more models means that we need to spend more time to analyse the results and understand them. This means that the schemes which generates more

models requires more human interaction. We do not have a metric for that but we need to keep it in mind. Table 4.3 summarizes the number of parameters with various behaviours (as in indicated Figure 4.8). This table shows that for the RMV scheme there is no clear behaviour about how the parameters evolve and all 27 parameters behave as in Figure 4.8b. In the GSV scheme, convergence was obtained for 9 parameters and 7 reached the limits (even after this limit was increased once) and geologically it is not possible to allow parameter to change by a further of 1.3 in $log_{10}$ scale. However in the LMV, all 19 parameters converged to a specific value. It is therefore easier to analysis the results for this scheme.

| Updating sch me | HM steps | Number of models(step) | Total number of models | Total CPU time, (processor days)* |
|---|---|---|---|---|
| Global single variable | 2 | $NTG$=4104 | 24626 | 137 |
| | | $K_h$=4104 | | |
| | | $K_z$=4104 | | |
| Regional multi variable | 1 | Edge=2720 | 6790 | 37.5 |
| | | Centre=4070 | | |
| Local multi variable | 1 | 3D= 3*66<br>6D= 3*524 | 1770 | 10 |

*Table 4.2: Summary of number of models used in history matching, total CPU time using 1 processor and total CPU time using cluster. *In this study CPU time to simulate each reservoir model using streamline simulator is around 8 minutes on an 3.4 GHz processor.*

| OUTCOME (FIGURE 4.8) | GSV | RMV | LMV |
|---|---|---|---|
| a | 9 | 0 | 19 |
| b | 6 | 27 | 5 |
| c | 5 | 0 | 3 |
| d | 7 | 0 | 0 |

*Table 4.3: Number of each type of parameter outcome for each scheme.*

After analysis of the parameters, the history matching results between the three schemes were compared. The first comparison is the misfit value for the final 10 models after history matching ($GSV_{Final}, RMV_{Final}$ *and* $LMV_{Final}$) as shown in Figure 4.24. It can

be seen that the GSV parameter updating scheme obtained a degree of improvement that was less than the other two approaches. For the RMV and LMV methods there was a very good improvement, the total production misfit of the targeted wells was drastically reduced, and the improvement was almost equivalent for all models.

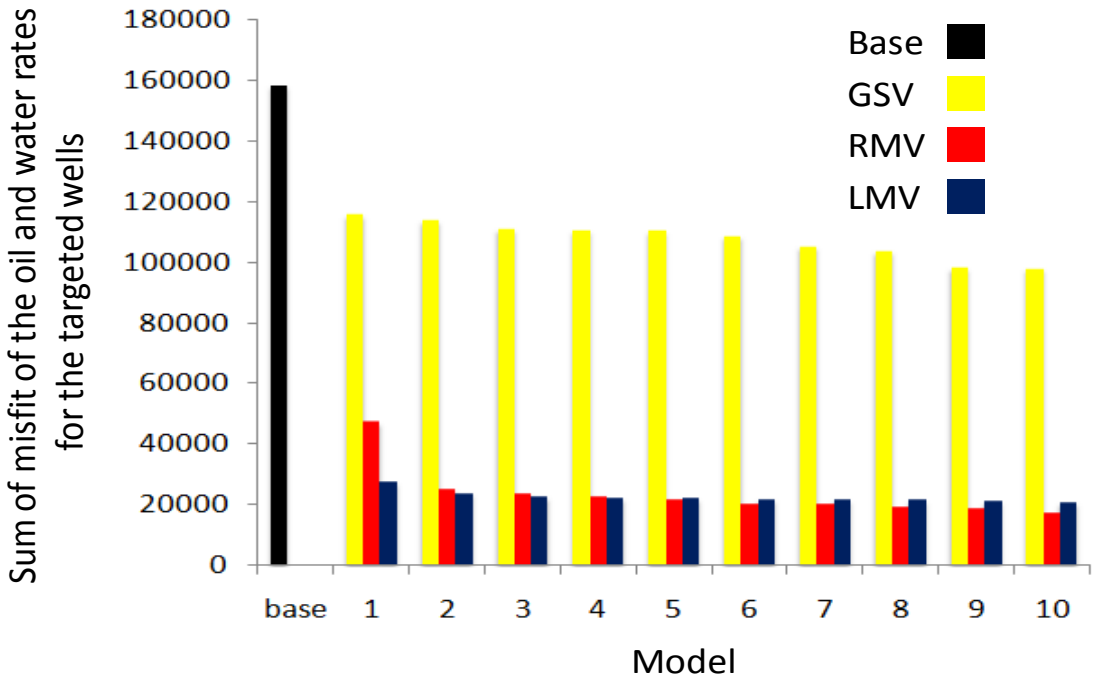


*Figure 4.24: Sum of misfits of the oil and water rates for the targeted wells for the best 10 models of each case. The normalized misfit value of base model by dividing over the number of observed data is 1100.*

Figure 4.25 shows that for the GSV case, even if there was some reduction of the misfit in the matching period, the updated models gave a poorer forecast than the base model. For the RMV and LMV cases the final 10 models gave a good forecast of the targeted wells. There was also a good correlation in the results. This means that if the updated reservoir model gave a good history match we get a reasonable forecast too.

For the best model (defined as the best combination of history and forecast misfit reduction) for both periods, we plotted the correlation of individual oil production misfits of each well and then the result was compared with the base model (Figure 4.26). The GSV case gave misfits that were close to the base case and there were high misfit values for both periods. In each of the RMV and LMV cases there was a big shift of the models toward zero which means that the well oil production misfit was reduced for both periods.

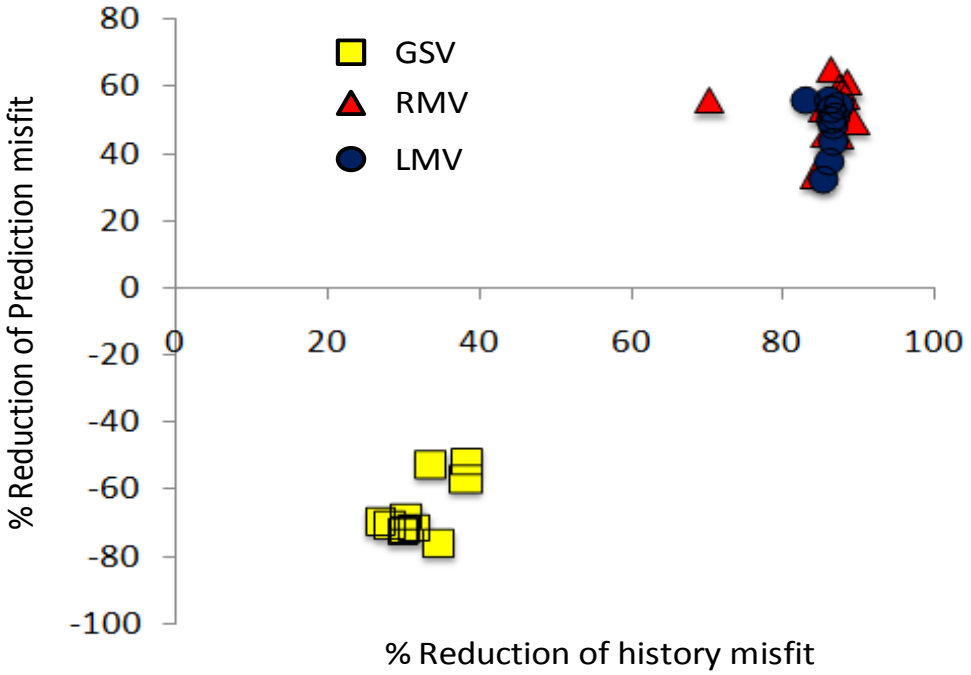


*Figure 4.25: Forecasting misfit reduction versus matching for the final 10 models of each case.*

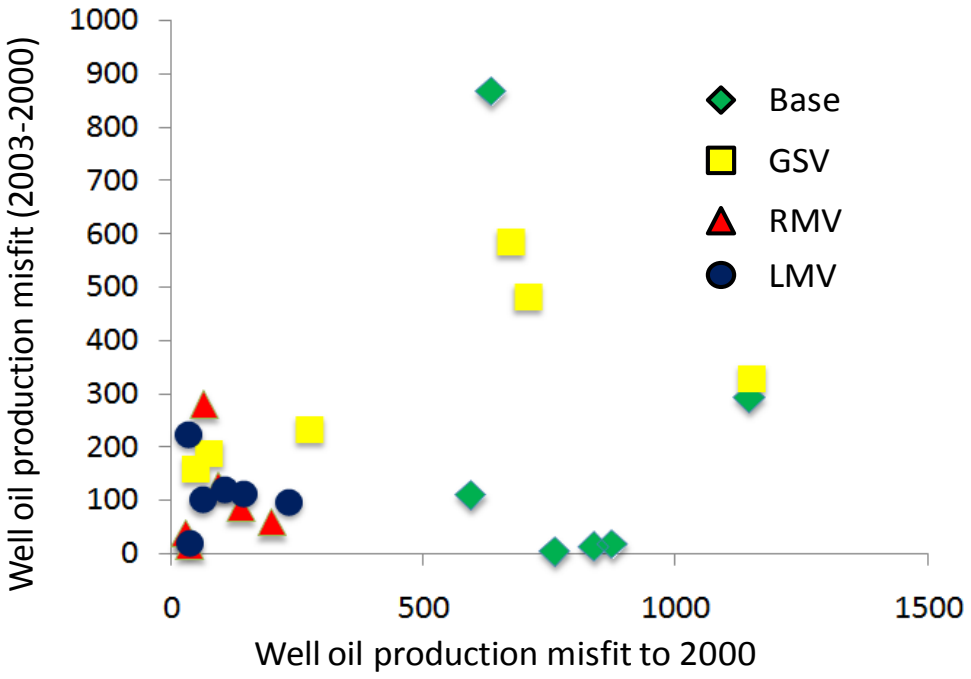


*Figure 4.26: Well oil production misfit in forecasting period versus history period for different schemes.*

One important outcome of this history matching was the degree of change that the reservoir model saw by updating parameters and how the fluid movement changed

because of that. In Figure 4.27 for the best reservoir model, the multipliers of each parameter was obtained in each region in the reservoir. The main result shown in that figure is that the horizontal permeability of the model was increased while net:gross and vertical permeability could increase or decrease. For example in Region 1 (indicated by the arrow in Figure 4.27 in the centre of the reservoir) lateral sweep of oil towards the well was increased following the increased horizontal permeability along with decreased net:gross and vertical permeability obtained from the RMV and LMV schemes. In GSV, however, increased vertical permeability was obtained.

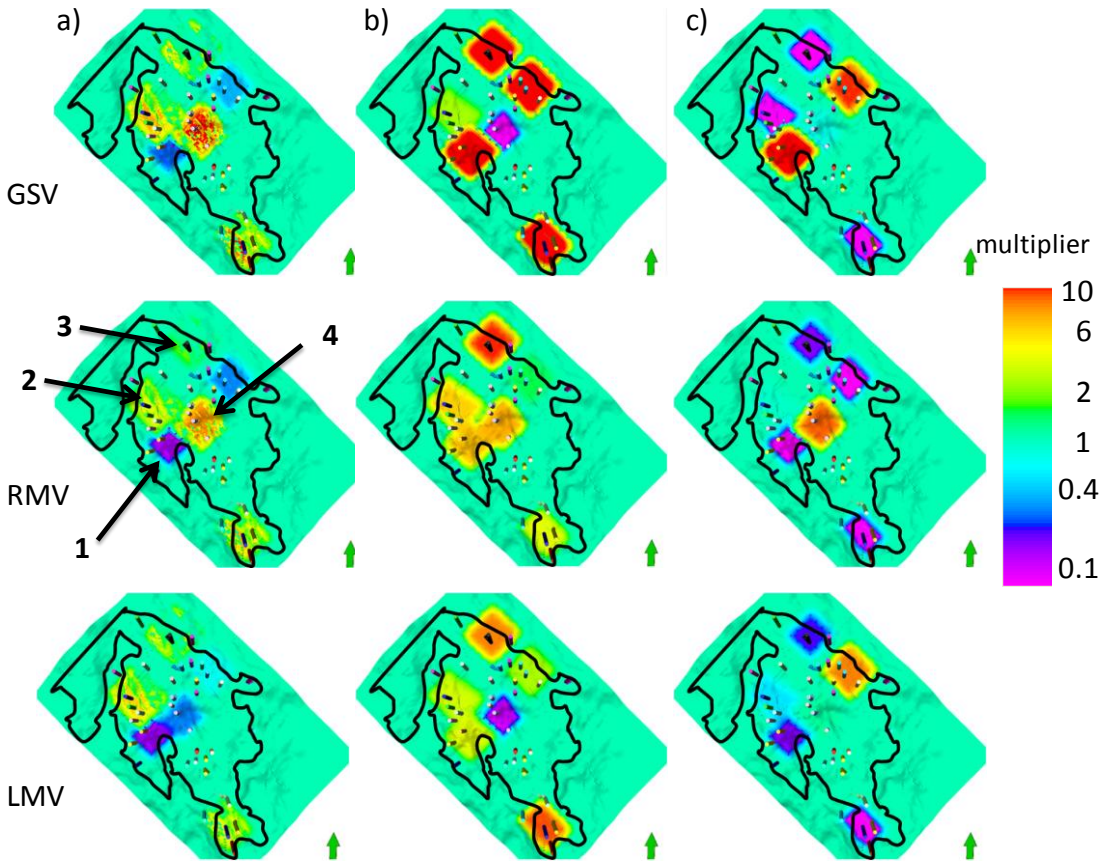


*Figure 4.27: Best parameter multipliers applied to update the base model in various cases for a) net:gross, b) horizontal permeability and c) vertical permeability.*

Region 2 is close to an injector and the lateral sweep was again increased as in Region 1 but here there was also reduction of shale volume by increasing net:gross. For this region there was almost the same behaviour for all history matching cases. Region 3, which was close to the edge of the reservoir as well as an injector, again saw increased lateral sweep of oil by updating the properties. Therefore it can be said that that injector has an important impact on the production well. Again, for this region there was a similar update for three cases. In the fourth region, which was in the centre of the

reservoir, the only apparent route for oil displacement was from the bottom aquifer. For the RMV and LMV approaches, the fluid displacement was controlled by increasing the ratio of vertical to horizontal permeability. In RMV both permeabilities were increased but more for the vertical direction and in LMV the vertical permeability was kept unchanged while the horizontal permeability decreased.

One general conclusion based on Figure 4.27 is that even for small reductions of the misfit value in the GSV case, the process of updating the reservoir was very similar to other approaches except that usually the degree of change was very large for this case. Therefore, it can be said that by considering only one variable at a time, the fluid movement was altered to increase/decrease lateral movement compared to other cases but updating was as not as efficient. The efficiency of fluid displacement could be increased by considering the change to all the parameters at the same time (RMV and LMV methods). Figure 4.28 shows the oil and water production rates for 4 wells as an example. It can be seen that by using the RMV and LMV approaches, the production profile of the wells can be matched better than the base model.

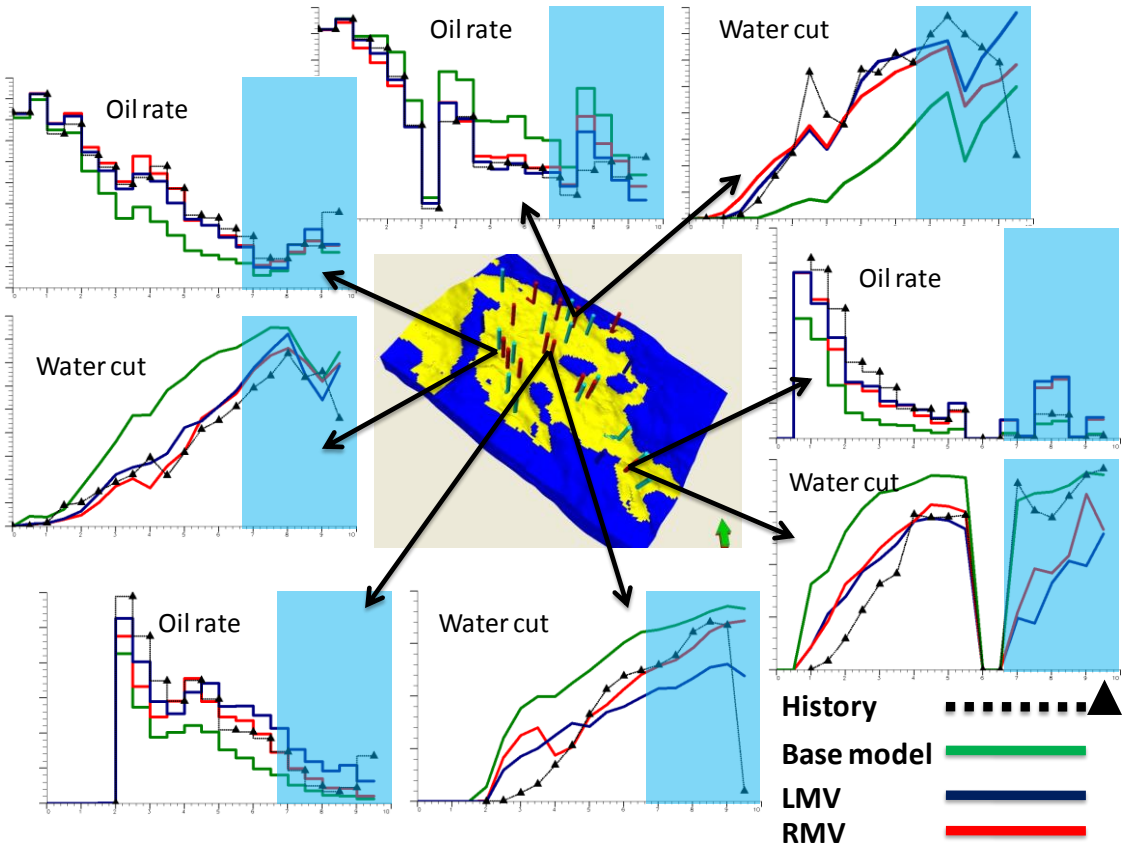


*Figure 4.28: Oil and water rate for best history matched model for 4 different wells.*

### 4.8 Which updating scheme should we use?

So far the application of various parameter updating schemes has described for a small history matching problem, including 6 wells only. This was carried out in order to investigate which scheme was most efficient and the results were analysed.

By adding more wells into the history matching study, the number of updated regions was increased as well. More reservoir parameter were needed changed thus increasing the dimension of the problem. As discussed several times during this thesis, increasing the dimension of the problem requires greater searching in the parameter space and this means significantly increasing the number of simulations. From this point of view the LMV approach would be more suitable because it needs fewer simulation models.

For the GSV method, obviously, the dimensionality is again a similar problem to the RMV. On top of that, for the GSV method, it is expected that undesirable changes in the geology of the reservoir could occur in this case. Thus, one variable will be updated at a time. The important point that needs to be considered for the LMV approach is that more precision is needed when choosing the regions to be updated in the reservoir in order to reduce the interaction between them to make sure that the final history matching result is unaffected. Ultimately from the whole discussion above it can be concluded that the LMV approach would be the best candidate for application in a history matching result including more production wells because it is faster, easy to follow the result and finally it gives the best representative models of the reservoir without destroying the geology.

### 4.9 History matching in Nelson including more wells

In this section the aim was to apply the LMV approach to a bigger history matching problem which includes nearly half of the wells and represents 84% of the total misfit of the oil and water for all 27 production wells.

13 wells were chosen for the study (Figure 4.3, red wells). Of these, seven wells were completed in the first geological interval only (Figure 3.7 shows the top view for each interval). Therefore, at these localities, the reservoir properties were updated only in

that interval. For each of these wells, there are only 3 variables modified. So that each sub-problem is three dimensional. The other 6 targeted wells were completed in both intervals, both of which were updated separately. Each of these cases is a six dimensional problem. Overall this was a 57 dimensional problem. Each sub-problem is considered in turn (though these could be treated simultaneously as in Sedighi and Stephen (2009) where misfit decomposition was used). The location of master pilot points were chosen to make sure that there is not an overlap between the regions to update that belong to each well. The interaction between the parameters was then reduced, though it cannot easily proven that there is none without more elaborate analysis.

After history matching, the 10 best parameter combinations from each pilot point location were selected and combined to generate a set of 10 best models overall. Figure 4.29a and 4.29b show the total oil production rate and total water cut of the field for one of the best models compared to the base model. There is a significant improvement in matching the production profile of field oil rate and water cut.

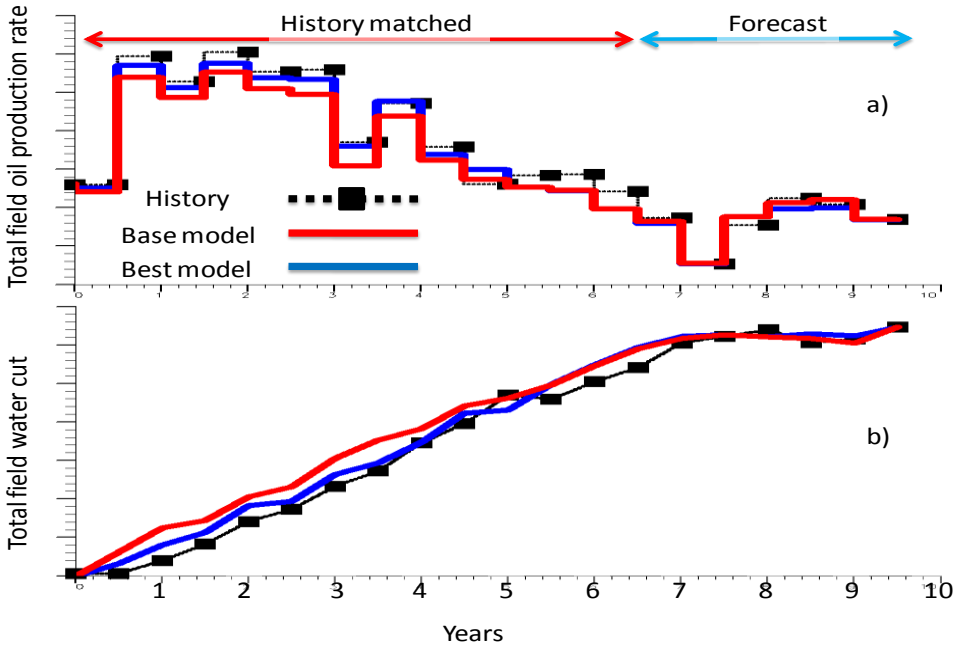


*Figure 4.29: (a) Total field oil production rates (b) and water cut for the best model compared to historical data and the base case model (for well by well analysis see Figure 4.33).*

To better understand how the reservoir parameters were changed as a result of history matching, the multipliers of each variable were plotted over the base reservoir model in Figure 4.30. On balance, parameter values were increased in the model although there are regions where decreases were necessary. Typically, the ratio of horizontal permeability versus vertical permeability increased from 10 to around 13 and this increase lead to increased edge drive from the aquifer and less bottom drive. This is better seen in Figure 4.31.

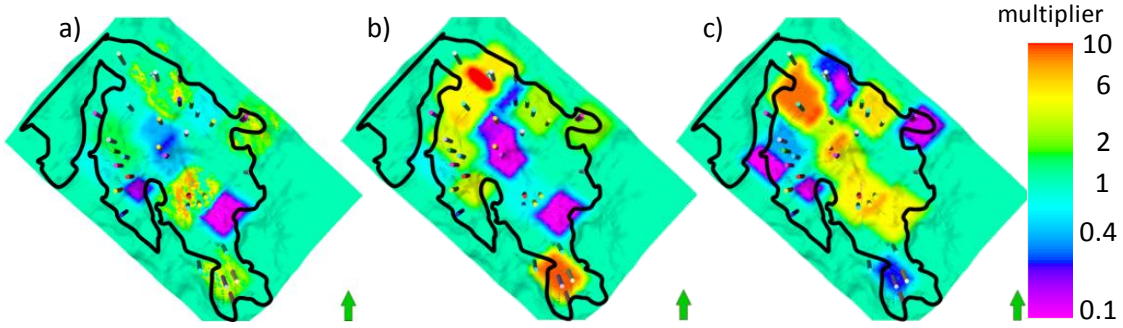


*Figure 4.30: Multipliers of parameter for the best reservoir model over the base model for a) net:gross, b) horizontal permeability and c) vertical permeability.*

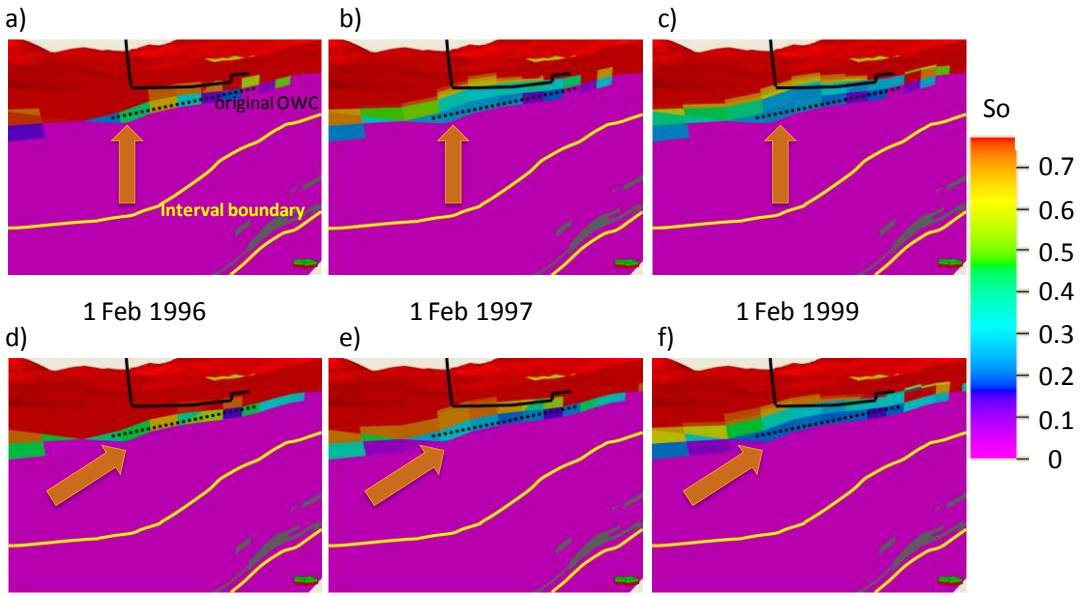


*Figure 4.31: Cross section of water movement near a well for the base model (a to c) and one of best models after history matching (d to f) in different time steps. The arrow shows the water discplacement from the aquifer toward the well. Because this is a 3D view so that the water oil contact does not look horizontal.*

Figure 4.32 shows the sum of misfits for oil and water for the targeted wells of the base model and the 10 best models after history matching. The misfits for the forecast periods along with the percentage reductions are shown. The history match misfit was reduced by around 70% for all models but for forecasting the reduction varies from 10 to 40%. Overall, model 9 was the best and the oil rate and water cut are plotted as an example for 4 wells in different locations to see the change of production profile (Figure 4.33). The forecast period also gave a good match.

Comparing the new history matching result with the previous study in section 4.6.3 shows that after adding 7 new wells into the study, addition to the same 80% reduction of misfit value for the previous 6 wells there was 50% reduction of misfit for the new 7 wells in matching period and 45% in forecasting period which was reasonable result.

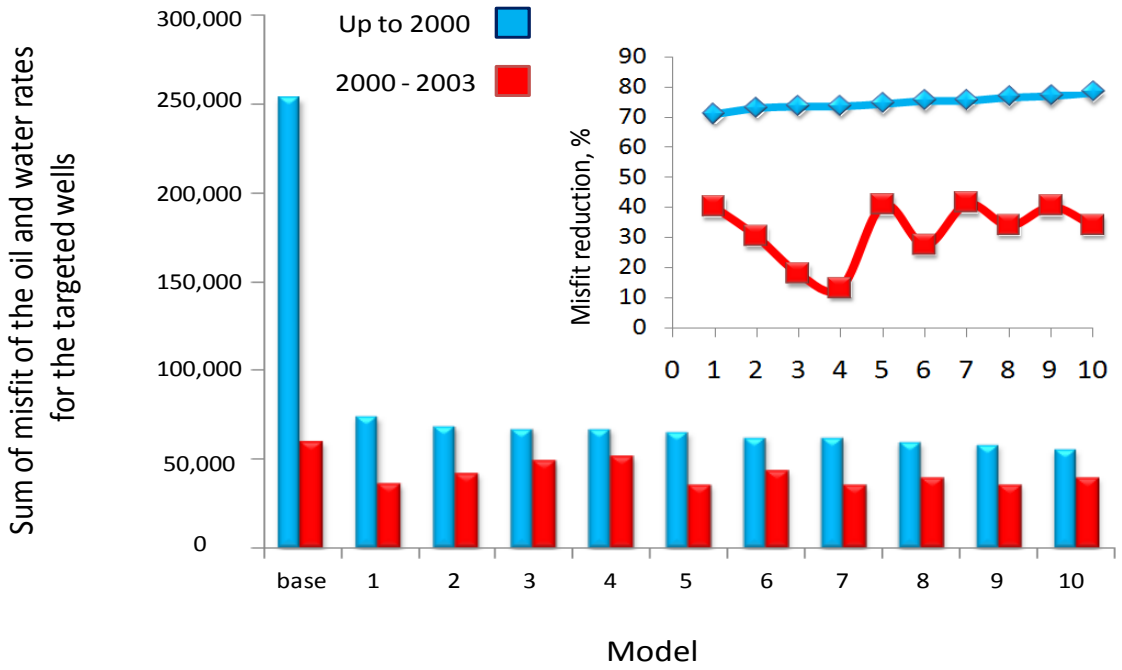


*Figure 4.32: Sum of misfits of the oil and water rates for the targeted wells for best 10 models in history and forecast period. The normalized misfit value of base model by dividing over the number of observed data is 860.*

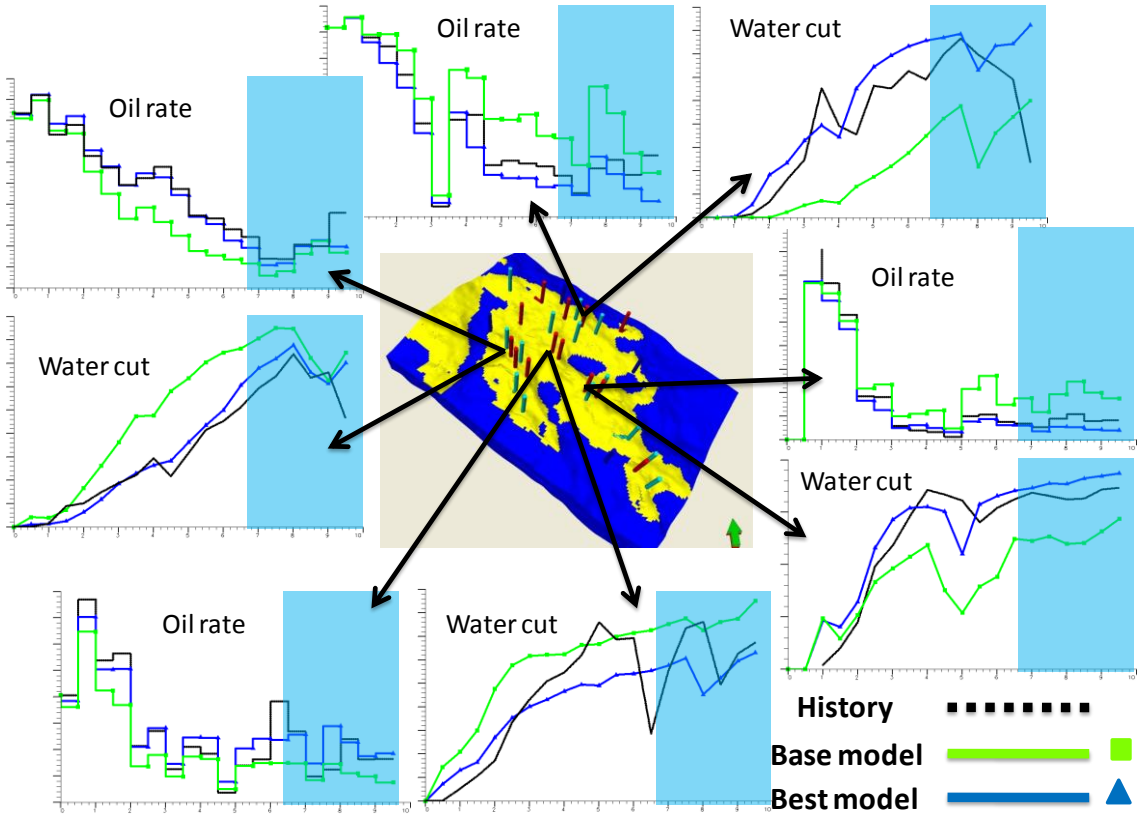


*Figure 4.33: Oil rate and water cut of 4 different wells in history and forecast (light blue) period.*

### 4.10 Well vicinity vs. streamline guided approach

In this chapter so far, an updating scheme has been introduced for history matching of Nelson based guided by streamlines and in the previous sensitivity study (Section 4.2.1) it was shown that this was an optimal method for choosing the right locations to make modifications to reduce the mismatch. On the other hand, the alternative and most used method for updating a reservoir often considers the region surrounding each well (Solorzano et al. 1973), as in Figure 4.34. In this case the assumption is that the region around the well is equally important in terms of improving the simulation of oil displacement from the aquifer or injector to the producer. In the following section we show the results of modifying the region surrounding the well. As above, the local multi-variable (LMV) scheme was used for each well to improve the same reservoir properties. The only difference here is the location of the pilot points. Again the reduction in the production misfit considered.

For 7 wells in the reservoir, the reduction of oil and water production misfits was plotted in Figure 4.35 and were compared to the results for the streamline guided approach. Also the trend of the reduction was compared to the original value of misfit for base reservoir model. The first observation from Figure 4.35 is that for all the regions there was a reasonable decrease in misfit value for the well vicinity approach but the streamline guided approach was twice as good.

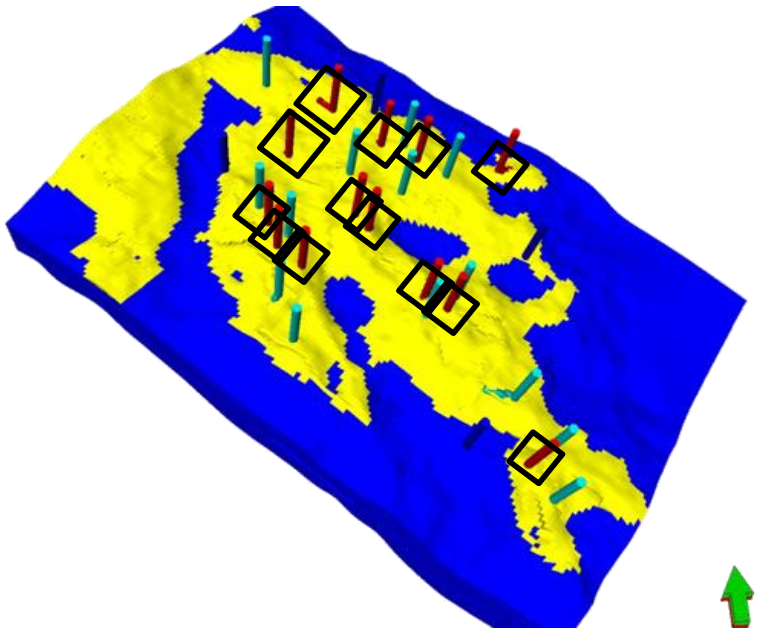

*Figure 4.34: Location of master pilot points in black box in the vicinity of each well*

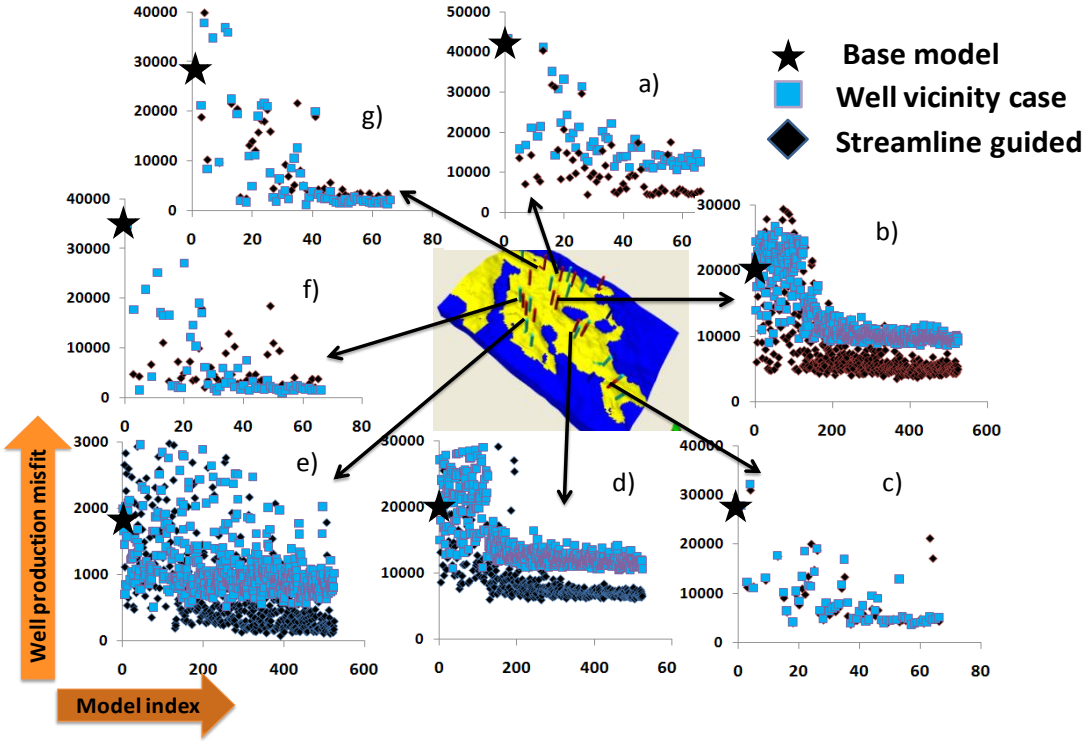


*Figure 4.35: Well production misfit through history matching for well vicinity and streamline case in different locations in the reservoir.*

After combination of the best models in each region the 10 best reservoir models were generated for the well vicinity approach. The sum of misfits of the oil and water rates were calculated for the targeted wells. Figure 4.36 shows the production misfit for base reservoir model and for the best 10 models for the streamline guided case and the well vicinity approaches. Overall, the well vicinity misfits are fifty percent larger than the streamline guided method (Figure 4.36a). Moreover, the forecast is worse if the streamline guide is not used (Figure 4.36b). In order to illustrate the improvement offered by using streamlines, the oil and water rates of the wells are plotted for different locations of the reservoir for the history matching and forecast periods (Figure 4.37).

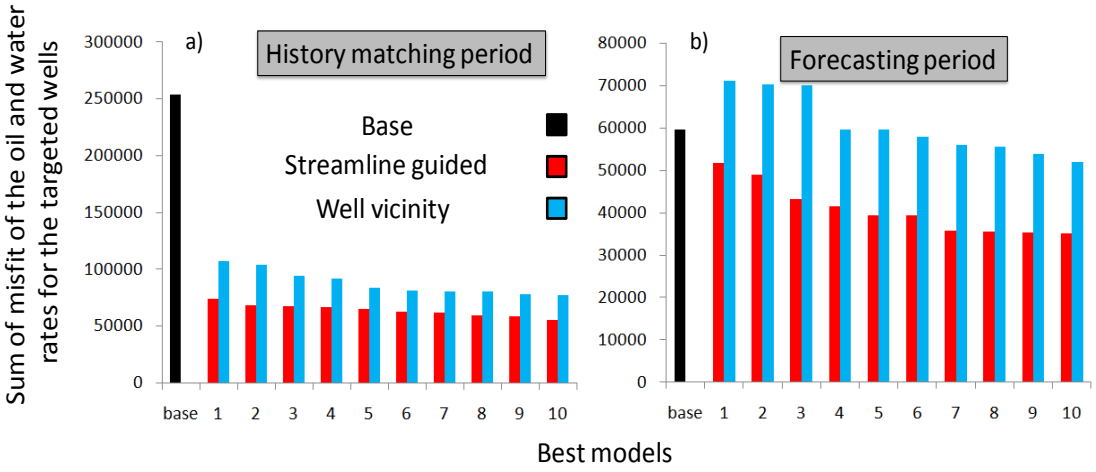


*Figure 4.36: Sum of misfits of the oil and water rates for the targeted wells in (a) history matching in matching period and (b) forecast period. The normalized misfit value of base model by dividing over the number of observed data is 860 in history matching period and 380 in forecasting period.*

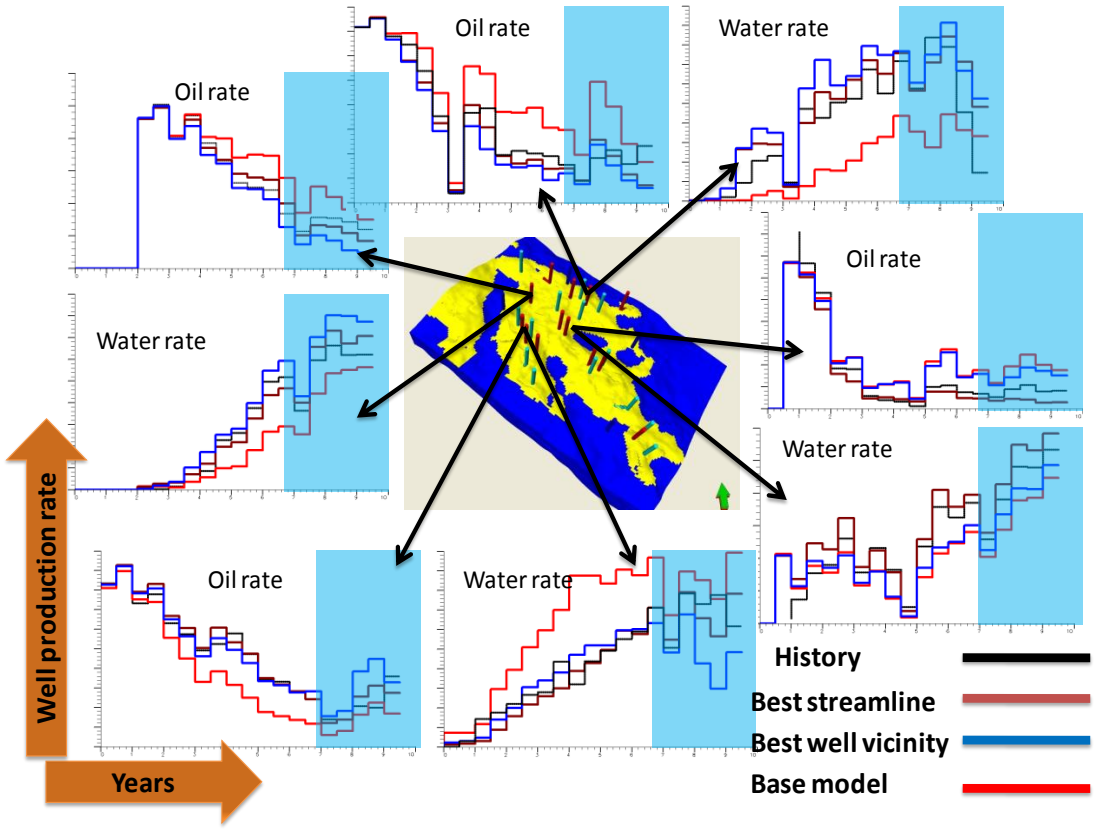


*Figure 4.37: Oil and water production rates for the best model from well vicinity updating and the streamline case in various location of the reservoir for history matching and forecasting (light blue shading).*

One important issue in history matching is the correlation of forecast versus the history matching misfit. We needed to know whether a good history matching model also gave a good forecast. For this purpose the improvement in the misfit forecast was plotted in Figure 4.38 versus history matching for the best 10 models chosen after matching for both streamlines and well vicinity cases. There are two main observations about this figure. Firstly, there is a broad correlation that better history matching models forecast better albeit with some deviation. Secondly the streamline guided models consistently matched history and forecasts better than those obtained with the well vicinity approach. An important consideration for the history matching process is how the reservoir was updated: were the new properties consistent with our prior geological knowledge? Figure 4.39 shows that the multipliers of parameters for the best model of the well vicinity cases were qualitatively similar to the results for the streamline guided study (Figure 4.30). On balance, there were increases to the variables across the model. These changes were very smooth in most of the regions for the streamline case but the well vicinity case results was more localized changes which may be less geologically valid.

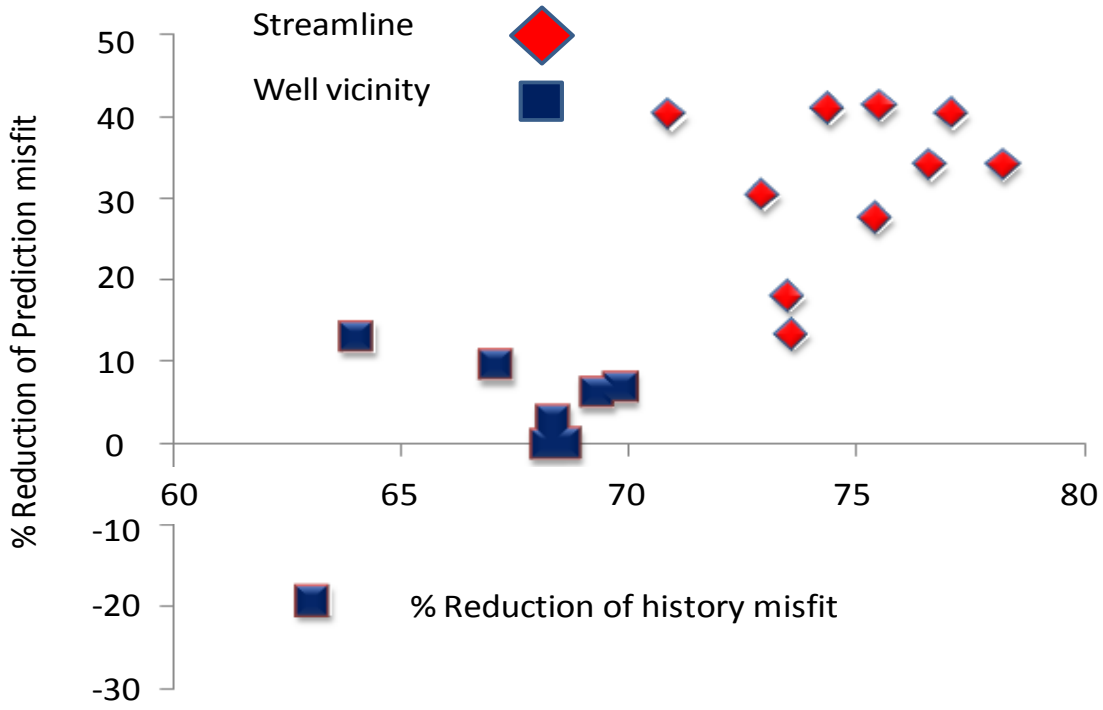


*Figure 4.38: Cross plot of misfit reduction in matching and forecast period for best 10 models of well vicinity and streamline based cases.*

Focusing on the region indicated by the arrows in Figure 4.39a, the well vicinity and streamline guided updates are quite different. This region belongs to a production well that was supported mainly by a water injector nearby. In the streamline case it can be observed that horizontal permeability increases lead to increased movement of water from injector to producer. On the other hand, updating the reservoir in the well vicinity resulted in increased net:gross only. This meant an increased volume of oil close to the well which delayed breakthrough to the well by slowing down the front propagation. Of course, because of the way simulator calculates transmissibility, net:gross increases lead to an increased effective horizontal permeability. The history matching result in Figure 4.37 shows that updating the reservoir guided by streamlines can better match this well and a better forecast was also achieved. It can be concluded that the streamline guided method was more accurate at selecting regions and then finding appropriate changes to make.

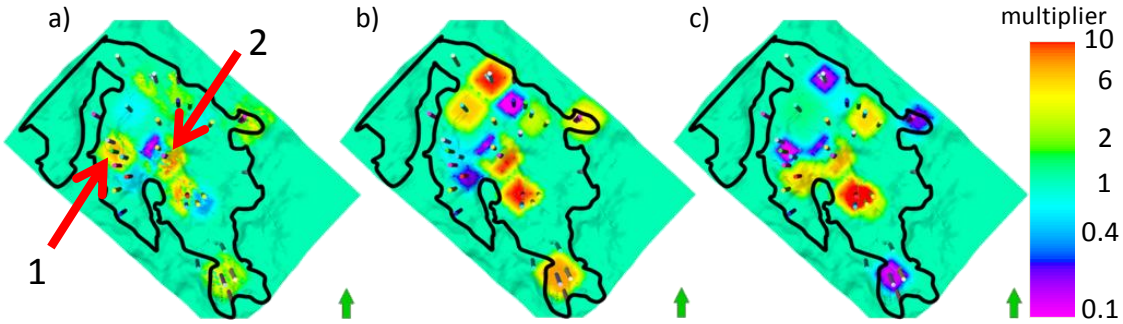


*Figure 4.39: Multipliers of parameter for the best reservoir model over the base model for a) net:gross, b) horizontal permeability, and c) vertical permeability.*

In the region indicated by Arrow 2 in Figure 4.39a, there is a production well which was supported by the aquifer below the reservoir. In the streamline guided case, by increasing the vertical permeability of the model and decreasing horizontal permeability and net:gross the distribution of shale was effectively modified in this part of the field so that there is more connectivity to the aquifer. In contrast, in the well vicinity case, all three variables increased near the well but net:gross and horizontal permeability were slightly decreased to the north-west. Figure 4.37 shows the production data for this well and it can be seen that the match in the well vicinity case was not good. This in itself indicates that while the water rate needed to be increased, the parameterization scheme did not allow it.

Apart from looking at the multipliers applied (Figure 4.30 and 4.39) the new values of the variables were also considered. Because on balance, properties increased, the focus is on the cells with large changes. In Figure 4.40 and 4.41 the cells in the reservoir were filtered out where variables are increased and the same filtering applied for the base model. Therefore, each parameter can be compared for the cells with multiplier greater than one in Figure 4.30 and 4.39.

Figure 4.40 shows that for the streamline guided case, even by increasing the parameter in the model the geological heterogeneity was retained in the reservoir. For net:gross, for example, in Figure 4.40a, the organized connected shales can be seen. Even though net:gross was increased, the organization remains after history matching. For the well vicinity case, however, it can be observed that this geological heterogeneity was lost in the model. For example in Figure 4.40b for horizontal permeability there was a region with relatively lower value of permeability compare to the rest of the cells. After history matching in Figure 4.40e again this heterogeneity can be seen. Even though parameters were increased, there was still a relatively low value of permeability compared to the rest of the cells. In the channel, permeability was increased but the channel shape remained. Again, it can be seen that in the streamline guided case, the parameters were changed more smoothly, areally, compared to the well vicinity case which had a more local effect around the well. Also, it can be observed that for some cells in the reservoir, net:gross increased to 1 which means that we expect the geology of those regions to be just sand.

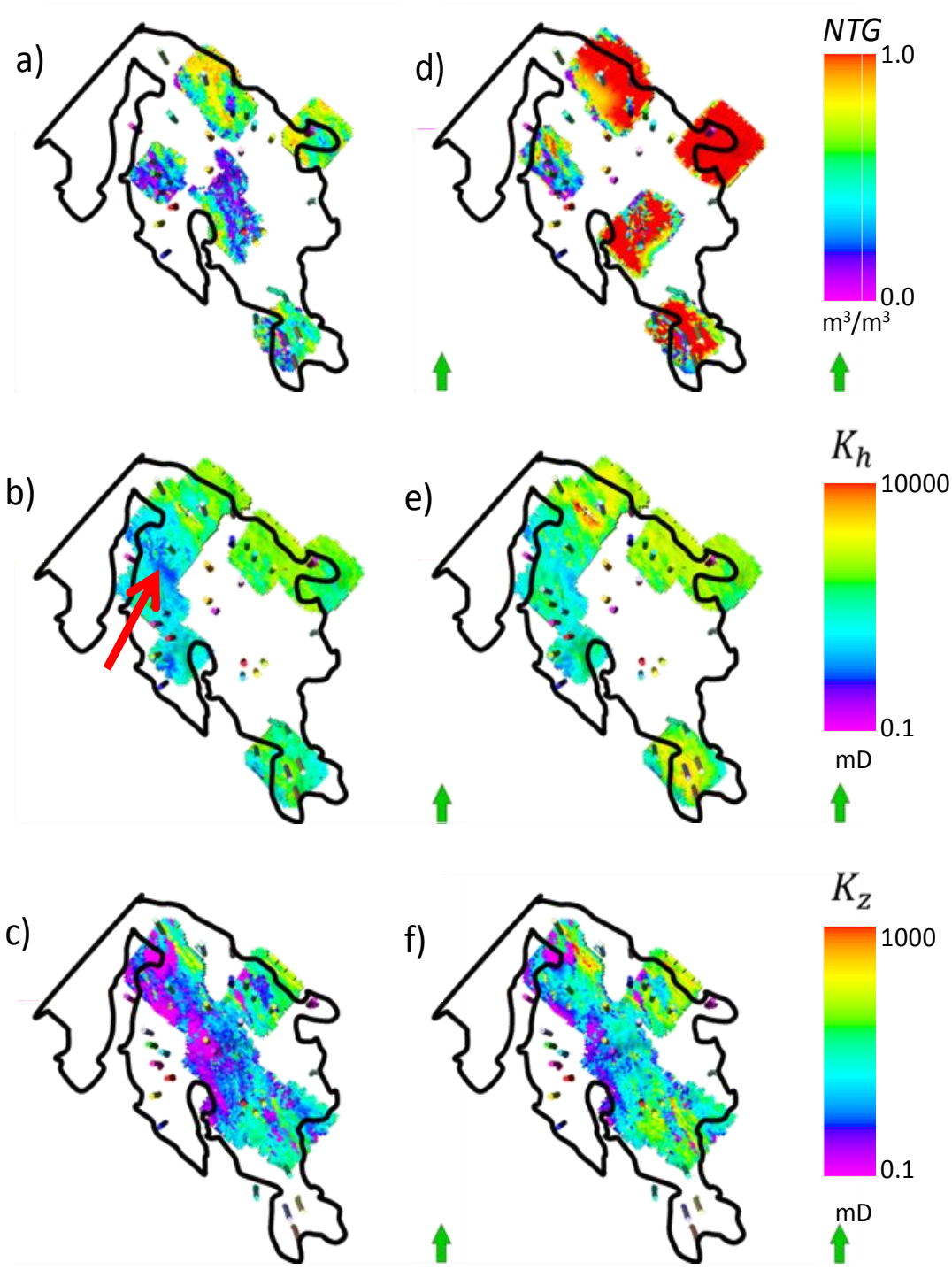


*Figure 4.40: Grid cell properties for those cells where increases were applied as a result of history matching showing a) net:gross, b) horizontal permeability and c) vertical permeability for the base case model and d) net:gross, e) horizontal permeability and f) vertical permeability for the best history matched model using streamlines. The black line indicates the boundary of the oil filled rock.*

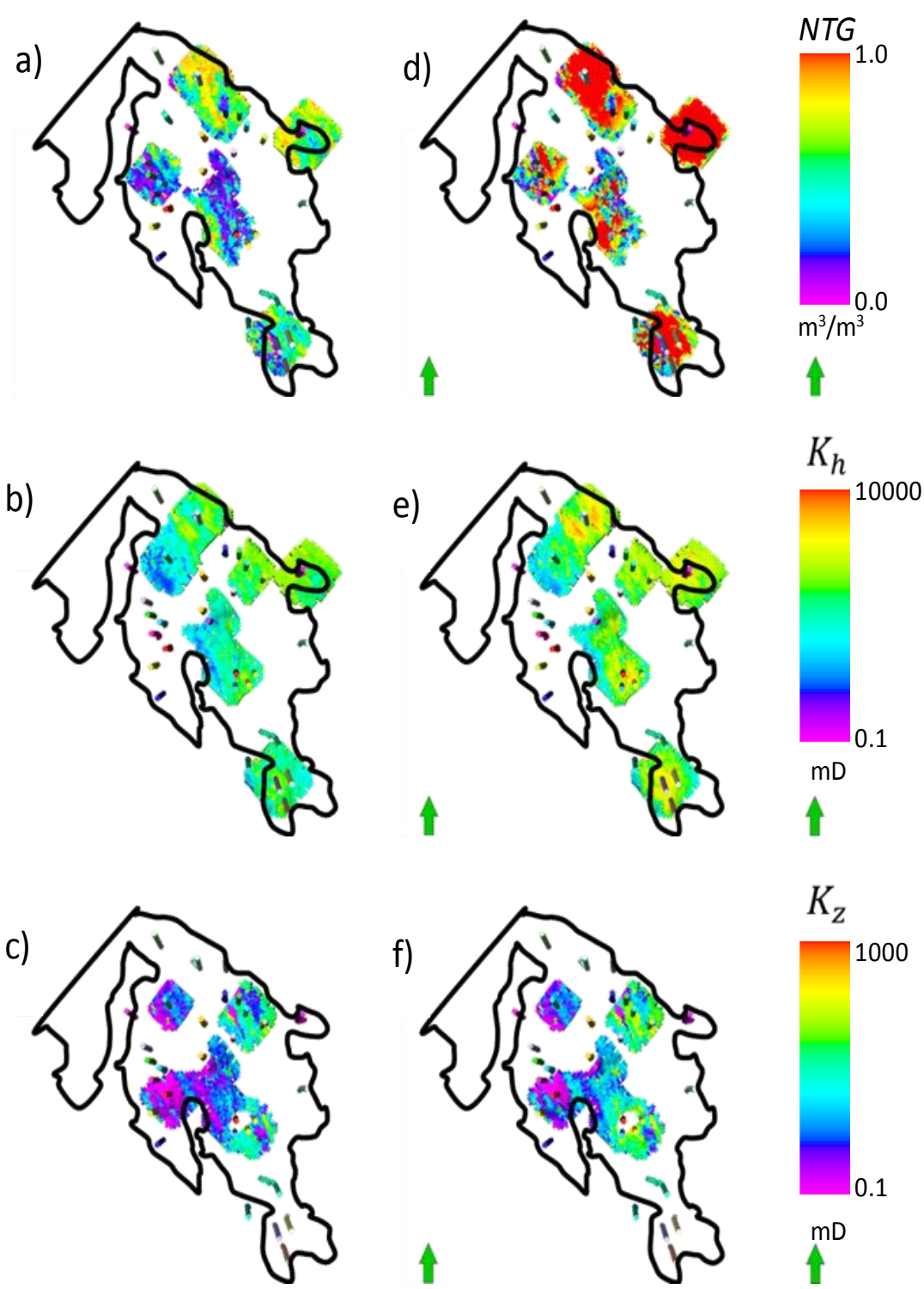


*Figure 4.41: Grid cell properties for those cells where increases were applied as a result of history matching showing a) net:gross, b) horizontal permeability and c) vertical permeability for the base case model and d) net:gross, e) horizontal permeability and f) vertical permeability for the best history matched model locating pilot points in the well vicinity.*

### 4.11 Discussion

From this chapter it can be observed that we can identify the best regions in the reservoir for updating using streamlines as a guide. It was found that this method was very useful in the Nelson field though there could be some fields where the approach requires more care in application. One case might be where we choose to update near a producer and then a new well is drilled during the history matching period. In this case the density of streamlines will be changed because of the impact of the new well. We would therefore need to history match in stages, perhaps focusing on the initial well configuration and then making further modifications once the new well is in place.

As an extension to this, we may consider that instead of focusing on the time steps with high misfit only, we could give equal importance to each time step. Then, from the beginning for each time step, we could map the streamlines towards the production wells and add pilot points to control changes to these streamlines. We would update the reservoir parameters successively for each time step by carrying updates onwards in time. If the new model can match the production profile of the well we can continue with this model otherwise we need to map the streamlines onto the new time step and by choosing new pilot point we update the reservoir through history matching.

Another case where the approach may require care is in a mature field with high well density. Finding the location to change may be problematic. On the one hand, this case may be easier to history match if the well separation is less than the correlation length of the permeability field. In this case we propose that smaller regions be considered for updating (i.e. single pilot points with appropriate Kriging parameters, including the variogram range). In this case the dimensionality of the history matching problem will increase.

In this study, three parameter updating scheme were introduced for better history matching. We first introduced the concept of each scheme and discuss the cases where we think each scheme can be applied successfully. We also discussed the limitations of each approach. In history matching problems where selected parameters seem to be independent, such as aquifer properties or fault transmissibilities we can use the GSV updating scheme in order to make the problem smaller and solvable by using AHM methods introduced in this study. On the other hand we can advise the use of the RMV scheme when history matching parameters are strongly dependent and also where there

were wells very close together with strong interaction. In such cases, by using the RMV approach, we can perform separate smaller history matching studies and therefore the AHM workflow more feasible. Finally LMV method is suitable for cases when we can separate different localities with negligible interactions. This scheme would be less costly in terms of CPU compare to the other two schemes and also the analysis of the result would be easier because of low history matching parameters.

In this chapter all schemes were tested on Nelson field and the local multi-variable scheme was found to be the best. The results confirmed the usefulness of this scheme and the match of the wells were improved and also there was a better forecast for the following three years. Comparing to other work in this research area for updating the reservoir, this method is more suitable for big reservoirs because it reduces the number of unknowns, saving CPU time. In most of the approaches presented previously, the whole simulation model was chosen for updating which increase the CPU drastically.
In order to investigate the optimum method of choosing the pilot point locations a sensitivity study was carried out for three wells and it was found that the streamline guide approach was the optimum way for choosing the region of the reservoir for updating. Also the history matching result was compared with a case where the pilot points were put in the vicinity of each well. It was found that the streamline guided history matching is more accurate and useful for the Nelson field.

# Chapter 5: TIME-LAPSE DATA NORMALIZATION

**Overview:**

So far history matching has been performed in Nelson by using production data only. One of the main goals in this project was application of 4D seismic data for better reservoir updating. An important step of the application of 4D seismic is data preparation. The physical meaning of the observed data needs to be understood as well as the units of measurement of the data.

As previously discussed in Chapter 3 (Section 3.7.2), the 4D seismic data that was used in this study consisted of phase shifted amplitudes which is in the same category as coloured inversion. The 4D signature was obtained from a Root Mean Square of signal between horizons and this was taken to represent relative pseudo-impedance. However, the unit of this data depends on how the original amplitude and phase shifted amplitude (pseudo impedance) data is calibrated. Based on the information we had, the full inversion and calibration was not performed for this data and so our observed data has a relative unit. More importantly the unit of the derived pseudo impedance attribute was different from the synthetic seismic impedance (introduced in Chapter 2, Section 2.4 and Chapter 3, Section 3.6). In the automatic history matching loop as defined in this study, the domain of seismic comparison is the impedance domain which is defined quantitatively in an objective function. Therefore in order to carry out a history matching successful we introduced a normalization scheme in order fill the gap of a proper and well calibrated seismic inversion and ultimately to bring the observed and synthetic data into the same units.

## 5.1 Normalization concept

In this chapter the focus is on the specific part of the Production and Seismic History Matching (PSHM) loop in the red box in Figure 5.1 where observed and predicted seismic signatures are compared.

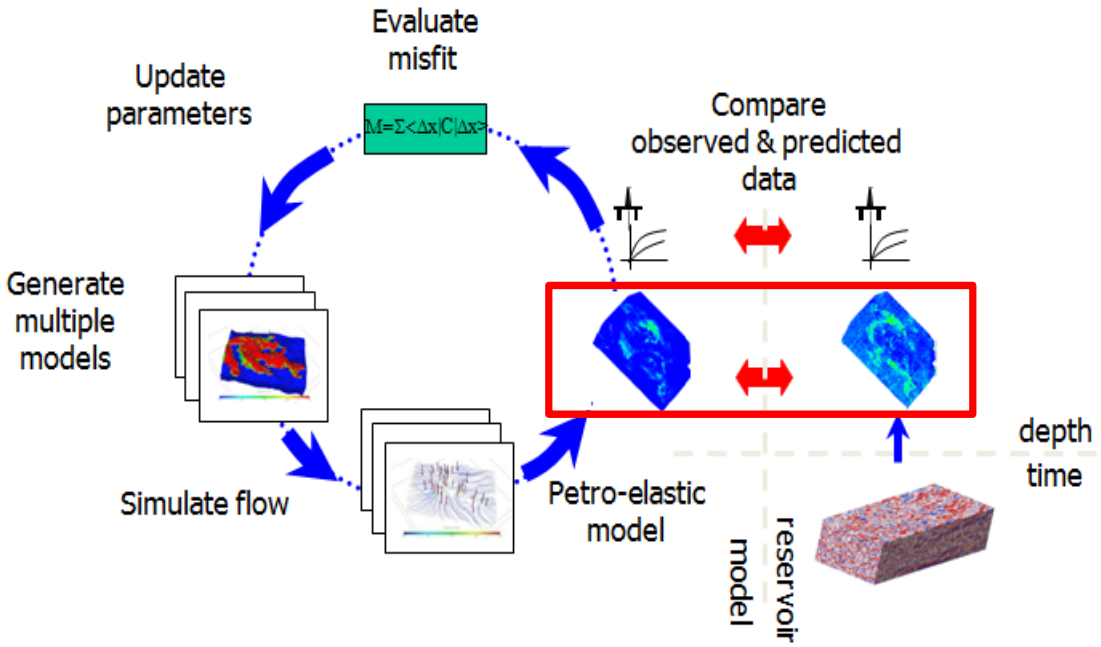


*Figure 5.1: Production and seismic history matching workflow. The red box is the area of study in this chapter.*

There are some difficulties here, however. The raw observed and the synthetic 4D signatures are incompatible in terms of the units of measurement. For the observed data we do not actually know these units due to the relative nature of the processing and inversion methods that have been used. Normalization is needed to get the data into equivalent dimensions (which is g/cc*km/s) for the predicted data. Figure 5.2 schematises how the observed data can be normalized. The raw observed map of change in impedances (Figure 5.2a) has a range from zero to several thousand in unspecified units. We consider that predicted changes in impedance from a simulation case (Figure 5.2b) may be used to derive a transformation equation. Figure 5.2c, shows as an example, the synthetic and real seismic data of a cross line in the reservoir. There is a similar trend for the data especially in the 4D seismic signal sections but there are differences, by orders of magnitude, between the data. The aim of this normalization study, then, is to convert the measured units of observed data (brown line) to the same units of synthetic data (blue line), which ranges from zero to 0.3 km/s g/cc. We assume that there is a degree of correlation between the synthetic and observed 4D seismic data that is approximately linear and so we derive such an equation using least squares regression. We approximate a linear forward seismic model, or a linear seismic inversion model. However if Backus upscaling (Chapter 2, Section 2.4.1) or Gassmann (Chapter 2, Eq. 2.5) or the fluid modulus law (Chapter 3, Section 3.6.1) are wrong then

the predicted impedance would not follow linearly with observed impedance. Similarly if the pseudo inversion via phase shifting and subsequent RMS do not provide a proper impedance then a linear model might be wrong.

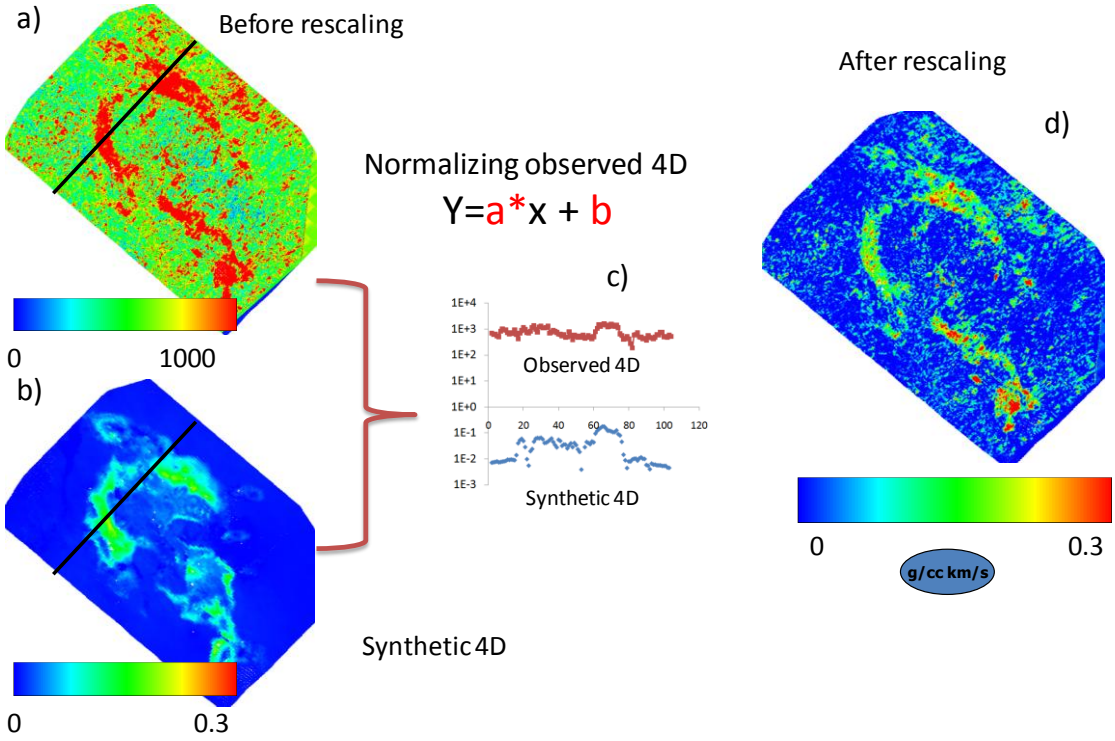


*Figure 5.2: Schematic of 4D seismic normalization. a) observed 4D seismic before normalization, b) synthetic 4D seismic, c) comparison of observed versus synthetic for the cross line shows in black colour in the maps and d) observed 4D seismic after normalization.*

## 5.2 Normalization approaches

For any 4D seismic history matching study we need to understand the 4D signal and analysis and interpretation helps to plan for history matching. However in this study for better normalization, the observed data needs to be understood first. For this purpose the 4D signature map (Figure 5.3a) was studied qualitatively to determine a link between production activity and the 4D seismic signal in the reservoir. The synthetic seismic data was calculated for the uppermost geological interval of Nelson (Figure 5.3b). The closed lines identified the regions were considered to contain 4D signal in the observed data (Figure 5.3a). There were also a number of production wells in this region.

As the Nelson field is a good example of saturated-dominated time-lapse seismic (Chapter 3, Section 3.6 and 3.7.3; McInally et al. 2003; MacBeth et al. 2005) it has been considered that this 4D seismic activity close to the production wells is the result of saturation change (water replacing oil). The synthetic 4D signature in Figure 5.3b shows that in the same region identified for observed data, there is a change of impedance for modeled data, but not exactly the same as observed data. Ultimately the aim is to remove these differences by PSHM.

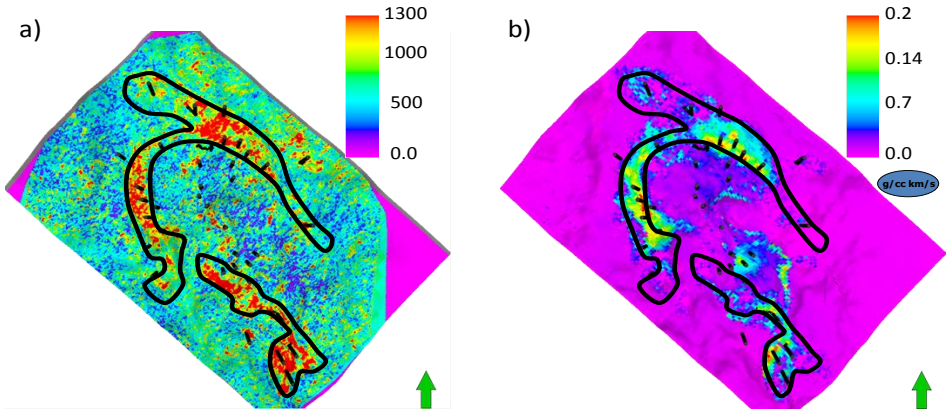


*Figure 5.3: Qualitative analysis of observed 4D seismic data by comparing a) observed data and b) synthetic data from the base model. The black lines indicate the main reservoir that is seismically active in this interval. All production and injection wells were also identified in the map as black lines.*

For the rest of the reservoir there is no defined 4D seismic signature. If there is some seismic activity in a region without other evidence of production activity then it can be considered as noise. This was the case outside of the reservoir region in Figure 5.3a. Based on this qualitative interpretation of 4D seismic data, the quantitative value of real and synthetic data was used in order to normalize the observed data.

### *5.2.1 Normalization procedure*

Two methods were defined for normalizing the observed 4D seismic signature:

***Map derived:*** Observed and synthetic 4D seismic signatures plotted for the simulation cells (either all or part thereof).

***Well derived***: Predictions from selected cells with well completions are compared. The focus was on those wells completed vertically and with good matching water cut. The latter indicates that there is a good prediction of saturation near the wells. Sub-horizontal wells are of reduced value however because a single water cut is obtained to

represent the near well saturation but this could be obtained from a number of different saturation distributions. Non-uniqueness is problematic here.

Figure 5.4 shows an example of calculating seismic data in the location of vertical wells. As shown in Figure 5.4a the observed data was chosen based on the data in the seismic bins corresponding to the simulation cells (red box in Figure 5.4a) in the location of vertical wells and arithmetic averaging was applied to the observed data within each simulation cell to obtain one value for this position. For the synthetic seismic (Figure 5.4b), the method which was introduced previously in Chapter 2 (Section 2.4) was used for calculation of compressional acoustic impedance for each simulation cell and Backus averaging (1962) was used vertically in order to get one value for the well (Chapter 2 ,Section 2.4.1).

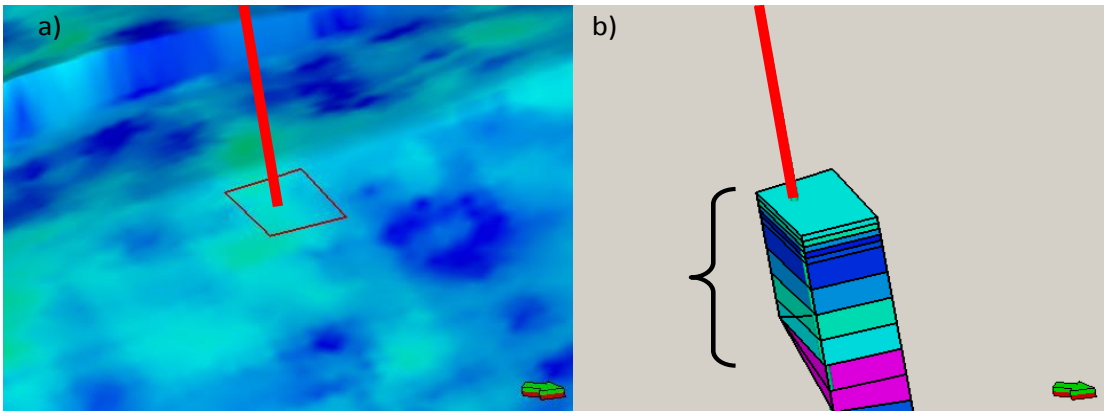


*Figure 5.4: Schematic of the location of a vertical well in a) seismic scale and b) reservoir scale. The red box shows the boundary of seismic bins at the same location of the simulation cell in b. Arithmetic averaging was used to calculate one value of real seismic in the red box and Backus (1962) averaging was used to get one value of synthetic seismic at the location of the well.*

Cross-plots for the two cases allowed us to derive an equation for normalization of the observed 4D seismic data. An example of the Well derived case is shown in Figure 5.5 where wells that match water cut closely at the survey times were used (Figure 5.5a) to derive Figure 5.5b. For the Well derived study it was assumed that when the simulated water cut of the vertical well matched reasonably with the historical data, it meant that the water saturation was also close to reality. In addition, the porosity and net:gross were also considered to be accurate at the well locations. This was quite reasonable given that the model was built based on the log data at the location of the wells.

There is a choice of models that can be used for normalization. The most obvious is the base case. Alternatively, a model updated via production history matching (PHM) could be used. In this study the best PHM model was obtained via the method in Chapter 4, essentially performing PSHM without the 4D seismic misfit.

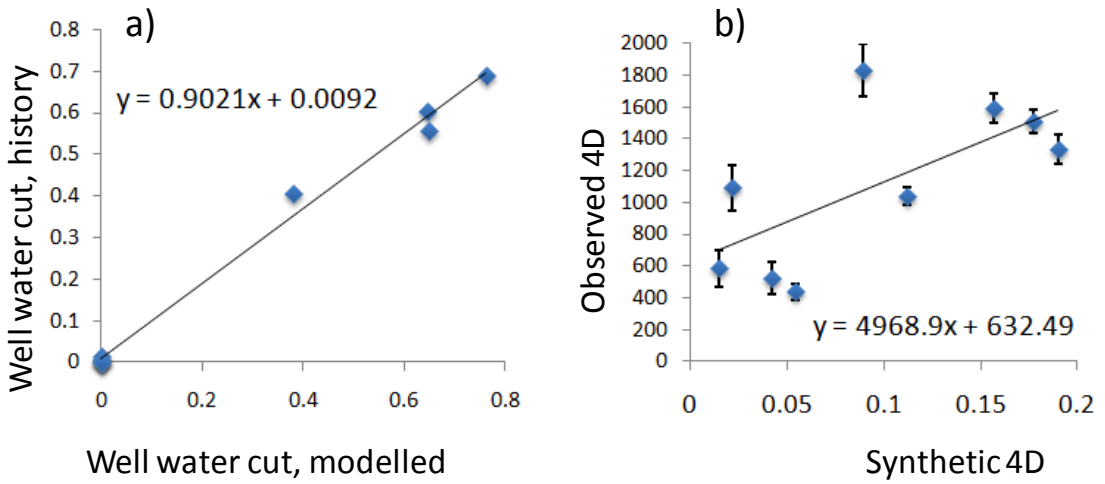


*Figure 5.5: Cross-plot of a) well water cut for history versus model and b) observed versus synthetic 4D seismic. The error bars in b are representative of standard deviation of observed seismic data for the bins at the location of each well.*

It is not clear, a priori, whether the Map derived approach is better than the well equivalent, nor is it clear whether the base case or the production matched model should be used. The following sections discus the approaches and the positives and negatives are summarised in Table 5.1.

In order to distinguish easily between the four cases, suitable names were chosen which we will use in the rest of the thesis. Well+base is for the case where normalization was based on well data only using the base case simulation model. Well+best is the same but instead of the base reservoir model, the best history matched model (PHM model) used. Map+base and Map+best are for Map derived cases by using base and best history matched model respectively.

| Options | Assumptions | Disadvantage |
|---|---|---|
| Map+base model | We trust our base model | 1- Biased by poorly matching areas (Figure 5.2)<br>2- Biased by noise (Figure 5.2) |
| Map+best model | Improved match is better | 1- PHM must be carried out.<br>2- Bias due to choosing a matched model |
| Well+base model | 1- Good matching water cut<br>2- Saturation dominated 4D seismic<br>3- $NTG$ and porosity correct | 1- Training data may be sparse<br>2- Partial completion of interval<br>3- We miss shut in wells |
| Well+best model | As above | As above except full field base case |

*Table 5.1: Assumptions and disadvantages of various 4D seismic normalization strategies, for modifying the base reservoir model through seismic and production history matching.*

The Map derived approach (using the full field model) is attractive because more data is used. However, the base case model may contain a number of regions where observations are not matched at a quantitative level but more importantly they may not match qualitatively either. This is most likely because the model requires updating. The production matched model is attractive in this case but changes may be made to the model that ultimately bias the search in PSHM because the seismic data is not yet matched. Therefore the results of PHM are discarded once the regression equation has been obtained for normalization. The downside is of course the cost of doing the history matching. It may also see bias if we are over optimistic about the accuracy of the petro-elastic model along with the near-well porosity and net:gross distributions in the model.

The Well derived approach is appealing because a good match is obtained at the wells and more data may be available if the production matched model is used. However, there is still a limitation of data with a small number of vertical wells present in the model and not all are significantly matched. Some are also inactive at the time of the 4D seismic survey and some only partially complete the reservoir interval leading to further non-uniqueness issues. This approach is also dangerous if the 4D seismic signature shows any pressure response. This was not believed to be the case for the

producers and there is no evidence for pressure response in the observed data, except around one injector.

All approaches based on the model assume that on average the net:gross distribution and porosity are modeled accurately enough. The possibility that this is not the case at the wells increases the resulting uncertainty, though we ignore that in this work. Similarly, the petro-elastic model capturing the effect of these properties on impedance must also be relied on.

### 5.3 Normalization of the data

Five regression equations were derived for normalization of the 4D seismic signature map. Figure 5.6 shows the observed versus synthetic 4D seismic data for different cases as introduced above. The straight lines show the regression equations that were obtained by least squares minimization.

The Map derived cross-plots are shown in Figure 5.6a and 5.6b and they are broadly similar. For the Well+base case (Figure 5.6c) the water cut data shows a good match for 8 wells out of the 12 vertical wells in this study. When the best history matched model (Well+best) was used it can be seen that the predicted water cut improved for another two vertical wells. However, in some of the locations where changes were made, there was more than one well present. In three of those cases, the water cut match of the wells that were not included in the misfit deteriorated and they have not been used in the cross-plot subsequently. It was also considered that an additional two wells should be discarded. One of these was shut in at the time of the 4D seismic survey and we cannot be sure that the saturation is correct then. The other well reaches the bottom hole pressure limit and so neither pressure nor rate match can be correct. These two wells are indicated in Figure 5.6d and the regression equation calculated with and without them.

In the first four normalization cases, the intercept of the regression equation was quite similar. The gradients of the lines were roughly doubled when the Well derived approach was used compared to using the map data. These differences resulted in the corresponding normalized maps (Figure 5.7).

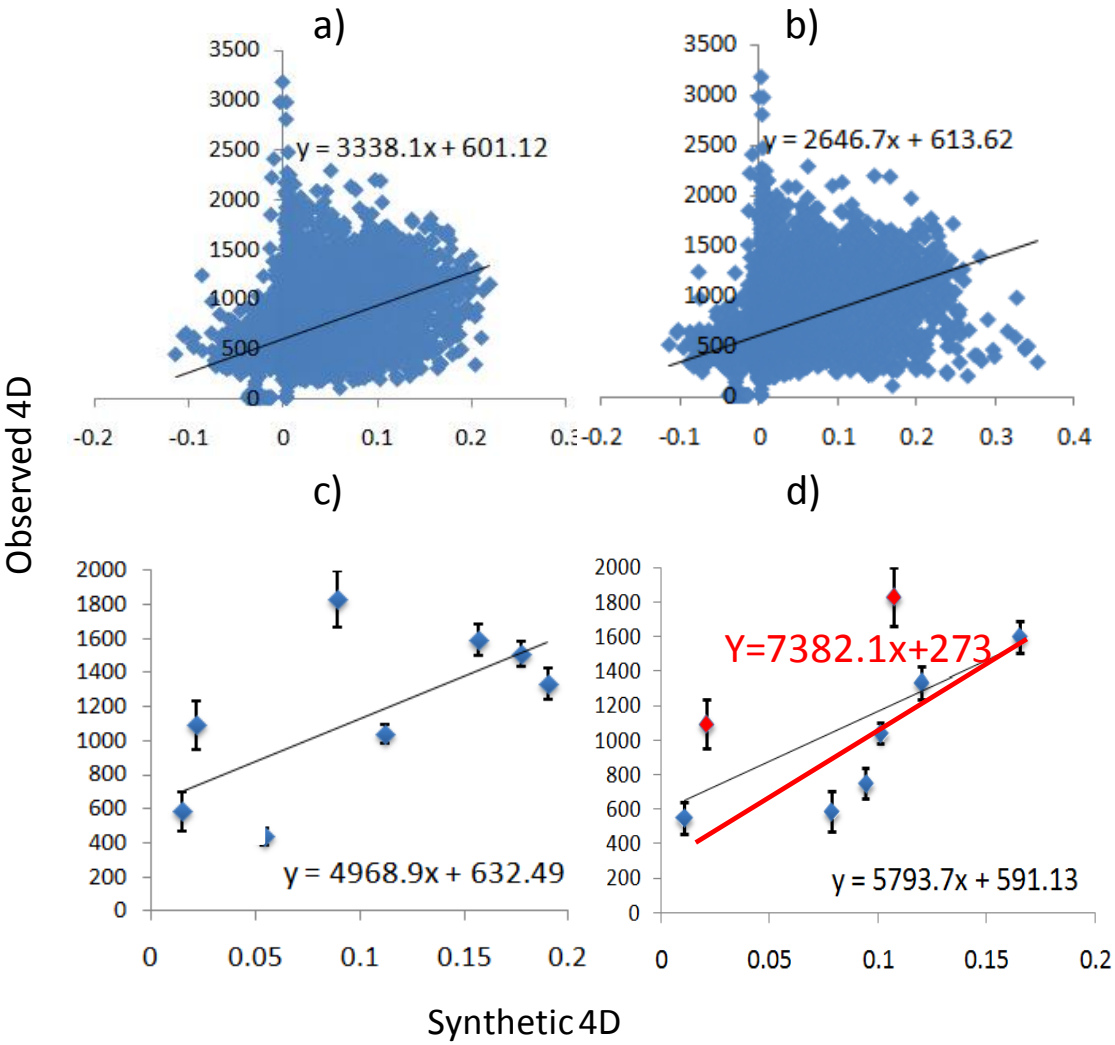


*Figure 5.6: Cross-plot of observed and synthetic 4D impedances for a) full set of simulation cells of the base model (Map+base), b) full set of simulation cells of the best model (Map+best), c) cells of vertical wells in the base model (Well+base) and d) cells of vertical wells in the best model (Well+best) (red line is obtained by ignoring two wells indicated by red symbols).*

The Map derived normalization produced quite a strong 4D seismic signature (Figure 5.7a and 5.7b), much stronger than the base case model suggested (Figure 5.7f). This possibly occurs because there are a number of regions in the observed data where there was no signature but the model predicted strong change. In other words the model needed to be modified further. There was also a lot of noise in the non-reservoir region of the map. The larger gradient in the regression equations from the Well derived normalization decreases the signature in the reservoir after normalization (Figure 5.7c-e) and they was appeared more like the base case. In Figure 5.7e the noise was accentuated because of the reduced intercept on the regression equation. It did not seem

to matter too much whether or not the best or base case models were used in either Map derived or Well derived normalization. The sum of squares of differences between the resulting normalized signatures and the base case model was calculated to confirm the above observations. It was noticeable, however, that the regression equations were not perfect in any of the cases and this can lead to additional uncertainty in the normalization.

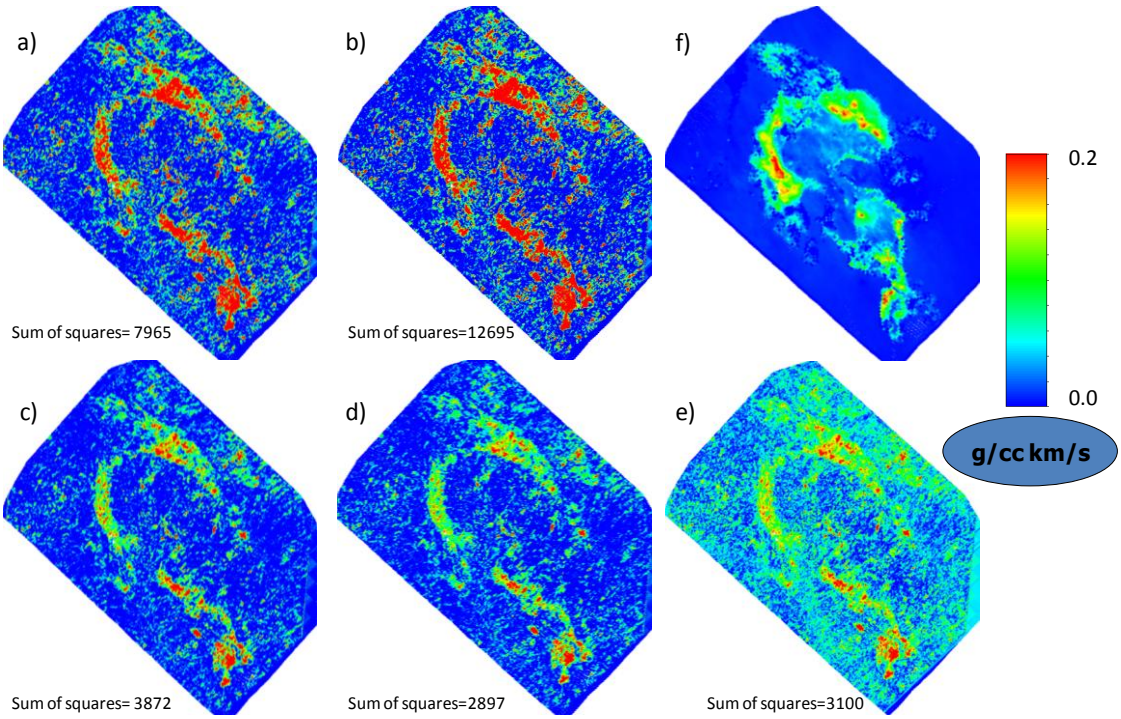


*Figure 5.7: Normalized observed 4D seismic obtained by using the regression equation of a) Map+base model, b) Map+best model, c) Well+base model, d) Well+best model, e) Well+best model with ignoring two wells and f) synthetic 4D seismic for base reservoir model (The sum of square of the differences between real and synthetic seismic of base reservoir model was calculated in each case).*

For better analyses of normalization results we need to consider two key points relating the magnitudes of 4D signatures and volume of water produced from wells. The first one was that based on the geological information in Nelson introduced in Chapter 3, there was a main shaly layer separating two reservoir intervals while there are a lot of wells completed in the first interval only. Because of that the water displacement towards the wells was more likely to be from lateral sweep rather than coning. The second important point is that because the reservoir is channelized there are large deposits of sand distributed, especially in the Channel Axis. These sand bodies are represented with a high value of net:gross in the reservoir. As long as the change of

impedance during the production is simply, directly, related to change of water saturation and net:gross value. Therefore the magnitude of the change in the signature was very important because when it was large it suggested that the reservoir needed a large water saturation change in the model via water displacement. This should be consistent with production activity, especially water breakthrough in the wells. On the other hand if the 4D seismic signature is smaller, then we do not require such a saturation change. Therefore for normalization of observed data, a regression equation similar to Figure 5.6c was preferred with a reasonable value of intercept and slope. An equation with large slope was obtained by ignoring the two wells above the line because of the same reason described for the red line in Figure 5.6d.

To use each normalized 4D seismic signature map in history matching, the data error needed to be estimated for use in the misfit in Eq. 2.19. This acted as a weight so that more accurate data was better matched. To obtain the data error, the non-reservoir 4D seismic signature was used and it was assumed that it consisted of noise that was typical of the part of the 4D signature containing signal as explained in Chapter 3 (Section 3.7.4). The non-signal part of the map was identified by setting a threshold in the data which was obtained visually from the maps. We acknowledge that this provides an estimate of the data error but it should be relatively close. A threshold of 1100 in the original data (Figure 5.8) was considered to be appropriate. The mean of the remaining signature is about 600, equivalent to the intercept of the regression equations in Figure 5.6. The standard deviation of this remaining data (values below the threshold if 1100 in Figure 5.8) is 186 which was calculated by Eq. 3.7 in Chapter 3. Then, this standard deviation was scaled for each normalized map by dividing by the gradient of each corresponding regression equation to get the normalized data error. For example for Map+base case in Figure 5.7, the standard deviation is:

$$\sigma = \frac{186}{3338.1} = 0.056 \tag{5.1}$$

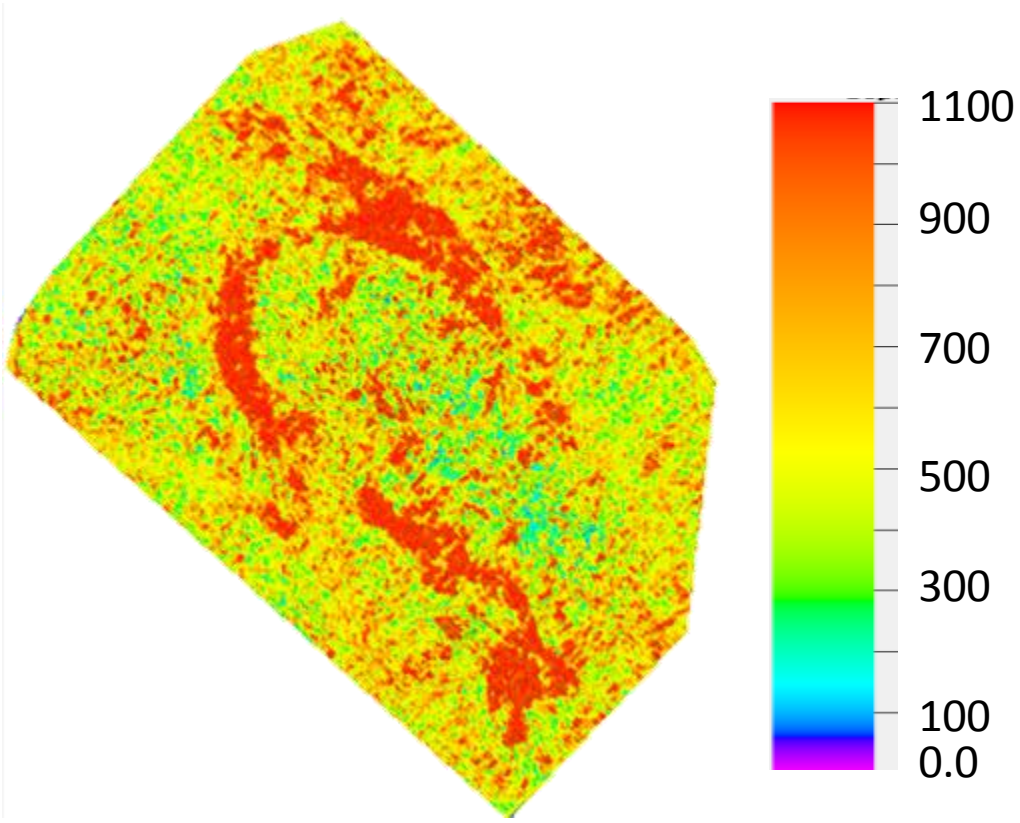


*Figure 5.8: Raw data observed 4D map before normalization. A coloured threshold of 1100 shows the 4D signals in the map.*

### 5.4 Using reservoir section for 4D seismic normalization

In addition to the normalization methods that were introduced in the previous section additional normalization approaches were defined based on reservoir sections in the model. The reservoir section was chosen by defining a threshold for base case 4D seismic maps before normalizing to see only the signature part in the reservoir section. Then the cells with 4D seismic value below this threshold were ignored. The rest of the cells were considered to represent signature in the reservoir section, and the cross-plot of observed and synthetic 4D seismic was plotted. For the synthetic 4D seismic the base and best reservoir models were used again. Figure 5.9a and 5.9b show the cross-plot of 4D seismic for base and best reservoir models respectively (in this case some false generation of signature was removed but not false absence).

Figure 5.9 shows that, first of all, the correlation of the observed and synthetic 4D seismic was very weak for both cases and for a long positive interval in the synthetic 4D seismic, the observed data was constant. The third observation was the negative slope. By using these equations, the 4D seismic attribute values that are higher than the

intercept were changed to negative amplitudes, whereas the cells with value below the intercept were changed to high positive amplitude. Negative values are not physically meaningful because we believe that there are no significant pressure signals and there are no regions of the reservoir where oil replaces water. For better understanding of this effect, the normalized 4D seismic map was plotted in Figure 5.10. Now it can be clearly seen that the part of the model that was below the threshold has a high amplitude value. Also, the signature from the active reservoir region is now negative.

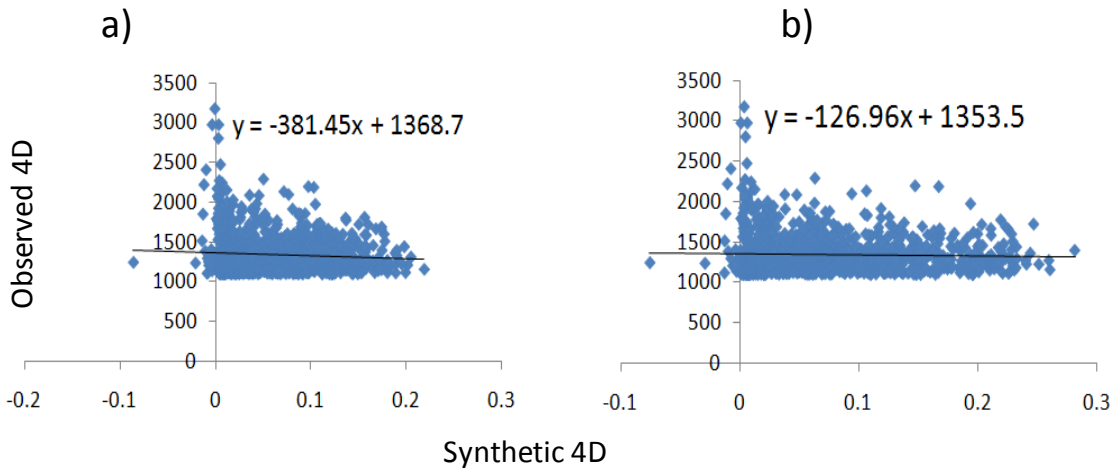


*Figure 5.9: Cross-plot of observed and synthetic 4D impedances for a) set of simulation cells in reservoir section only of the base model and b) set of simulation cells in reservoir section only of the best history matched model.*

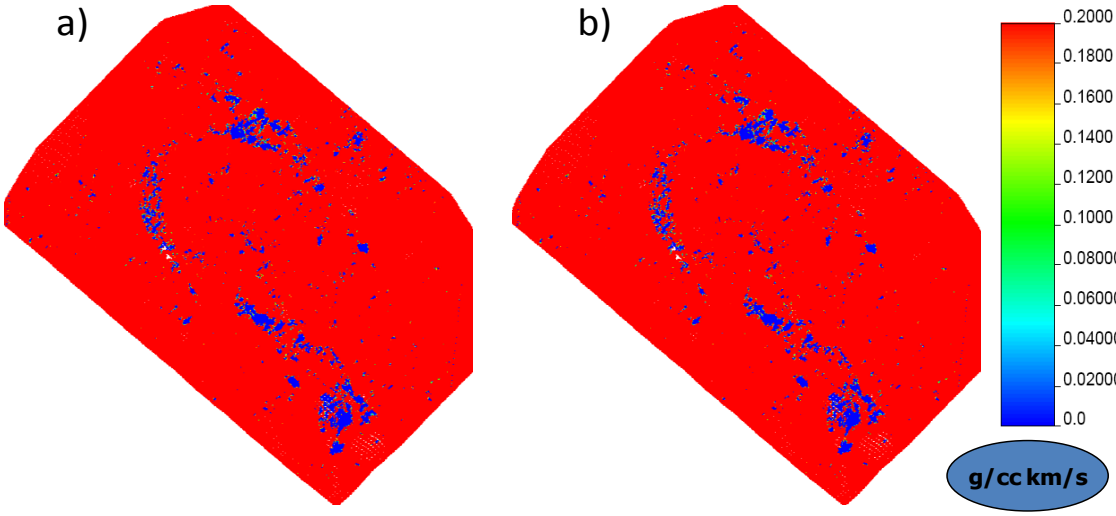


*Figure 5.10: Normalized observed 4D seismic obtained by using the regression equation of a) set of simulation cells in reservoir section of base model and b) set of simulation cells in reservoir section of best history matched model.*

## 5.5 NRMS filtering

So far, in the normalization schemes, all simulation cells, or some part thereof were used without considering any restrictions. For the next section it was decided to choose only the high quality part of the data by focusing more on the repeatability concept to reduce some uncertainty in the observed 4D seismic. The aim was to get more accurately normalized 4D seismic data.

For qualitative and especially quantitative use of 4D seismic, we need to know how repeatable our data are. One of the usual metrics for this is the "repeatability" of time-lapse seismic data. For this we mean that if everything is the same at two different times below in the sub-surface, the seismic trace should be identified. Determining whether this is the case is still a big area of research and because of a lot of factors in seismic acquisition it is almost impossible for us to have exactly the same traces.

The repeatability measure is based on calculating the Normalized Root Mean Square (NRMS) between two seismic traces at two different dates. To calculate this NRMS we usually focus on a part of the data set. Because we do not want to have the production effect, and usually we use the data from just above the reservoir section. Then we compare two different traces in this volume by calculating the root mean square (RMS) of the differences and we normalized that by dividing over sum of the RMS of each trace (Kragh and Christie 2002).

For two traces, $a_t$ and $b_t$, within a given window $t_1 - t_2$, the RMS of differences divided by the average RMS of the inputs is expressed as:

$$NRMS = \frac{200 \times RMS(a_t - b_t)}{RMS(a_t) + RMS(b_t)} \tag{5.2}$$

Where the RMS operator is:

$$RMS(x_t) = \sqrt{\frac{\sum_{t_1}^{t_2}(x_t)^2}{N}} \tag{5.3}$$

And N is the number of samples in the interval $t_1 - t_2$.

The value of NRMS is not intuitive and the range is not limited to 100%. For example the theoretical maximum of NRMS is 200% which is for the case when both traces are

anti-correlated. If both traces contain random noise, the NRMS value is 141% ($\sqrt{2}$). And if one trace is half the amplitude of the other, the NRMS would be 66.7%. For the Nelson field, we obtain the NRMS map of phase shifted amplitude 4D seismic data which is represented in Figure 5.11. From this picture it can be seen that there is a band in the middle where the NRMS is quite high.

In the literature some researchers allow 30% of non-repeatability whereas others are able to get 15% as the maximum value of non-repeatability, depending on the field of study and data (Craft et al. 2009). It is believed that, this is still a big range and there remains a question of which value exactly should be the best threshold that can be considered for the NRMS map.

For the Nelson field a 30% limit was chosen for this threshold to guide the calibration of observed 4D seismic and ultimately the time-lapse history matching. Using this threshold value, 10% of data over the Nelson map has been removed.

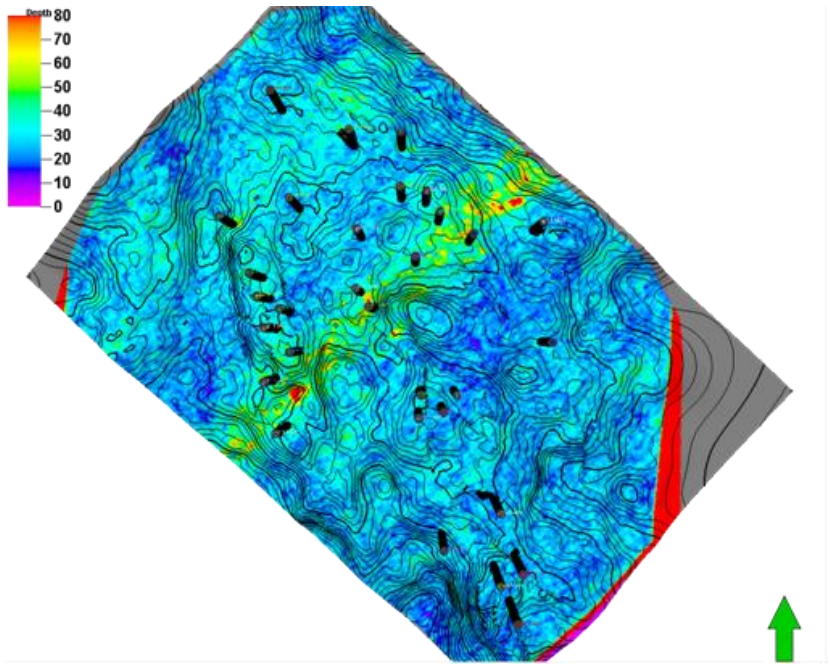


*Figure 5.11: The NRMS map for the 2000-1990 time-lapse data and for the first reservoir interval.*

## 5.6 Normalization of observed data filtered by the NRMS map

New observed maps were normalized by using the Map derived and Well derived options. As discussed earlier because of the uncertainty in the Map derived approach and lack of information in the Well derived approach it was decided to investigate a third approach between those normalization methods. The resulting cross-plots are shown in Figure 5.12.

The intercept for the equations in Figure 5.12a and b is around 600 which is the same as the average value of noisy part of data. This intercept is approximate because it converts the noisy part of the reservoir to zero on average. In the previous section (5.3) where the NRMS was not considered, this intercept was about 600 also for all four similar cases above.

By filtering the cells with high NRMS, the data at the position of the two vertical wells was removed as shown in Figure 5.12c and there were 6 points only in the cross-plot which was very sparse. After production history matching another well was lost with high water cut because it was not included in the history matching misfit. Therefore, it can be said that because of the lack of information for the Well derived study, it could not predict a reasonable value for the intercept of the regression equation. On top of that there is still another uncertainty in the normalization study which is not related to NRMS only. The first is from the fact that the reservoir parameters were considered to be reasonable at the well location where there may be uncertainty because of averaging issue when transforming from log scale to simulation scale. Secondly there is uncertainty in the equations used to calculate the synthetic seismic data because the equations came from lab studies and it is problematic to apply those to the simulation scale (Menezes and Gosselin 2006; Kazemi and Modin 2010).

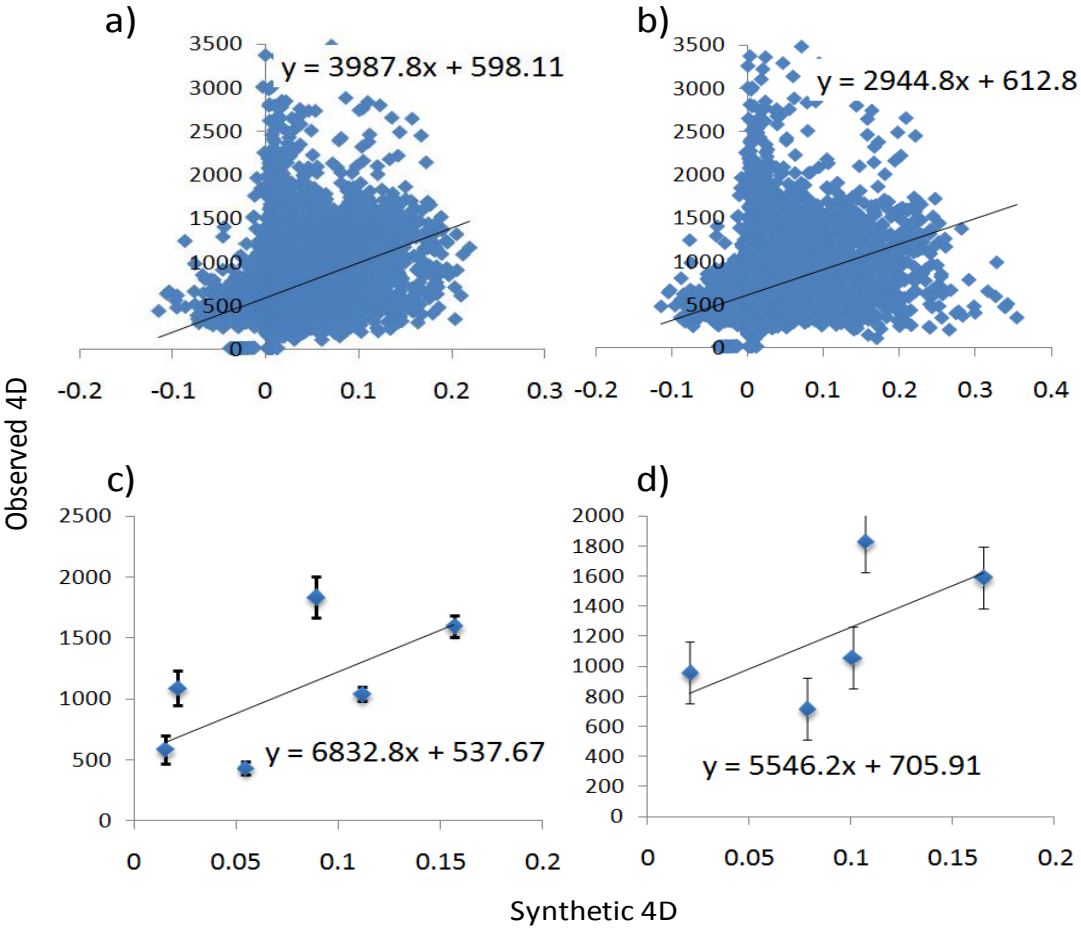


*Figure 5.12: Cross-plot of observed and synthetic 4D impedances for a) full set of simulation cells of the base model (Map+base+NRMS), b) full set of simulation cells of the best model (Map+best+NRMS), c) cells of vertical wells in the base model (Well+base+NRMS) and d) cells of vertical wells in the best model (Well+best+NRMS) (a part of data filtered by using NRMS equals to 30%).*

Focusing on the gradient which controls the 4D seismic signature it can be said that the gradient is lower for the Map derived cases compared to the Well derived cases. Therefore, a brighter 4D seismic signature for Map derived cases was expected compared to the Well derived. By comparing the new results with the previous study (Section 5.3) it can be observed that by filtering some data, the gradient of the regression equation increased except for the case in Figure 5.12d. Compared to previous study this increased gradient was something which was expected for Map derived but not for Well derived cases. It can be concluded therefore that after using NRMS as a filter a better gradient for the Map derived cases was found. After application of the above regression equations to normalization of observed data, we obtained the normalized maps as shown in Figure 5.13.

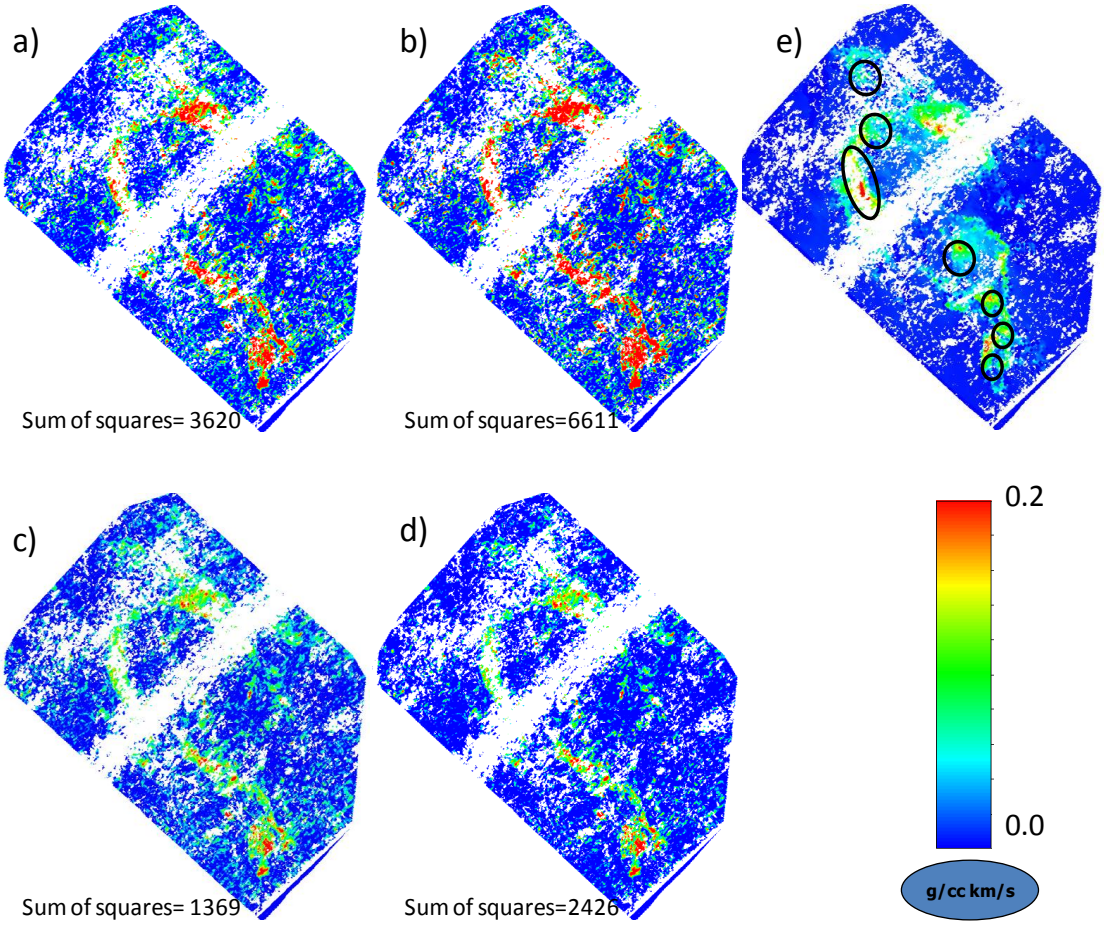


*Figure 5.13: Normalized observed 4D seismic obtained by using the regression equation of a) Map+base+NRMS model, b) Map+best+NRMS model, c) Well+base+NRMS model, d) Well+best+NRMS model from Figure 5.12 and e) the synthetic seismic data for base reservoir model. Black circles show the location of 15 production wells that under predict water rate for the base reservoir model.*

There is an important point which needed to be considered when the misfit values were compared. From Figure 5.13, for the Well derived cases, there was a lower sum of squares between the difference of real and synthetic data for the whole model. On the other hand for matching the production rates at the wells there should have been water displacement towards the wells, from the right location in the reservoir. Therefore in reality it was expected that 4D seismic signatures should have been seen in the reservoir to confirm the water sweep.

Looking at the production activity, the base model overestimated water production for the whole reservoir. For individual wells, 12 out of 27 wells over-predicted total water production and 15 under-predicted. It is very difficult to find an exact relationship between the production and seismic activity quantitatively because it would depend on a

lot of factors and it is out of the scope of this thesis. Qualitatively it can be said that in the black circles in Figure 5.13e which identify those 15 wells with under prediction of water production, it was expected that greater change in water saturation would occur leading to stronger 4D signatures.

Based on the discussion above for Well derived cases, even for cases where the misfit value was reduced in the black circles in the 4D maps (Figure 5.13e) the magnitude of seismic value was very close to synthetic seismic of the base model. This comparison suggests that after improving the simulation model in order to increase water sweep for those 15 wells, there should be a synthetic seismic map with stronger 4D values. This is not compatible with the Well derived observed data. Simply, it can be concluded that the Well derived observed map does not possess great enough 4D signature in order to be consistent with water sweep in the black circled areas. Based on the above discussion the Map derived data better captured the 4D seismic activity in the black circles.

## 5.7 2003-1990 4D seismic normalization

Normalization of the 2003-1990 4D seismic map is the goal in the prediction period. The same methods were used as for the 2000-1990 map. The difference here is that we did not use the NRMS map for the 2003-1990 period.

For this study the period of production in the field was 9 years. Therefore, additional water was produced from the reservoir compared to the previous 6.5 years of production. Thus it was expected that brighter 4D signatures would be observed in the reservoir after normalization. Figure 5.14 shows the normalization equation for different studies. The intercept of the equation was around 600 for Map+base and Map+best cases which was consistent with the previous discussion in section 5.3. For the Well+base case the intercept was lower than the expected value, however. On the other hand, the slope of the equation increased for this case so that the value of the real data also increased as well. Therefore, in Figure 5.15 it can be seen that the 4D signature was higher than the previous case (Figure 5.7). Because the estimation for the intercept was incorrect in the Well derived case, the normalized 4D is very noisy, as shown in Figure 5.15b. The large slope of the equation also reduced the 4D signature for that case.

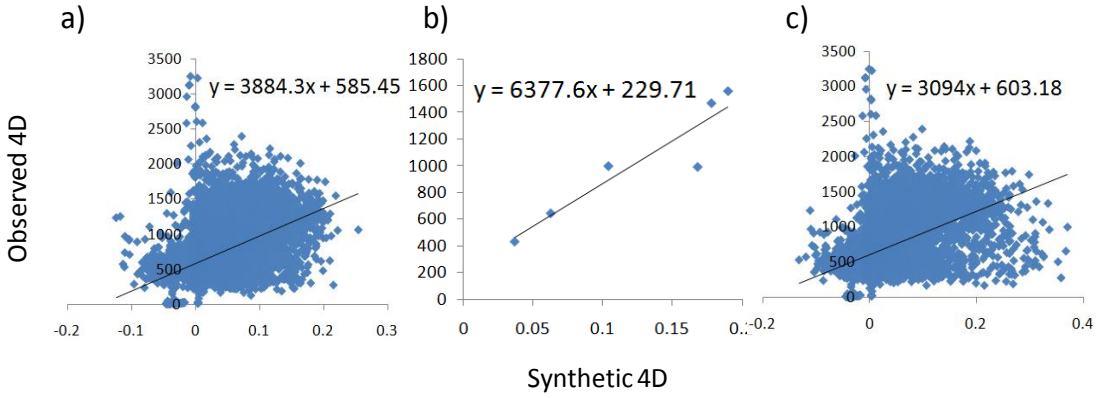


*Figure 5.14: Cross-plot of observed and synthetic 4D impedances for a) full set of simulation cells of the base model (Map+base), b) cells of vertical wells in the base model (Well+base), c) full set of simulation cells of the best model (Map+best).*

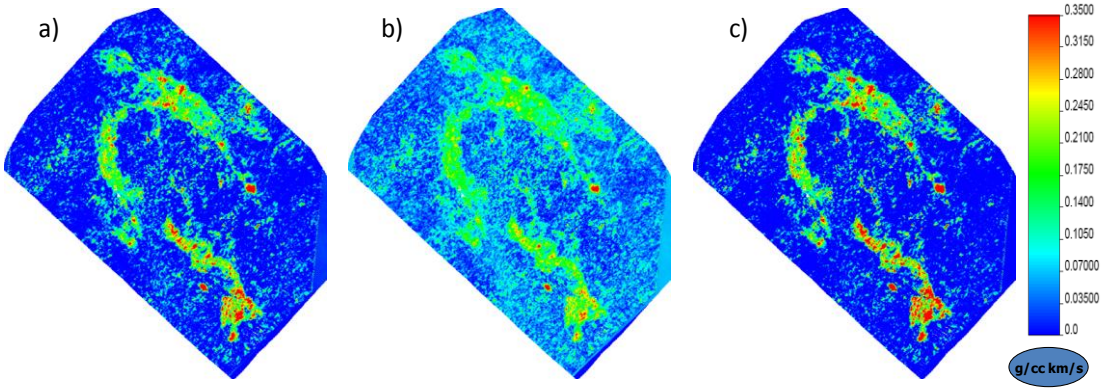


*Figure 5.15: Normalized 4D seismic map in 2003-1990 periods based on a) Map+base, b) Well+base and c)Map+best.*

## 5.8 Summary

In this chapter of the thesis, the aim was to investigate different ideas and methods that can be used for normalization of 4D seismic data. This study was challenging because in each case there were problems. Some assumptions were required which created uncertainties. In the last part of the chapter the concept of repeatability introduced in order to remove data with high uncertainty. In the next chapter the normalized 4D seismic map are used in order to history match of the Nelson field.

# Chapter 6: PRODUCTION AND SEISMIC HISTORY MATCHING USING STREAMLINE GUIDE APPROACH

**Overview:**

In this chapter of the thesis, we describe how the time-lapse seismic data for Nelson were integrated into the history matching process along with production data in order to constrain the reservoir model with both kinds of dynamic information. Almost all normalized 4D maps (derived in the previous chapter) were used in order to test the normalization scheme. Also we investigated which normalization method can provide the most suitable 4D map. The final aim in 4D seismic history matching is minimizing the objective function by reducing both production and seismic misfits. Therefore we define the most suitable normalized 4D map to be that which enables the biggest reduction of the total misfit value at the end of history matching study for both matching and forecasting periods. In addition, we observed different levels of signal/noise in produced normalized maps and as discussed in previous chapter (Sections 5.3 and 5.6), the seismic signature should be consistent with production activities. Therefore, other criteria for selecting the normalization would be based on consistency between seismic signature and production activity. By using various normalization processes, the resulting history matched models were different. The updated reservoir model that can better capture fluid flow movement in the reservoir in matching and forecasting periods is going to be a better candidate for final selection of history matched models.

## 6.1 History matching information

In this chapter similar to Chapter 4, the 13 worst matching wells were targeted with one master pilot point per well. These wells contributed to 84 per cent of the total production misfit. 7 of these wells were completed in the top geological interval so we did not change properties in the intervals beneath those locations. In this case each history matching problem was three dimensional. The other 6 remaining wells that we focused on were completed in both oil filled intervals where we updated the properties. The problem was therefore six dimensional for these regions. Overall, the problem was 57 dimensional using the local multi-variable approach and the problem was a combination of 7 three dimensional problems and 6 six dimensional problems. A

summary of relevant information about the history matching cases is presented in Table 6.1.

| | |
|---|---|
| Areas chosen for history matching | 13 areas based on the streamline guide (Chapter 4; Kazemi and Stephen, 2010) |
| Reservoir variables updated | $K_h$, $K_z$ and $NTG$ |
| Dimension per well | 3D for 6 areas in first interval only<br>6D for 7 areas in both intervals |
| NA parameters | 3D: $n_i$=16, $n_s$=10, $n_r$=5, total=66<br>6D: $n_i$=128, $n_s$=18, $n_r$=9, total=524 |
| Production wells chosen | Oil and water rates for 13 wells |
| 4D observed data | Re-scaled phase shifted amplitude |
| Parameterisation scheme | Local multi-variable (LMV) (Chapter 4 and Kazemi and Stephen 2010) |
| Pilot point information | Pilot points separation: ~500m<br>Kriging variogram range: ~1500m<br>The number of pilot points per master: 9 - 25 |

*Table 6.1: History matching parameters.*

**6.2 History matching results**

The 9 normalized 4D signature maps that were produced in Chapter 5 (Figure 5.7 and 5.13) were applied to the PSHM loop through identical history matching studies. From this process it was found that the production and seismic misfits were reduced by different degrees giving some improvement of the reservoir model for all 9 studies. However the aim here was to find out which normalized 4D seismic would be a better constraint of the reservoir in history matching. An example of misfit convergence is shown in Figure 6.1 where the trend of misfits during history matching is plotted for 3 different parts of the reservoir. In this figure, the production misfit is only shown for selected wells (the wells targeted in those areas). The seismic misfit was obtained for the whole reservoir but it was affected only by the region close to the specific well in each case.

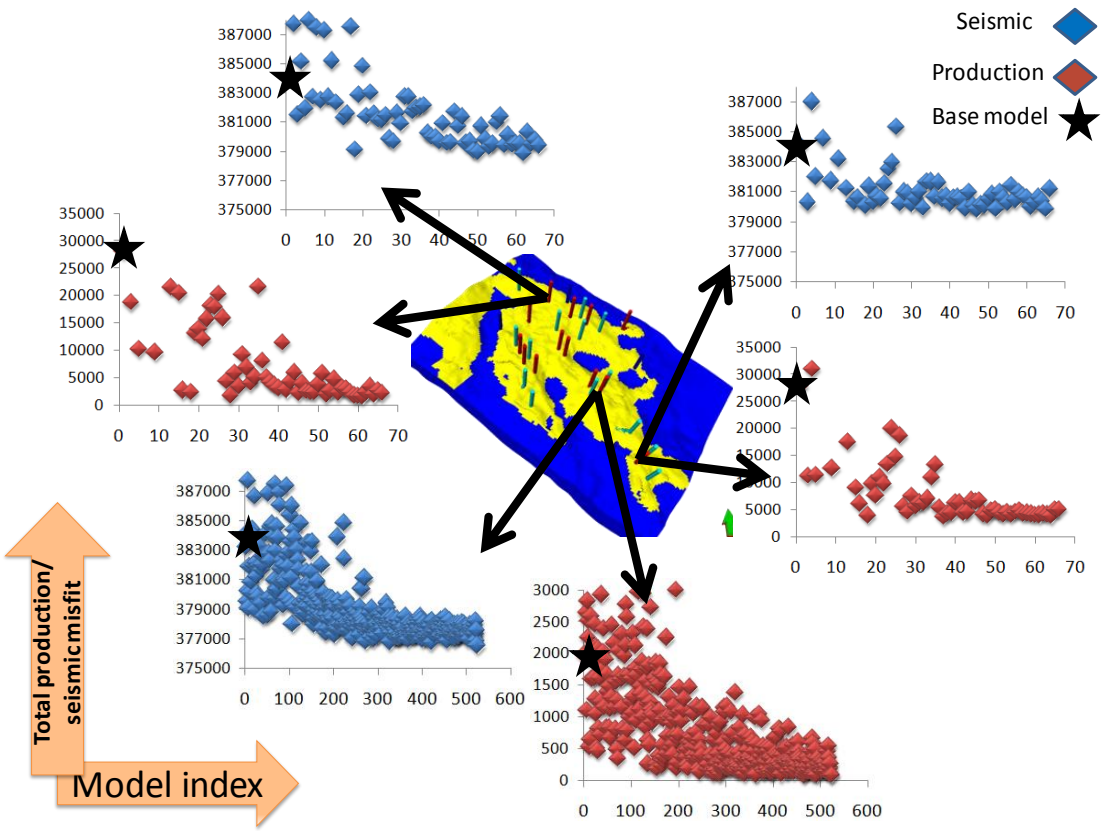


*Figure 6.1: Misfit reduction for seismic and liquid production rate for each well for 3 different areas of the reservoir.*

A local multi-variable (LMV) approach was used as described in Chapter 4 which means that each history matching case consists of seven 3 or 6 dimensional sub-cases. Each sub-case provided us with an updated set of parameters which was then amalgamated to obtain a better fitting model. We then built a set of the final 10 models by including modified reservoir parameter similar to procedure explained in Chapter 4 (Section 4.6.3). In this case we used abbreviation $LocalityPSHM_j$ $(j = 1,2,3,..,13)$ to show the final models. As an example the final model would be like:

$$LMVPSHM_{Final1} = f\left((NTG_1(u), KH_1(u), KZ_1(u))_{Locality_1}, \dots\dots, (NTG_1(u), KH_1(u), KZ_1(u))_{Locality_{13}}\right) \quad (6.1)$$

We performed 9 history matching studies (Map+base, Map+best, Well+base, Well+best, Well+best by ignoring two wells, Map+base+NRMS, Map+best+NRMS, Well+base+NRMS and Well+best+NRMS in Figures 6.3 and 6.4) therefore the above procedure was repeated to generate final 10 reservoir model for each study. Also we

made a comparison between misfit values when reservoir parameters were combined ($LMVPSHM_{Final}$) with individual history matching studies ($LocalityPSHM_j$) as shown in Figure 6.2. For each locality we added the misfit value of the best history matched model (Eq. 6.2) and added the misfit of non-targeted wells in order to calculate the total reduction of misfit across the reservoir. This figure shows that after combination of parameters updated in localities ($LMVPSHM_{Final1}$) the reduction of misfit value is as good as the sum of misfits obtained by modifying individual localities.

$$misfit_{locality} = misfit_{LocalityPSHM_1} + .. + misfit_{LocalityPSHM_{13}} + misfit_{non-targeted\ wells} \quad (6.2)$$

The reduction of the misfits for the best overall model was compared in Figure 6.3 and 6.4. The seismic misfit reductions are shown although the observed data was different in each case. From Figure 6.3 several observations can be made. From black bars (reduction of field production misfit) it can be seen that regardless of the choice of normalization method the misfit was reduced for all production wells. Well+best shows a smaller reduction of the misfit compared to the others which was probably due to the nature of the observed 4D map for which the gradient of the regression equation was large (Figure 5.6d) and thus the magnitude of the normalized 4D signals was small.

For the 4D seismic misfit reduction (blow bares) there is a variable degree of improvement to the predicted 4D signature. The best improvement of 4D seismic data occurred with the least improvement in production misfit. Also, the two Map derived cases saw the poorest improvement although these were poorer matching models in any case. It has been noted that the reduction of the 4D seismic misfit was somewhat lower than for production data. This was because the change in 4D signature was quite localized and much of the 4D misfit actually came from noise in the non-reservoir region (around 50 per cent). The production misfit was of course very localized and is relatively more affected by changes during PSHM. On the other hand, what mattered for the inversion process was the absolute change in each misfit. The balance of these absolute changes was controlled by the estimated data error, which was smaller for the two well derived cases using the best PSHM model.

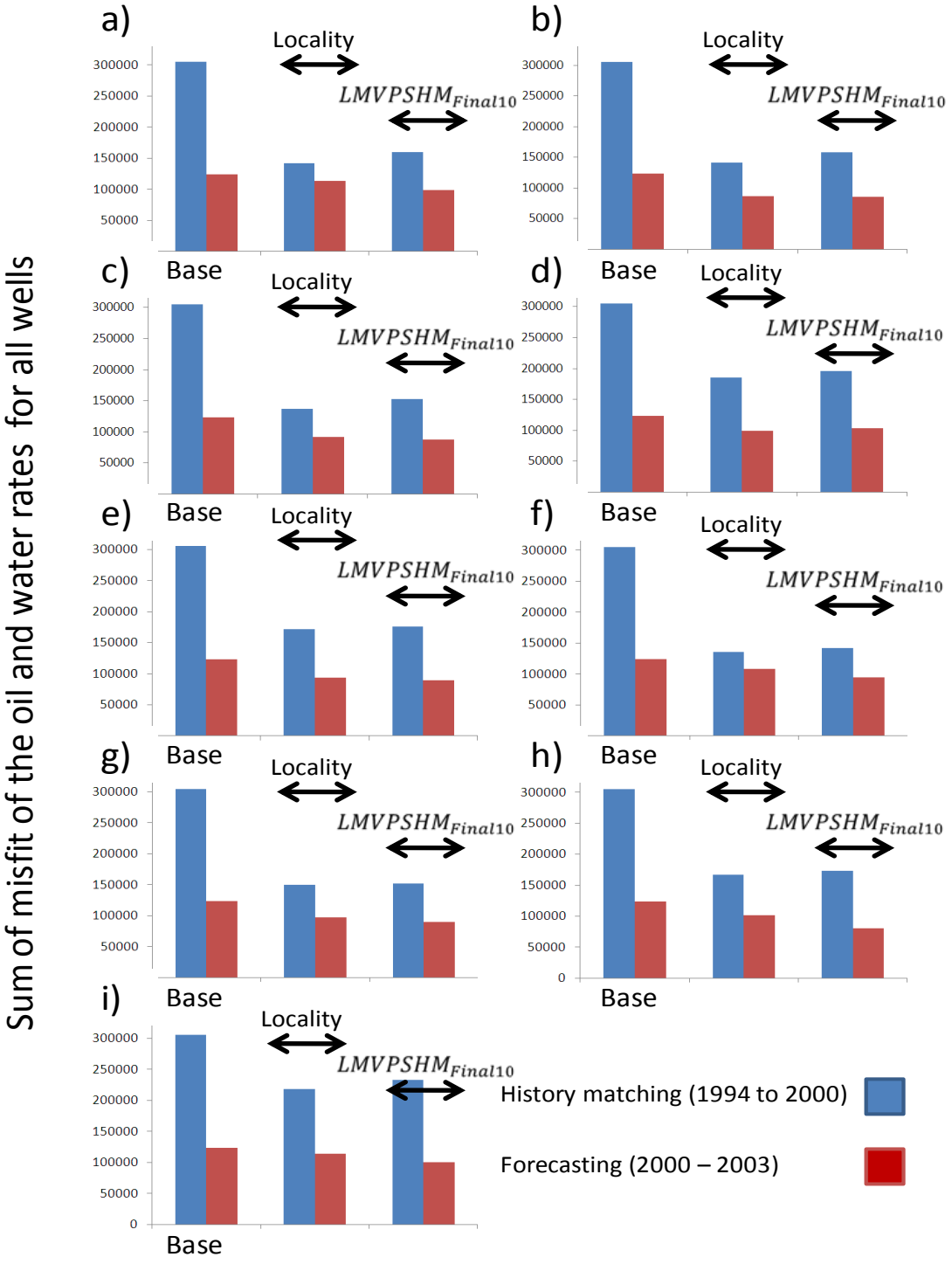


*Figure 6.2: Sum of misfits of the oil and water rates for all wells, comparing the model generated by combination of parameter in each locality ($LMVPSHM_{Final1}$) with sum of misfits value for each locality (Eq. 6.2) for a)Map+base, b)Map+best, c)Well+base, d)Well+best, e)Well+best with ignoring two wells, f)Map+base+NRMS, g)Map+best+NRMS, h)Well+base+NRMS and i)Well+best+NRMS*

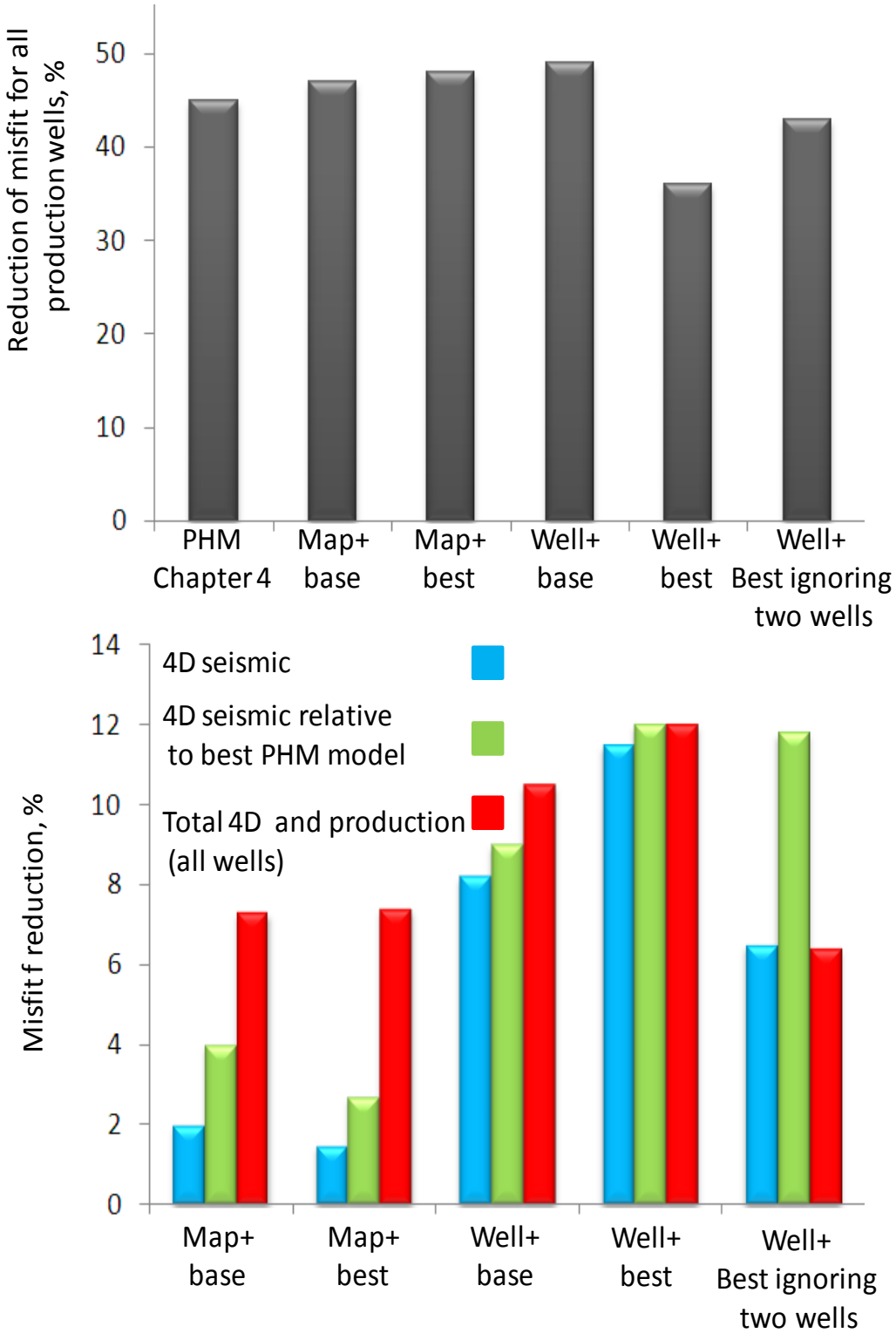


| Seismic misfit of base models (in millions) | 2.39 | 2.65 | 2.54 | 2.22 | 2.37 |
|---|---|---|---|---|---|

*Figure 6.3: Reduction of misfits of production and 4D seismic data for the best reservoir model from each history matching case. Reductions are compared to the base case model except for green bars which is a comparison to the best PHM model .*

Green bar (4D seismic relative to the best PHM model) shows the reduction in 4D seismic misfit following PSHM compared to the best model from PHM. Clearly the best PHM model saw an increase in 4D seismic misfit in a number of regions and the value of seismic is demonstrated. Red bar shows the combined reduction in misfit and finally the small table in Figure 6.3 the seismic misfit of base reservoir model is presented. This was used in the calculation of seismic and total misfit reductions. These statistics depend on the weighting of the production and seismic misfits which came from the data error estimates. In this study we estimate the data error with a calculation of the standard deviation for both production and seismic data as discussed in Chapter 3 (Section 3.7.4). In a Bayesian framework, weighting is based on the relative accuracy of data measurements and the model estimates. The misfit will be lower for less accurately measured data. However, extra weighting could be used in different cases. For example if the field operator was aware of some uncertainties in the processing of the data we can include that in the objective function ($\beta$ *in Eq.* 1.2). This would be equivalent to an adjustment upwards of the estimated data error. On the other hand, where measurements are thought to over-sample and provide no new information, then, separate weighting may be introduced. This may occur in cases of 4D signatures that vary very slowly spatially or production data that does not diverge from simple behaviours but is measured at very high frequencies. Another important issue for 4D seismic is the accurate estimation of noise and signal in the data which is difficult and should be discussed case by case. All history matching were performed in order to increase the ability of reservoir models to predict the future behaviour of the reservoir. On the other hand the main advantage of using 4D seismic is often as a constraint on the simulation model adding more information spatially from the reservoir. Therefore in this study the best history matched model was chosen where the model was good enough to match the history of the reservoir with a reasonable forecast capability.

To discuss Cases 4 (Well+best) and 5 (Well+best, ignoring two wells) further, it seems that for Case 5 normalization amplified the noise (Figure 5.7e) that, ultimately, the inversion process tried to match along with the signal in other areas. While the misfit appears better after PSHM it is possible to end up with a predicted signal that may match the normalized data but not reality. This would occur if we have used the wrong data in the normalization process or failed to account for the additional uncertainty created in that process. For Case 4 a large slope was derived in the regression equation. Therefore, post-normalization, a smaller change in saturation was interpreted. This

could have resulted in changes to properties in a direction contradictory to what was required to improve the match to the wells. This was particularly likely to have been the case if we determined that the 4D signature was more accurate than it actually was. This observation can be made in 5 production wells out of the targeted 13 (for the best history matched model) where the total amount of water produced in the matching period for these 5 wells was underpredicted by 16%. However in Well+base case which was chosen as the best result for these 5 specific wells, there was a good match for the total amount of water produced and it was just 5% higher than historical production data.

By using the NRMS filtered normalized observed map, another set of history matching results was generated. Figure 6.4 summarizes the production and seismic misfit reductions of the best model which improved the misfit value in the matching period.

Figure 6.4 shows that in the Map derived cases there was a very good reduction of the total production misfit of the whole reservoir and this was even better than for the production history matching case (PHM). However, for the Well derived cases, an unsatisfactory regression equation was obtained, from the normalization study (and observed maps in Figure 5.13c and d) because of the sparse amount of information. Those observed 4D maps did not show a strong enough 4D signature especially in the black circles in Figure 5.13e. If the observed data is not of reasonable quality, ultimately the workflow will end up with an unrealistic history matched model.

Looking at the reduction of the seismic misfit it can be seen that for the all cases, the misfit value was reduced by some percentage. In the Well derived cases this reduction was around twice that of the Map derived cases. The reduction of the seismic misfit alone was sufficient, however, the production misfit cannot be improved also. This was the case for the Well+best+NRMS in this study.

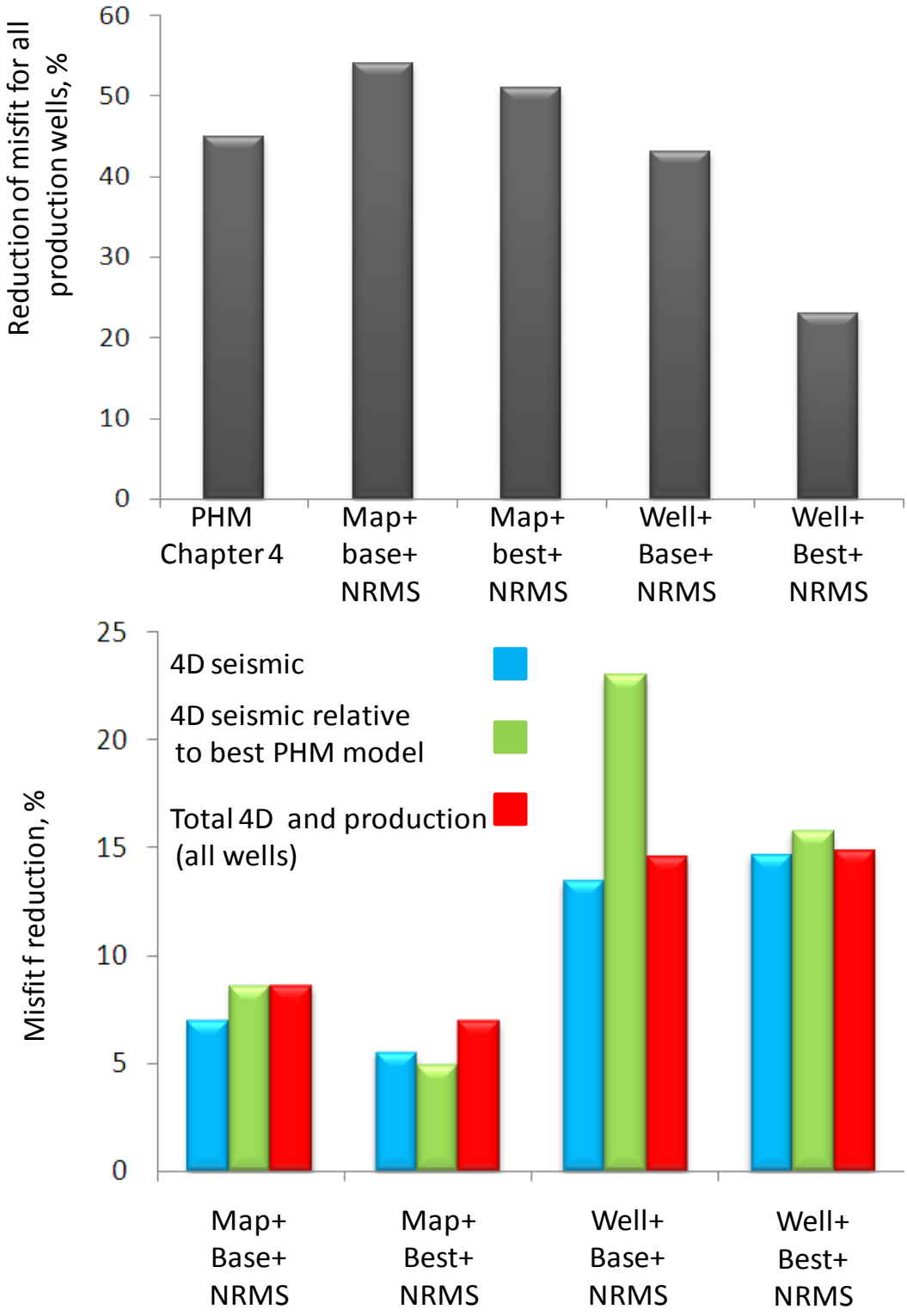


| Seismic misfit of base models (in millions) | 1.28 | 1.49 | 1.54 | 1.31 |
|---|---|---|---|---|

*Figure 6.4: Reduction of misfits of production and 4D seismic data for the best reservoir model. Using the 4D seismic normalized map filtered by NRMS.*

Each normalized observed 4D map was compared against the synthetic seismic for the best history matched model obtained using production data only. Green bar (4D seismic relative to best PHM model) in Figure 6.4 shows that using production data only for history matching failed to honour the seismic data and at the end of history matching, the best model was worse, seismically, than the base model that we started with. This result shows the importance of using appropriate 4D data to constrain history matching in order to better capture the fluid activity in the reservoir.

For Well+base case (in Figure 6.3) we compared the progress of the reduction of misfit values through history matching with production and seismic data as well as total misfit (summation of production and seismic misfits). Figure 6.5 shows the misfit reduction for 5 different localities. Total misfit reduction could be due to reducing either or both of seismic and production values. Also, the total reduction might occur despite counter-directional change of misfit values (i.e an improvement to production misfit may occur at the expense of an increased seismic misfit or vice versa and are accepted so long as there is net reduction of the total). However, Figure 6.5 shows the same trend of reduction for both seismic and production misfit. Figure 6.6 shows the cross plot of misfits for 5 wells.

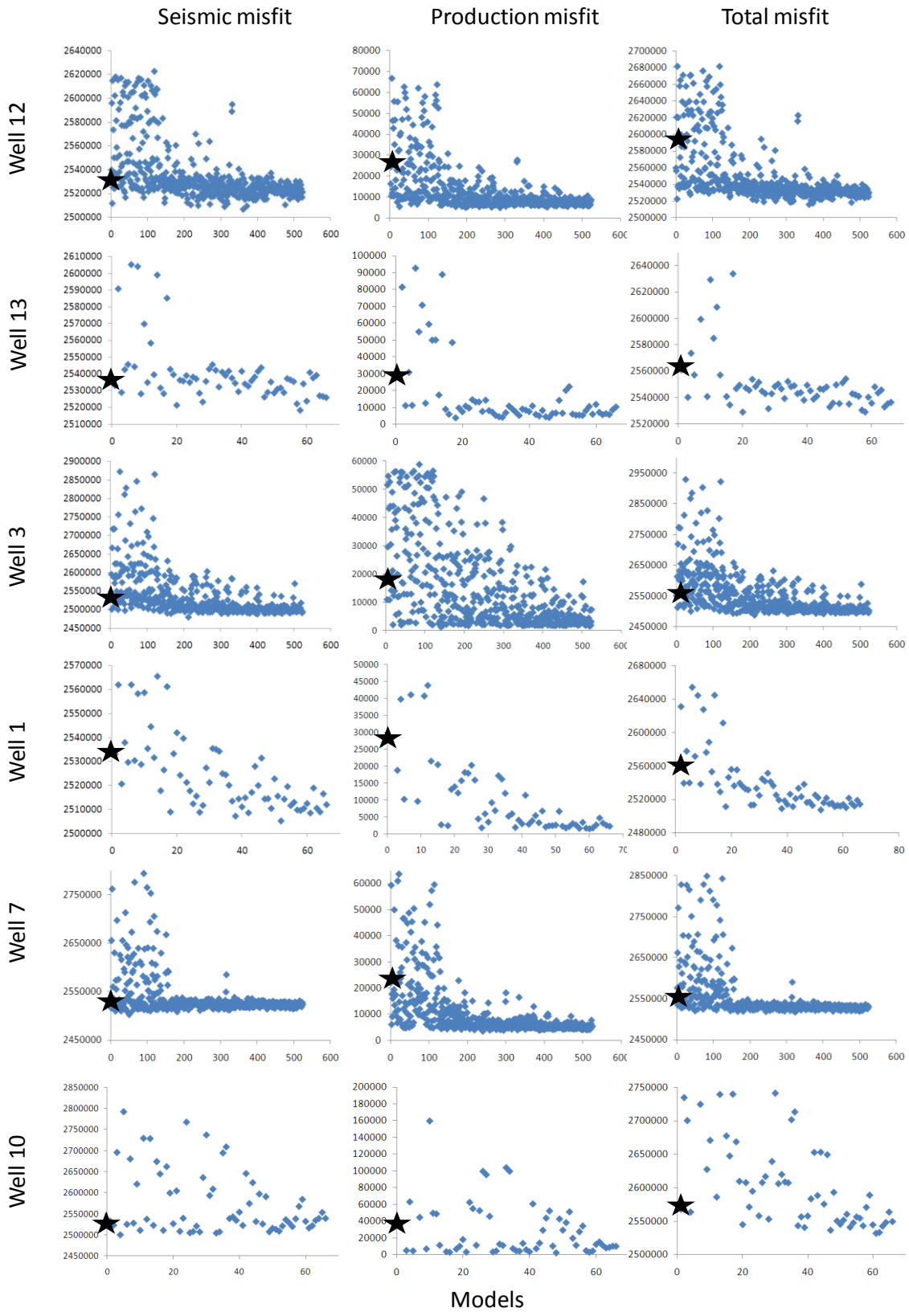


*Figure 6.5: Reduction of seismic, production and total misfit value through the 4D seismic history matching process (for Well+base case) for different wells (well names are based on Figure 3.35).Black stars show the misfit value for base simulation model.*

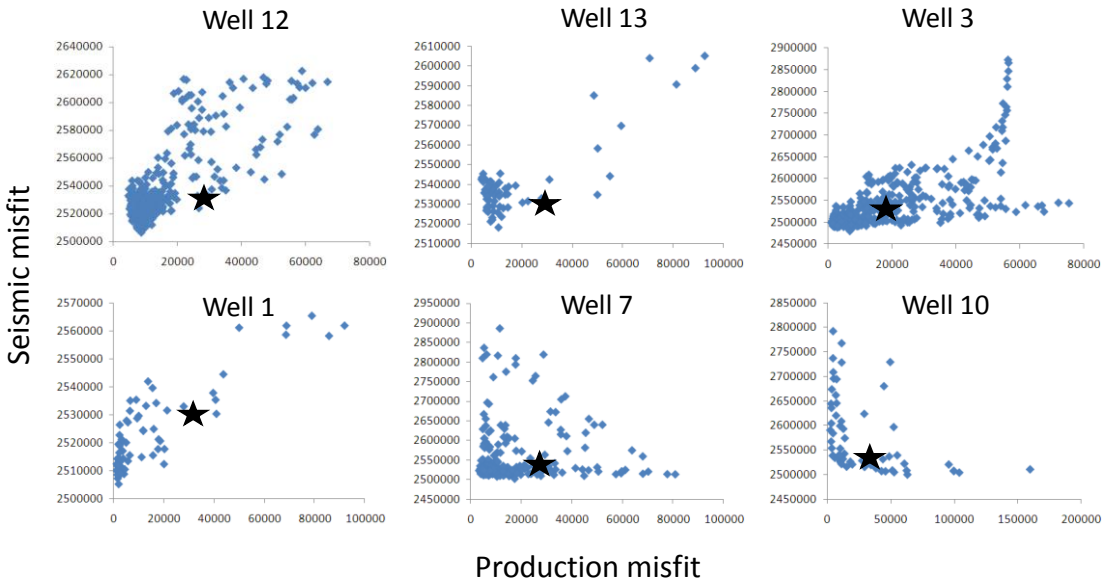


*Figure 6.6: Cross plot of seismic and production misfits for wells presented in Figure 6.5. Black star shows the misfit value of production and seismic for base simulation model.*

For all wells in Figure 6.5 we also obtained a history matching results using production data only (PHM in Chapter 4). For two selected wells (Well 10 and 12) we kept all individual reservoir model generated through production history matching (PHM). Then for all models run for PHM study, simulation was performed again and in this time the misfit value for both production and seismic data was calculated. Note that for calculation of seismic misfit above we needed observed 4D data. In order to be consistent with Figure 6.5, we used the data obtained from the Well+base normalization case. Then we compared the reduction of production and seismic misfit during the progress of history matching as shown in Figure 6.7. The result shows that when production data only was used in history matching, the reduction of seismic misfit was negligible. Also the reduction of production misfit itself was in the same order compared to seismic and production history matching studies (presented in Figure 6.5). Figure 6.8 shows cross-plot of misfit values for two selected wells in Figure 6.6.

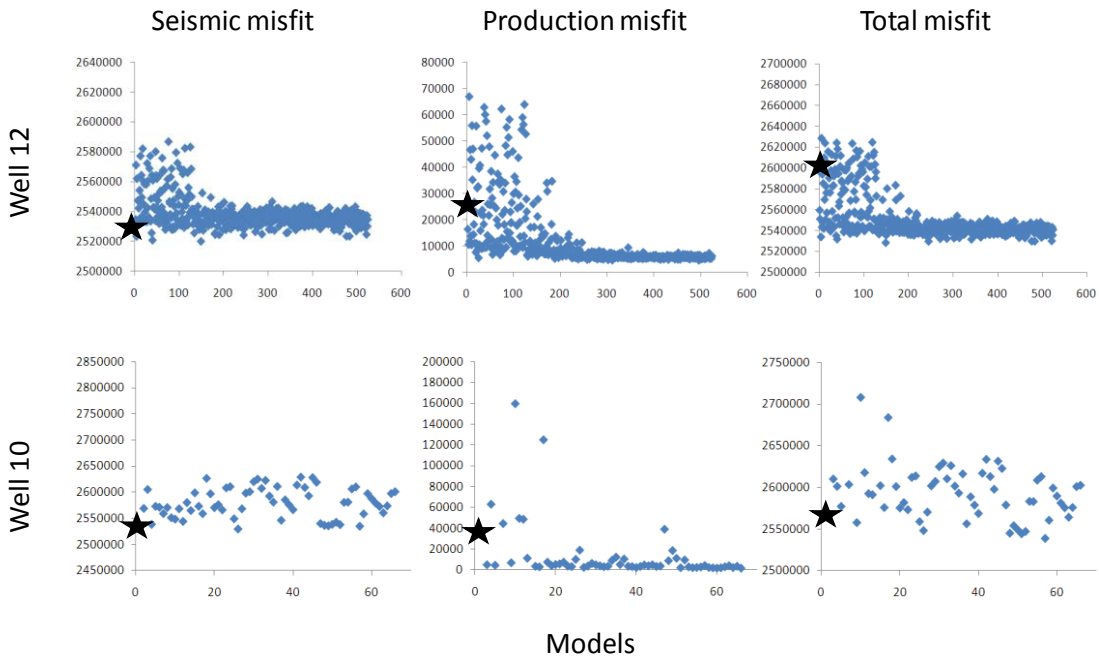


*Figure 6.7: Reduction of seismic, production and total misfit value through PHM. Note that seismic and total misfit were calculated after history matching process (for seismic misfit calculation Well+base map used) (well names are based on Figure 3.35). Black stars show the misfit value for base simulation model.*

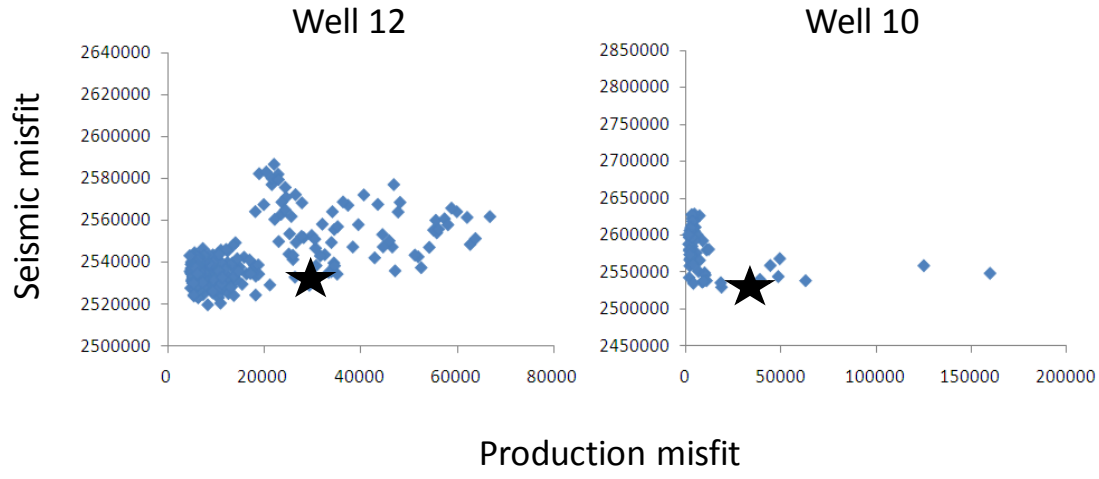


*Figure 6.8: Cross plot of seismic and production misfits for wells presented in Figure 6.7. Black star shows the misfit value of production and seismic for base simulation model.*

Figure 6.9 shows the 4D signature prediction of the best history matched model for each normalization approach. Comparing each model with the base model (Figure 5.7f) a general improvement of seismic in the middle of the reservoir was observed for cases other than the Well+best (ignoring two wells) case (Figure 6.9e corresponding to Figure

5.7e). For the PHM case the 4D signature in the centre of the reservoir was increased, where we retained some of the false signature removed in the other cases. The Map derived normalization cases, Figure 6.9a and 6.9b, also resulted in a stronger predicted signature in certain regions to match the normalized observed data in Figure 5.7a and 5.7b.

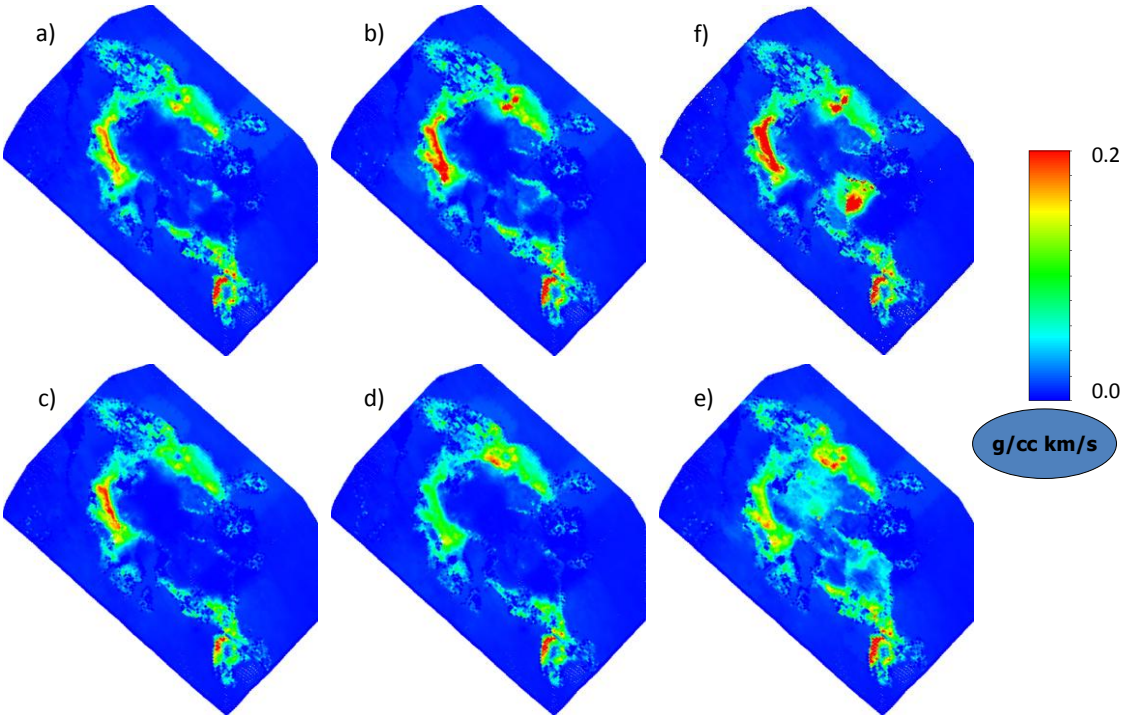


*Figure 6.9: The best synthetic 4D impedance maps after history matching where raw date was normalized using a) Map+base, b) Map+best, c) Well+base, d) Well+best, e) Well+best by ignoring two wells and finally f)the PHM model with no seismic.*

Similar results were obtained when using NRMS for filtering observed 4D seismic data as shown in Figure 6.10. From Figure 6.10 it can be seen that for all four cases there was improvement obtained in the centre of the reservoir, seismically, compared to the best production history matching case (Figure 6.10e) where a false seismic signature appeared in the centre of the model. This happened because the reservoir was controlled by production data only which resulted in the wrong modification of the reservoir parameters to match the wells.

Also for the Map derived cases it can be seen that in the black circles introduced in Figure 5.13e, a stronger 4D signature was observed. This was expected so that more water displacement occurred in each cell and consequently more water production.

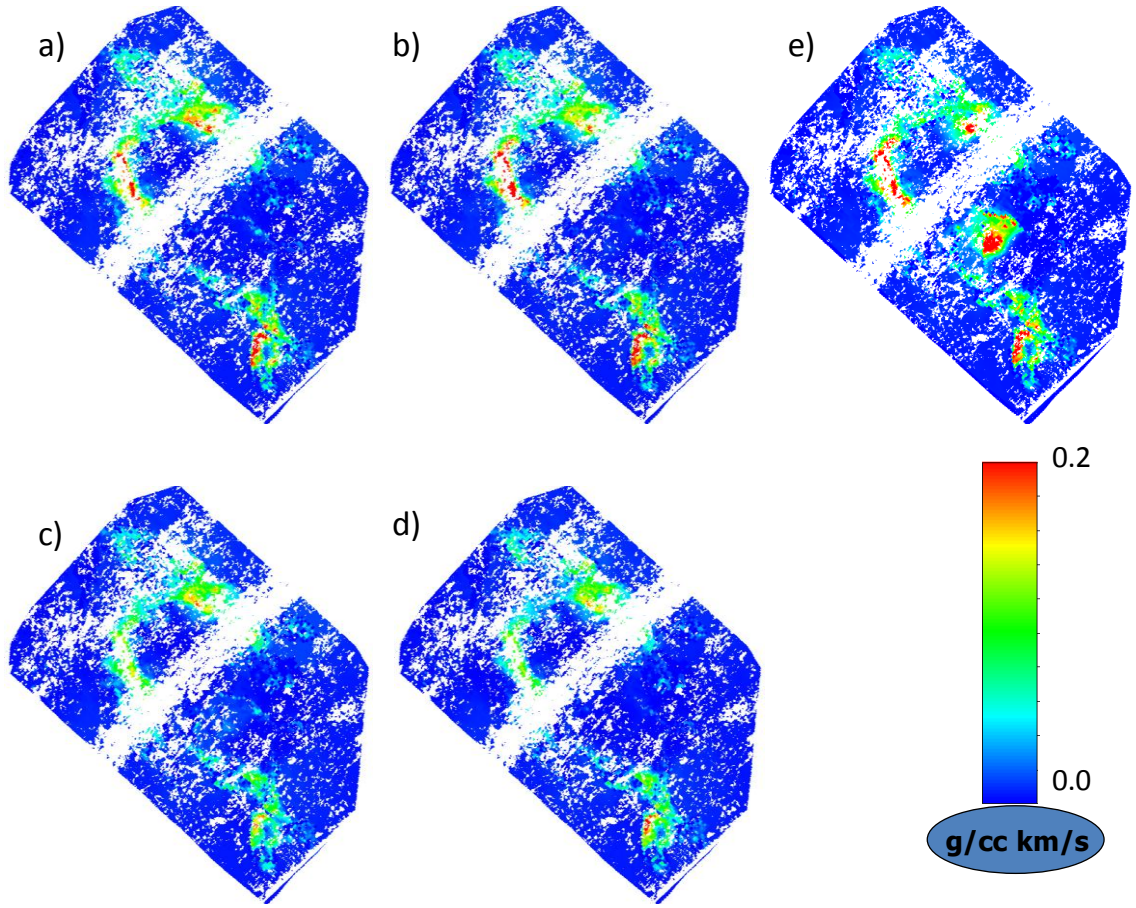


*Figure 6.10: The best synthetic 4D data after history matching for a) Map+base+NRMS, b) Map+best+NRMS, c) Well+base+NRMS, d) Well+base+NRMS, and e) PHM model.*

### 6.3 Updated reservoir model

The updated reservoir model was compared in each case with the best production history matching case in Figure 6.11 by plotting the multipliers used to change each reservoir parameter during history matching. It is clear that the change at the pilot points was not consistent for all three variables. Some regions saw reduced net:gross but others saw an increase. The effect of increasing net:gross alone was to increase the 4D signature for a given saturation change. However, the increased pore volume slowed down the movement of the fluids, possibly reducing water saturation increase, particularly ahead of the front. There were several regions where the horizontal and vertical permeabilities were changed in the same direction (up or down) although the degree of change varies. The regions indicated by the arrows labelled "1" and "2" in Figure 6.11 saw a different change between the PHM and PSHM cases. Horizontal permeability was reduced and vertical permeability was increased in the PHM case while in the PSHM case, the horizontal permeability increased and vertical permeability

was increased or decreased. The net effect was that edge water drive was decreased for the PHM case and the opposite for the PSHM cases where edge water drive was generally increased elsewhere.

The same figure was generated for the NRMS study (Figure 6.12). It can be seen that, generally, for the each of the PSHM cases, the horizontal permeability of the reservoir was increased while net:gross and vertical permeability were increased in some places and were decreased in others. Region 1 and 2 show the locations in the reservoir where some 4D activity was over predicted in the reservoir after history matching using production data only (the PHM case) while in the PSHM cases that false 4D signature was removed after history matching. It can be seen that for Region 1 changes were made to match the wells by increasing vertical permeability such that the model had more bottom drive displacement. Comparing that with the same region in Figure 6.12b it can be seen that for the PSHM cases, the horizontal permeability was increased to increase water drive from the edge of the reservoir. The result was improved well matches and also the seismic effects were captured in the correct location. In Region 2 for PHM all parameters were reduced while in PSHM cases horizontal permeability was increased.

Regions 3 and 4 in Figure 6.12 belonged to two of the black ellipses in Figure 5.13e where the base reservoir model underpredicted water production. It can be seen that in the Map+best+NRMS case, the fluid displacement was controlled in Region 3 by increasing horizontal permeability and decreasing vertical permeability. This increased edge drive towards the production wells. In Region 4, the water sweep was controlled from the injector to those producers by increasing net:gross and horizontal permeability. Comparing with the Well+base+NRMS case it can be seen that for Region 4, the vertical permeability was decreased with no change to net:gross.

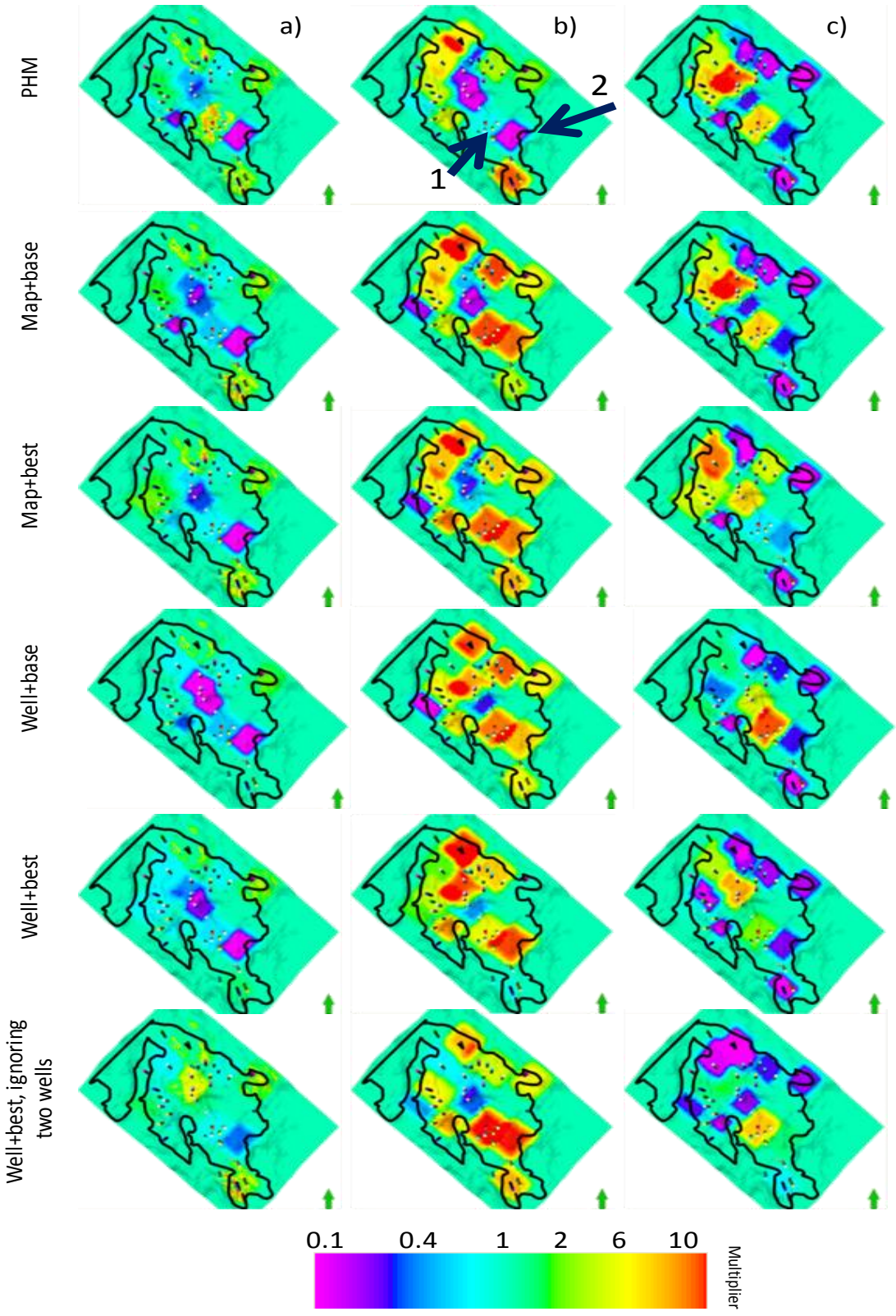


*Figure 6.11: Multipliers of properties changed in the base model via history matching for a) net:gross, b) horizontal permeability and c) vertical permeability in log scale. Note that actual changes to net:gross were limited so that unity was not exceeded and this is not reflected in the above plot.*

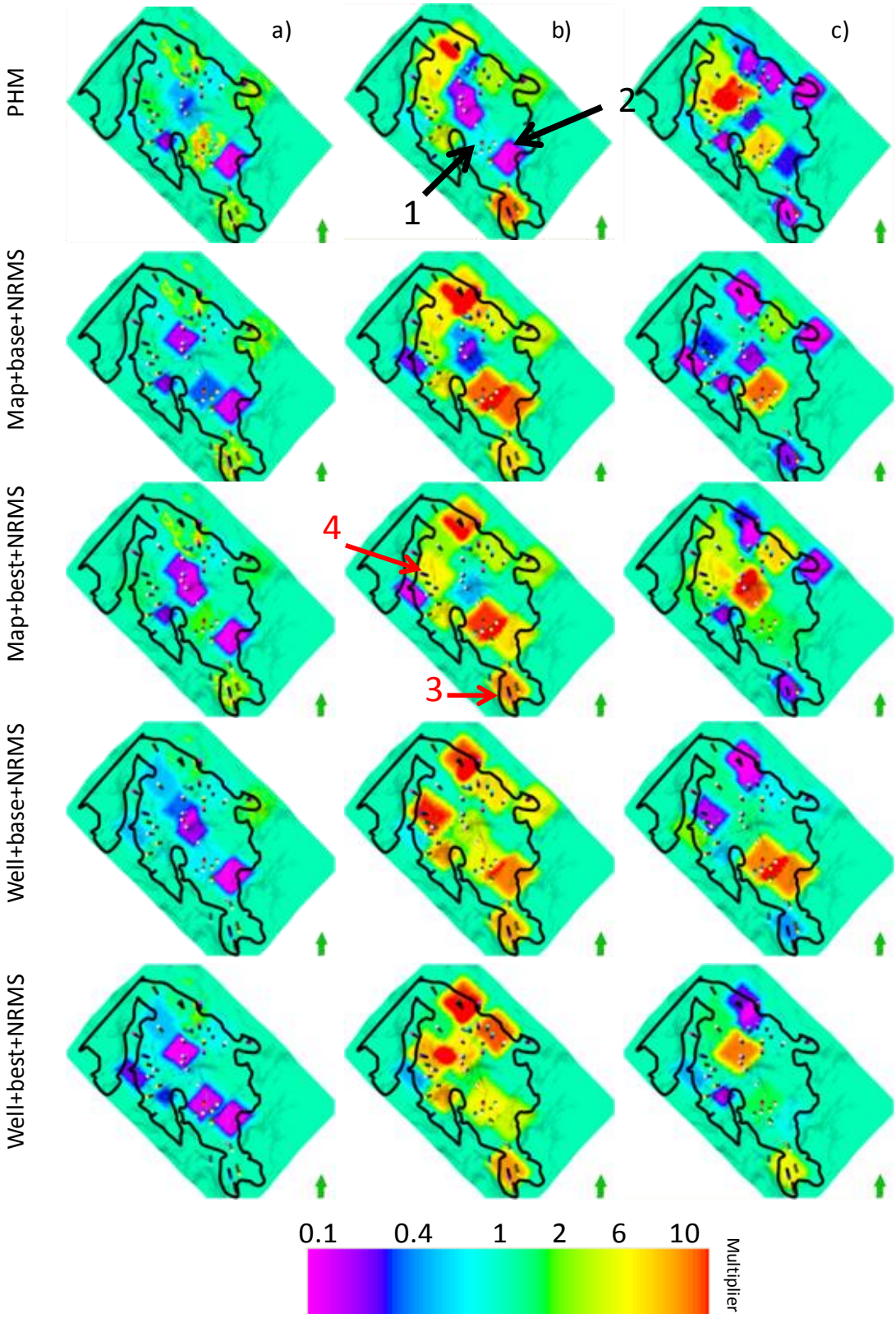


*Figure 6.12: Multipliers of properties changed in the base model via history matching for a) net:gross, b) horizontal permeability and c) vertical permeability in log scale. Note that actual changes to net:gross were limited so that unity was not exceeded and this is not reflected in the above plot.*

### 6.4 Forecast accuracy

In this section each history matching result is investigated for its capability to predict the future behaviour of the reservoir (i.e. beyond the history matching period to forecast from 2000 up to 2003). For this purpose the well production data between 2000 and 2003 were used to measure the forecast accuracy of the best 10 models from each case. We know that because the history matching is non-unique we do not expect the forecasts to be the same. Figure 6.13 shows the best forecast result and the average of all 10 forecasts.

The average misfit reduction (calculated over the best 10 models) for the PHM forecast falls in the middle of the PSHM cases. However, the global benefit of using 4D seismic data in the misfit is seen in Figure 6.13 where the best PHM model forecast is surpassed by the forecast from all the PSHM cases. The differences between the forecasts for the PSHM cases are also interesting. The Well+base normalization gives better forecasting models than the other normalization options.

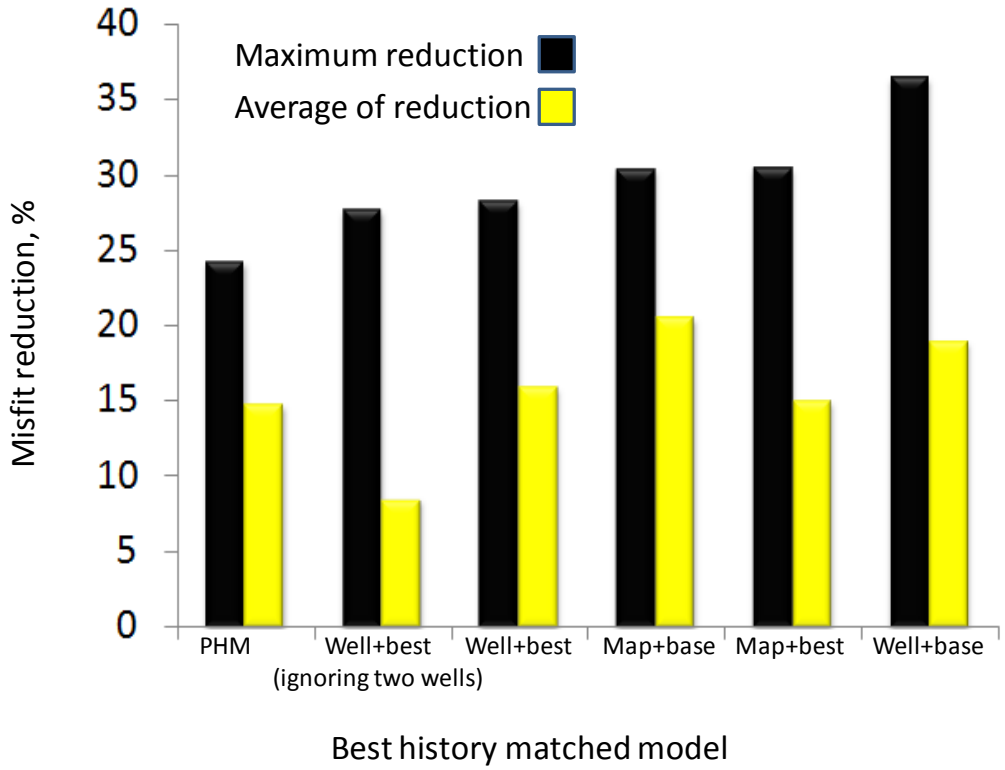


*Figure 6.13: Misfit reduction by percentage for the best history matched model of each case by considering all production wells. This is only for the cases where NRMS filtering was not used.*

From Figure 6.14 it is clear that the Well+best normalization was less successful at improving the reservoir match part but the forecast was reasonably improved. For the Well+base case for some models a good reduction in misfit for the matching and forecasting periods was obtained. The Map derived results were located somewhere between the Well+best and Well+base cases on the cross plot. There is reasonable improvement in the misfit value for both periods but not as good as Well+base case. All four cases show a range of forecasting accuracy.

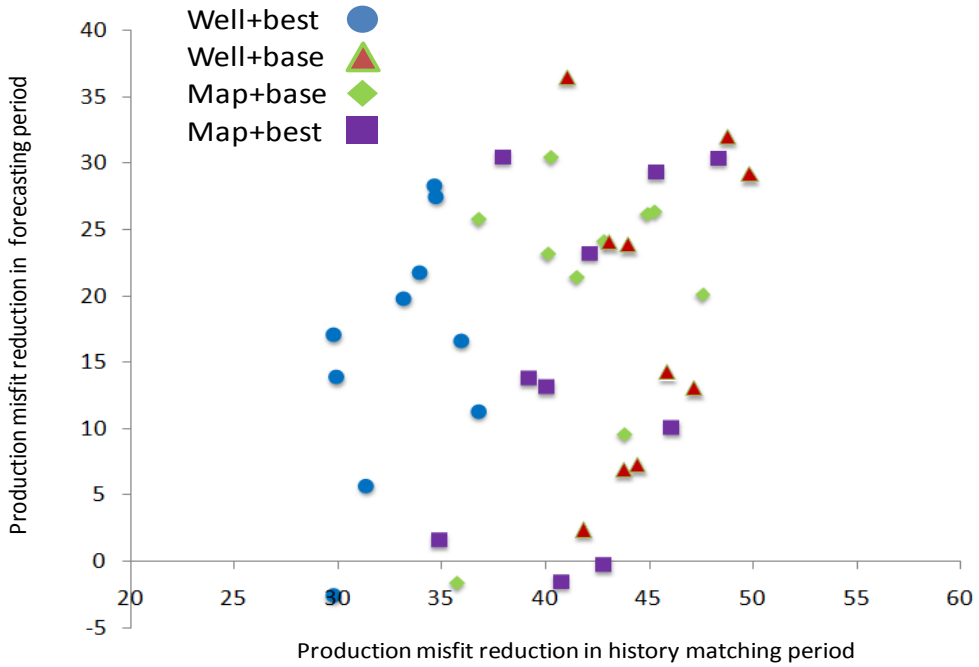


*Figure 6.14: Reduction of total production misfit in forecasting versus matching periods for different history matching studies.*

The above result can be compared to similar cases where NRMS filter was applied. Figure 6.15 shows the misfit reduction of the best 10 history matched models and it can be compared with the result with Figure 6.14.

Figure 6.15 shows that the Map derived cases gave better reduction of misfit values for both matching and forecasting periods, mainly because of an appropriate regression equation that was used to generate normalized 4D seismic signatures for these cases. Comparing this study with the result presented in Figure 6.14, it can be seen that when NRMS filtering was not applied then more vertical wells were used in the cross-plot and a more reasonable equation was derived for normalizing the observed data. As we discussed previously, the intercept and the gradient was better estimated for Well+base

case (Chapter 5, Figure 5.6c). An inappropriate regression equation resulted in a search in the wrong direction resulting in poorer forecasts, as shown in Figure 6.15. On the other hand, a more appropriate normalization study for Map derived cases yielded a better history matching result with almost 50% reduction of misfit in the matching period and more than 25% for the forecasting part, as shown in Figure 6.15. In this study the criteria for choosing the best history matched model used the actual production misfit value (for the all production wells) for both matching and forecasting periods. For each model in Figure 6.14 and 6.15 the sum of misfits of oil and water rates for the all wells are calculated at the end of the production history at 2003 and the result are plotted versus the same misfit value but for the matching period (1994 to 2000) as shown in Figure 6.16. From Figure 6.16a it can be concluded that for history matching studies where NRMS was not used for normalization of 4D seismic data, the best result was for the Well+base case because of lower misfit value in X and Y axes. The next best results were obtained for Map+best. On the other hand, by using NRMS in the normalization studies, after history matching, the best result are observed for the Map+best+NRMS case and the less reduction of misfit was observed for the Well+best+NRMS case.

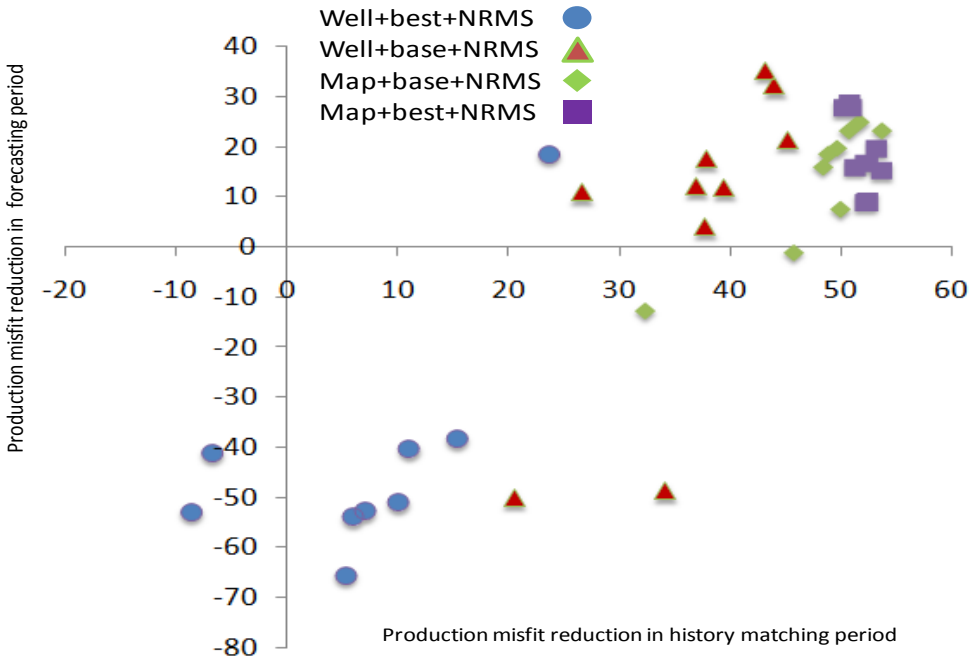


*Figure 6.15: Reduction of total production misfit in forecasting versus matching periods for different history matching studies.*

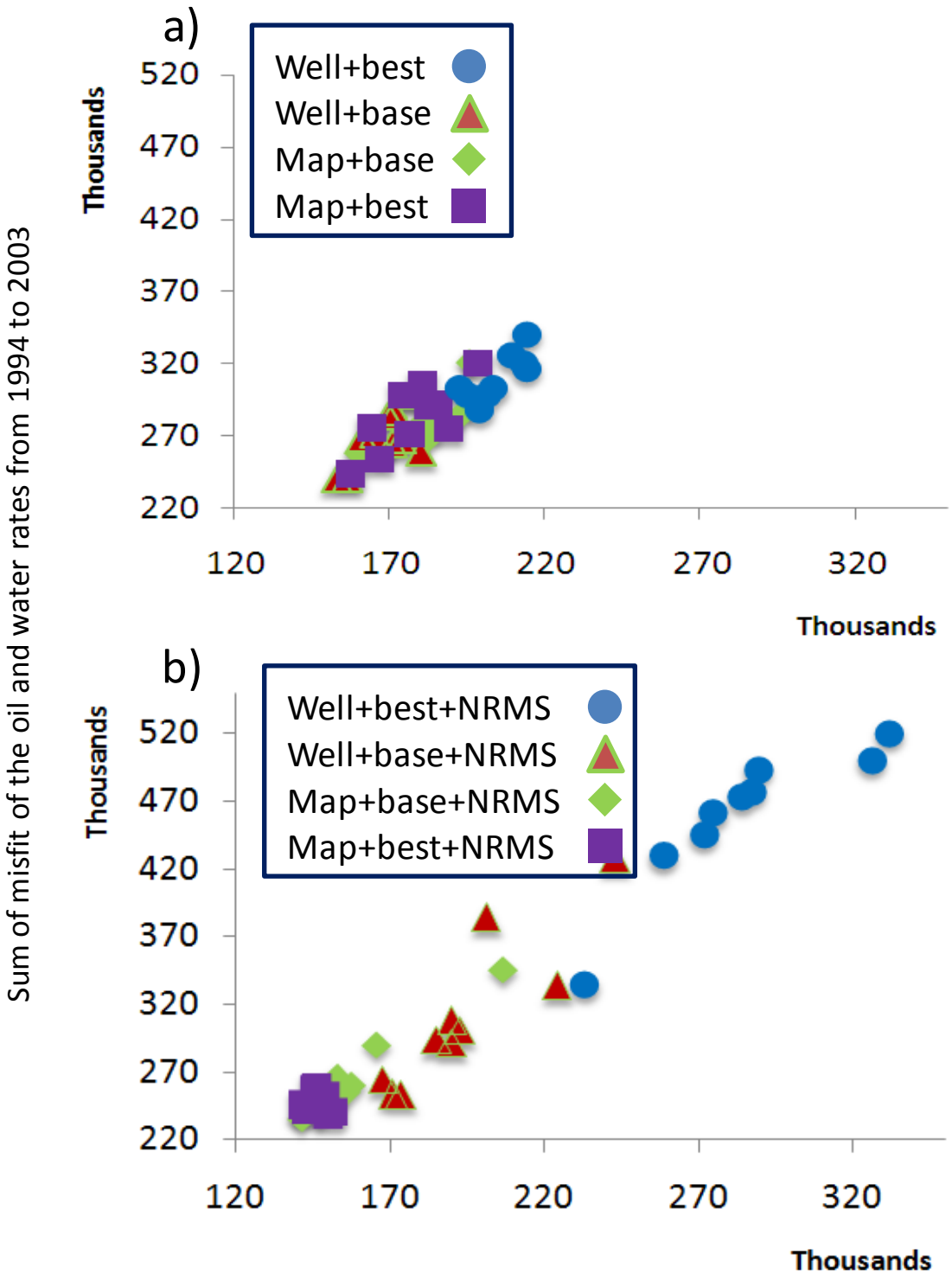


*Figure 6.16: Sum of misfits of the oil and water rates for all wells from 1994 to 2003(history plus forecasting period) versus the same property but for 1994 to 2000 (history period only ) Showing history matching cases in a) Figure 6.3 and b) Figure 6.4. Note that the misfit value of base reservoir model is 300,000 and 430,000 for the history and history plus forecasting periods respectively.*

Figure 6.17 shows a comparison of the oil and water production profiles for the best models of PHM and PSHM (Map+best+NRMS). The best PSHM case better matched the history of the wells and was better at forecasting than the PHM case. The two labelled wells (Wells 1 and 2 in Figure 6.17) are also shown even though they were not included as target wells for history matching. By integrating 4D seismic data, however, there was also improvement to those wells. This observation is additional evidence of the benefit of using 4D seismic in the history matching study.

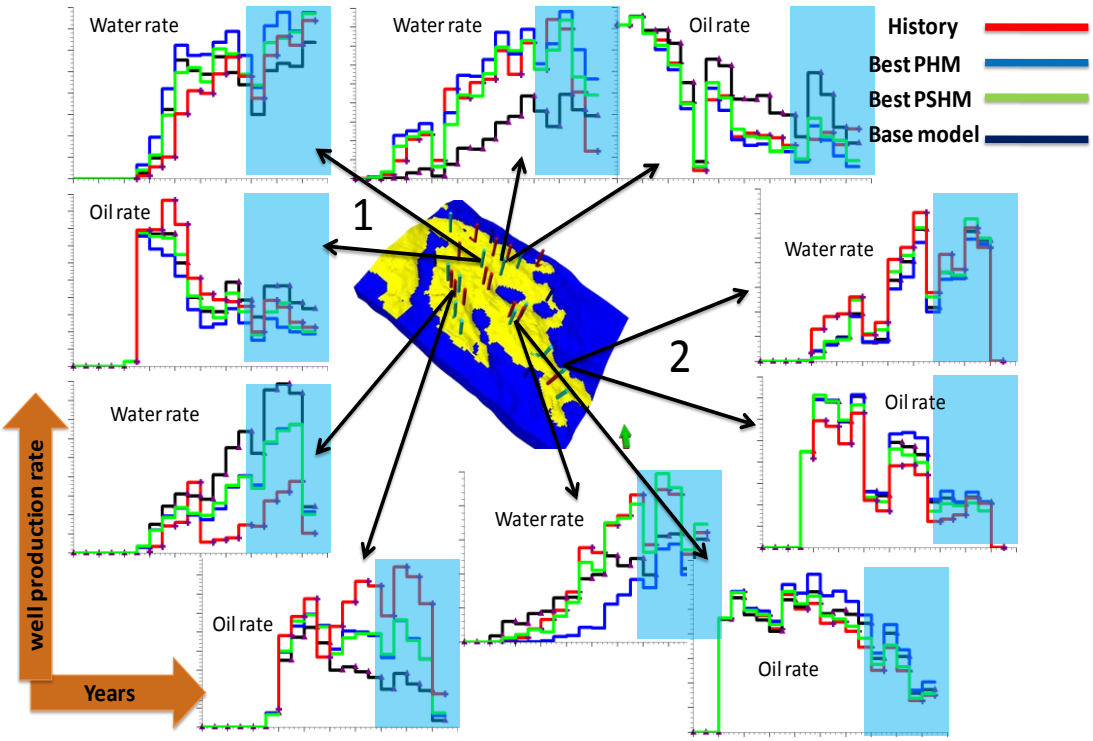


*Figure 6.17: Oil and water production rates in matched and forecast periods (light blue) for the best history matched model using production data only (blue) and for the best model using both production and seismic data (Map+best+NRMS) (green).*

## 6.5 4D seismic map prediction

Figure 6.18 shows the normalized observed 4D seismic data for 2003 which was calculated based on the Map+best approach (Chapter 5, Section 5.7), and it is compared with the predicted 4D map of the reservoir up to 2003 for the best history matched model (Well+base). The result shows that improvement on the seismic forecast was obtained in most of the regions in the reservoir but especially in the middle of the model. The seismic misfit was reduced by 7% for this case.

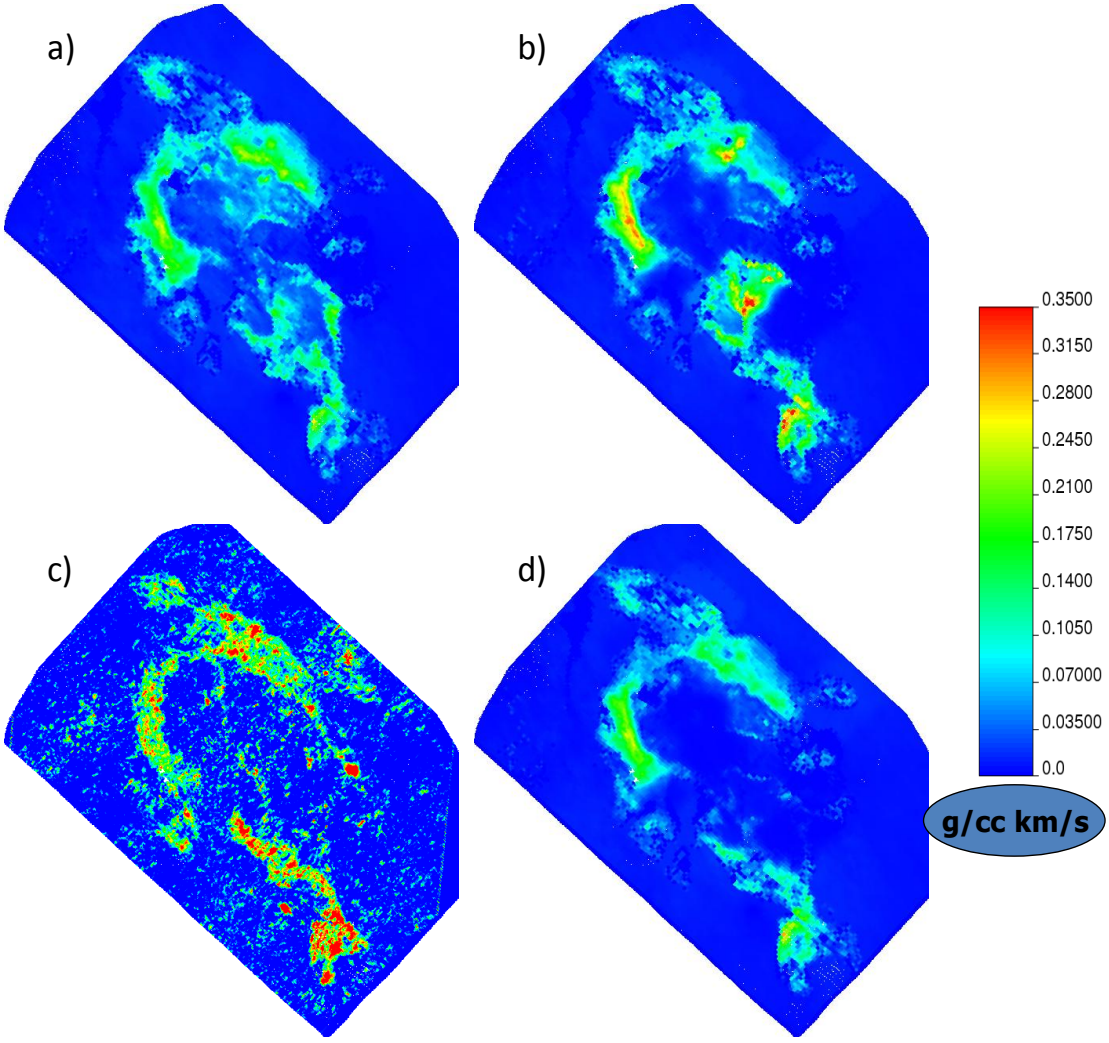


*Figure 6.18: The 4D seismic data for (a) the base reservoir model, (b) PHM model, (c), the normalized observed data (Map+best) and (d) and the best seismic and production history matched model Well+base (Figure 6.3).*

**6.6 Does NRMS help the history matching process?**

One important investigation in this study was the effect of using the NRMS filter in normalization of the observed data. The importance of NRMS filtering appeared mainly in the Map derived results (Figure 6.15) where we compared them with the similar result in Figure 6.14. It can be seen that the reduction of misfits for both periods was greater for the NRMS study compared to non-NRMS study and also the best 10 models are more correlated between the updated models to better capture the well production activity in both periods.

The best history matched model was compared in each case in Figure 6.3 and 6.4. As discussed previously because of the regression equation used for normalization in the

Map+base and Map+best cases, a large 4D signature was observed over the active regions of the reservoir which was not consistent with the production activity. Because of this inconsistency between seismic and production it can be seen that in Figure 6.3 the reduction of total production misfit was not as good as the NRMS case (Figure 6.4) where a more acceptable normalised 4D map was observed based on consistency with production. Also the seismic misfit reduction itself was very small in Map+base and Map+best cases. This was because of the effect of the production misfit, which prevents the seismic from pushing the parameter search in the opposite direction required to improve the well match. Of course there could be several other reasons that make the matching of production data in the opposite direction of matching 4D seismic such as choosing wrong parameters to update, using a incorrect petro-elastic model, choosing the wrong location to update the reservoir and etc.

The NRMS and non-NRMS cases were all similar in that history matching with seismic and production data together resulted in models that better predicted seismic compared to the PHM case. This is shown in blow bars in Figure 6.3 and 6.4. Also the combined production and seismic misfit was reduced or each PSHM case according to red bars of the same figures.

According to the comparison of the results it can be concluded that if the NRMS filter was not used, the best normalized 4D will be generated based on the Well+base case. Integration of that normalized data into the history matching resulted in greater reduction of total production misfit. When the NRMS map was used to filter the cells with low repeatability, the resulting normalized observed map for the Map derived cases provided even better reduction of total production misfit compared to the non-NRMS filtered cases.

Figure 6.19 shows the multiplier of parameters for the Well+base case and Map+best+NRMS case where the best history matching result was observed. It can be seen that the degree of change was quite similar for some parameters in different regions. However for analysis, it is better to focus on specific regions as indicated by the black ellipses in Figure 5.13e where more water displacement was expected. In Region 1 in Figure 6.19, the ratio of horizontal to vertical permeability was increased for Map+best+NRMS case to increase the edge drive support. The same change occurred for Well+base but the $k_h : k_v$ did not increase as much as previous case. In

Area 2 for the Map+best+NRMS case, the water movement observed from injector to producer was better captured by increasing all parameters. However in the Well+base case the vertical permeability decreased. Therefore, there is less effect of bottom drive displacement. The Map+best+NRMS case for Region 3 showed increased permeabilities whereas in Well+base there was also increased permeabilities but to a lesser degree.

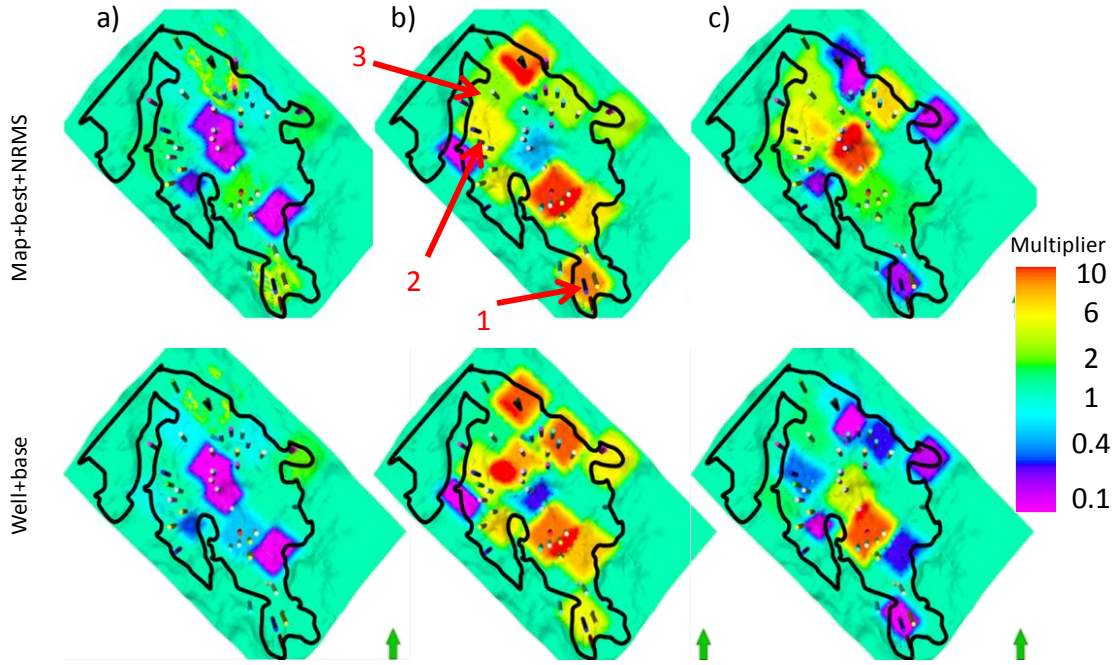


*Figure 6.19: Multipliers of best reservoir model for two different cases over the base model for a) net:gross, b) horizontal permeability and c) vertical permeability in log scale.*

## 6.7 Possible geological change in the reservoir after history matching

One important question after history matching is how do changes to parameters relate to changes to the geology of the reservoir. In this section two updated reservoir models from previous studies were considered. These two models were better representative of the reservoir in terms of the reduction of the misfit values. Then the reservoir properties were compared with the base reservoir model as shown in Figure 6.20. In the Well+base case the net:gross value was increased up to 0.95 (north of Nelson field) which means a high proportion of sand was added to the reservoir. This change of net:gross was made in the Channel Axis. However, the horizontal permeability was also increased to a maximum 5000 mD in the north of Nelson field. On the other hand,

in the Interchannel sands, the reservoir became shalier because of reduction to the net:gross but the horizontal permeability is still high in some regions.

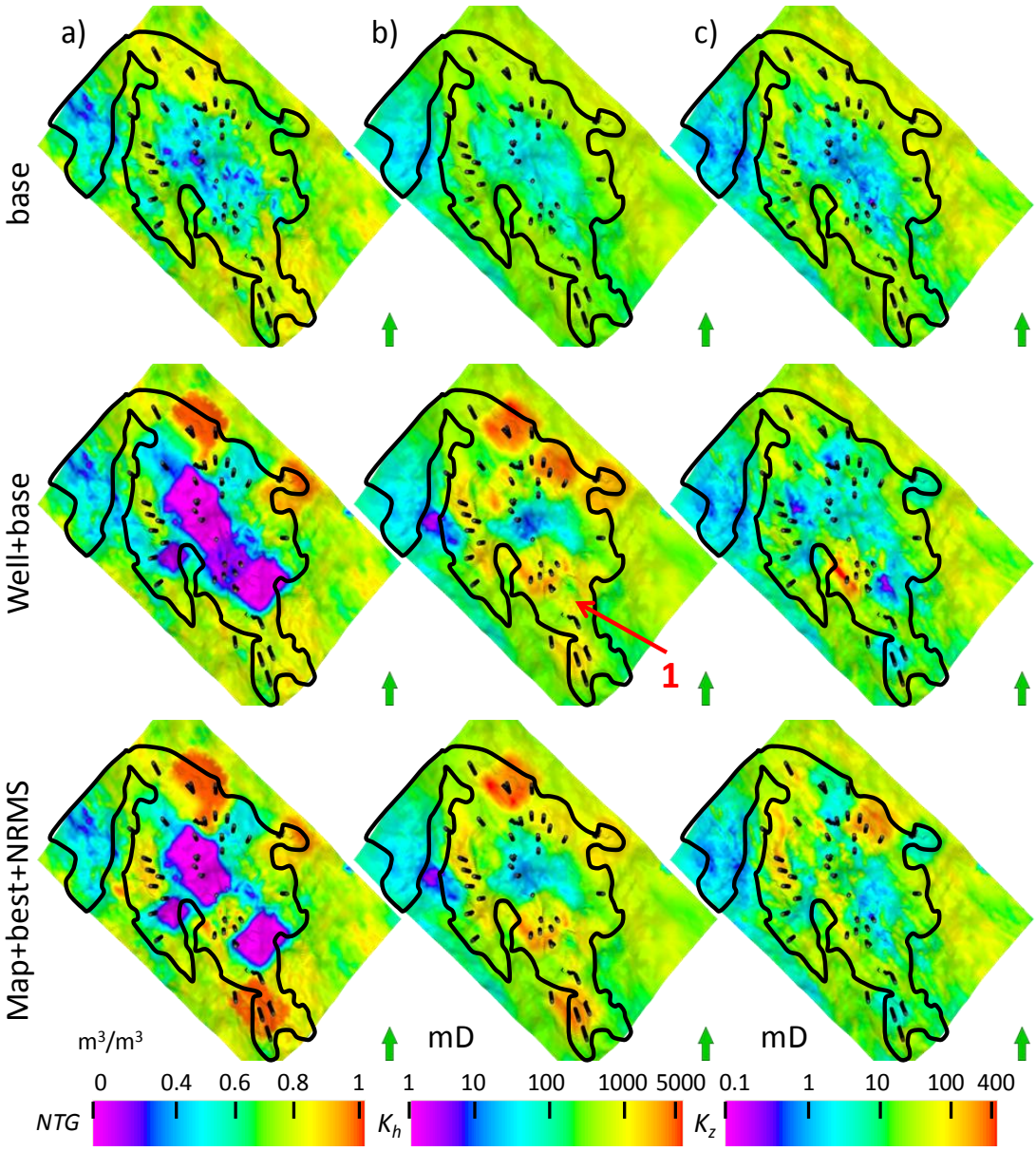


*Figure 6.20: Average reservoir properties in first reservoir interval for different history matching studies. (a) net:gross, (b) horizontal permeability and (c) vertical permeability.*

For the Map+best+NRMS case similar to the Well+base case in the Channel Axis (North of Nelson) we increased the net:gross value which meant the presence of more sand and the horizontal permeability also increased. In the Interchannel there is low net:gross value because there was more shale but the horizontal permeability was increased in this part of reservoir. As an alternative for changing net:gross, which ultimately changes the horizontal cell to cell transmissibility in the reservoir, it is

possible to define some equivalent change to porosity and permeability instead. For example adding 10% to net:gross is equivalent to increasing porosity and horizontal permeability by the same amount. However, the petro-elastic model is a function of shale volume and porosity separately which is related to net:gross in this study, therefore changing net:gross will affect synthetic impedance data too. We may therefore interpret net:gross and porosity increases differently.

All the changes in the reservoir properties, illustrated in Figure 6.20, are categorized in one of the possibilities explained before in Figure 3.11 in Chapter 3. As an example, Region 1 in Figure 6.20 saw decreased net:gross, increased horizontal permeability and decreased vertical permeability as in Case 4 in Figure 3.11.

### 6.8 Using automatic history matching technique for seismic normalization

In the previous chapter we investigated various normalization techniques. We derived a regression equation linking observed and predicted data using the whole map or by using near well seismic only for wells that match production data. There are some alternative approaches that we can consider as future work research topics. These might be to use only the active reservoir or regions where predicted and observed data show a similar degree of signal. An additional alternative approach would be to consider a wider area around wells and treat the normalization regionally.

In this section we further discuss potential future research work on normalization. The aim was to use the automatic history matching technique in the normalization study. In Chapter 5 (Section 5.4) we used the active reservoir section for the normalization study and we observed inconsistencies such that the seismic signal was converted to noise and vice versa. In this section, therefore, we decided to use some specific parts of the reservoir in order to perform the normalization. For success, the targeted parts of the reservoir should show a good quality of seismic signature in the observed data which also needs to be consistent with production activity such as water displacement from the aquifer or nearby injector. Also the quality of observed seismic can be checked with repeatability also (discussed in Chapter 5, Section 5.5).

The aim here was to normalize the local 4D signature to the local predicted signal and then improve the latter by history matching. We considered two important assumption

here. Firstly, the 4D signal in the selected region should have very low uncertainty (high signal/noise ratio) and secondly, the petro-elastic model should be valid again with a very low uncertainty. Then we need to consider that the predicted and observed data are not in the same units. Therefore, the challenge is to update selected reservoir parameters (that affect synthetic data) in order to reduce the differences between observed and synthetic impedance in selected regions of the reservoir. It is worth mentioning that the aim here was not to perform a history match study; we just updated the reservoir parameters that affect synthetic seismic impedance in the reservoir in order to make it closer to observed data. Then we use the ratio of real to synthetic data for deriving normalization equation.

Two boxes were chosen in the reservoir, one is close to well A1 (A1) in the south and another is close to well N6 in the North-East (N6) (Figure 6.21). N6 produced 6% of the total water production from the whole field from 1994 to 2000 and A1 produced 3%. Therefore there is a good production activity for these two wells. There are two injectors close to both wells so it was expected that water should move from those injectors and the aquifer. Both producer wells were completed in the first reservoir interval. Therefore, it was expected that fluid displacement occurred in that interval only. The two boxes shown in Figure 6.21 were chosen for their proximity to the production wells and there is a good signature because of water sweep.

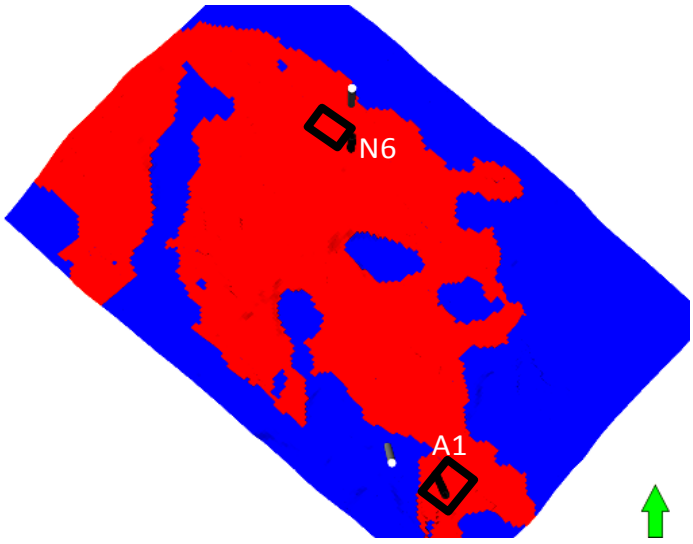


*Figure 6.21: Areas chose for normalization study close to well N6 and A1.*

Figure 6.22 shows the magnified view of the above two locations in the simulation model. It can be seen that the synthetic seismic generated based on the base reservoir

model can predict the 4D signature in the chosen box. On the other hand the production profile for both wells shows that the total water production for the base reservoir model was almost twice reality. Therefore, the wells overestimate the produced water. Based on the production activity and predicted 4D signature for the base model, it was concluded that the 4D signature did not change enough close to the well or else it was changed in the wrong location. In A1 more 4D signature should be in the black box around the well and in N6 the magnitude of 4D signature should increase.

Two separate history matching studies were performed for each case. In order to have an accurate calculation of the misfit value in the objective function, the normalized map of Well+base case was used for history matching studies. As previously discussed there were reasonable arguments in order to consider this normalized map as good observed data.

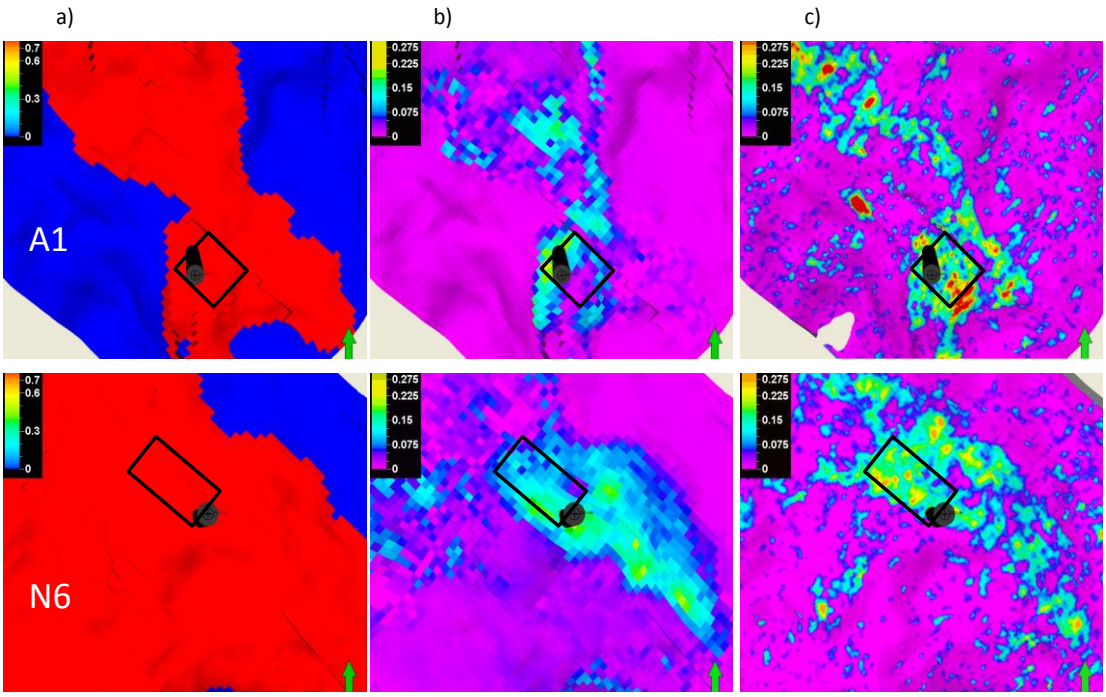


*Figure 6.22: Magnification of two areas chosen for normalization in a) the simulation model b) synthetic seismic time-lapse data for base model and c) observed time-lapse seismic. Top row is A1, bottom row is N6.*

Pilot points were located in these areas (black box in Figure 6.22) following the history matching workflow introduced in Chapter 4 and this chapter. Horizontal and vertical permeability was considered as well as net:gross as the unknown reservoir parameters.

Then, automatic history matching was performed to match the synthetic 4D and real seismic data for each area using 4D seismic data only.

As discussed previously one of the difficulties for the Well derived cases was that the number of points that were used in the study was sparse. In this method, the number of cells were increased to 40 and 60 simulation cells for A1 and N6 respectively. After history matching in A1, the misfit value of 4D seismic for the simulation cells in the black box reduced by only 0.2%. Figure 6.23 shows the cross-plot of seismic data for the cells surrounded by the black box in A1.

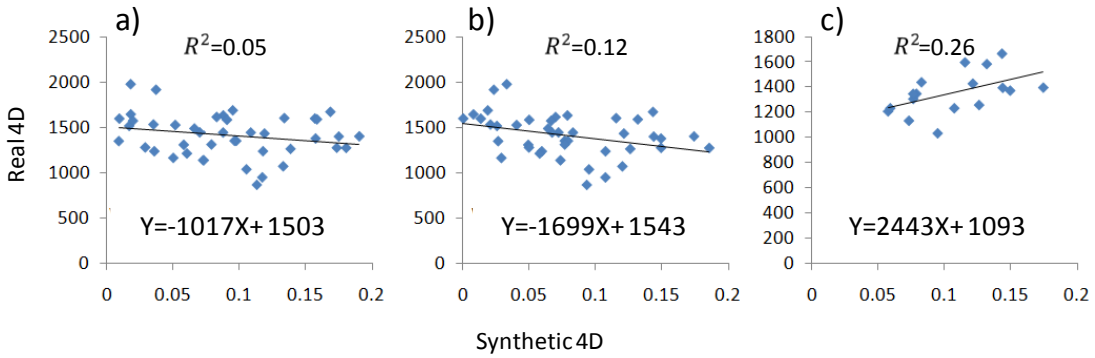


*Figure 6.23: Cross-plot of observed and synthetic 4D impedances for a) set of simulation cells in area belong to A1 in Figure 6.21 and for the base model, b) set of simulation cells in area belong to A1 and after history matching and c) same as (b) but ignoring the poorly matching region.*

From the regression equation in Figure 6.23 we can see that even after history matching the correlation between real and synthetic data was still negative (Figure 6.23b). From the linear correlation between water saturation and 4D seismic signature in the reservoir we deduced that improving reservoir properties in this part of the model did not affect the water displacement enough in order to generate sufficient 4D seismic signatures.

In order to obtain the best correlation between 4D seismic data in the selected cells, we ignore those points where the differences between real and synthetic 4D seismic is higher than 50% (the poorly matching region) and we cross-plot the rest of the cells which are represented in Figure 6.23c.

In N6, after history matching, we obtained 1.27% reduction of the total seismic misfit value by updating reservoir properties in the black box which is good for such a small

part of the whole reservoir. In Figure 6.24 we can see that from the anti-correlated equations between the data in the reservoir box before history matching (Figure 6.24a) we obtained a better correlation between the data afterwards (Figure 6.24b). However, both intercept and slope of the regression equations were still very high. For this case, because we chose the box based on the location of 4D seismic signature only a significant improvement from history matching was not expected. Similar to A1 we ignored the points with large differences between observed and synthetic 4D seismic (the differences between observed and synthetic values were more than 50%) and we cross-plot for the rest of the cells (Figure 6.24c). Now we get a better correlation between our real and calculated 4D seismic for this specific part of the reservoir.

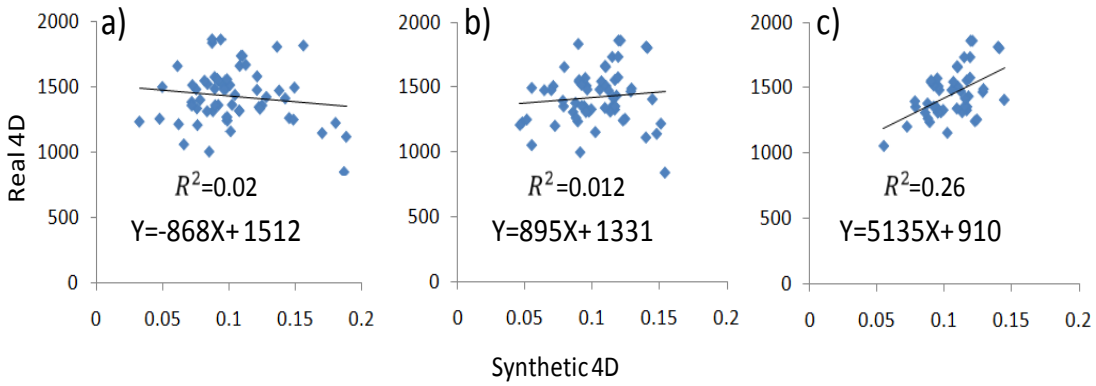


*Figure 6.24: Cross-plot of observed and synthetic 4D impedances for a) set of simulation cells in area belong to N6 in Figure 6.21 and for the base model, b) set of simulation cells in area belong to N6 and after history matching and c) same as (b) but ignoring the data with high error.*

By considering these two parts of the reservoir for normalizing 4D seismic data, we ended up with the maps presented below in Figure 6.25. The 4D seismic signature observed in this figure is very low compared to well activity in the reservoir which means that normalization was not accurate enough. This was due to signal/noise ratio and it was better, therefore, that we did not use that as an approach to normalize observed 4D seismic. As previously mentioned this study was just an idea and there are various issues that need to be considered in order to test it to be a useful method for seismic normalization.

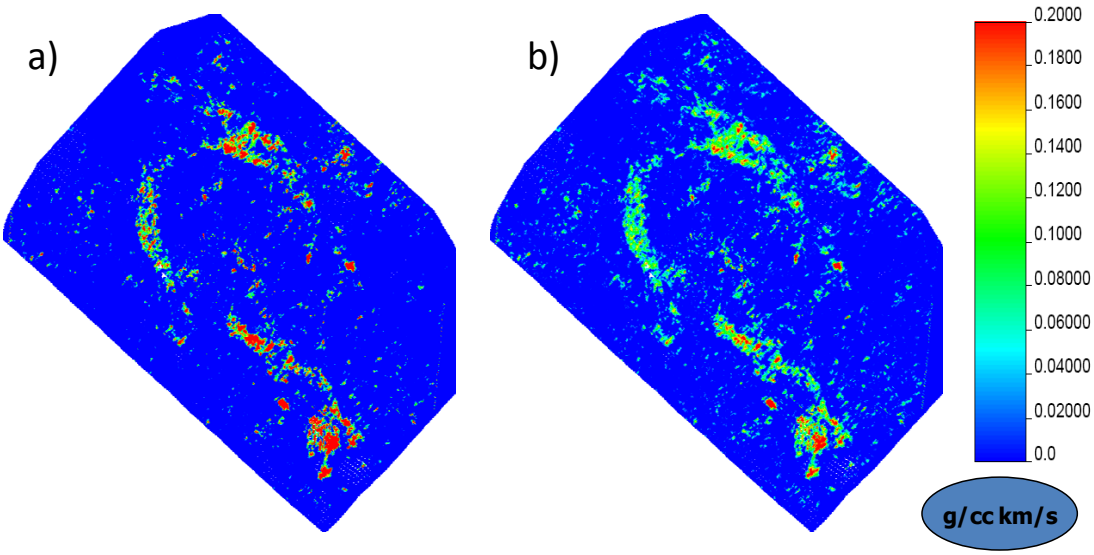


*Figure 6.25: Normalized observed 4D seismic obtained by using the regression equation of a) study based on A1 and equation in Figure 6.23c and b) study based on N6 and equation in Figure 6.24c.*

## 6.9 Discussion

In this chapter we analysed and discussed various seismic history matching studies. The input 4D maps used in the objective function were the normalized 4D data that was discussed in Chapter 5. However, the normalization study did not provide a unique answer and we obtained various 4D maps showing different levels of signal and noise. We tested all generated normalized maps in this chapter by including them in the AHM loop. We found that when we ignored highly uncertain seismic bins identified with the NRMS map, the normalization technique provide more reasonable 4D data. By reasonable we mean that after normalization more satisfactory reduction of both production and seismic misfits was observed.

By history matching using production data, we usually want to change the model to reduce or increase production rates of water appropriately. The prediction error may arise for different reasons such as simulating the wrong degree of edge or bottom drive from the aquifer, or incorrect estimation of channelling, fingering or other physical dispersions. If the predicted water production rate is too high, for example, we can reduce water movement laterally by: homogenizing the permeability field to reduce channelling; reduce permeability to slow down connection to the aquifer laterally; or increase the NTG (or porosity) to slow down water movement; or perhaps account for numerical dispersion by upscaling the relative permeability curves (Kyte and Berry

1975). It is also possible to reduce bottom water drive by decreasing the vertical permeability or explicitly place shale barriers near the well. It is also very possible that by reducing flow horizontally to the well, we increase it vertically and vice versa. Production data alone does not give information about which of these options are best and the problem is therefore very non-unique. Saturation dominated 4D seismic data can provide more information, however, if we use it in history matching. A weak 4D signature a few grid cells from the well indicates low levels of lateral drive and that we do not want to induce it. A strong signature requires that we retain the edge drive mechanism. In this chapter it has been shown how the 4D data is useful in this respect.

Normalizing 4D seismic signatures is essential for quantifying misfits in history matching. In many cases well tie information is not present and some form of model based approach is necessary. We are always caught in a dichotomy, however, that the model does not predict accurately and some regions of the field must be selected where it is believed that the match is good. In this study a 'blind' approach using maps were compared to one where the wells were considered to match on saturation. The normalized data resembled the base case model in magnitude of the signal although regions of mismatch were clear. During history matching the match was improved somewhat, particularly by removing some of the false signature.

In this thesis, the seismic data was normalized by using model data just once and the normalized data were fixed for duration of history matching studies. It may be preferable to include the normalization parameters in the history matching loop. However, some assumptions need to be considered for this approach. For example reservoir properties should have low uncertainty because they will be used for generating synthetic seismic and we need to be sure about the synthetic seismic data at least for some regions in the reservoir. This is quite an important assumption which cannot easily validated for a reservoir. On the other hand the petro-elastic model itself need to be validated which is again not possible for many fields. On the other hand it would be difficult to define an appropriate objective in order to measure misfits in this case and we may have the problem of non-uniqueness of the result. As a summary, by including the normalization parameters in history matching we may find parameters by reducing the misfit function but on the other hand, this method makes the observed data more like the synthetic data rather than change the model to achieve the opposite. We

may, therefore, lose the real value of using observed data as a constraint for updating reservoir model.

However, this approach could be considered in future work but it is possible that such an approach will result in increasing non-uniqueness and that there may be too many solutions that all fit with different regression equations. By tying the regression to the wells, a single regression equation seems more satisfactory and may be more stable in the inversion process. It also serves to give a good starting point if inclusion of the normalization process in the loop is considered.

For NRMS studies there is still an important question of what the best threshold value for NRMS should be at which we apply the filtered. In this study 30% was used ad-hoc just to investigate the importance of NRMS filtering.

## 6.10 Summary

Previously in Chapter 5, a study for normalizing observed 4D data was performed in order to preparation for use in the history matching loop. It was found that the best map that can show 4D activity qualitatively related to the production activity was for the case where seismic data was cross-plotted in the location of vertical wells and for the base reservoir model. However, there were a lot of production wells in Nelson which under-predicted water production in the base reservoir model. According to the previous discussion in Chapter 5, more water was needed for lateral sweep. Therefore it was expected that stronger 4D signals should be observed close to the location of those production wells. Then, by using that normalized map in history matching we also improved our model seismically such that we obtained a good reduction of total production misfit.

As an alternative to that approach in another study, the NRMS map was used to filter the seismic data. From the normalization study it was found that by using the Map derived approach with NRMS filtering, the gradient of the regression equation increased compared to the equivalent Map derived case without NRMS and decreased compared to the Well derived case (also without NRMS filtering). Therefore the NRMS based equation avoided the problems of over estimated 4D signature. Also it was better than

the unfiltered Well derived cases at predicting the 4D activity especially for the wells that underestimated total water production for the base reservoir model.

By using this new normalized 4D map in history matching of the reservoir greater improvement of the total production misfit of the reservoir was obtained with a good reduction of seismic misfit as well.

# Chapter 7: HISTORY MATCHING IN NELSON BY UPDATING GEO-BODY TYPES

**Overview:**

The first requirement in any manual or automatic history matching technique is to decide what reservoir properties need to be updated, including where and how they should be changed. This process is called parameterization. Even with the major developments in the computer technology it is still not practical to deal with a high dimensional inverse non-linear problem. Suitable parameterization is therefore very important.

In Chapter 2 (Section 2.1.1), we discussed various parameterization techniques that can be applied in history matching. In the Nelson field, we decided to use pilot points with Kriging. The main advantage of this technique was that the continuity of reservoir parameters was preserved through updating in the history matching process.

In Chapter 4 (Section 4.2), the best locations for updating the model were found by using the streamline guide and it was observed that a good improvement in matching the production rates was obtained. On the other hand, as part of another study in Chapter 4, a suitable parameter updating schemes was used in order to mix the best set of parameters at the right location in the reservoir (LMV method introduced in Section 4.3.3) to reduce the number of unknowns. We updated the model in a more feasible way, therefore, where pilot points with Kriging were used for parameterization. That parameterization scheme was used in Chapters 4 and 6 in order to perform production and seismic history matching in Nelson field. The change in reservoir properties were mainly local for the best reservoir models obtained after history matching studies in Chapter 4 and 6. The question here was could we apply another parameterization scheme in order to update the whole reservoir instead of making local changes?

The work in this chapter is based on an alternative parameterization method also introduced in Chapter 2 (Figure 2.1, Option 2B) where the reservoir parameters were changed based on the geological features. In this chapter the reservoir model was updated by improving the parameters in geo-body types. Geo-bodies were identified as "Environment" variables by the operator (see Chapter 3, Section 3.4). The advantage of

this parameterization technique was that reservoir properties were modified in a more geologically consistent manner in each geo-body type through the history matching process. However, one important question in this technique was that, whether or not reservoir parameters can be updated in the regions where we lack observed dynamic data (in the locations far from production activities or observed seismic signatures). Therefore, the aim of this chapter was to compare the history matching result of two different parameterization techniques; geo-body updating and pilot points with Kriging.

## 7.1 History matching method

Figure 7.1 shows the history matching workflow for the study in this chapter. From stage one, the important geo-body types (termed Channel Axis, Channel Margin and Interchannel introduced in Chapter 3) need to be defined in order to change the properties within to ultimately improve the match in production (and time-lapse seismic) data. In this stage some sensitivity analysis needs to be performed in order to investigate which geo-body type has more influence on the production activities and fluid flow in the reservoir. Also, the appropriate parameters need to be chosen for modification. This stage may be different field by field. In Nelson, however, the geological information and also fluid flow pattern information from the model supplied by the operator of the field was used to choose the parameters for updating. Based on that information there are shale bodies all over the reservoir and in different geo-body types. The amount of shale is lower in the Channel Axis sands, higher in Channel Margin and highest in Interchannel; an example can be seen in Chapter 3, Figure 3.7. Based on this observation it is important to consider updating all three variables net:gross, horizontal and vertical permeability in order to control shale bodies in the reservoir. The appropriate modification of those parameters helps to control water displacement from injectors and aquifer toward production wells.

In the second stage the appropriate parameter updating technique needs to be applied. The previous history matching studies (Chapters 4 and 6) were based on a parameterisation method called Pilot Point with Kriging as part of a Local Multi-Variable scheme which is a local parameter updating method to reduce the dimension of the problem. In this work the geo-body types were considered as the elements defining the regions that needed to be updated through history matching by assigning a multiplier for different variables inside each of them. The important question remains as to which

geological feature should be modified in the history matching process to get the best update of the reservoir (parameter updating). Stages 3, 4 and 5 of this workflow were discussed previously in Chapter 4 (Section 4.1). In a case obtaining unsatisfactory history matching results we can return to stage 1 or 2 to change the parameters or consider different combinations of geo-body types.

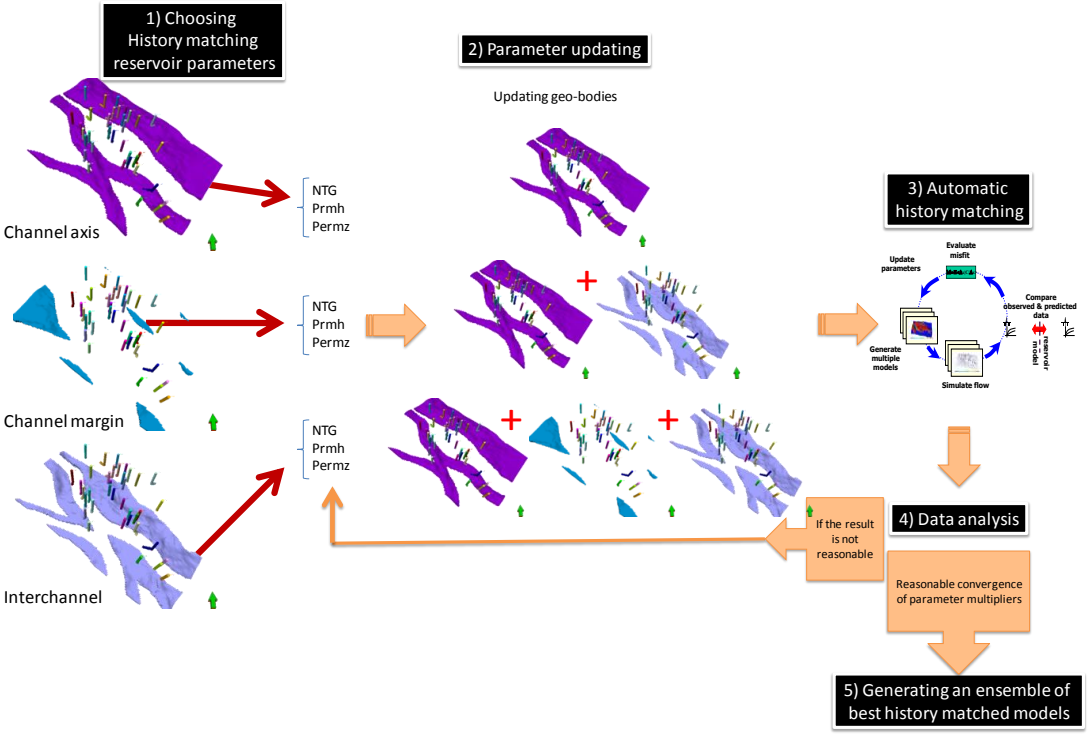


*Figure 7.1: History matching workflow based on updating reservoir properties in geo-body types.*

Previously, in Chapter 3, interpreted geo-body types were described in the Nelson field. In Figure 3.7 it can be seen that almost all the wells are located in the Channel Axis in the second interval and in the Channel Axis and Channel Margin in the first interval. By considering different combinations of geo-body types a set of problems with different dimension was generated. There were two strategies for updating the reservoir. In one case, the parameters of each geo-body type were modified in a uniform manner across the whole reservoir and in the second one each geo-body type was split into two parts based on the reservoir intervals. Based on the dimension of the problem, a different number of models was considered for the initial set of model ($n_i$) to search the parameter space sufficiently. Also appropriate values were chosen for $n_s$ and $n_r$ to explore and exploit different combinations of the parameters in order to find the best history matching result.

Compared to previous history matching studies, a different parameter updating scheme (global multi-variable) was used in order to update geological bodies appropriately and this scheme will be discussed in the following section.

An important issue in this study is the range of multiplier value that needs to be considered for each parameter. It is very important to ensure that this range of multiplier does not change the properties of the reservoir in a way that is inconsistent with geological information. In this study the reservoir will be updated based on geo-body types, each of which contains many simulation cells with a wide range of values for various reservoir properties. Therefore we need to makes sure that the cells that already have a high parameter value do not increase significantly. The range of multipliers was 0.1 to 10 and sampled on $log_{10}$ scale.

For the Channel Axis, there is a wide range of values for different parameters such as net:gross, horizontal and vertical permeability from low to high as previously shown in Figures 3.29 and 3.30. Based on the assumption that the shale distribution is uncertain, it is possible that a cell that was originally considered as a shale with a low value of net:gross or permeability can be converted into sand with high values of those properties. It should be considered, however, that through the history matching process, the properties of the cells that already contain high values of permeabilities are not further increased. For this reason the cells that have permeability set greater than 1000 mD (the highest permeability is 1700 mD, as discussed in Chapter 3) were counted for the first and second intervals and it was found that there were 1000 cells in the first interval and 40 in the second interval (in a disorganized distribution) which is negligible compared to 500,000 cells in the simulation model. For the Interchannel the number of cells with a high value of permeability was 60 and 7 in the two intervals respectively.

For the geo-body types located below the reservoir, and named here as Aquifer, the maximum value of horizontal permeability is 1000 mD. Therefore, the range of multiplier was reasonable for this facies as well.

## 7.2 Global multi-variable approach

In this approach the idea was to update the parameters in the most influential geo-body types (to capture the water displacement toward the wells) globally in the reservoir by

updating several variables at the same time. Here the term global is used to mean that because of the lateral extension of the geo-body types throughout the reservoir, parameters are updated globally geographically.

Figure 7.2 illustrates a set of history matching studies that were performed. The first 4 sets of studies were 3D problems where net:gross, horizontal and vertical permeability was updated in each geo-body type, one at a time. The goal of this part of the study was to investigate the importance of updating each geo-body type.

Then, the most important geo-body types were combined such that the dimension of the problem increased to 6, 9, 12 and 15 in this order to find the best way of updating parameters. Up to the 12D case, it was considered that each geo-body type in both reservoir intervals should be changed in the same way. In the 15D problem, however, the reservoir was updated separately by intervals. This kind of parameter updating of the reservoir was very helpful for finding the right geo-body type in the reservoir to change and prevented changing the regions where no change was needed. It is worth mentioning again that by increasing the dimension of the problem, the number of models that we need to run increases as well.

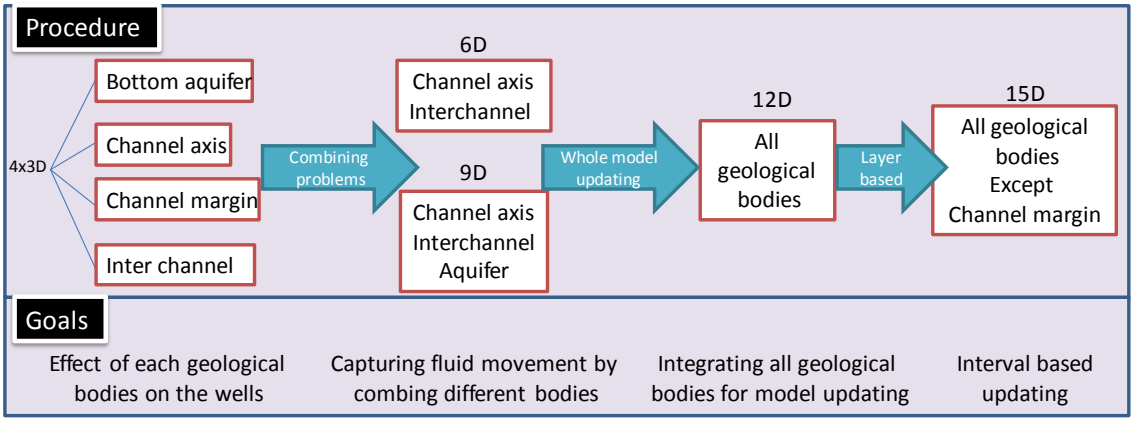


*Figure 7.2: Main history matching studies performed to globally update reservoir properties in geo-body types.*

### 7.3 Production history matching result

Table 7.1 shows a summary for different history matching cases. We can see the geo-body types that were combined in various ways and the total number of simulation models was increased with the dimension of the problem. As discussed previously, we

considered a limit of 4000 as the maximum number of model. The Well+base normalized 4D seismic data were considered observations for the cases where production and seismic history matching was performed in this study.

The first results were obtained for the 3D problems. Figure 7.3 shows the reduction of total production misfit by updating the parameters in each geo-body type. It can be concluded that apart from the Interchannel, the geo-body types were very important for reduction of the misfit. For some parameters there was a convergence to a specific value, while others approached the upper limits. It was not very important to analyze these results precisely because the aim of history matching was not to change just one geo-body type. As discussed previously, it was essential to update different reservoir parameters simultaneously. By updating geo-body types in various combinations, the best 10 models were obtained with lowest misfit as an ensemble of updated reservoir models.

| | | | | | | |
|---|---|---|---|---|---|---|
| Reservoir variables updated | $k_h$, $k_z$ and net:gross | | | | | |
| History matching dimension | 3D for sensitivity of each individual geo-body type<br>6D – including Channel Axis and Interchannel geo-bodies only<br>9D- including bottom aquifer, Channel Axis and Interchannel geo-bodies<br>12D- including all geo-body types<br>15D- all geo-body types except Channel Margin geo-bodies (interval based) | | | | | |
| NA parameters | | **3D** | **6D** | **9D** | **12D** | **15D** |
| | $\mathbf{n_i}$ | 16 | 128 | 1024 | 2000 | 3058 |
| | $\mathbf{n_s}$ | 10 | 18 | 28 | 36 | 46 |
| | $\mathbf{n_r}$ | 5 | 9 | 14 | 18 | 23 |
| | **total** | 66 | 524 | 4104 | 2720 | 4070 |
| Production wells chosen | Oil and water rates | | | | | |
| 4D observed data | Normalized phase shifted amplitude (Well+base) | | | | | |
| Parameter updating scheme | Global multi-variable | | | | | |
| History matching period | 1994 to 2000 | | | | | |
| Forecasting period | 2000 to 2003 | | | | | |

*Table 7.1: Main elements for history matching runs.*

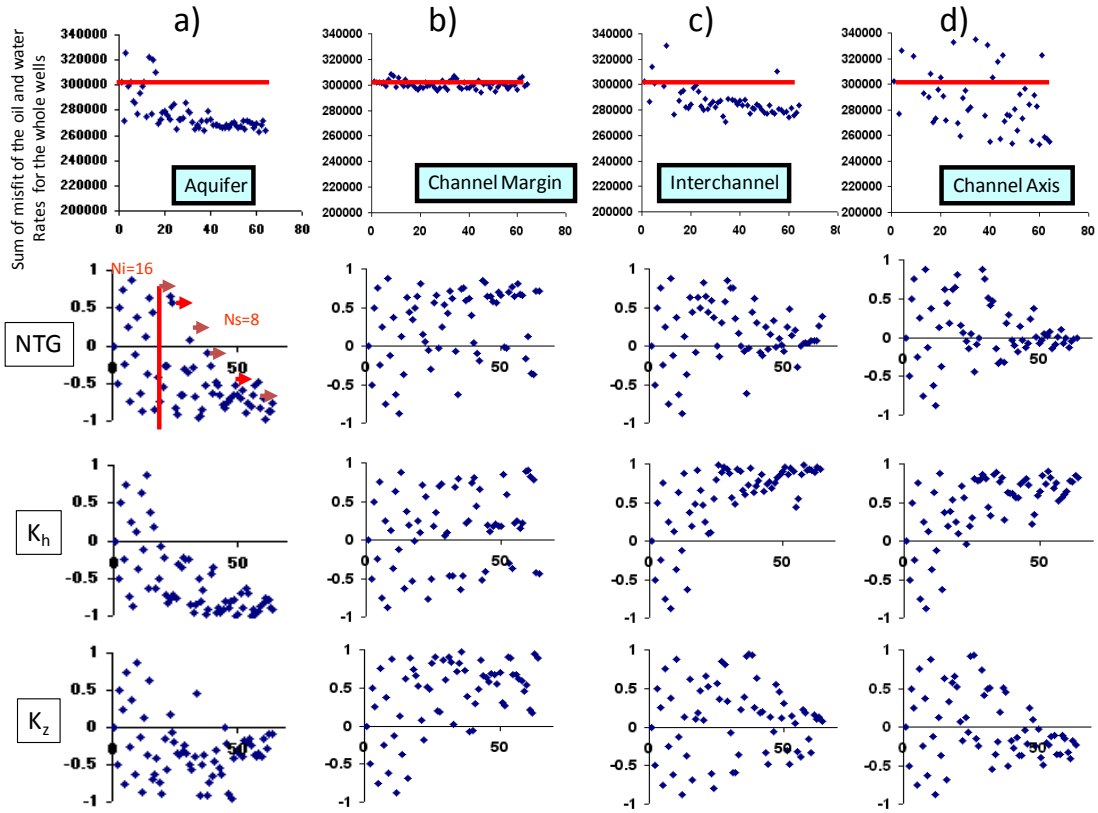


*Figure 7.3: Reduction of sum of misfits of the oil and water rates for the all wells for each 3D history matching problem (top plots) and the convergence of various reservoir parameters to the final result (lower plots). various 3D history matching runs were performed for updating properties in a) aquifer, b) Channel Margin, c) Interchannel and d) Channel Axis. The red lines in the top plots are representative of the misfit value of the base reservoir model. Also, as an example, the boundary for the initialisation models ($n_i$) is shown as a vertical red line in the NTG for (a) following by red arrows which is the number of iterations to repeat generating $n_s$ models .*

In Figure 7.4, it can be observed that in the history matching period, the sum of misfits of the oil and water for the all wells were reduced for the models and the highest was for the 12D problem and lowest for the 6D problem. In the forecasting period the result shows poorest reduction of the misfit for the 12D problem and the highest reduction was for the 15D problem. According to Figure 7.5, generally, the best result was obtained for the 15D case which gave the highest reduction of misfit in the matching and forecasting periods. For the 6D case, where two geo-body types were updated, the correlation between the points in the Figure 7.4 is low and sometimes a small reduction of history matching misfit gives a large reduction in forecasting. The 12D problem, where we updated all geo-body types was considered to be is the worst case because of

the poor improvement in the forecast. The point to note with the 12D problem is that the Channel Margin was included in the history matching whereas in Figure 7.3 it can be seen that updating this part of the model by itself did not affect matching the wells. By increasing the dimension of the problem the volume of parameter space was increased drastically and the optimization algorithm (NA) needed to search a much bigger volume of parameter space in order to find the best parameters. In the 15D case where PHM updated the parameters in all geo-body types except the Channel Margin, the misfit was improved in both matching and forecasting periods. It can be seen, also, that the best model stands out from the rest of models in the 15D case. The reason for that is because the dimension of history matching is very high so it was not possible to run enough models in order to observe convergence for the variables.

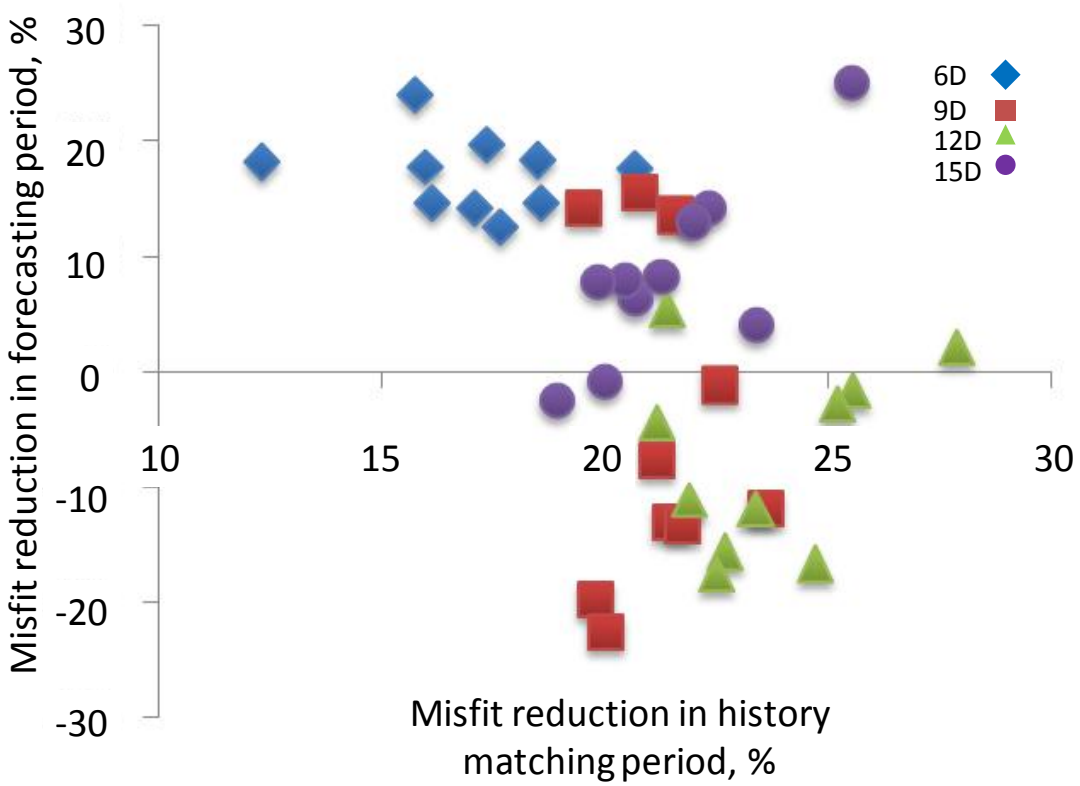


*Figure 7.4: Reduction of total production misfit in forecasting versus matching periods for different history matching studies.*

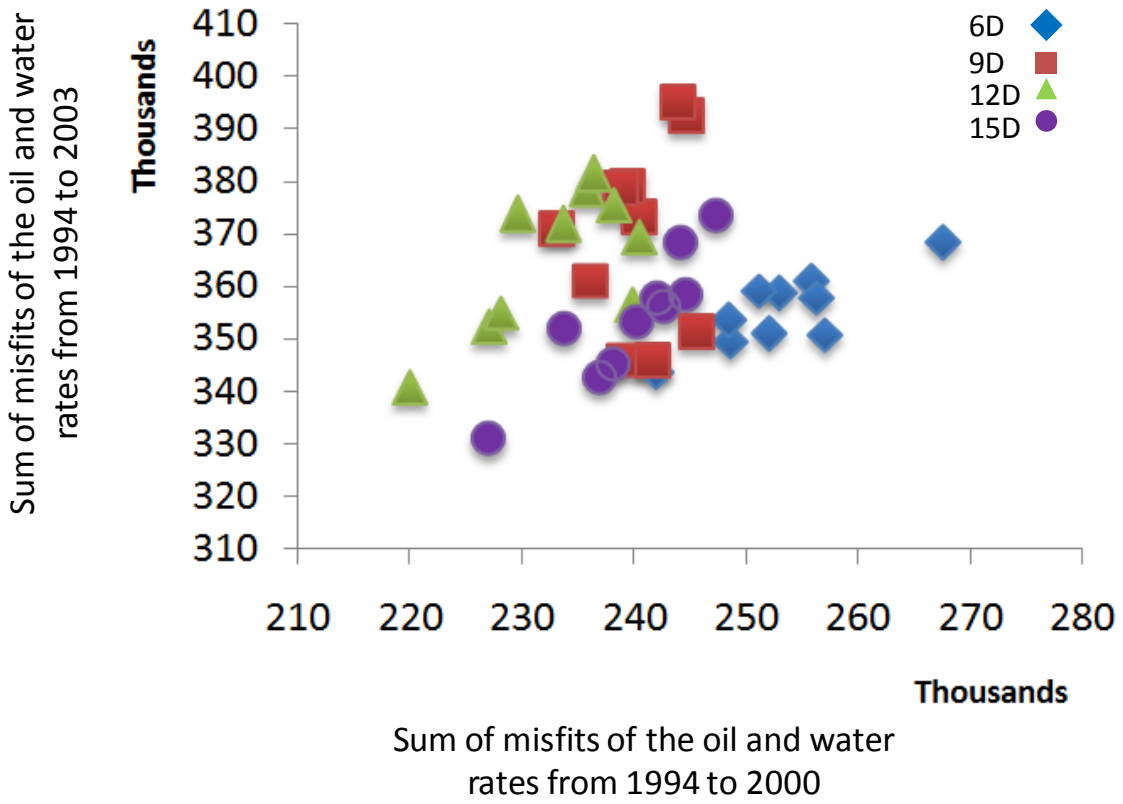


*Figure 7.5: Sum of misfits of the oil and water rates for all wells from 1994 to 2003 (history plus forecasting period) versus the same misfits for the history period from 1994 to 2000. Note that the misfit value of the base reservoir model is 300,000 and 430,000 for the history period and history plus forecasting period respectively.*

Figure 7.6 shows how the parameters were changed after history matching in each case. Looking at the 12D problem in history matching, it can be seen that the horizontal permeability increased drastically in the Interchannel region. Because of the increased dimension of the problem, a greater search of the parameter space was required and so the process could not converge.

In the 9D and 15D cases, the same locations of the reservoir were updated but in the 15D case two reservoir intervals were considered separately. From Figure 7.6 it can be seen that the parameters were changed in the same direction but generally the degree of change is less in the 15D case which means smoother changes to the reservoir. The average value of parameter multiplier for the net:gross of the 15D case and the horizontal permeability of 12D case confirm that for these two cases convergence was obtained. For the 12D case, the important point was the lack of freedom by updating the reservoir model in each geo-body type throughout the reservoir without

distinguishing between the two reservoir intervals. In the 15D problem, net:gross of bottom aquifer was increased in order to provide additional water for displacing oil.

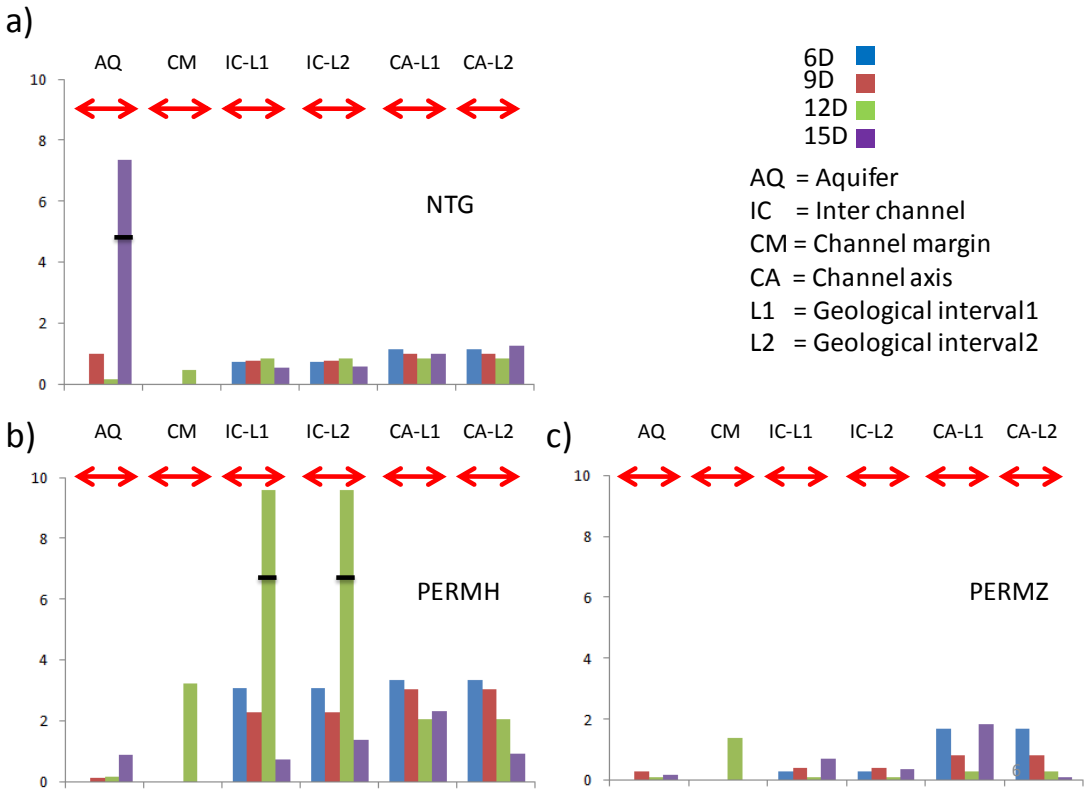


*Figure 7.6: The multipliers of various reservoir parameters; a) net:gross, b) horizontal permeability and c) vertical permeability for the best history matched models. Note that in 6D and 9D problems only one Channel Axis and Interchannel geo-body type was altered for the both reservoir intervals therefore the multiplier of parameters is same for each geo-body type in 1st and 2nd interval as shown in the this figure. Three black lines in the bars show the average value of multiplier for the best 10 history matched model.*

Figure 7.7 and Figure 7.8 show the new values for the reservoir variables that were obtained for the best reservoir model in each case. In those figures, the arithmetic average of each variable was calculated over each interval for the base and best models. It can be seen that for the 6D problem the degree of change was quite large for horizontal permeability in the Channel Axis and the Interchannel in the 12D case. The vertical permeability was also decreased considerably in Interchannel for the 12D case.

Comparing the 9D and 15D results it can be seen that the trend of change was very similar between facies except in the aquifer region. The net:gross was increased in the Channel Axis and decreased in the Interchannel. The horizontal permeability was

increased in both geo-body types and the vertical permeability was increased in Channel Axis and was decreased by a small amount in Interchannel.

In the second interval (Figure 7.8) there was a sharp increase of horizontal permeability in the reservoir for 6D, 9D and 12D cases whereas for the 15D case there was a reasonable change of parameter. Similar to the first interval, the net:gross was increased in the Channel Axis and was decreased in the Channel Margin. The horizontal permeability was quite similar to the base model and vertical permeability decreased in the Channel Axis.

As discussed previously in Chapter 3, based on the geological information for the various geo-body types, it was expected that the Channel Axis would be of better quality reflecting more sands and that shale should exist mainly in the Interchannel sands. From Figure 7.7 and 7.8 it can be seen that for the 12D problem, the Channel Axis was made more shaly by decreasing net:gross and that shale was very well connected horizontally because of decreasing vertical permeability. Therefore, as a conclusion, it is not possible to accept the history matching result of the 12D case.

After history matching in 6D and 9D cases in the second interval more sand was added to the Channel Axis by increasing net:gross and there is also a good connection vertically in the sand because of a higher value of vertical permeability. On the other hand the horizontal permeability seems to be wrong in these two cases because in the location of Interchannel with a low value of net:gross the permeability increased.

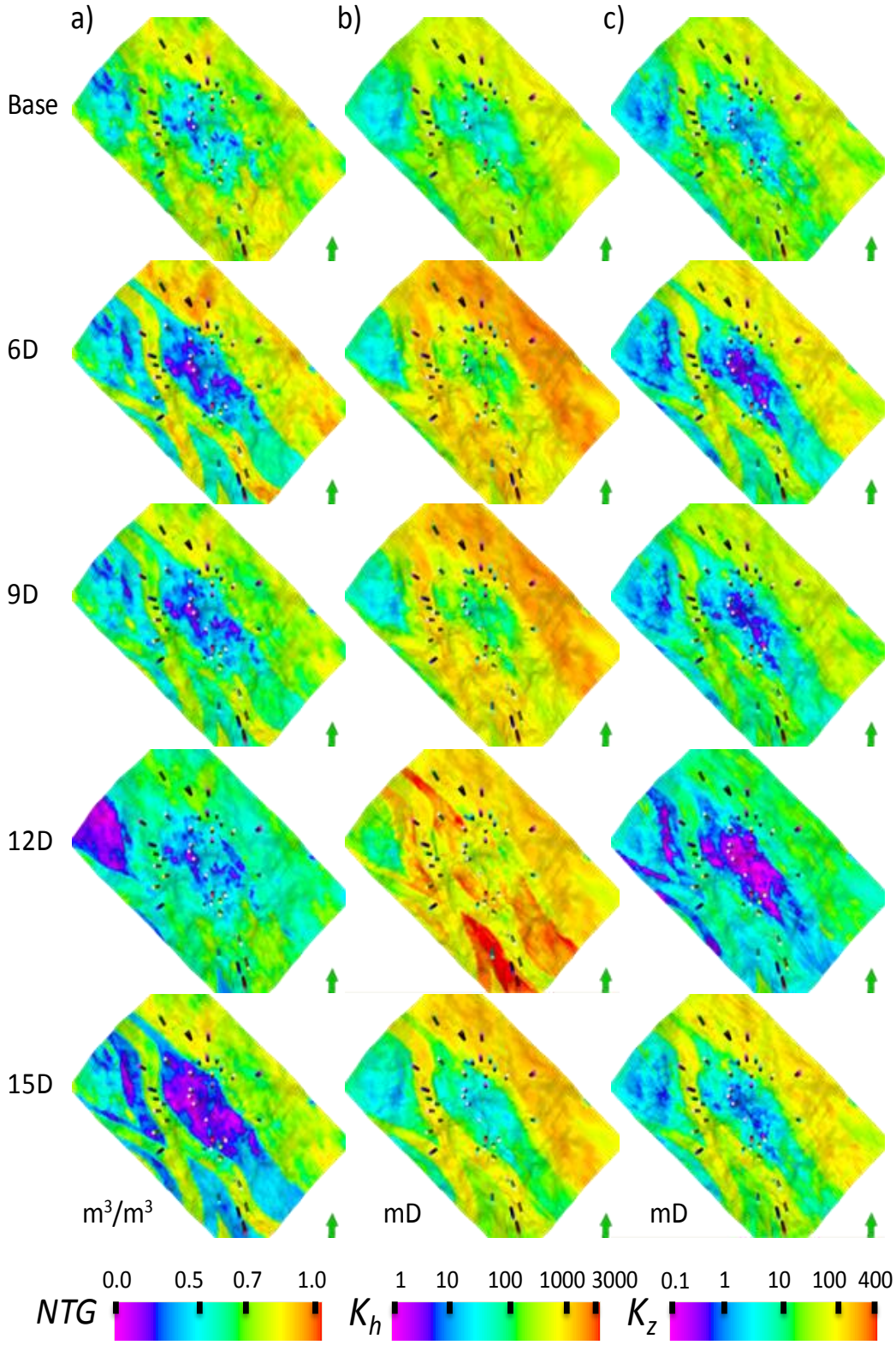


*Figure 7.7: Average reservoir properties in first reservoir interval for different history matching studies. (a) net:gross, (b) horizontal permeability and (c) vertical permeability.*

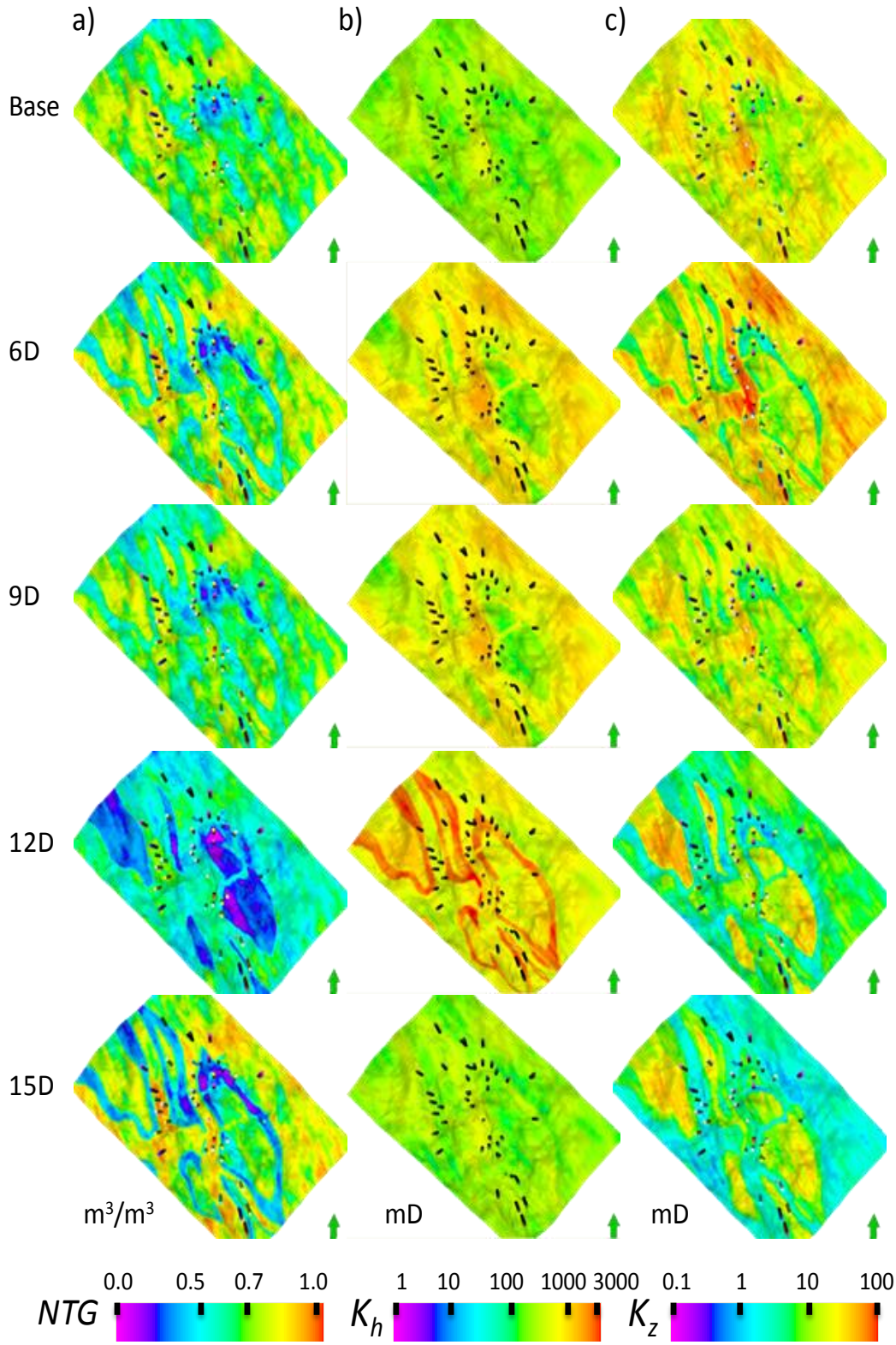


*Figure 7.8: Average reservoir properties in second reservoir interval for different history matching studies. (a) net:gross, (b) horizontal permeability and (c) vertical permeability.*

### 7.4 Production and seismic history matching

Up to this point in the study, production data only was used in history matching and best result was observed for the 15D problem. The best normalized 4D data from the previous study (Well+base, Chapter 5, Figure 5.7c) was then used in the history matching process for the 15D case by using the global multi-variable approach as a parameter updating scheme. The seismic history matching result was compared to the previous result obtained for production history matching case.

The reduction of misfit value for the best 10 models are shown in Figure 7.9. Comparing PHM and PSHM, it was observed that with the latter, there were some models similar to the PHM outcomes such that the reduction of misfit in the matching period was equivalent.

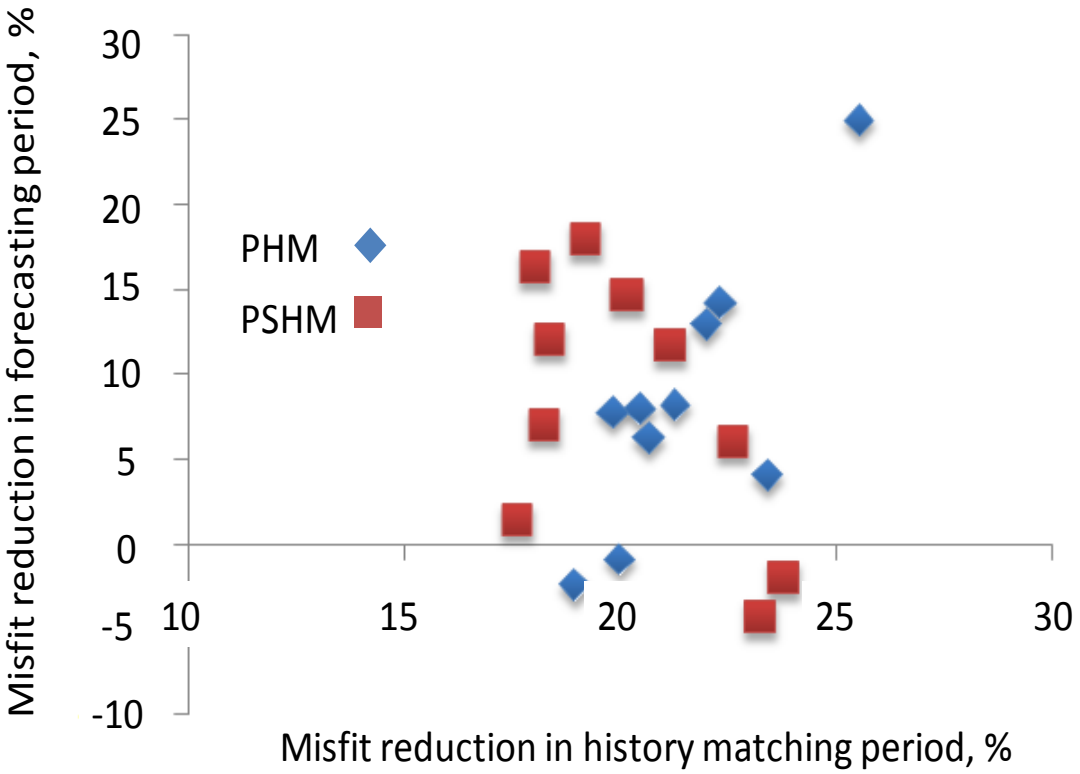


*Figure 7.9: Reduction of total production misfit in forecasting versus matching periods for different history matching studies.*

The point that needs to be considered for the PSHM case is that because there was significant lateral change to the reservoir model via the geo-body types, there was potential for a reduction in quality of the fit of matching the seismic data. The synthetic seismic data was generated for the best updated model as shown in Figure 7.10. There

were some improvements to the model seismically in different areas, mainly in the centre of the reservoir where there was a good improvement in the model. A 7% reduction of seismic misfit after history matching was obtained.

In seismic history matching, the aim was to match the time-lapse seismic in the region that seemed to contain signal. From the observed 4D map in the Nelson field (Figure 7.10b) it can be seen that usually that signal was in the edge of the reservoir where there was water sweep from injectors or the aquifer. By updating the reservoir laterally the problem that occurred was that, the inversion loop sought to match the noisy part of the observed data and thus we got a lower quality perdition.

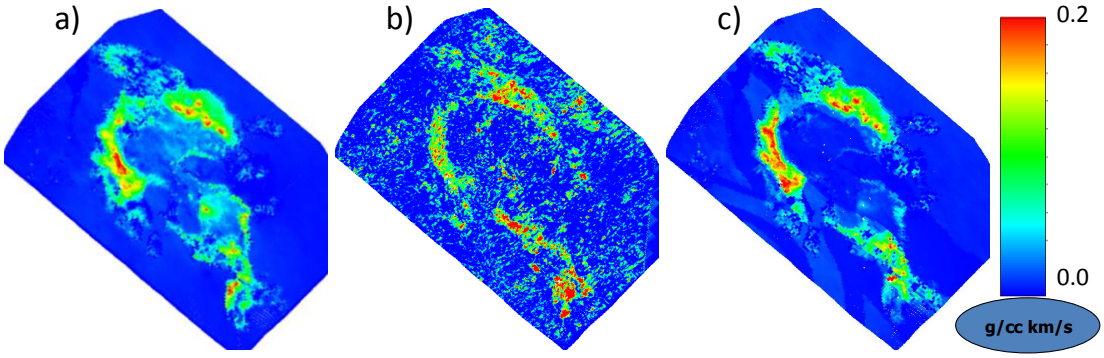


*Figure 7.10: Synthetic 4D seismic map (2000-1994) for (a) base reservoir model, (b) observed map and (c) best history matched model.*

Another problem that occurred here was that the net:gross was changed laterally everywhere in the reservoir even in the non-reservoir section. On the other hand the synthetic seismic data was generated by a set of equations (Chapter 2, Section 2.4 and Chapter 3, Section 3.6) which averaged vertically using pore volume weighted averaging. There was therefore a direct influence of net:gross. Erroneous synthetic seismic data were generated by changing net:gross in non-targeted areas in the reservoir (where thee is no observed 4D signal). These synthetic data were compared to observed data for every model during the history matching loop and therefore it had a negative effect on the process.

Because of above two problems, it was not expected that the final model would be found just by using time-lapse seismic data in the history matching process with the geo-body type updating scheme alone.

Further analyses were made by comparing the change in the best reservoir model after history matching studies. Figure 7.11 and Figure 7.12 show the average reservoir properties for the best history matched model, in both matching and forecasting periods. In the first interval it can be seen that a similar degree of change was obtained for both PHM and PSHM cases. In the second interval the parameters are different and for both horizontal and vertical permeabilities an increase of parameter was obtained in the Channel Axis.

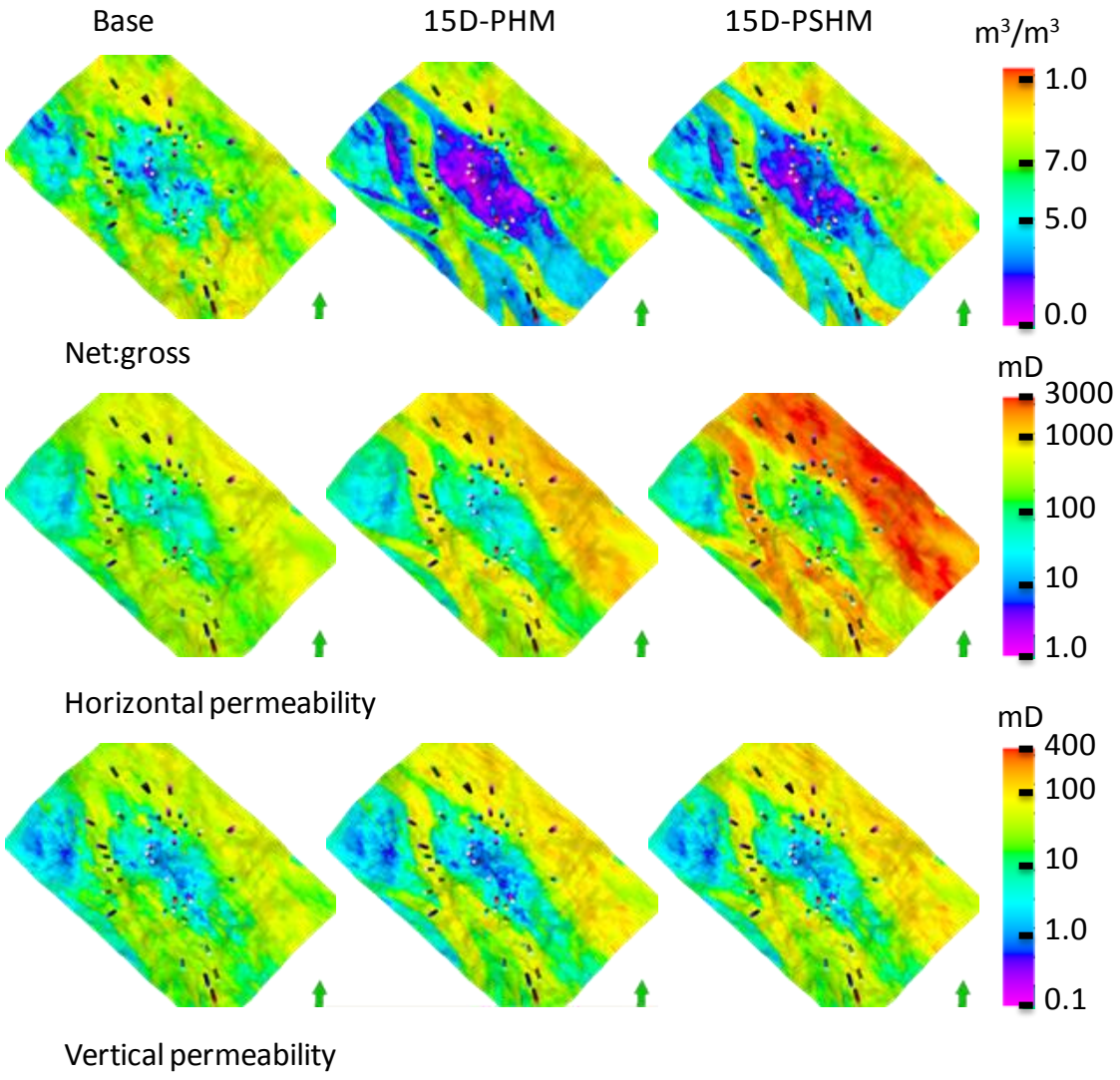


*Figure 7.11: Average reservoir properties in the first reservoir interval, comparing the PHM and PSHM studies.*

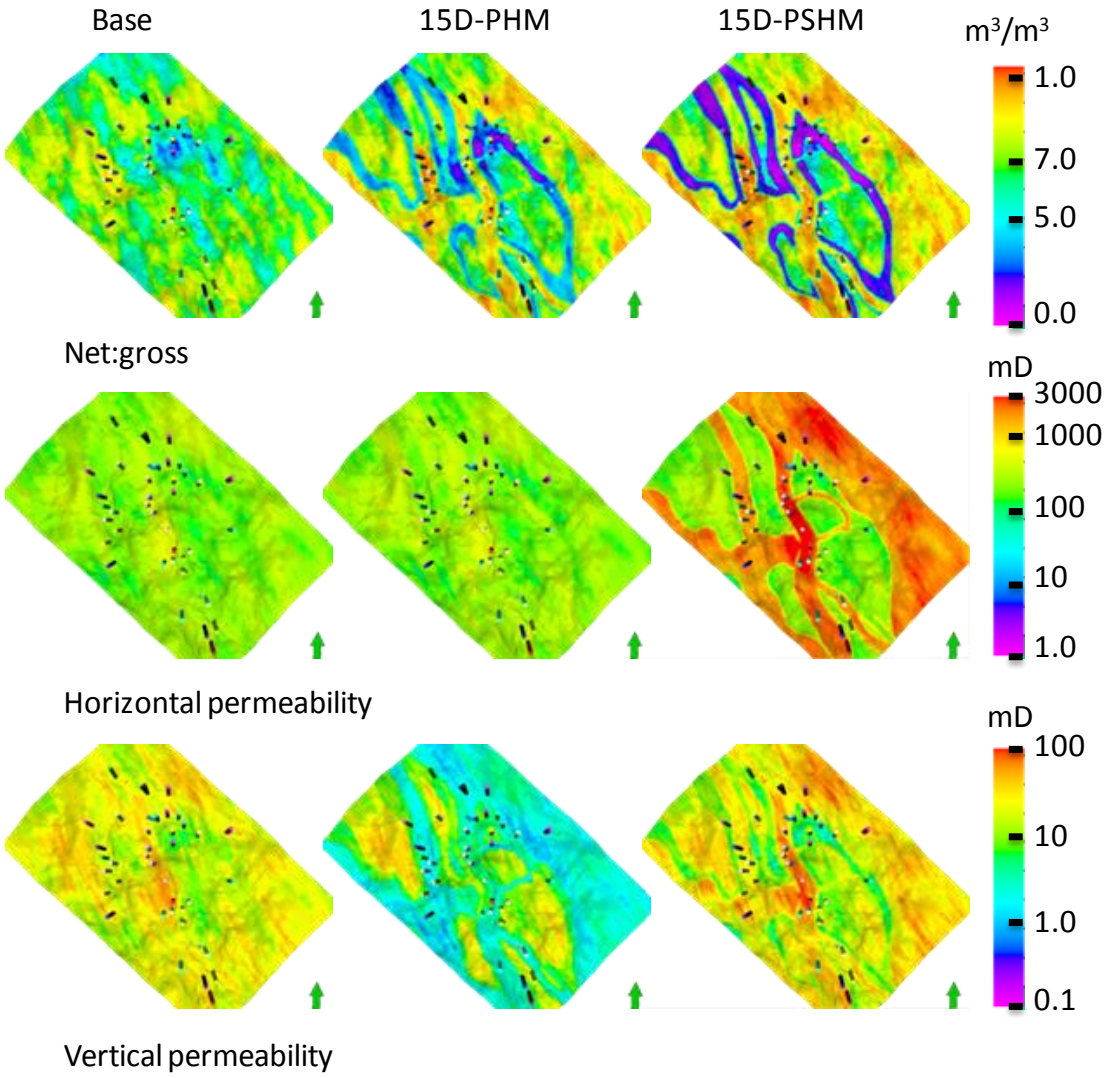


*Figure 7.12: Average reservoir properties in second reservoir interval, comparing PHM and PSHM study.*

## 7.5 Global updating versus local updating in history matching

The aim in this section was to compare the result of global updating of geo-body types (previous sections) with the previous study (Chapters 4 and 6) where the pilot point method was used as a geostatistical tool for changing the reservoir model. In Table 6.1 we can see the information for the history matching runs such as the number of regions to update, the dimension of the problem, the models that were needed for each run and so on.

Figure 7.13 shows the comparison between production history matching (PHM) and production and seismic history matching (PSHM) cases when the model was updated by using pilot points and when updated based on geo-body types only.

Figure 7.13 shows that there was a clear difference between the pilot point and geo-body types updating schemes. In the pilot point cases, a better reduction in misfit was observed in both periods whereas the misfit reduction is almost half for geo-body type updating cases. This result occurred because the regions to update (i.e the pilot point locations) were chosen based on the streamline guide, which was very efficient, whereas in the geo-body types updating cases, the model was updated throughout the facies.

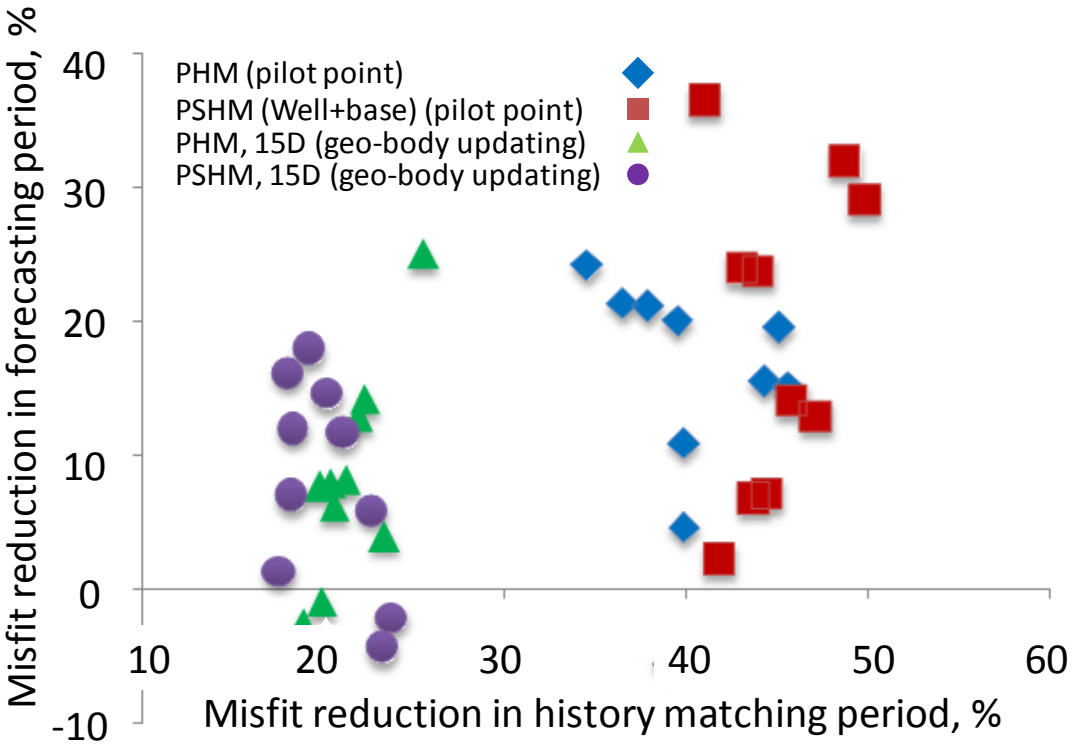


*Figure 7.13: Reduction of total production misfit in forecasting versus matching periods for different history matching studies.*

In Table 7.2 the misfit reduction of total production and seismic data is summarized for best reservoir models that give the lowest misfit in both matching and forecasting periods.

### 7.6 Combining geo-body type updating and the pilot point method

Looking at the reduction of production misfit values in the geo-body types updating study it can be concluded that this method of updating the reservoir did not sufficiently improve history matching of the well data as much as the previous study (Chapter 6). The main reason for this result is because lateral updating of the reservoir affected the

production performance of the wells differently (some were improved while some made were worse).

| History matching case | All production wells misfit reduction, % | 4D seismic misfit reduction (%) |
|---|---|---|
| 1. PHM | 45 | ---- |
| 2. PSHM, well+base | 49 | 8.2 |
| 3. Geo-body types updating, PHM, 15D | 22 | ----- |
| 4. Geo-body types updating, PSHM, 15D | 19 | 7.3 |

*Table 7.2: Reduction (%) of production and seismic misfit in history matching period for different studies.*

The best PHM case reported in Table 7.2 (row 4, geo-body types updating, PHM, 15D) was chosen as the representative of the geo-body types updating scheme. The well water production misfit was plotted for all wells in Figure 7.14 in order to compare the misfit value of each well before and after history matching. It can be seen that for almost half of the wells there is a better match after history matching but there are still some that require improvement. The first 9 wells in the figure (i.e worst matching after history matching) were chosen and their locations are specified in Figure 7.15.

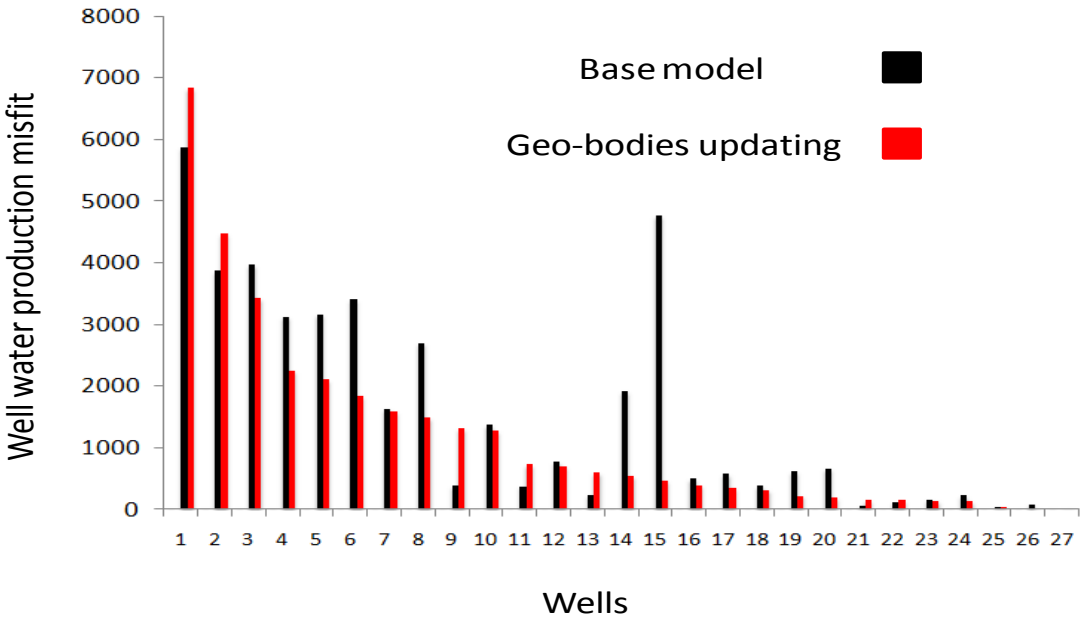


*Figure 7.14: Well water production misfit for the base model (black) and best history matched model after geo-body type updating (red) from 1994 to 2000.*

6 out of the 9 wells in Figure 7.15 are located in the Channel Axis geo-body types in both reservoir intervals (Figure 3.7) and the other 3 are in the Interchannel in the first interval (Figure 3.7a and Figure 7.15) and Channel Axis in the second interval (Figure 3.7b).

Wells 5 and 8 in the Interchannel, over predicted water rates in the base reservoir model whereas Well 7 under predict water rate. Because of that difference in the well activity of the base reservoir model it was better to consider two different strategies in order to improve the match of the wells. However, in the geo-body type updating scheme all of the production wells in the Interchannel were used in the objective function and we tried to improve them globally throughout history matching.

In the eastern Channel Axis, water production was over predicted for wells 1 and 3 but under predicted for Well 4. Similarly in the western Channel Axis wells 2 and 9 under predict water production and Well 6 over predicted.

The idea then was that to improve these 9 wells after updating the geo-body types, master pilot points should be located close to each well based on the streamline guide concept (Chapter 4, Section 4.2). It was then possible to obtain further updates to the reservoir properties by the local multi-variable scheme around each of the 9 wells. Table 7.3 shows the history matching information. Four wells (1,2,3 and 9) were completed in the first interval only and the rest of the wells in both intervals. We therefore defined two history matching problems of 3D and 6D for each case.

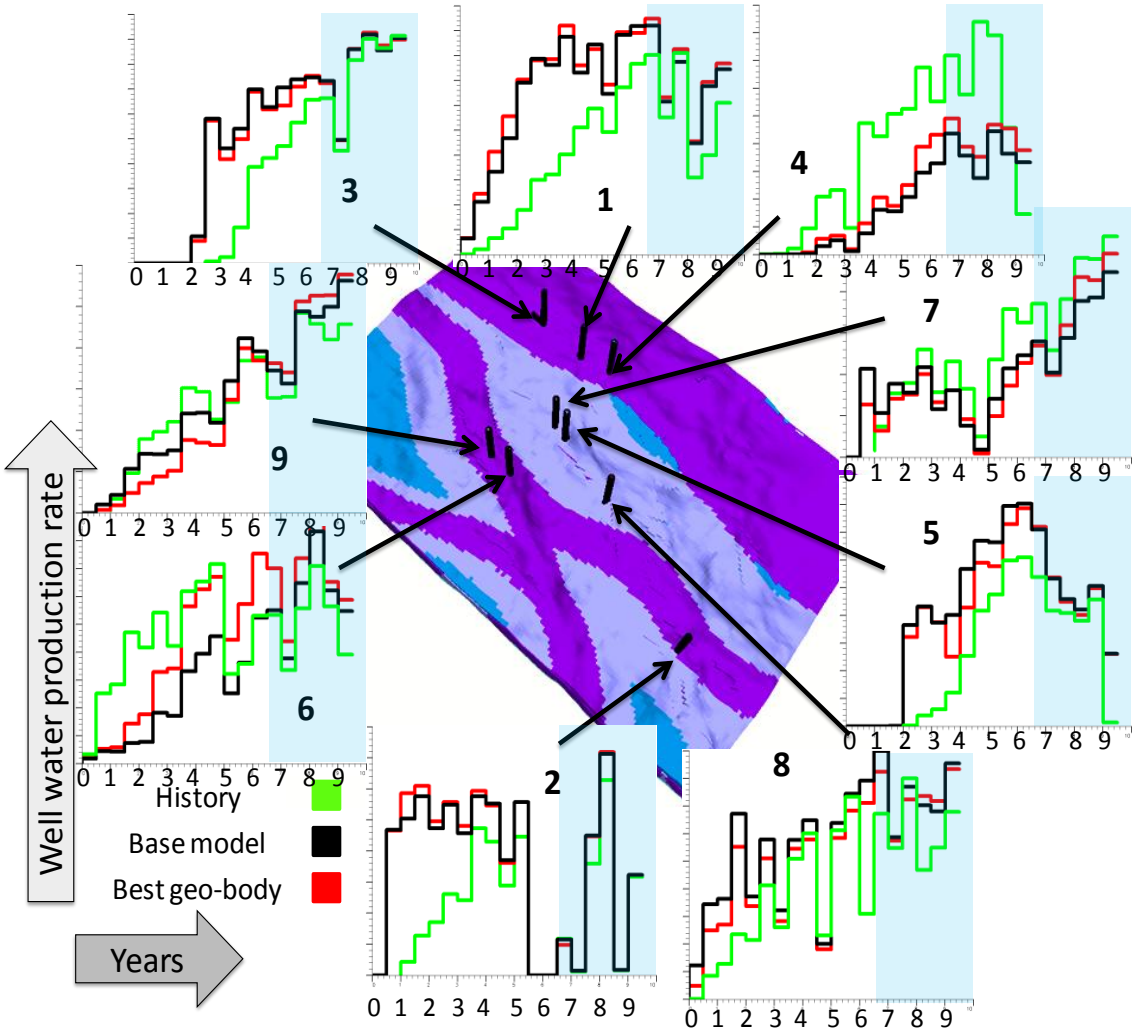


*Figure 7.15: Well water production rates for the worst matched wells. The well number is based on the number in Figure 7.14.*

| | |
|---|---|
| Regions chosen for history matching | 9 regions based on streamline guide (Chapter 4) |
| Reservoir variables updated | $k_h$, $k_z$ and net:gross |
| Base reservoir model | Best history matched from geo-body types updating (PHM) |
| Dimension per well | 3D for 4 regions in first interval only<br>6D for 5 regions in both intervals |
| NA parameters | 3D: $n_i$=16, $n_s$=10, $n_r$=5, total=66<br>6D: $n_i$=128, $n_s$=18, $n_r$=9, total=524 |
| Production wells chosen | Oil and water rates |
| Parameterisation scheme | Local multi-variable (Chapter 4) |
| Pilot point information | Pilot points separation: ~500m<br>Kriging variogram range: ~1500m<br>The number of pilot points per master: 9 - 25 |

*Table 7.3: Main information for different history matching studies.*

After performing history matching for each individual well, the best 10 models for each region was chosen and combined in order to get the final 10 models for the reservoir as a whole.

The procedure for generation of 10 models was completely similar to Chapter 4 (Section 4.6.3 and Eq. 4.4). The production misfit values when reservoir parameters were combined ($LMV_{Final}$) was compared with individual history matching studies ($Locality_j$ ) as shown in Figure 7.16. This figure shows that after combination of parameters updated in localities ($LMV_{Final1}$) the reduction of misfit value is as good as the sum of misfit for localities.

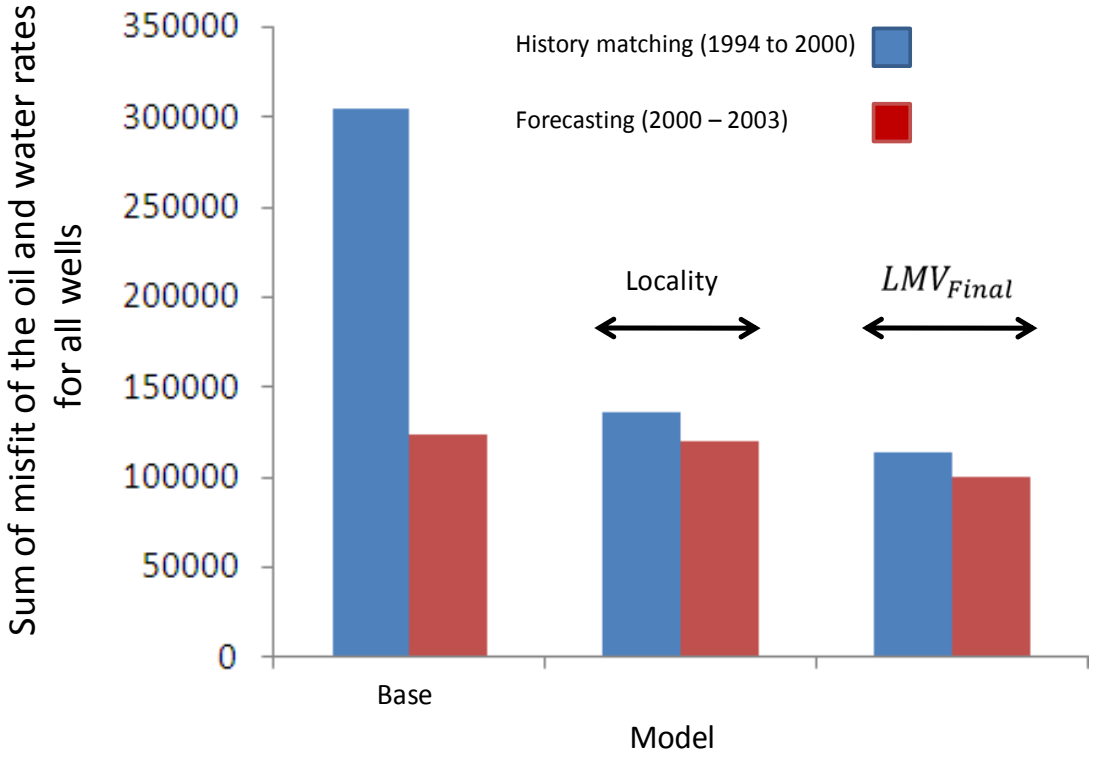


*Figure 7.16: Sum of misfit of the oil and water rates for all wells, comparing the model generated by combination of parameter in each locality ($LMV_{Final1}$) with sum of misfit value for localities (Eq. 6.2).*

Figure 7.17 shows the cross plot of misfit reduction for the final models and it is possible to compare the result to the previous study (Figure 7.13). It can be seen that for new result there was further reduction of production misfit values 25% to almost 62% in history matching period. However, in the forecasting period, the reduction of the misfit was quite similar to the previous geo-body type updating cases in Figure 7.13.

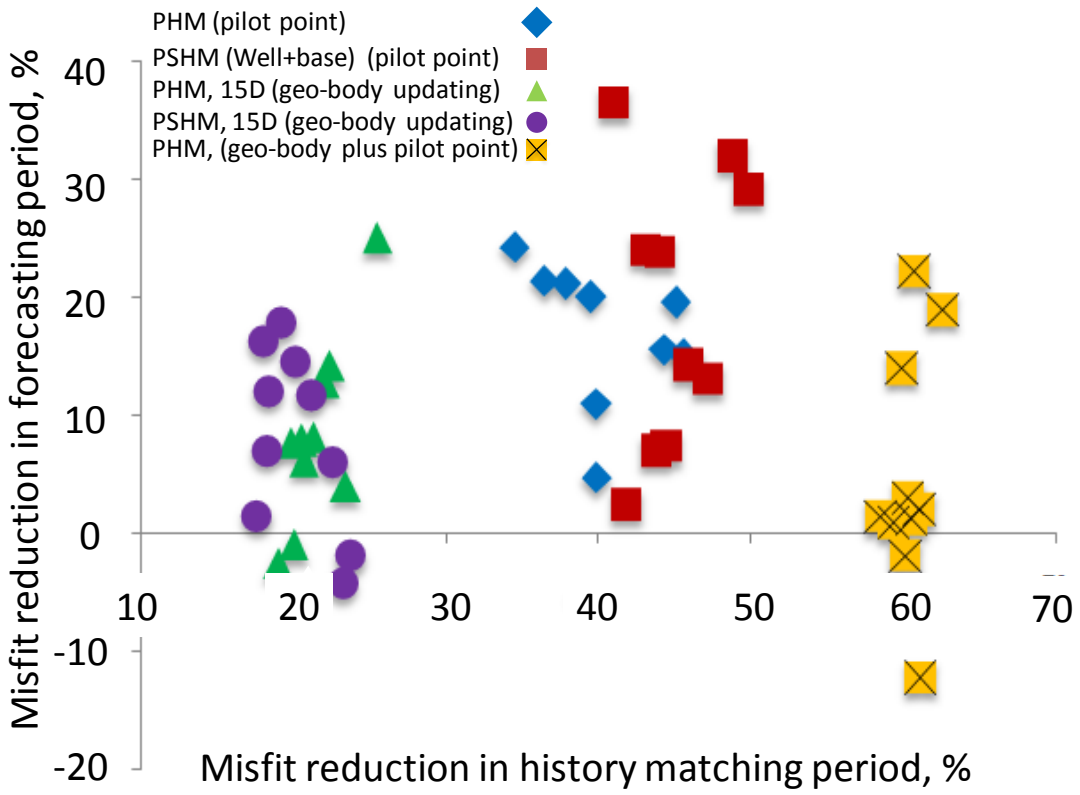


*Figure 7.17: Reduction of total production misfit in forecasting versus matching periods for different history matching studies.*

Figure 7.18 shows the water production misfit of all production wells after history matching using the pilot point method (pilot points were applied after geo-body types updating). According to this figure, a satisfactory result was achieved after local updating of the reservoir model for the 9 wells that were not improved sufficiently by the geo-body types updating scheme. There is only one well with an increase of misfit value after updating the reservoir and the reason is that the well was not included in the misfit during the history matching study. By looking at the well water production rates of the 9 wells for the best history matched model (Figure 7.19) the improvements can be seen.

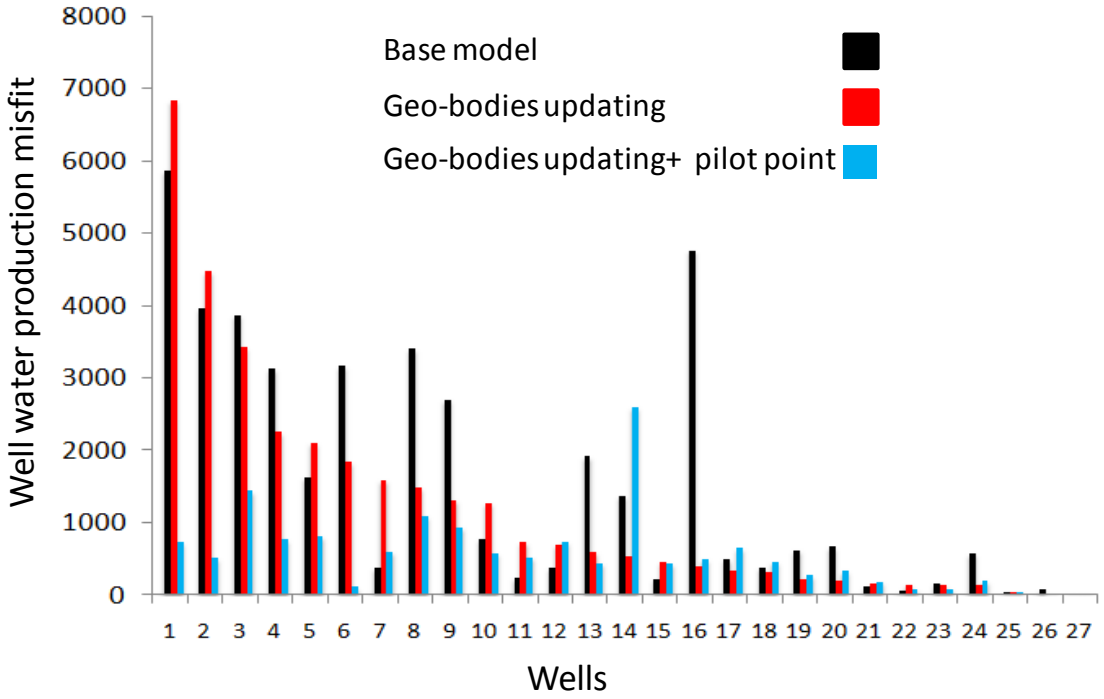


*Figure 7.18: Individual well water production misfits for the base model (black) and best history matched model after geo-body type updating (red) from 1994 to 2000.*

Figure 7.20a and 7.20b shows the average reservoir properties in the first and second reservoir intervals of the best models respectively. The multiplier of each variable converged to provide the result presented in this figure. It can be seen that after local history matching of the reservoir for wells 5 and 7 in the Interchannel geo-body types more shale was introduced by decreasing net:gross in the top interval while more sand was introduced by increasing net:gross in the lower interval. However the top interval was adjusted so that it contained very well connected shale due to the low vertical permeability set. More lateral sweep was observed by increasing the horizontal permeability. In the second interval, both horizontal and vertical permeability were increased but the magnitude of increase in the horizontal permeability was bigger. For Well 8 in the Interchannel geo-body type more sand as added in the first interval and again more lateral water displacement was observed from the aquifer by decreasing vertical permeability. On the other hand, in the second interval there is a small decrease of net:gross but it remains high. After local updating of the reservoir close to Well 8, both horizontal and vertical permeabilities decreased.

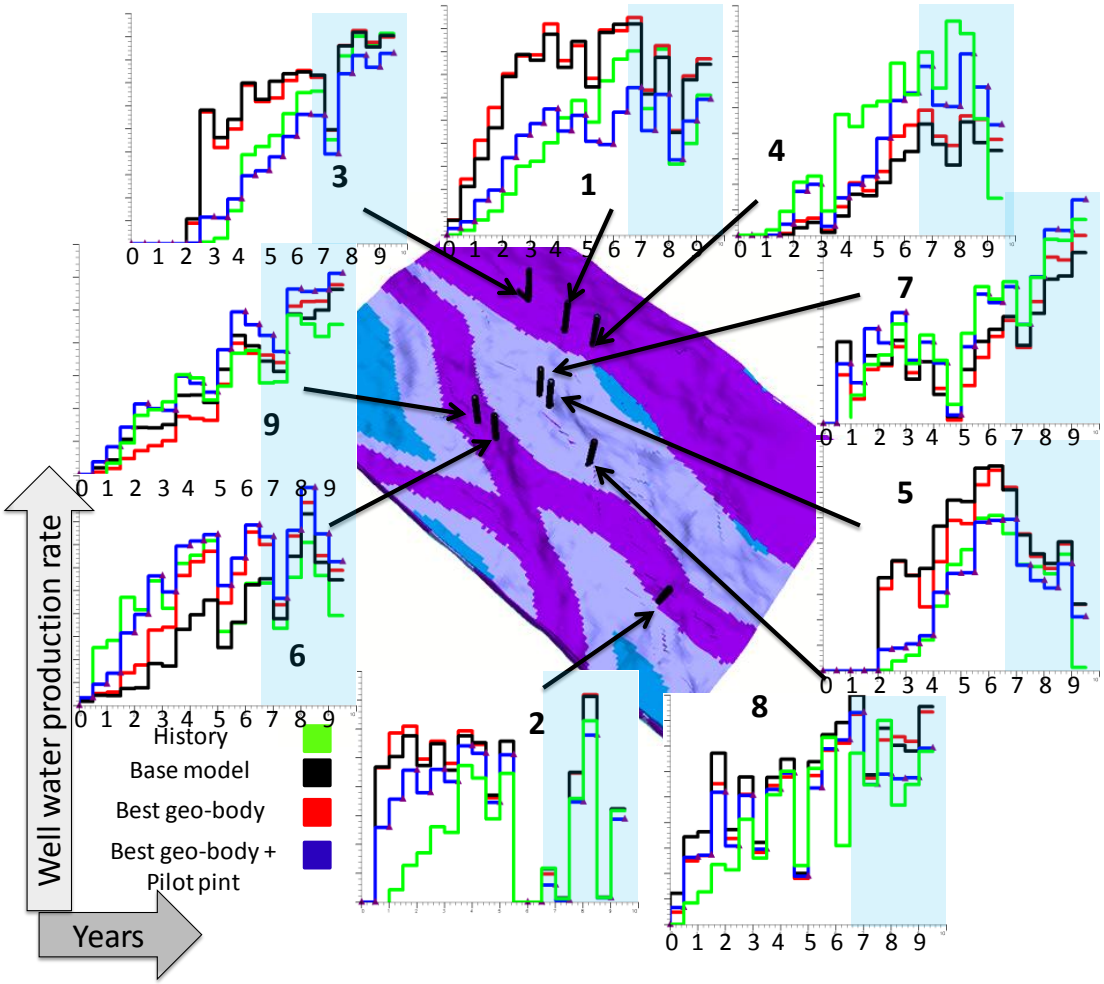


*Figure 7.19: Well water production rate for individual well, comparing the best history matched model after geo-body type updating and then further reservoir improvement via pilot point application.*

For wells 1, 3 and 4 in the eastern Channel Axis, the net:gross tended to one, therefore, such that more sand was added. For Well 3, the fluid displacement was the result of increased to more lateral flow by increasing horizontal permeability and decreasing vertical permeability. For Well 1, horizontal permeability was decreased and there was almost no change in vertical permeability. For Well 4 both permeabilities were increased close to the well.

In the second interval, there was a big change in the properties of the Channel Margin after local updating of the reservoir close to these three wells (1, 3 and 4). The Channel Margin in the second interval was made more sandy after increasing net:gross and there was a high value of permeabilities therefore the reservoir is very well connected for fluid displacement.

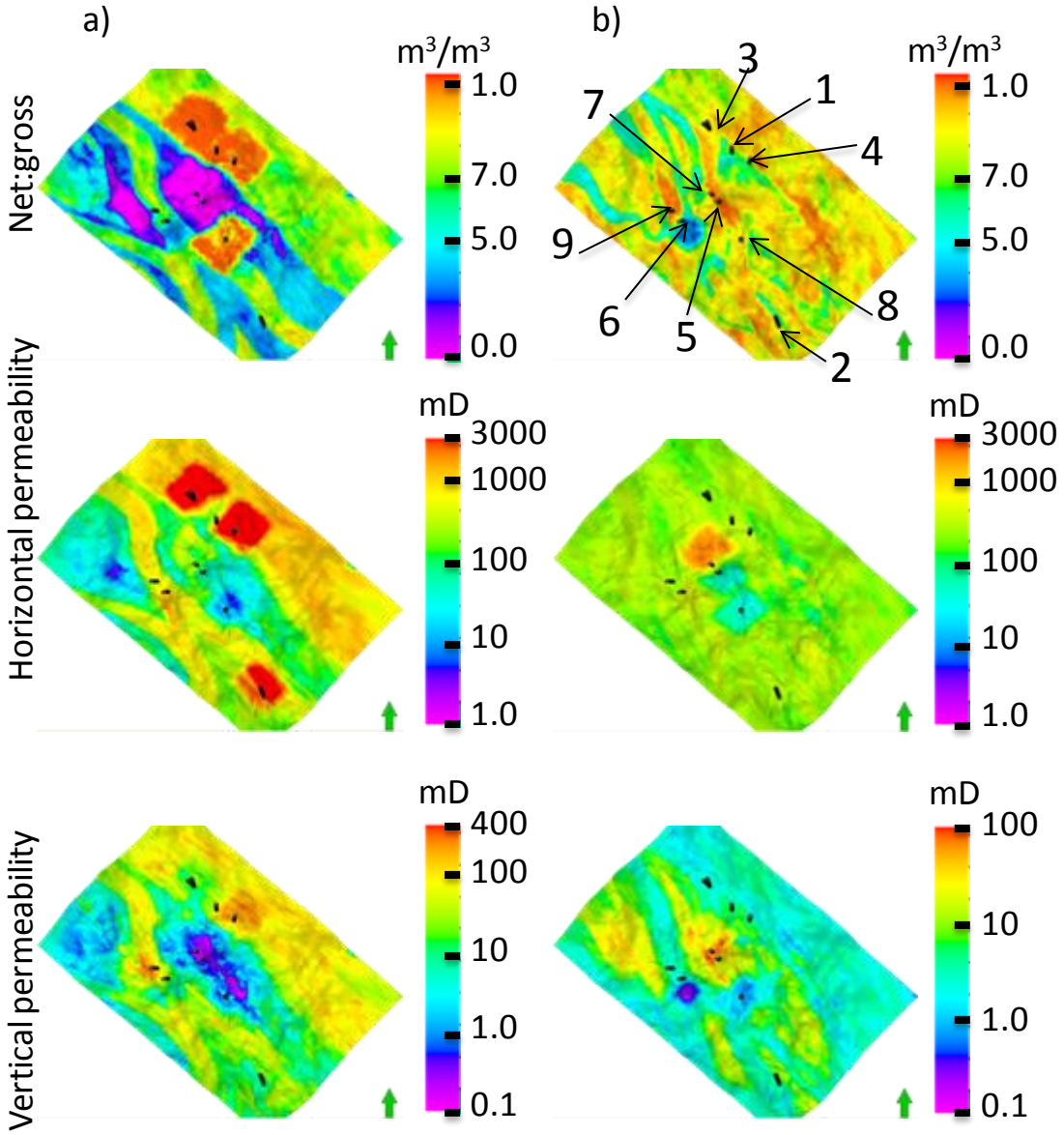


*Figure 7.20: Average reservoir properties of the best history matched model after integrating geo-body type updating and the pilot point method in a) first and b) second intervals. The numbers indicates the location of the well that study. The properties of base model were presented in Figures 7.11 and 7.12.*

In the western Channel Axis for Well 9, net:gross was decreased in the Interchannel geo-body type close to the well which was followed by decreasing horizontal permeability and increasing vertical permeability. Therefore it can be concluded that close to this well there was more shale in the Interchannel which was disconnected because of high vertical permeability. For Well 6 there was some change in Channel Axis by decreasing net:gross, increasing horizontal permeability and decreasing vertical permeability. These changes of the reservoir suggest locally more shaly region in the reservoir. Close to Well 2 there was no change in net:gross but horizontal permeability

were increased and vertical permeability decreased. The model predicted more lateral displacement close to this well after history matching.

In the second reservoir interval there were more sand in the Channel Axis close to Well 9 but for Well 6 there was a shaly region which was very well connected with a vertical barrier in that part of the reservoir. For Well 2 more sand was added in the Channel Axis with a little decrease of vertical permeability which makes the fluid displacement more laterally.

The change of reservoir parameter in this case can be compared to the similar history matching study, which was shown in Chapter 4 where we described how all of the reservoir properties were updated for individual wells using the pilot point method. The properties for the best reservoir model were plotted in Figure 7.21, which can be compared to Figure 7.20. The general comparison between these two figures is that different reservoir properties were obtained after history matching. Both cases show large increase of net:gross in some places in the reservoir. The drawback for both results is that 4D seismic data were missing for history matching of the field. By properly including time-lapse seismic data, more satisfactory results were observed as shown previously in Chapter 6 (Figure 6.20). This comparison confirms the importance of integrating 4D seismic data appropriately as useful constrain to history matching in order to find a better representative of the reservoir.

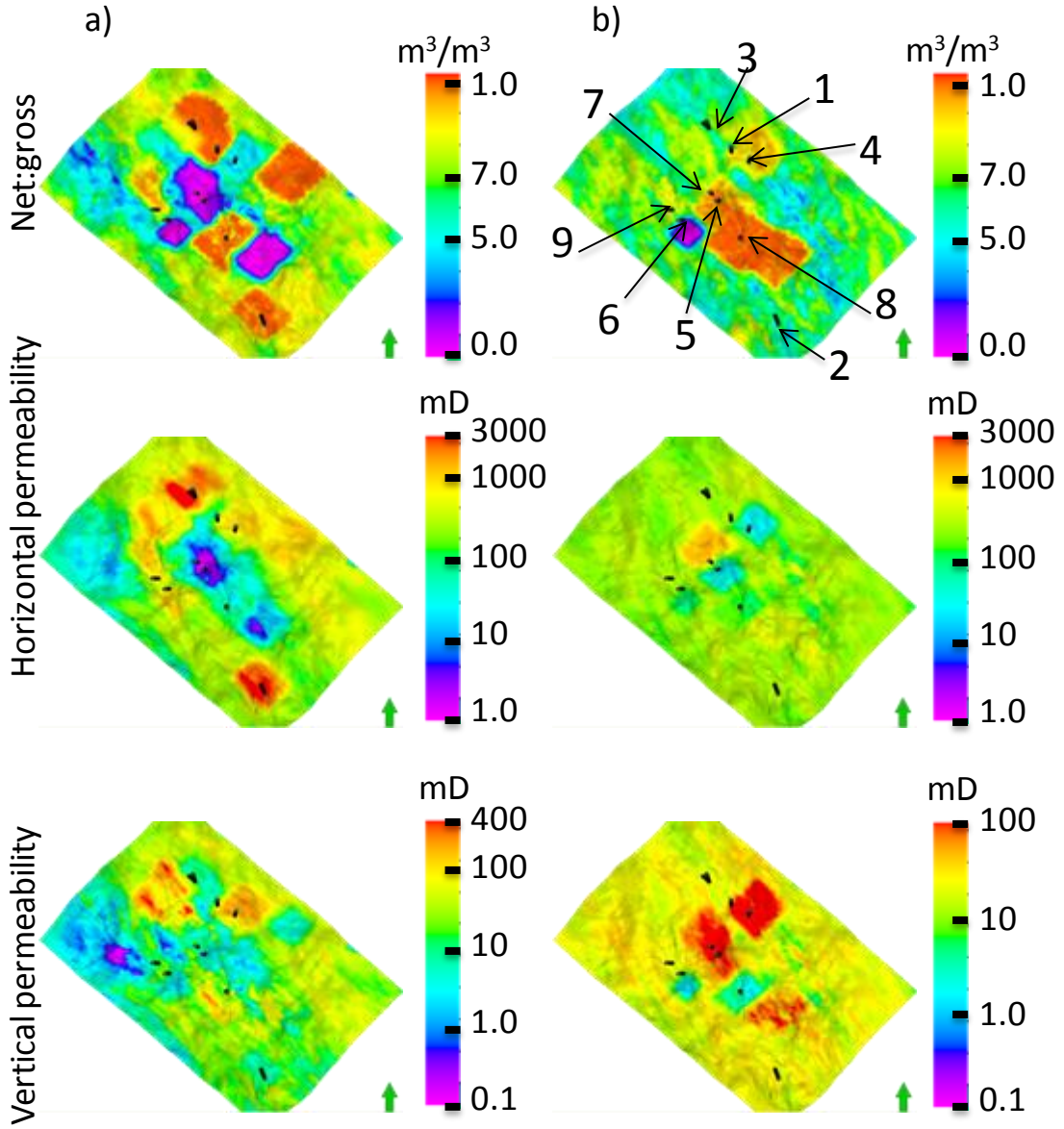


*Figure 7.21: Average reservoir properties of the best history matched model using production data only and pilot point as parameterization (Chapter 4) in a) first and b) second intervals. The numbers indicates the location of the well that study. The properties of base model were presented in Figures 7.11 and 7.12.*

### 7.7 Summary and discussion

In this chapter the idea of improving the reservoir was based on geo-body type updating schemes was tested. Instead of changing the reservoir in some localities based on the streamline guide concept of Chapters 4 and 6 the whole geo-body type was considered. The same reservoir parameters were considered for updating during the history matching process as in Chapter 4 and 6. Also various combinations of geo-body types

were considered at the same time in the reservoir in order to make sure that best change has been applied to the model.

The best result was achieved in production history matching when the reservoir updates were applied in separate intervals for all geo-body types except the Channel Margin which did not have significant influence on fluid displacement. On the other hand using time-lapse seismic data did not help to make improvements. The reservoir was updated laterally during the history matching process, including the non-signal region to search properly in the parameter space.

Because of unsatisfactory results obtained for some production wells after updating geo-bodies, local updating was performed close to those wells by using pilot point method and local multi-variable scheme guided by streamlines. After history matching a more satisfactory result was obtained by around 60% reduction of the misfit in the matching period and 20% in forecasting. However, the degree of change in the reservoir properties was higher than previous studies observed in Chapter 4 and Chapter 6.

As a summary, based on the study in this chapter, we observed that between the geo-body updating scheme (which changed parameters over large areas without considering their continuity) and pilot points with the Kriging method (which updated reservoir locally but preserved the continuity), the better parameterization scheme is the latter in this field. This is because for the geo-body updating scheme there are many regions in the reservoir where reservoir parameters were updated without any observed production or seismic constraint (such as the aquifer region which was out of reservoir section). In addition, the history matching problems for some wells were different in a geo-body type (Section 7.6). For example one well had the problem of over predicting water rates in the base reservoir model whereas one well under-predict water. Therefore, through updating reservoir parameters in geo-body scheme there were an average improvement of the misfit of the wells but not as sufficient as using pilot point method.

In this study we observed that, the streamline guided approach for selecting pilot points (Chapter 4, Section 4.2) and the LMV parameter updating scheme (Chapter 4, Section 4.3) were two important methods which need to be considered in addition to pilot points in order to get a reasonable reduction of misfit value in history matching studies.

# Chapter 8: SUMMARY, CONCLUSIONS AND RECOMENDATIONS

The general aim of this thesis was integration of 4D seismic data with traditional production data in order to properly update the simulation model using an appropriate automatic history matching workflow.

In general, all history matching problems need to be solved by using an appropriate strategy. This strategy is very case dependent. Therefore, the first step of this work was to investigate the reservoir to understand the field properly including the geology, the range of values for different reservoir properties, the uncertainty of various variables in the reservoir (such as, aquifer properties, location of faults, errors in production measurements and 4D seismic data etc). Also we needed to know which parameters have the most significant influence on fluid movement in the reservoir in order to predict the correct amount of fluid production.

In this study we did not possess full information about the reservoir. Therefore, a part of our understanding was based on information and recommendations from the field operator. According to our understanding of the reservoir, the aim of history matching was estimation of shale volume and distribution that ultimately controls water movement from the aquifer and injectors to the producers. On the other hand, an important part of this work was using 4D seismic data to constrain the flow model. 4D seismic signatures could be used for matching due to saturation change.

In this thesis we integrated various tools in an automatic framework in order to have a useful tool that may be applied to history matching of oil and gas fields. This framework consisted of streamline simulation, pilot point and Kriging, a petro-elastic model, an objective function and the neighbourhood algorithm. Obviously there are some drawbacks and limitations for each component that will be discussed later in Section 8.5. On the other hand, four studies were performed in order to make automatic history matching more amenable. We showed how we can use streamline simulation to optimally choose the updating region in the reservoir. We introduced three different updating schemes in order to appropriately combine history matching parameters. A normalization study was performed to make sure that observed and synthetic seismic

data are in the same scale of units and finally geo-body updating scheme was implemented as an alternative approach for parameterization of Nelson field. A lot of history matching studies performed in order to apply our proposed method on field data.

### 8.1 Streamline guided approach and parameter updating schemes

After choosing the appropriate property for updating, the second step in our strategy was selection of the regions to update in the reservoir. Updating the selected reservoir property in all simulation cells takes a very long time and therefore history matching is not practical. In this work we used streamlines in order to choose the regions to update in Nelson. Streamlines have the capability to show the path of water movement from the source to the producers. Our idea was that we select the regions to update in this path and try to update reservoir properties there. On the other hand by using streamlines it is also possible to exactly find the cells that were in the path but selecting those cells only. Obviously to use model derived streamlines we trust our base case reservoir model and the only unknown of history matching was the updating reservoir properties in the selected paths. In this thesis, as long as we believed that these paths were also uncertain, therefore, we chose a wide region involving most of the streamlines as regions to update in Nelson.

One important issue in history matching of Nelson was the way that parameters were updated. In this work we used the pilot points with Kriging as a geostatistical tool. This method was very useful in order to smoothly update the properties in the reservoir. After choosing the reservoir properties the regions for updating, we also addressed how the parameters can be combined efficiently while also getting reliable models after history matching. Considering different combinations of parameters for updating parameters also defined the dimension of the history matching problem. The dimension of the problem was an important factor for us because we used Neighbourhood Algorithm as an optimization algorithm and for the first search in the parameter space, it required as many models as 2 to the power of the history matching dimension. In this work we introduced three different parameter updating schemes called GSV, RMV and LMV. In summary, the GSV is suitable for cases where the effect of properties chosen for updating are independent, such as fault transmissibilities, aquifer properties etc. The RMV is suitable for the cases where there is strong dependency between properties chosen for updating. Also there were wells very close together with strong interaction.

In that case, updating the reservoir parameters by regions influenced all wells. The LMV method is suitable for cases where there are local dependencies between the properties selected for updating but the regions to update are independent. We tested all methods for a small history matching problem considering 25% of production wells. In terms of saving CPU time and the level of satisfaction of the history match and forecast that was obtained, the LMV method was the best scheme. Thus in our case, the properties selected for updating were dependent and we chose the regions in order to have maximum independence. We also compared the streamline guide for parameter updating with a traditional approach using the cells symmetrically in the vicinity of the well. We observed that the streamline case provided us with better results.

We then applied the LMV method to a bigger problem that then included 50% of production wells (represents 84% of the total misfit of the oil and water for all 27 production wells) and we obtained satisfactory results. However, because there is a phased development for the reservoir, we consider that we should use the LMV method with some caution. For example, if a new production well is completed in the vicinity of an older one it may have some effect on the path of the streamlines. Therefore, we may need to change the regions selected for updating at different time steps. We recommend the RMV method for the cases where there is a high density of production wells in a region.

## 8.2 Normalization of 4D seismic data

For integrating time-lapse seismic data we introduced the concept of normalization. The main reason for this study was that there were differences between the unit of measurement for synthetic and observed seismic data. The synthetic seismic used in this study was p-wave elastic impedance with the unit of g/cc*km/s. However, the observed data consisted of phase shifted amplitudes which is similar to elastic impedance and the units were unknown. Two methods were considered for the normalization study; Map derived and Well derived. The former was based on using impedance data for all simulation cells and the latter was based on using the information at the location of vertical wells with a good water cut match. The idea of normalization was to consider a regression equation derived from the cross-plot of the synthetic and observed seismic data by using either well or map information. From the Map derived case we observed a cross-plot of low correlation and for the Well derived cases there

were sparse points. Alternative subsets of the observed and predicted data were used. One idea was based on using data in the reservoir section only, another focussed on two specific parts of the reservoir and the last idea used the repeatability map (NRMS) in order to filter the observed seismic data. By considering 30% as maximum non-repeatability we filtered out 10% of observed data.

Various maps were produced after normalization. The analysis of the maps was based on qualitative comparison between the 4D signature in the reservoir and production activity in various parts of the field. For example we considered a low ranking for the normalized map that showed a 4D signature in the regions where there were no production wells or water displacement was unlikely. Generally, the normalized maps, derived after filtering the observed data were more acceptable in terms of comparing production activity and 4D signature. However it was not easy to reject completely any of the normalized datasets at this stage. Therefore, we decided to use all of them in history matching with the exception of two cases. These were the cases where the reservoir section was considered for the study and where we chose two specific parts of the reservoir for normalization.

The problem with focusing on the reservoir section was that the synthetic seismic data was derived from the base reservoir model before history matching. The synthetic seismic data contained false predictions due to errors in the model. Therefore, we could not expect to derive an accurate normalization equation. In the second study, even by using the best history matched model, the problem was that the best model was constrained by production data only. Therefore, there was no guarantee of predicting the right synthetic seismic prediction throughout the reservoir.

In the second exception, focusing on just two regions, the point was that there was no guarantee that the selected regions chosen for normalization was the best choice for study.

In addition to the ideas used in this work we also have some recommendations which can be used in addition to the normalization study. In this case the calibration of 4D seismic could be performed at the wells. For calibration we need to have information from log data such as sonic logs. We can then calculate the impedance data at the location of the well. Then it is possible to calibrate observed data throughout the

reservoir but this is no easy task. Another recommendation is that instead of deriving one single regression equation we can derive different equations for different regions in the reservoir.

Some additional ideas for a normalization study are:

- Consider different regression equations instead of one equation for different regions in the reservoir.
- Integrate the normalization parameters into the history matching and try to find the best parameters.
- Select some regions in the reservoir where we have true 4D signature with a good match of model and observation and then derive the regression equation on that region.

### 8.3 Production and seismic history matching

After preparing observed seismic data we integrated them into history matching of Nelson. The constraint of the production and seismic history matching (PSHM) studies in Chapter 6 were exactly the same as previous history matching study using production data only (PHM case in Chapter 4) and we just added 4D seismic data as a constraint. The results show that for all Map derived cases (including NRMS filtered) we obtained better result compared to the production history matching case. With the Well derived normalization studies, the improvement was not as good as the PHM case, except for the Well+base case. The forecasting ability also was improved for the Map derived and Well+base cases more than the PHM study. The lowest misfit for both matching and forecasting periods were obtained from Well+base and Map+best+NRMS. In the all PSHM cases in terms of seismic prediction, the best history matched model compared to the observed seismic data reasonably well. Using production data only gave a poor seismic prediction and predict wrongly some 4D signature in the reservoir. Whereas in seismic history matching cases, the best model did not predict those unwanted signatures.

The history matching result was more satisfactory when we used the normalized map that had a better consistency with production activity as qualitatively observed in Chapter 5. Also the result emphasized the importance of choosing the right 4D seismic data in order to get a reasonable result.

In terms of updating the reservoir we got the best history matched model by increasing the sand content in the Channel Axis by increasing net:gross and permeabilities. The Interchannel was changed to be more shaly after history matching. Comparing the best PSHM model with best PHM model we got different models. There was greater continuity of shale for PSHM cases compare to PHM.

As a general recommendation for this work we propose that in order to save time when integrating all normalized 4D maps in the history matching study, we can revisit the normalization procedure and introduce a more quantitative tool to link the 4D signature to production activity in different parts of the reservoir. In such a case we can only choose the best normalized map and use that in the study. However another important issue in normalization is the concept of signal/noise ratio of seismic data which could have a strong influence on the study and we need to have a better understanding of that.

### 8.4 History matching by updating geo-body types

The last part of this study was updating the reservoir in a wider region based on geo-body types. Using the streamline guide approach and pilot points with Kriging we obtained some updates to the reservoir which were local within geo-bodies. For example there was a big region of Channel Axis in the north of the field and the selected region to update was only a part of the channel. The idea for this chapter was that instead of updating a part of a geo-body type we updated all parameters everywhere. Similar to previous studies, we had the problem of limited CPU time, made worse by increasing the number of history matching unknowns. Thus, we started by investigating the importance of updating reservoir properties in each individual geo-body type. Then we considered different combinations of geo-body types in the history matching study and the best history matching result was observed by considering all geo-body types except the Channel Margin, and each was treated separately for the reservoir intervals. The history matching was performed first by using production data only and then both production and the best preferred normalized 4D seismic data (from Chapter 6) used in the history matching study. The history matching result observed here was not as good as previous results especially for PSHM (geo-body type updating) case. The main reason why we could not get a good result is that production wells did not all require the same modification to the model. For example some wells underpredicted water rates

while neighbours did the opposite. However in history matching all production data was included in the objective function. Therefore, trying to match some wells made others worse. In PSHM geo-body type updating study there was another issue. Updating net:gross throughout the geo-body type, including the part where there was no 4D signature observed, introduced false predicted signature.

As an alternative case, we also combined the geo-body type updating schemes with the pilot points with Kriging approach in order to further modify the reservoir for those wells that were not improved by geo-body types updating. We only applied the method using production data only. The result showed that, the reduction of misfit is higher than all previous studies in the matching period. However in forecasting, the improvement was the same as PHM (Chapter 4) case and lower than PSHM (Well+base) case. In terms of the degree of modification to the reservoir we increased the amount of sand and shale in the Channel Axis and Interchannel for the combined geo-body plus pilot point case.

As general conclusions of this thesis it can be said that the best strategy found for history matching of the field was to use streamlines to help us to choose regions for updating. Then a proper normalization of time-lapse seismic data filtering by NRMS map makes 4D data ready for integration with production history of the wells. In this case the seismic and production history matching improved the misfit of sum of oil and water production rate for the whole wells by 50% in matching period and 30% in forecasting period. The properties of the best history matched model were also satisfied based on the geological information which was available for the field.

### 8.5 Limitations of automatic history matching method used in this study

Generally the methods discussed and applied in this thesis could be applicable in history matching of any oil or gas field; however, there are some limitations that need to be considered.

The fluid flow simulation method used in this thesis was based on the streamlines method (Schlumberger Geoquest Manual, 2007). The benefit of this approach is faster calculations. However, the maximum benefit from streamlines is obtained in fields with low pressure variation through the life of production and where pressure stays above

bubble point. In previous versions of Frontsim it was important that there were only two phases (oil and water) in the reservoir but in the newest version, the software provider expressed that this software can be use for three phase flow too. As advice, we recommend that the accuracy of simulation output needs to be checked against any potential speed up for three phase flow cases before starting a history matching study. Apart from that our workflow works with finite difference simulator (Eclipse) as well.

The pilot point method with Kriging was used in this study. This parameterization approach needs to be used with care when the reservoir properties are highly heterogeneous. In this case the number of pilot points, their location, values of parameter multipliers and the semi-variogram used in Kriging should be defined carefully. Also, for cases where there are different reservoir intervals (or perhaps rock types) with strong heterogeneity, it is very important to use the Kriging method in a suitable reservoir interval or within facies.

The petro-elastic model is an important part of a seismic history matching study. Usually, for a given field, empirical equations are obtained in order to calculate fluid and rock bulk moduli. However, the derived equations are based on lab data and therefore the uncertainty of those equations needs to be quantified. On the other hand Gassmann's equation, which was used here for fluid substitution, is based on some assumptions such as the porous medium contains only one type of solid with an homogenous mineral and the pore space is statistically isotropic. These assumptions could be invalid in some fields and therefore may result in large errors in the synthetic seismic calculation (e.g. fractured reservoirs).

The objective function that was used in this study was based on the estimation of uncorrelated data errors for both production and seismic data. However this estimation needs to be quantified for each history matching case. If production data is measured with higher frequency, the chance of data error correlation will be increased. Also there is the possibility that there is correlation of seismic noise which should be investigated. This is more likely to be important if comparisons of observations and predictions are made at the seismic measurement scale. In such a case we need to calculate the covariance matrix and it's inverse and used that in the objective function. Of course, first we need to identify the noise and separate it from the signal. It is worth mentioning that the covariance matrix could be large and therefore it will increase the CPU time for

calculation of misfit function. Soldo (2005) found that partial sampling of the data produced a useful fast estimation and others (Aanonsen et al 2003; Gosselin et al 2003; Liu 2005) have used templates to estimate covariance using standard models.

The neighbourhood algorithm that was used as the optimization method in this study is a powerful tool for finding the global minima of inverse problems. One important limitation of this algorithm is that for a high dimensional problem we need to run a lot of simulations in order to properly search the parameter space. Otherwise, the chance of finding the minima decreases. The high dimensionality is something which could be a problem of a lot of fields. However, in the parameter updating scheme study we used some techniques in order to overcome to this problem. As a conclusion we advise that for a high dimensional history matching problem, if different parameter updating schemes do not work, NA needs to be compared, or perhaps replaced, with other optimization methods (discussed in Chapter 1).

In this study we showed how we can identify the best regions in the reservoir for updating using streamlines as a guide. We found this method was very useful in the Nelson field though there could be some fields where the approach requires more care. One case might be where we choose to update near a producer and then a new well is drilled during the history matching period. In this case the density of streamlines will be changed because of the impact of the new well. We would therefore need to history match in stages, perhaps focusing on the initial well configuration and then making further modifications once the new well is in place. We note though that this streamlines based approach can be used in any field where streamline simulation is possible. It is not limited to the same conditions needed to get speed up from streamlines such as relatively stable pressure changes.

Another case where the approach may require care is in a mature field with high density of wells. Finding the location to apply changes may be problematic. On the one hand, this case may be easier to history match if the well separation is less than the correlation length of the permeability field. As such, we propose that smaller regions be considered for updating (i.e. single pilot points with appropriate Kriging parameters, including the variogram range). Then, the dimensionality of the history matching problem will increase. An alternative inversion routine would be preferable and so a Genetic Algorithm may be more appropriate.

In this study we showed that normalizing 4D seismic signatures is essential for quantifying misfits in history matching. This method was based on well data with a good water cut match and map data. In cases where the wells were not matched at all, we may have problem using this technique. Similarly, the method would be improved with pressure data. We used a liner regression equation for deriving the normalization equation. This linear equation may not work if the petro-elastic model has a high uncertainty (and therefore synthetic data would be wrong). On the other hand if 4D seismic data has a high ratio of noise/signal it would be difficult to simply normalize data.

## 8.6 Conclusions

***For streamline guided and parameter updating scheme studies***

1. The well vicinity approach for updating can be used to reduce the misfit in history matching but forecasts are not so good.
2. By using streamlines as a guide to identify the optimal region to update reduces the misfit in the history and forecast periods.
3. Overall, the better the match to history, the better the forecast, indicating a distinct correlation.
4. Geological concepts are better preserved using the streamline guide rather than the well vicinity approach.
5. The streamline guided approach works very well in a local multi-variable method.
6. Other updating schemas (GSV and RMV) could be considered for history matching studies.

***For normalization study***

1. Normalization of observed seismic data needs to be performed in order to prepare data for integration into the history matching study.
2. The Map derived and Well derived methods can be used for normalizing observed data by predicting seismic signatures in the region that we expected to see seismic signal. However the normalized maps need to be used in history matching study in order to choose the best map.

3. Using NRMS was very useful in order to filter out the observed data that had a high degree of uncertainty. The regression equation and normalized maps were more acceptable from this study.
4. The normalization study could be influenced by signal/noise ratio in the reservoir.
5. Normalization or calibration needs to be applied for any observed 4D impedance data that was not generated by a full inversion process.
6. For other field applications, for successful normalization, we need to have quantitative information about different uncertainties in the petro-elastic model and observed seismic data.

***For automatic production and seismic history matching study***

1. Integrating appropriate time-lapse data with production data helped history matching of Nelson and we got a better forecast.
2. The normalized map, filtered by NRMS, was a better constraint for the history matching study and the production and seismic misfit value was reduced further in this case.
3. Using production data alone for history matching cannot capture properly the fluid movement far from the wells so the matched model predicts some unwanted 4D signature in the reservoir.
4. Using production data only resulted in a different updated model compared to using both seismic and production data in history matching. This would be important for the future plan of field development for choosing the best location for new wells in the reservoir.

***For geo-body updating study***

1. The history matching of Nelson based on geo-body type updating did not as good a result as previous production and seismic history matching cases.
2. There is no guarantee of finding a reasonable history matching by updating the reservoir in the regions where there is no production and 4D seismic evidence.
3. Combination of geo-body type updating scheme and pilot point method improved the history matching result as good as previous seismic and production history matching using pilot point only.

# Appendix A

## A.1 Simple Kriging

Figure A1.1 shows the concept of simple Kriging in a 3 dimensional case in order to find an appropriate value of reservoir property ($X$) at location $u_0$ as a function of known properties in other four locations. This function between the points will be defined as a weighted linear equation as shown in Eq. A1.1. The index $i$ refers to a particular location in the reservoir which is representative of the centre of a 3-D grid. $u_i$ is the vector for $i$ location.

$$X^*(u) = m(u) + \sum_{i=1}^{n} w_i(X(u_i) - m(u_i)) \quad \text{(A1.1)}$$

$m$ represents the expected mean value of variable $X$ and is defined by the user. $n$ is the number of data points and $w_i$ is the weighting function between the points.

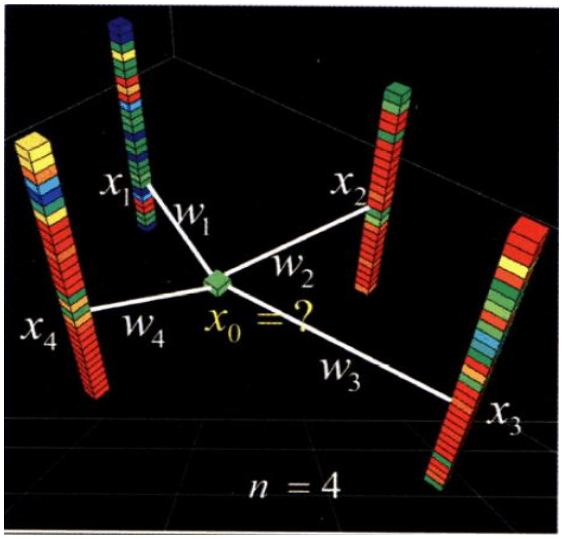


*Figure A1.1: Simple Kriging in 3D (Doyen 2007).*

The only unknowns are the weighting terms. The goal is to determine $w_i$ that minimize the variance of the estimator.

$$\sigma_E^2(u) = Var\{X^*(u) - X(u)\} \quad \text{(A1.2)}$$

Under this constraint that $E\{X^*(u) - X(u)\} = 0$. The $X(u)$ is decomposed into residual, $R(u)$, and mean value, $X(u) = R(u) + m(u)$. Under this circumstance that $X(u)$ is correlated random variable the estimation error $X^*(u) - X(u)$ is a linear

combination of random variables representing residuals at the data point, $u_i$, and the estimation point, $u$:

$$X^*(u) - X(u) = \sum_{i=1}^{n} w_i R(u_i) - R(u) = R^*(u) - R(u) \quad \text{(A1.3)}$$

Using the rule for variance of linear combination of random variables:

$$Var\{X^*(u) - X(u)\} = Var\{R^*(u) - R(u)\} \quad \text{(A1.4)}$$

$$\sigma_E^2(u) = Var\{R^*(u)\} + Var\{R(u)\} - 2Cov\{R^*(u), R(u)\} \quad \text{(A1.5)}$$

Therefore:

$$\sigma_E^2(u) = \sum_{i=1}^{n} \sum_{j=1}^{n} w_i w_j C_R(u_i - u_j) + C_R(0) - 2\sum_{i=1}^{n} w_i C_R(u_i - u) \quad \text{(A1.6)}$$

where $C_R$ is the covariance of residuals. To minimize the error variance, the derivative of Eq. A1.6 is taken with respect to each of the Kriging weights and each derivative is set to zero to make the following system of equations.

$$\sum_{j=1}^{n} w_i C_R(u_i - u_j) = C_R(u_i - u) \qquad i = 1, \dots, n \quad \text{(A1.7)}$$

Because the mean is constant, the covariance for $X(u)$ is the same as residual component,$C = C_R$, so that the above equation can be written as:

$$\sum_{j=1}^{n} w_i C(u_i - u_j) = C(u_i - u) \qquad i = 1, \dots, n \quad \text{(A1.8)}$$

The weights will be obtained by solving a system of equations called the *Kriging system* as shown in Eq. A1.8. Figure A1.2 shows a Kriging system where we have three points in the example. The $C_{ij}$ represents the spatial covariance of distance vectors $h_{ij}$ between data points $i$ and $j$ and the diagonal elements of the matrix are all equal to the variance of $x$ ($\sigma_x^2 = \sigma^2$).

$$C_{ij} = C(h_{ij}) = C(u_i - u_j) \quad \text{(A1.9)}$$

On the right hand side of the *Kriging system* (Figure A1.2) there is a matrix which is for spatial covariance of the distance vector between the three data points and the position $u_o$, where we want to calculate the property. The covariance value will be calculated from the curve represented in Figure A1.2 therefore for each $h_{ij}$ there is a value for $C_{ij}$. This curve would be representative for the whole simulation model and it is calculated for various reservoir properties that were used as variables in the history matching study. The known parameters in Eq. A1.1 (such as $x_1$, $x_2$, $x_3$ in Figure A1.2) would be the location of the pilot points in the reservoir. The number of pilot points defines the dimension of the matrix in Figure A1.2. More details about this function can be found in GSLIB (Deutsch and Journel 1998). From the *Kriging system* we can calculate the weighting matrix with calculation of inversion for covariance matrix.

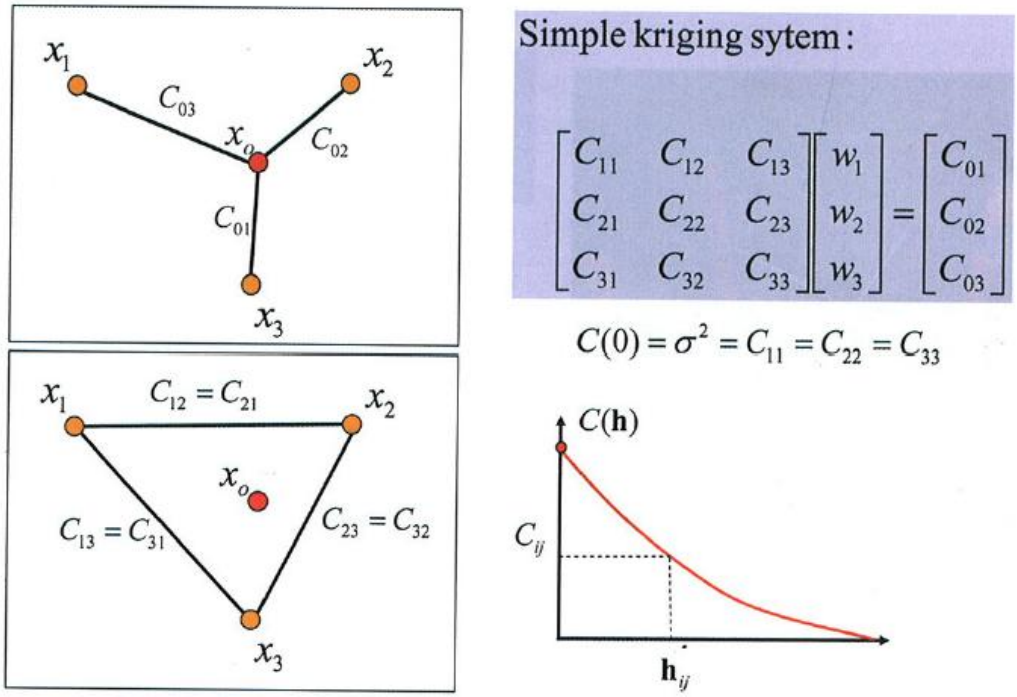


*Figure A1.2: Definition of simple Kriging system (Doyen 2007).*

**A.2 Streamline simulation**

The simulator uses the streamline tracing concept to generate the streamtubes (Schlumberger Geoquest Manual, 2007). In this process we consider the starting point, the streamline path and the stopping criteria for the streamlines. There are three properties which need to be specified to define the streamlines which are Time Of Flight (TOF), flow rate and a pointer which relates the streamline to a unique cell in the underlying numerical grid. The first two properties are defined in points along the streamline and the third property is for each segment between the points defining the

streamline. These pointers are important for picking up relevant information defined on the grid blocks. Figure A2.1 shows an example of the points on the streamline and the segments between the points.

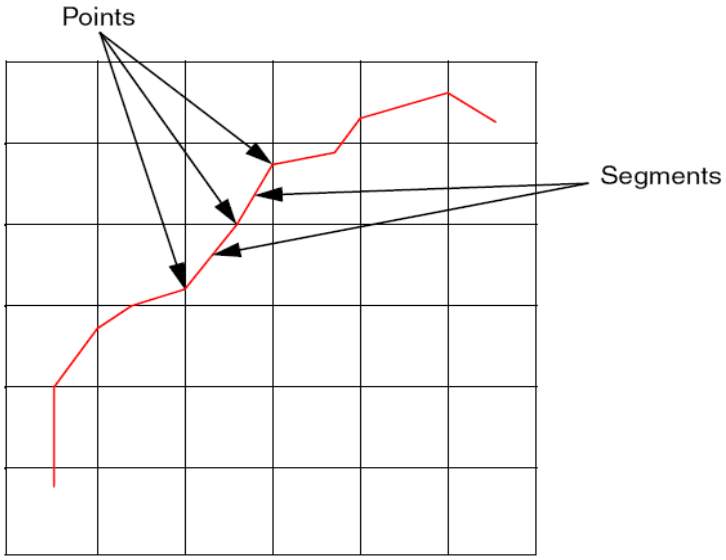


*Figure A2.1: Streamline tracing through grid, showing points and segments between the points (Schlumberger Geoquest Manual, 2007).*

The streamline is based on the streamtube concept which means that instead of computing the fluid flow equations in 3 dimensions (3D) we compute them through the streamtube in a 1D domain. In streamline simulation the equations are based on a finite difference Implicit Pressure and an Explicit Saturation (IMPES) formulation so that the pressure solution is separated from the equations solving the fluid movement (Schlumberger Geoquest Manual, 2007).

As illustrated in Figure A2.2 the streamline starts from an initial model with defined pressure and saturation from initialization of the reservoir. Then the pressure equation will be solved for the 3D grids which ultimately provides us with the Darcy velocity in the reservoir. Streamlines are calculated in the model and saturation is mapped onto them. After calculation of the saturation equation on each streamline (and solving gravity segregation if necessary), the saturation will be mapped from streamlines back to the grid cells and based on the new saturation, the pressure equation will be solved for next time step.

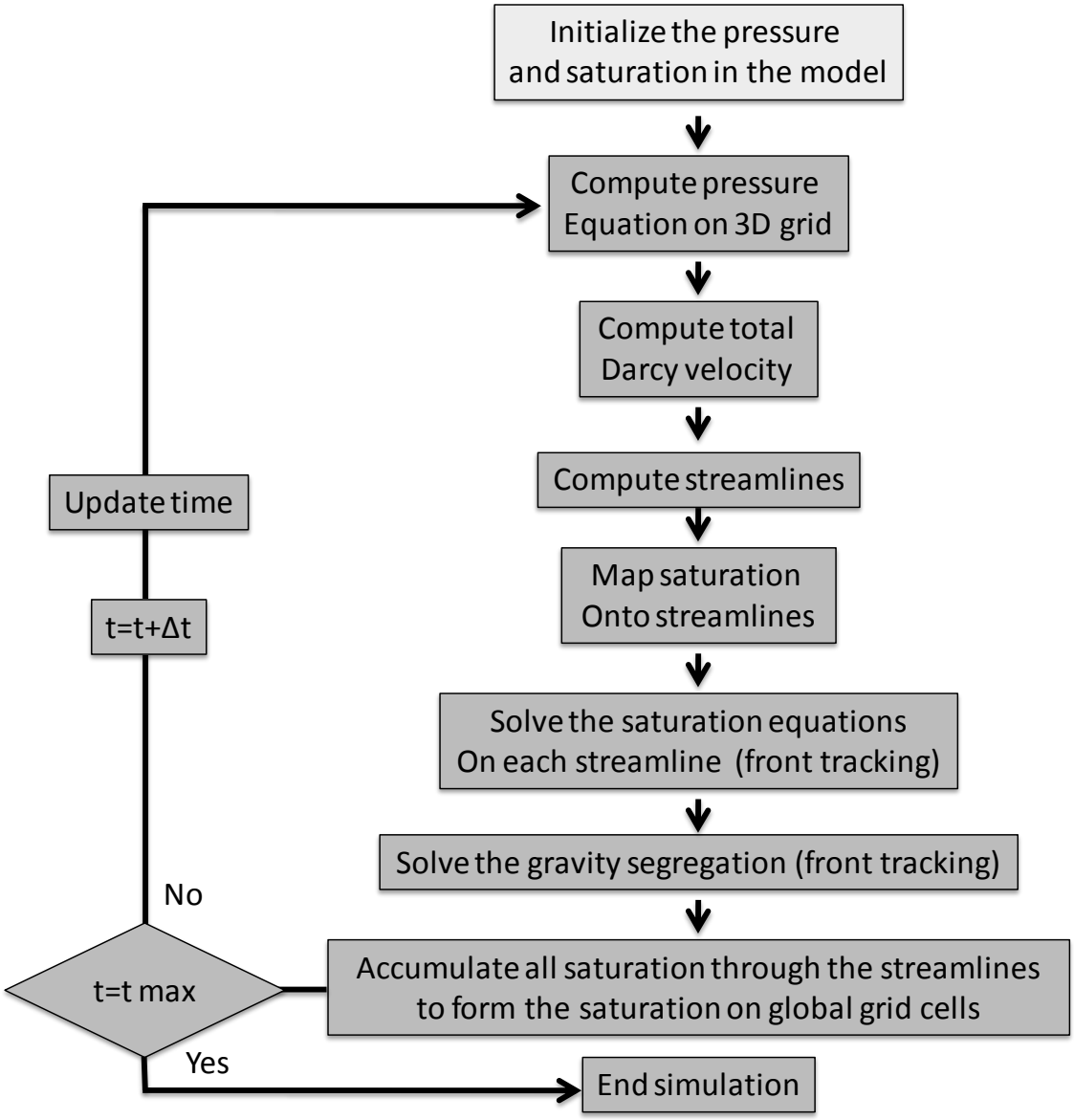


*Figure A2.2: Algorithm for streamline simulation.*

The streamline can be thought as a line in the centre of streamtubes and the pore volume in any segments will be calculated from the TOF and flow rate. As an example, in the segment $i$ the pore volume is:

$$PV_i = dTOF_i \times Q_i \tag{A2.1}$$

Where the $dTOF$ is the time of flight in the segment and $Q$ is the total flow rate into segment $i$ in Figure A2.1. The algorithm used to trace the streamline through a single cell is the Pollock method (Pollock 1988). This method is based on some assumptions such as uniform flow rates on each cell face, linear variation of velocity field in

different coordinates and orthogonal grids and the total Darcy velocity will be used to calculate the total flow rate in and out of each cell.

The full details of calculating the inference point and exit point can be found in the references (Pollock 1988) but the general information we need to know here is that the starting point for streamlines is a point in a source or sink (injector or producer position) or in a cell that was not visited by computed streamlines generated in previous time steps. The stopping point for a streamline is where streamlines reach a source or sink or when the flow rate is less than some defined minimum. In our work we adjust the simulator to consider all cells for calculating streamlines.

# Appendix B

**Overview:**

As discussed in Chapter 2, there are two important elements in the streamline simulator. These are the controls on the density of generated streamlines in the reservoir and also the length of time step over which the reservoir pressure is fixed before it needs to be recalculated in order to update the pressure profile in the reservoir. There is a direct relationship between the CPU usage and number of streamtubes and number of times pressure recalculate in the reservoir (Schlumberger Geoqueat Manual (2007).

These two parameter need to be tuned in each specific field in order to have a reasonable accuracy while simulating the model in a short period of time. The content of this appendix is about investigating of those two parameters.

## B.1 Streamline density number (SLD)

The streamline density number is an important parameter in streamline simulator especially when the reservoir field is very big with a lot of simulation cells. By adjusting a reasonable value for this parameter it is possible to save a lot of CPU time in order to make the simulation faster by keeping the accuracy of calculations. Figure B.1 shows an example of streamtubes in Nelson field in a specific time step for different values of SLD. In this study 5 different SLD numbers were considered for simulation of the base reservoir model (supplied by operator). The maximum SLD considered was 1 followed by 0.5, 0.1, 0.05 and 0.005 as shown in Figure B.1.

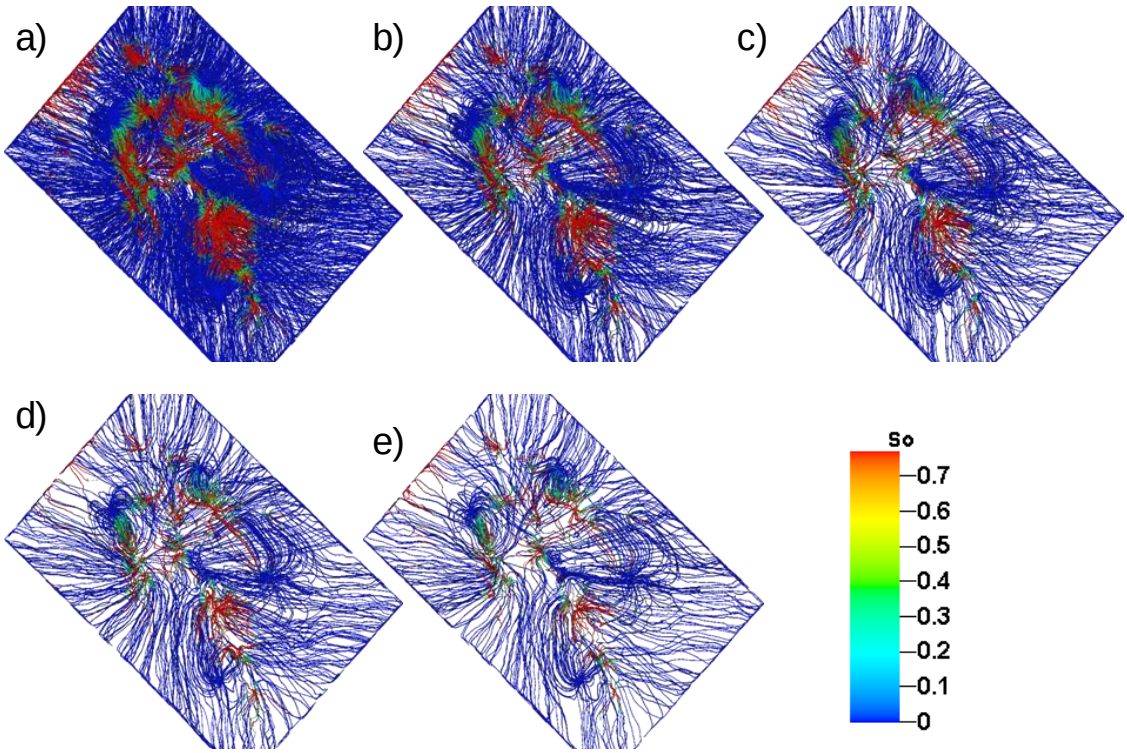


*Figure B.1: The density of streamlines in the reservoir for different value of SLD, a) 1, b) 0.5, c) 0.1, d) 0.05 and e) 0.005.Note that for better visualisation this figure shows a fraction of streamlines (10% for all cases).*

Biannual production history data (total liquid rates) was used as the constraint of wells in the simulation model. For each SLD case a simulation was performed and the sum of misfits for oil and water production rates of all production wells were calculated using Eq 2.29 (considering the production part only). The same reservoir model was also used in the Eclipse simulator and the misfit calculate for that case. Figure B.2 shows the misfit value for each case plotted versus the CPU time. It can be seen that by increasing SLD the accuracy of streamline simulator to capture the flow behaviour in the reservoir increases and therefore a lower misfit value will be observed for the wells. It seems that there was a critical value of SLD such that for SLD greater than 0.05 there was no change in the misfit value. It can be concluded, therefore, that increasing SLD above 0.05 does not make any significant change in the production rates at the wells. It was also interesting that the misfit value for the all streamline cases is lower than the Eclipse case even for a low value of SLD.

In Figure B.3 it can be seen that except SLD=0.005 the other cases show the same trend for oil production of the field and they are closer to the field water history of Nelson.

A Set of comparisons were performed between the output of Eclipse and streamline simulator. Figure B.4 shows that the streamline simulator better predicts the field oil production rate compared to Eclipse.

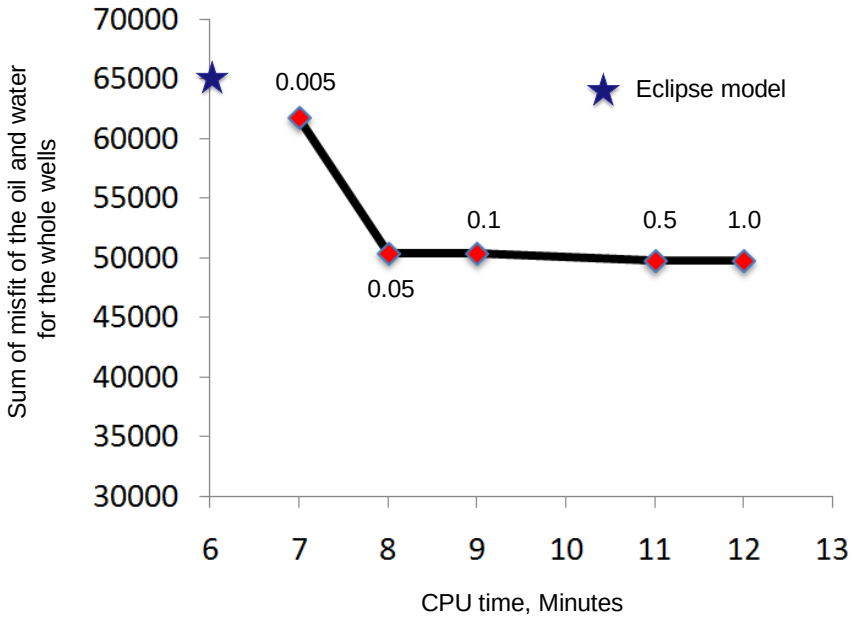


*Figure B.2: The sum of misfit of the oil and water for all wells versus CPT time. The number in the line shows the SLD belongs to each case.*

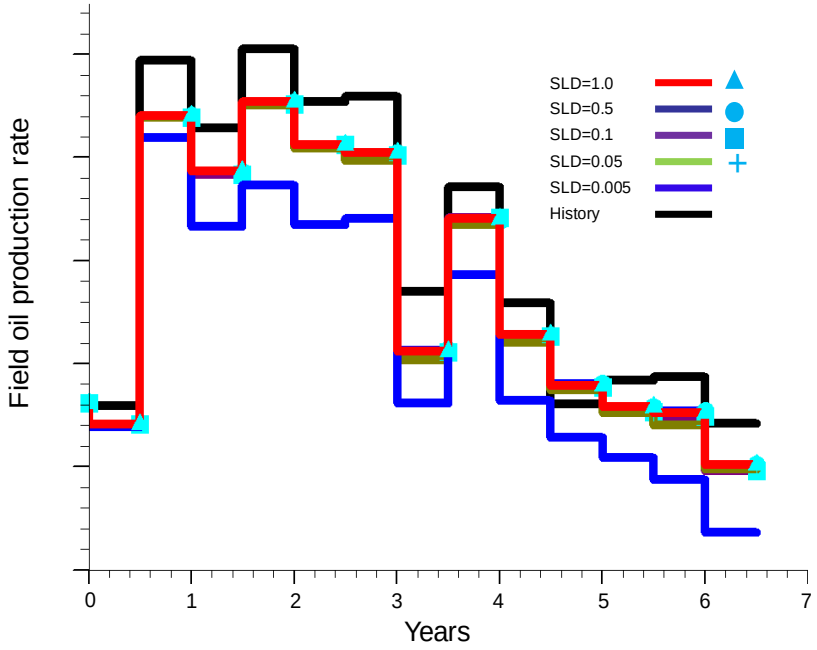


*Figure B.3: Field oil production rate for different streamline cases with changing the SLD number. Note that the field production rate for SLD=1, 0.5, 0.1 and 0.05 are almost the same.*

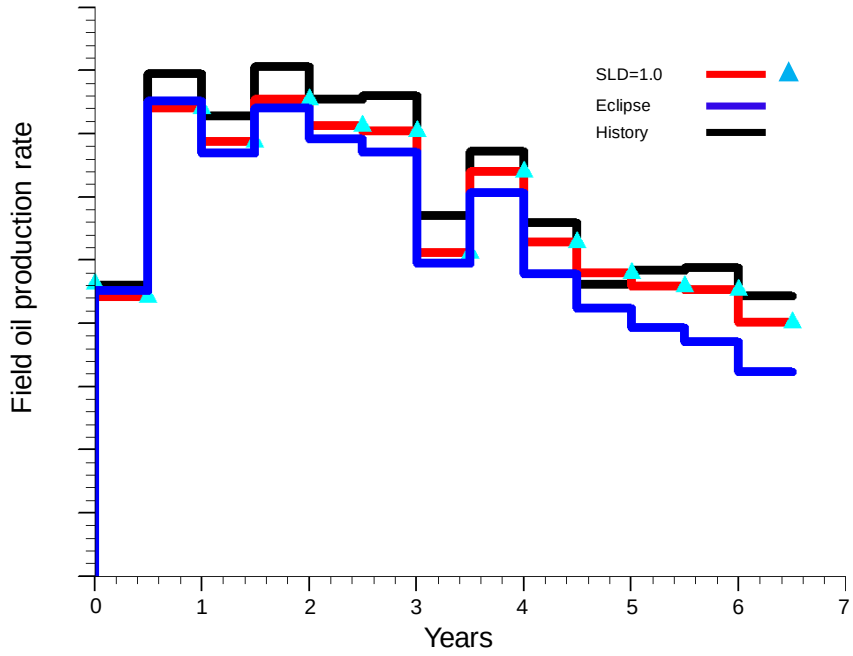


*Figure B.4: Field oil production rate for streamline and Eclipse cases.*

For each individual wells, the differences between observed and measured water production rate were calculated for the Eclipse and streamline model (SLD=1.0) using Eq. 2.29. Figure B.5 shows that almost for all wells the misfit value for Eclipse cases is higher than streamline case which means more accuracy of base case streamline simulator to model the reservoir.

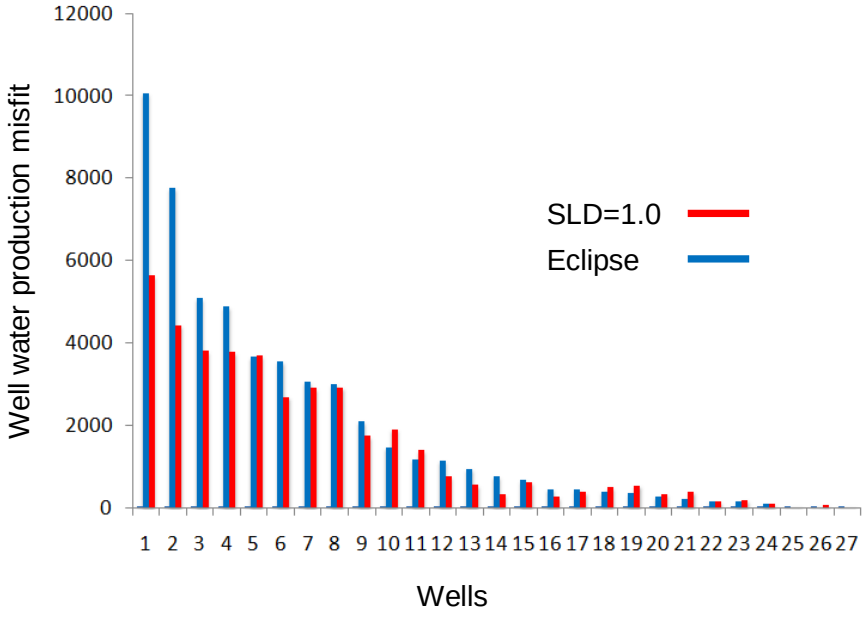


*Figure B.5: Well water production misfit for Eclipse and streamline base mode with SLD=1.0.*

The oil saturation of the Eclipse model was subtracted from the streamline cases (for all simulation cells at the end of history matching period (6 years of production). Then the cell with zero values were filtered out and an arithmetic averaging was performed in order to generate a 2D map for the whole reservoir as shown in Figure B.6.

Figure B.6 shows that except for SLD=0.005 for the rest of the maps the saturation difference happens mainly at the edge of the reservoir and in the rest it is almost zero. The differences shows that at the edge streamline is generated at lower oil saturation compared to the Eclipse model which mean that more oil moved towards the wells. This observation is consistent with the Figure B.4 which shows higher oil production rate for the streamline case. For SLD = 0.005 there are more differences in oil saturation. At the edge streamline shows lower saturation and at the centre Eclipse shows lower value. The conclusion here is that the streamline simulation without a reasonable number of streamtubes could not reasonably simulate the fluid flow in the reservoir.

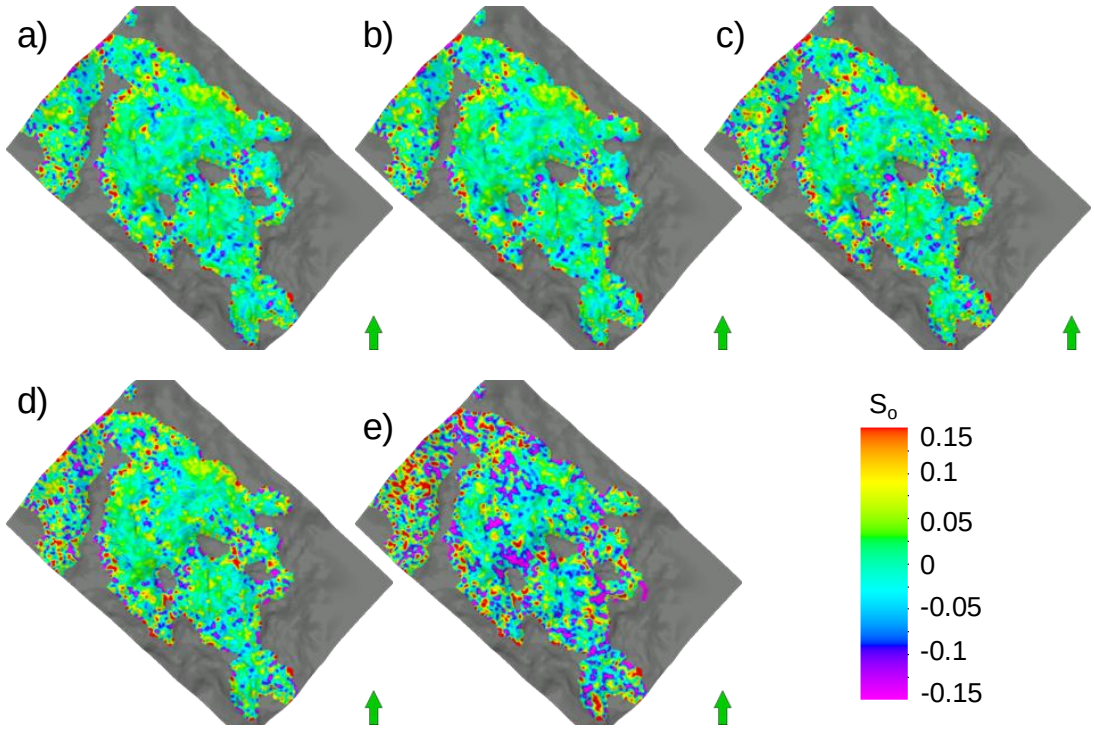


*Figure B.6: The differences of oil saturation at the end of production period between Eclipse and streamline case (averaged vertically) for, a) SLD=1.0, b) SLD=0.5, c) SLD=0.1, d) SLD=0.05 and e) SLD=0.005.*

Figure B.7 shows the comparison between the streamline case with SLD=1.0 to other streamline cases. According to the results presented in Figure B.6 it can be seen that as the density of streamline decreases in the reservoir the differences of oil saturation increases and the highest difference is for SLD=0.005. Except SLD=0.005, for the rest of cases the oil saturation difference is almost zero laterally in the reservoir and there are just a few cells in the edge of the reservoir which the differences can be observed.

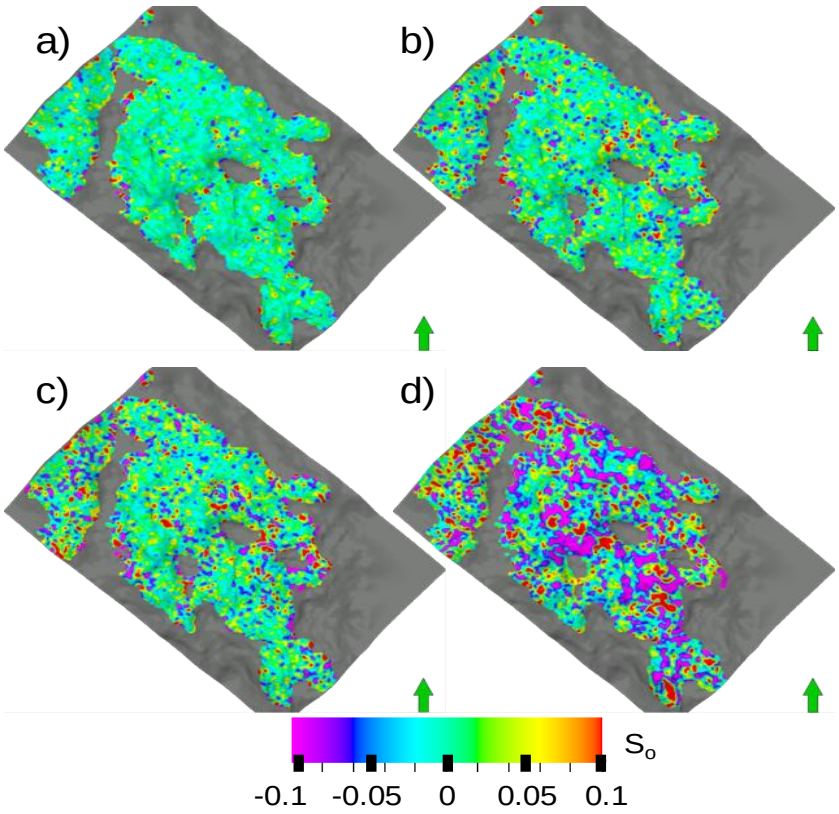


*Figure B.7: The differences of oil saturation at the end of production period between high density streamline case (SLD=1.0) and different streamline cases with lower SLD, a) SLD=0.5, b) SLD=0.1, c) SLD=0.05, d) SLD=0.005.(for all maps vertical arithmetic averaging performed)*

According to the misfit value observed in Figure B.2, it was decided to chose the SLD=0.05 as the optimum value of streamline density could be used generally for this field in order to have a reasonable result in a short period of time.

**B.2 The pressure calculation time steps**

As previously discussed in Chapter 2, Section 2.3 one of criteria for using streamline simulator was that pressure should not change drastically in the reservoir. In order to

check that criteria in Nelson field, the pressure difference for biannual time steps calculated by using Eclipse simulator as shown in Figure B.8. According to this figure every 6 months (time step used in this study) the differences between two following time steps calculated for all simulation cells. This figure shows that, there is a small reduction of pressure between the time steps.

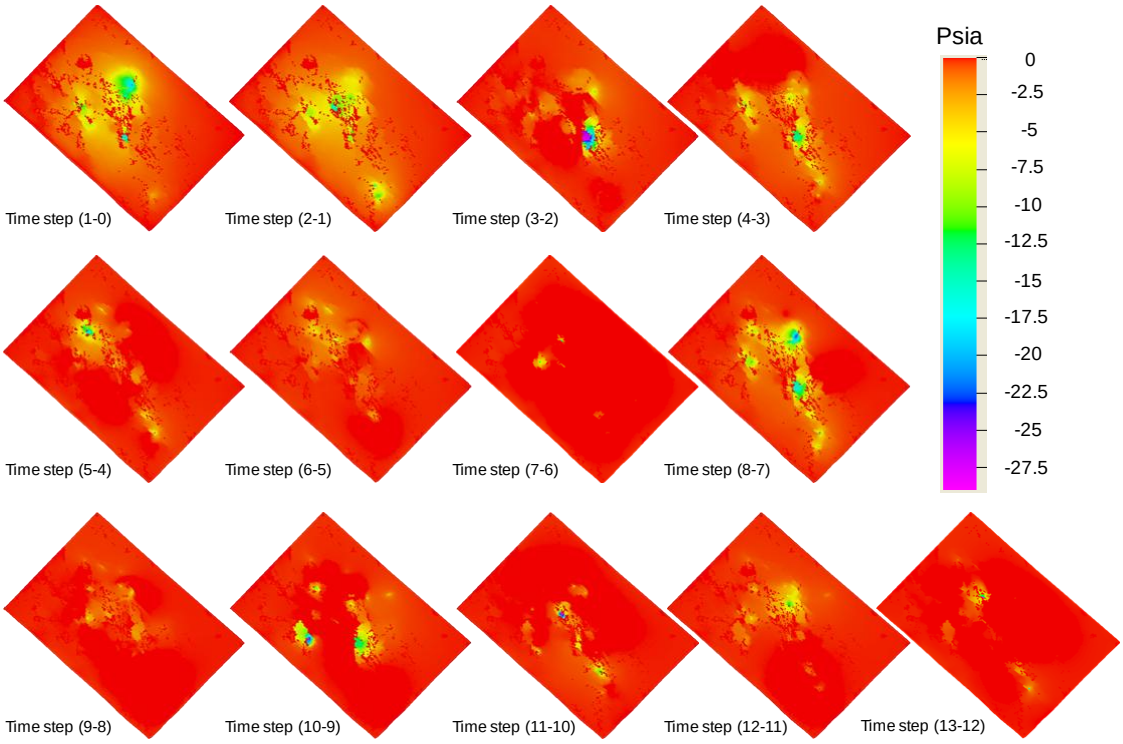


*Figure B.8: 2D maps for the change of reservoir pressure between six monthly time steps, modelling by Eclipse simulator.*

Three different cases were considered in order to investigate the effect of number of time steps for appropriately recalculation of pressure in the reservoir. In the previous cases the pressure was recalculated every 6 months. The streamline cases with SLD=0.05 was chosen as one case in addition to another two cases in which the production history data represented “quarterly” and “monthly”.

The sum of misfits of oil and water production rate for all wells was calculated for the quarterly and monthly cases. The misfit increases with the number of pressure change time steps (compared to the biannual case) therefore as normalization the misfit value of all cases was divided by the number of time steps for each case.

Figure B.9 shows that by increasing the number of time steps, the CPU time also increases while on the other hand there is an increase in the normalized misfit value as

well. On the other hand in the CPU axis there is a shift that shows Eclipse model takes longer to simulate the model. Also the gradient of misfit change is sharper for streamline case which is because of the point that during each time steps the pressure is constant in streamline simulation therefore more differences should be appears between three streamline cases.

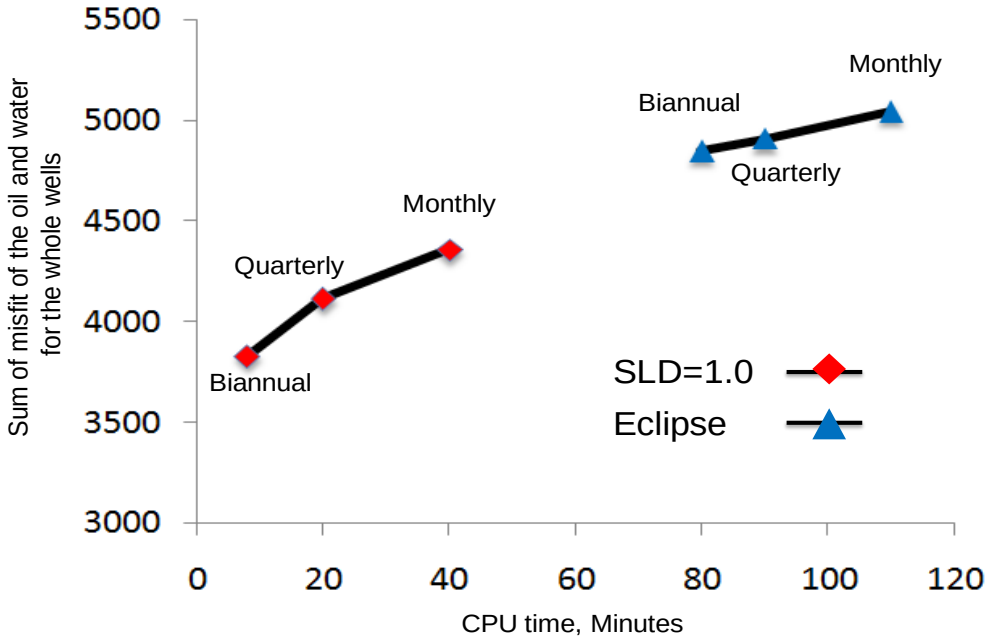


*Figure B.9: The sum of misfit of the oil and water for the whole wells versus CPU time. The misfit value was normalized in each case by the number of time steps.*

Figure B.10 shows the difference between oil saturation of the biannual case and the other two cases (quarterly and monthly time steps), It can be seen that after changing the number of time steps for recalculation of pressure, the difference in final oil saturation is almost zero.

In Figure B.11 it can be seen that the reservoir pressure is almost the same for different cases and therefore the difference between final reservoir pressure is very close to zero. The main reason for this is the fact that the general reduction of reservoir pressure is very small during the whole production period in Nelson (Figure 3.19) therefore recalculating the pressure every 6 month captures the pressure distribution in the reservoir.

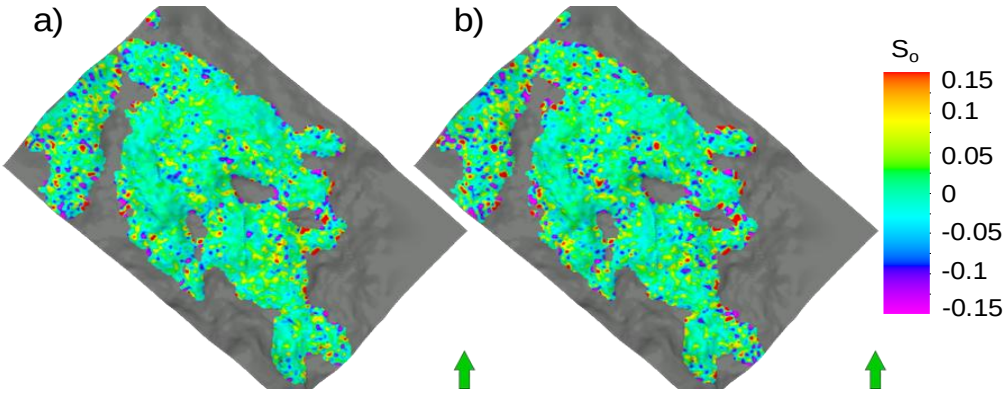


*Figure B.10: The differences of oil saturation at the end of production period between streamline with biannual time step and, a) streamline with monthly time step and, b) streamline case with quarterly time steps (the arithmetic averaging performed for both maps).*

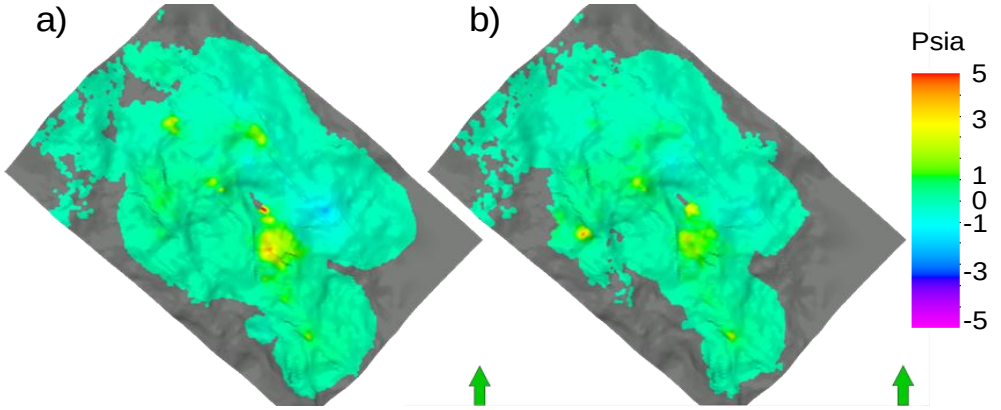


*Figure B.11: The average of pressure difference at the end of production period between streamline with biannual time step and, a) streamline with monthly time step and, b) streamline case with quarterly time steps.*

Based on the discussion above considering streamline simulation with a density of 0.05 for streamline and calculating pressure every 6 month provide a reasonable accuracy of the result in a short period of time therefore it was decided to use those values for the whole thesis.

# References


Aanonsen, S. I., Aavatsmark, I., Barkve, T., Cominelli, A., Gonard, R., Gosselin, O., Kolasinski, M., Reme, H. (2003). "Effect of scale dependent data correlation in an integrated history matching loop combining production data and 4D seismic data." SPE 79665, SPE reservoir simulation symposium, Houston, Texas, U.S.A., 3-5 February 2003.

Aanonsen, S. I., Nævdal, G., Oliver, D. S., Reynolds, A. C. and Vallès, B. (2009). "The Ensemble Kalman Filter in Reservoir Engineering—a Review." SPE 117274, *SPE Journal* **14(3)**, pp. 393-412.

Agarwal, B. and Blunt, M. J. (2004). "A Streamline-Based Method for Assisted History Matching Applied to an Arabian Gulf Field." *SPE Journal* **9(4)**, pp. 437-449.

Aggio, A. and Burns, C. S. (2001). "Seismic visualization for dynamic and static reservoir characterization." EAGE 63rd Conference & Technical Exhibition, Amsterdam, The Netherlands, 11-15 June 2001.

Arenas, E. M., Oldenzeil, T. and Van Kruijsdijk, C. P. J. W. (2001). "History matching reservoir model to Time-Lapse seismic using pilot point method." EAGE 63rd Conference & Technical Exhibition, Amsterdam, The Netherlands, 11 - 15 June 2001.

Arenas, E. M., Van Kruijsdijk, C. and Oldenziel, T. (2001). "Semi-Automatic History Matching Using the Pilot Point Method Including Time-Lapse Seismic Data." SPE 71634, SPE Annual Technical Conference and Exhibition, New Orleans, Louisiana, U.S.A., 30 September–3 October 2001.

Arroyo-Negrete, E., Devegowda, D., Datta-Gupta, A., and Choe, J. (2008). "Streamline-Assisted Ensemble Kalman Filter for Rapid and Continuous Reservoir Model Updating." SPE-104255-PA, *SPE Res Eval & Eng* **11 (6)**, pp. 1046–1060.

Avseth, P., Mukerji, T & Mavko, G. (2005). "Quantitative seismic interpretation: applying rock physics tools to reduce interpretation risk." Cambridge 2005.

Back, T. (1996). "Evolutionary algorithms in theory and practice." *Oxford University press.*

Backus, G. E. (1962). "Long-wave elascit anisotropy produced by horizontal layering." *J. Geophysical Research*, **(67)**, pp. 4427- 4440.

Baker, R. O. (2001). "Streamline Technology: Reservoir History Matching and Forecasting = Its Success, Limitations, and Future." *Journal of Canadian Petroleum Technology*, April 2001, **Vol.40, No. 4**, pp. 23-27.

Batzle, M. and Wang, Z., (1992). "Seismic properties of pore fluids." *Geophysics*, **(57)**, pp. 1396-1408.

Bentley, L. R. (1998). "On incorporating time-lapse seismic survey data into automatic history matching of reservoir simulations." CREWES Research Report, **(10)**.

Bissell, R. C., Dubrule, O., Lamy, P., Swaby, P. and Lepine, O., (1997). "Combining Geostatistical Modelling With Gradient Information for History Matching: The Pilot Point Method." SPE 38730, SPE Annual Technical Conference and Exhibition. San Antonio, Texas, 5-8 October 1997.

Boyd-Gorst, J. and Garnham, J. (1999). "Nelson field rock physics model on the Sele shale and Forties sandstone."

Bratvedt, F., Bratvedt, K., Buchholz, C. F., Gimse, T., Holden, L, Holden, H. and Risebro, N. H. (1993). "Frontline and Frontsim. Two Full Scale, Two-Phase, Black Oil Reservoir Simulators Based on Front Tracking." *Survey of Math. Ind.*, **3**, pp. 185.

Bratvedt, F., Bratvedt, K., Buchholz, C.F., Holden, L., Holden, H. & Risebro, N.H. (1992). "A New Front-Tracking Method for Reservoir Simulation." SPE 19805 , *SPE Reservoir Engineering*, **7**, pp. 107-116, , February.

Bratvedt, F., Gimse, T. and Tegnander, C. (1996). "Streamline computations for porous media flow including gravity." *Transport in Porous Media*.

Bryant, S. and Raikes, S. (1995). "Prediction of elastic-wave velocities in sandstones using structural models." *Geophysics*, **(60)**, 1995.

Caers, J., (2003). "History matching under training-image based geological model constraints." SPE J. **(7)**, pp. 218–226.

Castro S, A probabilistic approach to jointly integrate 3D/4D seismic, production data and geological information for building reservoir models. PhD Thesis, Stanford University, USA, 2007.

Chavent, G., Dupuy, M. and Lemonnier, P. (1975). "History Matching by Use of Optimal Theory." *SPE J.* **15(1)**, pp. 74-86.

Chen, W. H., Gavalas, G.R., Seinfeld, J.H. and Wasserman, M.L. (1974). "A New Algorithm for Automatic History Matching." *SPE J.* **14(6)**, pp. 593-608.

Cheng, H., Kharghoria, A., Zhong, H. and Datta-Gupta, A. (2005). "Fast History Matching of Finite-Difference Models Using Streamline-Based Sensitivities." *SPE Reservoir Evaluation & Engineering* **8(5)**, pp. 426-436.

Christie, M., Subbey, S., Sambridge, M. S. and Thiele, M. (2002). "Quantifying Prediction Uncertainty in Reservoir Modelling using Streamline Simulation." 15th ASCE Engineering Mechanics Conference. Columbia University, New York, 2-5 June 2002.

Coats, K. H., Dempsey, J. R. and Henderson, J. H. (1970). "A New Technique for Determining Reservoir Description from Field Performance Data." *SPE Journal* **10(1)**, pp. 66-74.

Clifford, P. J., Trythall, R., Parr, R. S., Moulds, T. P.,Cook, T., Allan, P. M. and Sutcliffe, P. (2003). "Integration of 4D Seismic Data into the Management of Oil Reservoirs with Horizontal Wells Between Fluid Contacts." SPE 83956, Offshore Europe, Aberdeen, UK, 2-5 September 2003.

Craft, K., Hays, D., Docherty, P., Paffenholz, J. and Smit, F. (2009). "An Ocean Bottom Seismic Node Repeatability Study." 71st EAGE Conference & Exhibition, Amsterdam, The Netherlands, 8 - 11 June.

Dadashpour, M., Martin Landrø, M. Kleppe, J. (2007). "Nonlinear inversion for estimating reservoir parameters from time-lapse seismic data." *J. Geophys. Eng.* **(5)**, pp. 54–66.

De Marsily, G. H., Levendan, G., Boucher, M. and Fasanino, G. (1984). "Interpretation of Interface Test in a well Field Using Geostatistical Techniques to Fit the Permeability Distributions in a Reservoir Model." In: G. Verly et al., Editors, Geostatistics for natural resources characterization. **Part 2**, D. Reidel Pub Co (1984), pp. 831–849.

De Souza, R. M., Machado, A. F., Munerato, F.P. and Schiozer, D. J. (2010). "Iterative history matching technique for estimation reservoir parameters from seismic data." SPE 131617, SPE EUROPEC/EAGE Annual Conference and Exhibition, Barcelona, Spain, 14-17 June 2010.

Deutsch, C. V. and Journel, A. G. (1998). "GSLIB Geostatistical Software Library and User´s Guide." 2n Edition, Oxford University Press, New York.

Dong, Y. and Oliver, D. S. (2005). "Quantitative Use of 4D Seismic for Reservoir Description." *SPE Journal*, March 2005, pp. 91-99.

Doyen, P. M. (2007). "Seismic Reservoir Characterization." *An Earth Modelling Perspective*. EAGE 2007.

Eberhart-Phillips, D., Han, D-H., and Zoback, M.D. (1989). "Empirical relationships among seismic velocity, effective pressure, porosity, and clay content in sandstone." *Geophysics*, **(54)**, pp. 82-89.

Emanuel, A. S. and Milliken, W. J. (1998). "History matching finite difference models with 3D streamlines. " SPE 49000, SPE Annual Technical Conference and Exhibition. New Orleans, Louisiana, 27-30 September 1998.

Emerick, A. A., De Moraes, R. J. and Rodrigues, J. R. P. (2007). "History Matching 4D Seismic Data with Efficient Gradient Based Methods." SPE 107179, SPE Europec/EAGE Annual Conference and Exhibition held in London, United Kingdom, 11–14 June 2007.

Evensen, G. (1994). "Sequential Data Assimilation with a Non-Linear Quasi-Geostrophic Model Using Monte-Carlo Methods to Forecast Error Statistics." *J. Geophys Res.*, **99 (C5)**, pp. 10143-10162.

Fagervik, K., Lygren, M., Valen, T. S., Hetlelid, A., Berge, G., Dahl, G. V. and Sønneland, L. (2001). "A Method for performing History Matching of Reservoir

Flow Models using 4D Seismic." SEG International Exposition and Annual Meeting, San Antonio, Texas, 9-14 September 2001.

Fagervik, K., Lygren, M., Valen, T. S., Hetlelid, A., Berge, G., Dahl, G. V., Sønneland, L., Lie, H. E. and Magnus, I. (2001). "History matching of flow models using 4D seismic." EAGE 63rd conference and technical exhibition, Amesterdam, The Netherland, June 2001.

Falcone, G., Gosselin, O., Maire, F., Marrauld, J. and Zhakupov, M. (2004). "Petroelastic modeling as key element of 4D history matching: A field example.", paper 90466, presented at 2004 SPE Annual Technical Conference and Exhibition, Houston, Texas, September, 26-29.

Fletcher, R. (1987). "Practical methods of optimisation." Wiley.

Floricich, M., Soldo, J., and MacBeth, C. (2004). "An Engineering Approach for Pressure and Saturation Estimation from Time-Lapse Seismic Data." In XII Congreso Venezolano de Geofisica, Caracas, Venezuela.

Floris, F.J.T., Bush, M.D., Cuypers, M., Roggero, F., Syversveen, A. R. (2001). "Methods for quantifying the uncertainty of production forecasts: a comparative study." *Petroleum Geoscience* **(7)**, pp. 87– 96.

Foster, D. G. (2008). "Lessons Learned From Over 20 Years of 4-D Deployment." SPE 113542, SPE Indian Oil and Gas Technical Conference and Exhibition. Mumbai, India, 4-8 March 2008.

Francis, A. M. and Syed, F.H., (2001). "Application of relative acoustic impedance inversion to constrain extent of E sand reservoir on Kadanwari Field." Presented at SPE/PAPG Annual Technical conference, 7-8 November 2001, Islamabad, Pakistan.

Gassmann, F. (1951). "Uber die elastizitat poroser medien." *Vier. Der Natur. Gesellschaft*, (**96)**, pp. 1–23.

Geman, S. and Geman, D. (1984). "Stochastic relaxation, Gibbs distribution and the bayesian restoration of images," *IEEE Trans. Patt. Analysis Mach. Int*, **6**, pp. 721–741.

Goldberg, D. E. (1989). "Genetic algorithms in search, optimization and machine learning." Addison–Wesley, Reading, MA.

Gosselin, O., Van den Berg, S., Comineli, A. (2001). "Integrated history matching of production and seismic data." SPE 71599, SPE Annual Technical Conference and Exhibition held in New Orleans, Louisiana, 30 September- 3 October 2001.

Gosselin, O., Aanonsen, S. I., Aavatsmark, I., Cominelli, A., Gonard, R., Kolasinski, M., Ferdinandi, F., Kovacic, L. and Neylon, K. (2003). "History matching using Time-lapse seismic (HUTS)." SPE 84464, SPE Annual Technical Conference and Exhibition, Denver, Colorado, U.S.A., 5-8 October 2003.

Guérillot, D. and Pianelo, L. (2000). " Simultaneous Matching of Production Data and Seismic Data for Reducing Uncertainty in Production Forecasts." SPE 65131, SPE European Petroleum Conference, Paris, France, 24–25 October 2000.

Guerin, G., He, W., Anderson, R. N. and Xu, L. (2000). "Optimisation of reservoir simulation and Petrophysical Characterization in 4D seismic." OTC 12102, Offshore Technology Conference, Houston, Texas, 1-4 May 2000.

Hammersley, J. M., and Handscomb, D. C. (1964). "*Monte Carlo Methods*." Chapman and Hall, New York, 1964.

Hatchell, P., Kelly, S., Muerz, M., Jones, C., Engbers, P., Van Der Veeken, J., and Staples, R. (2002). "Comparing Time-Lapse Seismic and Reservoir Model Predictions in Producing Oil and Gas Fields." EAGE 64th Conference & Exhibition, Florence, Italy, 27-30 May 2002.

Hoffman, B. T. and Caers, J. (2005). "Regional probability perturbations for history matching." *Journal of Petroleum Science and Engineering* **(46)**, pp. 53– 71.

Holland, J. H. (1975). "Adaptation in Natural and Artificial Systems." University of Michigan Press, Ann Arbor.

Hong, T., Sen, M. K., Stoffa, P. L., Klie, H., Thomas, S. G., Rodriguez, A. and Wheeler, M. F. (2007). "Integrated Time-lapse Seismic Inversion for Reservoir Petrophysics and Fluid Flow Imaging." SEG/San Antonio Annual Meeting, Texas at Austin, 23-28 September 2007.

Hongliu, Z. and Backus, M. (2005). "Interpretive advantages of 90° -phase wavelets: Part1-Modeling." *Geophysics*, **70(3)** pp. C7-C15. May-June 2005.

Huang, X., Meister, L. and Workman, R. (1997). "Reservoir characterization by integration of Time-Lapse seismic and production data." SPE38695, SPE Annual technical conference and exhibition, San Antonio, Texas, 5-8 October 1997.

Huang, X., Meister, L. and Workman, R. (1998). "Improvement and sensitivity of reservoir characterization derived from time-lapse seismic data." SPE 49146, SPE Annual Technical Conference and Exhibition, New Orleans, Louisiana, U.S.A., 27-30 September 1998.

Huang, X., Will, R., Khan, M., Stanley, L. (1999). "Reconciling Time-lapse Seismic Data and Production Data: Application to a Gas Field." SPE 56732, SPE Annual Technical Conference and Exhibition, Houston, Texas, U.S.A., 3–6 October 1999.

Huang, X. R. (2001). "Integrating time-lapse seismic with production data: A tool for reservoir engineering." *The Leading Edge*, **(20)**, pp. 1148–1153.

Huang, X. and Lin, Y. (2006). " Production optimization using production history and time-lapse seismic data." SEG/New Orleans 2006 Annual Meeting.

Jin, L., Sen, M. K., Stoffa, P. L. and Seif, R. K. (2007). "Optimal Model Parameterization in Stochastic Inversion for Reservoir Properties Using Time-lapse

Seismic and Production Data." SEG/San Antonio Annual Meeting, Texas at Austin, 23-28 September 2007.

Jin, L., Stoffa, P. L. and Sen, M. K. (2009). "Stochastic Inversion for Reservoir Properties Using Parallel Learning-Based VFSA and Pilot Point Parameterization." SPE 118818, SPE Reservoir Simulation Symposium, The Woodlands, Texas, USA, 2-4 February.

Johnston, D.H. (1997). "A Tutorial on Time-Lapse Seismic Reservoir Monitoring." paper OTC 8289 presented at the 1997 Offshore Technology Conference, Houston, 5–8 May.

Kazemi, A. and Modin, D. (2010). "Optimization, Uncertainty Analysis and Upscaling of Rock-Physics Models." SPE130303, SPE EUROPEC/EAGE Annual Conference and Exhibition, 14-17 June 2010, Barcelona, Spain.

Kazemi, A. and Stephen, K. D. (2008). "Improved Reservoir Description of the Nelson Field Via Seismic History Matching." EAGE 3942 presented at the 70th EAGE Conference and Exhibition, Rome, Italy, 9-12 June.

Kazemi, A. and Stephen, K. D. (2009). "Automatic Seismic and Production History Matching in Nelson Using Different Updating Schemes." presented at the 71st EAGE Conference and Exhibition, Amsterdam, The Netherlands, 8-11 June.

Kazemi, A., Stephen, K. D. and Shams, A. (2010). "Seismic History Matching of Nelson using Time-lapse Seismic Data: An Investigation of 4D Signature Normalization." SPE 131538, SPE EUROPEC/EAGE Annual Conference and Exhibition, Barcelona, Spain, 14-17 June.

Kazemi, A., Stephen, K. D. and Shams, A. (2011). "Improved normalization of time-laspe seismic data using NRMS repeatability data to improve automatic production and seismic history matching in the Nelson field." SPE 143628, SPE EUROPEC/EAGE Annual Conference and Exhibition, Vienna, Austria, 23-26 May.

Kazemi, A. and Stephen, K. D. (2011). "Automatic production and seismic history matching by updating locally and by geological environment in the Nelson field." SPE 143629, SPE EUROPEC/EAGE Annual Conference and Exhibition, Vienna, Austria, 23-26 May.

Kirkpatrick, S., Gelatt Jr., C.D., and Vecchi, M.P. (1983). "Optimization by Simulated Annealing, " *Science* (1983) **(220)**, pp. 671-680.

King, M. J. and Datta-Gupta, A. (1998). "Streamline simulation: A current perspective." *In Situ*, **22(1)**, pp. 91-140.

Kragh E and Christie P (2002). " Seismic repeatability, normalized RMS and predictability." *The Leading Edge* **(21),** pp. 640–7.

Kretz, V., Le Ravalec-Dupin, M. and Roggero, F. (2002). "An integrated reservoir characterization study matching production data and 4D seismic." SPE 77516, SPE Annual Technical Conference and Exhibition, San Antonio, Texas, U.S.A., 29 September- 2 October 2002.

Kunka, J. M., Williams, G., Cullen, B., Boyd-Gorst, J., Dyer, G. R., Garnham, J. A., Warnock, A., Wardell, J., Davis, A. and Lynes, P (2003). "The Nelson field, Blocks 22/11, 22/6a, 22/7, 22/12a, UK North Sea. " *United Kingdom oil and gas fields, commemorative millennium volume.* Geological society, London, Memoir, **(20)**, pp. 617-646.

Kuster, G. T., and Toksoz, M. N. (1974). "Velocity and attenuation of seismic waves in tow-phase media: Part I. theoretical formulations: " *Geophysics,* **(39)**, pp. 587–606.

Lancaster, S. and Whitcombe, D. (2000). "Fast Track Coloured Inversion." 70th Annual International Meeting of the Society of Exploration Geophysicists. p1572-1575

Landa, J. and Horne, R. (1997). "A Procedure to Integrate Well Test Data, Reservoir Performance History and 4-D Seismic Information into a Reservoir Description." SPE 38653, SPE annual technical conference and exhibition, San Antonio, Texas, U.S.A., 5-8 October 1997.

Le Ravalec-Dupin, M. and Noetinger, B. (2002). "Optimization with the gradual deformation method." *Mathematical Geology* **34(2)**, pp. 121-138.

Liu, N. (2005). "Automatic History Matching of Geologic Facies." PhD Thesis, University of Oklahoma graduate college, Oklahoma, USA.

Liu, N. and Oliver, D. S. (2004). "Automatic History Matching of Geologic Facies." *SPE Journal* **9(4)**, pp. 429-436.

Lolomari, T., Bratvedt, K., Crane, M., Milliken, W. J. and Tyrie, J. J. (2000). "The Use of Streamline Simulation in Reservoir Management: Methodology and Case Studies. " SPE 63157, SPE Annual Technical Conference and Exhibition. Dallas, Texas, 1-4 October 2000.

Levy, A. V. and Montalvo, A. (1985). "The Tunnelling method for global optimization." *SIAM J. of Sci. and Stat. Comp.* **1**, pp. 15.

Lygren, M., Dahl, G. V., Fagervik, K., Nickel, M., Borgos, H. G., Skov, T., Hetlid, A., Berge G. and Sønneland, L. (2002). "Use of reservoir flow models in quantitative 4D analysis." EAGE 64th Conference & Exhibition, Florence, Italy, 27-30 May 2002.

Lygren, M., Fagervik, K., Valen, T. S., Hetlelid, A., Berge, G., Dahl, G. V., Sønneland, L., Lie, H. E. and Magnus, I. (2003). "A method for performing history matching of reservoir flow models using 4D seismic data." *Petroleum Geoscience*, **(9)**, pp. 85–90.

MacBeth, C. (1995). "How can anisotropy be used for reservoir characterisiation?" *First Break,* **13(1),** pp.31-37.

MacBeth. C. (2007). "Time-lapse course 2007."

MacBeth, C., Stephen, K. D. and McInally, A. (2005). "The 4D Seismic Signature of oil-water Contact Movement Due to Natural Production in a Stacked Turbidite Reservoir." *Geophysical Prospecting*, **53(1)**, pp. 183-203.

MacMillan, D. J., Pletcher, J. L. and Bourgeois, S. A. (1999). "Practical Tools To Assist History Matching. " SPE 51888, SPE Reservoir Simulation Symposium. Houston, Texas, 14-17 February 1999.

Maschio, C. and Schiozer, D. J. (2005). "Assisted History Matching Using Streamline Simulation." *Petroleum Science and Technology* **23(7)**, pp. 761 - 774.

Matheron, G. (1971). "The theory of regionalized variable and its applications." Les Cahiers du Centre de Morphologie Mathematique de Fontainebleau, n5, published by the Ecole Nationale Superieure de Mines du Paris.

Mattax, C. and Dalton, R. (1990). "Reservoir Simulation." SPE Monograph Volume 13, Society of Petroleum Engineers, Richardson, Texas.

McInally, A.T., Redondo-López, T., Garnham, J., Kunka, J., Brooks, A. D., Stenstrup Hansen, L., Barclay, F. and Davies, D. (2003). "Optimising 4D fluid imaging." *Petroleum Geoscience*, **9(1)**, pp. 91- 101.

Menezes, C & Gosselin O. (2006) "From logs scale to reservoir scale:Upscaling of the petro-elastic model." SPE 100233 presented at SPE/Europec Annual Conference and Exhibition, Vienna, Austria, 12-15 June 2006.

Metropolis, N., Rosenbluth, A., Rosenbluth, M., Teller, A., and Teller, E. (1953). "Equation of State Calculations by Fast Computing Machines." *Journal of Chemical Physics*, **21**, pp. 1087−1092.

Mezghani, M., Fornel, A., Langlais, V. and Lucet, N. (2004). "History matching and quantitative use of 4D seismic data for an improved reservoir characterization." SPE 90420, SPE Annual Technical conference and Exhibition,Houston, Texas, U.S.A., 26-29 September 2004.

Milliken, W. J., Emanuel, A. S. and Chakravarty, A. (2000). "Applications of 3D Streamline Simulation to Assist History Matching. " SPE 63155, SPE Annual Technical Conference and Exhibition. Dallas, Texas, 1-4 October 2000.

Mindlin R, Compliance of elastic bodies in contact, Journal of Appl. Mech., vol. 16, (1949).

Mosegaard, K. and Sambridge, M., (2002). "Monte carlo analysis of inverse problems." *Inverse Problems*, **18**, R29–R54.

Murphy, W., Reischer, A., and Hsu, K. (1993). "Modulus Decomposition of Compressional and Shear Velocities in Sand Bodies," *Geophysics*, **(58)**, pp. 227-239

O´Donovan, A.R., Smith, S.G. and Kristiansen, P. (2000). "Foinhaven 4D Seismic – Dynamic Reservoir Parameters and Reservoir Management." SPE 63294, presented at the SPE Annual Technical Conference and Exhibition, Dallas, Texas, 1– 4 October, 2000.

Ouenes, A., Brefort, B., Meunier, G. and Dupere, S., (1993). "A New Algorithm for Automatic History Matching: Application of Simulated Annealing Method (SAM) to Reservoir Inverse Modeling." SPE 26297, Society of Petroleum Engineers.

Parr, R. S., Marsh, M. and Griffin, T. (2000). "Interpretation and Integration of 4-D Results into Reservoir Management, Schiehallion Field, UKCS." SEG 2000 Expanded Abstracts, Calgary, Canada, 6-11 August 2000.

Pollock, D. W. (1988). "Semianalytical Computation of Path Lines for Finite-Difference Models". *Ground Water*, **(26)**, pp. 743-750.

Portella, R. C. M and Emerick, A. A. (2005). "Use of Quantitative 4D-Seismic Data in Automatic History Match." SPE 94650, SPE Latin American and Caribbean Petroleum Engineering Conference, Rio de Janeiro, Brazil, 20-23 June 2005.

Portellaand, R. C. M. and Prais, F. (1999). "Use of Automatic History Matching and Geostatistical Simulation to Improve Production Forecast." SPE 53976, Latin American and Caribbean Petroleum Engineering Conference. Caracas, Venezuela, 21-23 April 1999.

Reuss, A. (1929). "Berechnung der fliessgrense von mishkristallen *Z. Angew.*" *Math. Mech.* **(9),** pp. 49–58.

Roggero, F. (1997). "Direct Selection of Stochastic Model Realizations Constrained to Historical Data." SPE38731. Presented at the SPE ATCE, San Antonio, Texas, 5-8 October, 1997.

Roggero, F. and Hu, L. Y. (1998). "Gradual Deformation of Continuous Geostatistical Models for History Matching." SPE 49004, SPE Annual Technical Conference and Exhibition. New Orleans, Louisiana, 27-30 September 1998.

Roggero, F., Ding, D. Y., Berthet, P., Lerat, O., Cap, J. and Schreiber, P.E. (2007). "Matching of Production History and 4D Seismic Data—Application to the Girassol Field, Offshore Angola." SPE 109929, SPE Annual Technical Conference and Exhibition held in Anaheim, California, U.S.A., 11–14 November 2007.

Sambridge, M. S. (1999). "Geophysical inversion with a neighbourhood algorithm-I. Searching a parameter space." *Geophys.J.Int.*, **(138)**, pp. 479-494.

Sambridge, M. (1999b). "Geophysical Inversion with a Neighbourhood Algorithm – Appraising the Ensemble." *Geophysical Journal International*, **138(2)**, pp. 727–746.

Sambridge M. (2001). "Finding Acceptable Models in Nonlinear Inverse Problems Using a Neighbourhood Algorithm." *Inverse Problems*, **(17)**, pp. 387–403.

Sambridge, M. and Mosegaard, K. (2002). "Monte carlo methods in geophysical inverse problems." *Reviews of Geophysics* **(40)**, pp. 3.1–3.29.

Schlumberger Geoqueat Manual (2007), Schlumberger.

Schlumberger Fronstim simulator (2007), Schlumberger.

Sedighi, F. and Stephen, K. D. (2009). "Faster Convergence in Seismic History Matching by Efficient Parameter Searching." SPE 121210 EUROPEC/EAGE Conference and Exhibition, Amsterdam, The Netherlands, 8-11 June.

Shepherd, M. and Gill, C. (2009). "Locating the remaining oil in the Nelosn field, UKCS." 2009.

Simmons, G. and Wang, H. (1971). "Single crystal elastic constants and calculated aggregate properties: A handbook (2nd Edition)." MIT Press, 1971.

Skjervheim, J. A., Evensen, G., Aanonsen, S. I. and Johansen, T. A. (2007). "Incorporating 4D Seismic Data in Reservoir Simulation Model Using Ensemble Kalman Filter." *SPEJ* **12 (3)**, pp. 282–292.

Soldo, J. (2005). "Quantitative Integration of Time-Lapse Seismic Data." PhD Thesis, Heriot-Watt University, Edinburgh, Scotland.

Solorzano, L. N., Arredondo, S. E. and Enrique, S. (1973). "Method for Automatic History Matching of Reservoir Simulation Models." SPE 4594, Fall Meeting of the Society of Petroleum Engineers of AIME. Las Vegas, Nevada, 30 September-3 October 1973.

Staples, R., Stevens, T., Leoutre, E., Jolley, S. and Marshall,J. (2005). "4D seismic history matching – the reality." EAGE 67th Conference & Exhibition, Madrid, Spain, 13 - 16 June.

Stephen, K. D., Soldo, J., MacBeth, C. and Christie M. (2005). "Multiple Model Seismic And Production History Matching: A Case Study." SPE94173. Proceedings of the 14th Europec Biennial Conference held in Madrid, Spain, 13-16 June 2005.

Stephen, K. D., (2006). "Measuring the value of time-lapse (4D) seismic as part of history matching in the Schiehallion UKCS field." Presented at the 10th European Conference on the Maths of Oil Recovery held in Amsterdam, the Netherlands, 4-7 September, 2006.

Stephen, K. D. and MacBeth, C. (2006). Seismic History Matching in the Schiehallion UKCS Field. *First Break*, **24**, pp. 43-49, April, 2006.

Stephen, K.D., Soldo, J., MacBeth, C. and Christie, M. (2006). "Multiplemodel seismic and production history matching: a case study." SPE-94173-PA, *SPEJ* **11 (4)**, pp. 418–430.

Stephen, K.D. (2007). "Scale and process dependent model errors in seismic history matching." *Oil & Gas Science and Technology—Revue de l'IFP* **62 (2), pp.** 123–136.

Stephen, K.D., Shams, A. and MacBeth, C. (2007). "Faster seismic history matching in UKCS reservoir." SPE 107147, SPE Europec/EAGE Annual conference and exhibition, London, United Kingdom, 11-14 June 2007.

Stephen, K. D. and MacBeth, C. (2008). "Reducing Reservoir Prediction Uncertainty by Updating a Stochastic Model Using Seismic History Matching." SPE 100295, *SPE Reservoir Evaluation & Engineering* **11(6)**, pp. 991-999.

Stephen, K. D., Shams, A. and MacBeth, C. (2009). "Faster Seismic History Matching in a UKCS field." SPE107147-PA, *SPE RE* **12 (4),** pp. 586-594.

Tan, T. B. (1995). "A Computationally Efficient Gauss-Newton Method for Automatic History Matching." SPE 29100, SPE Reservoir Simulation Symposium. San Antonio, Texas, 12-15 February 1995.

Tarantola, A. (1987). "Inverse Problem Theory - Methods for Data Fitting and Model Parameter Estimation." Elsevier Science Publishers, Amsterdam 1987.

Trani, M., Leeuwenburgh, O., Arts, R. J., Brouwer, J. H. and Douma, S. (2009). "The value of streamlines based localization in the assimilation of 4D seismic data with the Ensemble Kalman filter." 71st EAGE conference and exhibition, Amsterdam, The Netherlands, 8-11 June.

UKCS North Sea rock physics analysis, Nelson Field, Enterprise Oil, December 1997

UK DTI, 2009. www.og.decc.gov.uk/pprs/full_production.htm

Van Ditzhuijzen, R., Oldenziel, T., and Van Kruijsdijk, C. P. J. W. (2001). "Geological parameterization of a reservoir model for history matching incorporating time-lapse seismic based on a case study of the Statfjord field." SPE 71318, SPE Annual Technical Conference and Exhibition, New Orleans, Louisiana, U.S.A, 30 September- 3 October 2001.

Vasco, D. W., Datta-Gupta, A., He, Z., Behrens, R., Rickett, J. and Condon, P. (2003). "Reconciling time-lapse seismic and production data using streamline models: the Bay Marchand field, Gulf of Mexico." SPE 84568, SPE Annual Technical Conference and Exhibition, Denver, Colorado, October 5-8 2003.

Voigt,W. (1928). "Lehrbuch der kristallphysik: Teubner."

Voronoi, M.G. (1908). " Nouvelles applications des parame`tres continus a` la the´orie des formes quadratiques." *J. reine Angew Math*, **(134)**, pp. 198–287.

Waggoner, J.R. (2000). "Lessons learned from 4D projects." *SPE Res. Eval. & Eng*, **(3)**, pp. 310.318.

Waggoner, J. R., Cominelli, A. and Seymour, R. H. (2002). "Improved reservoir modelling with Time-Lapse seismic in a Gulf of Mexico gas condensate reservoir." SPE 77514, SPE Annual Technical Conference and Exhibition, San Antonio, Texas, U.S.A., 29 September- 2 October 2002.

Walker G. Allan, P., Trythall, R., Parr, R., Mash, M., Kjelstadli, R., Barkved, O., Johnson, D. and Lane, S. (2006). "Three case studies of progress in quantitative seismic-engineering integration." *The Leading Edge*, **25(9)**, pp. 1161-1166.

Wang, S., Zhao, G., Xu, L., Guo, D. and Sun, S. (2005) "Optimization for automatic history matching" *International journal of numerical analysis and modeling* **(2)**, pp. 131-137

Watson, A. T. and Lee, W. J. (1986). "A New Algorithm for Automatic History Matching Production Data." SPE 113479, SPE Unconventional Gas Technology Symposium. Louisville, Kentucky, 18-21 May 1986.

Williams, G. J. J., Mansfield, M., MacDonald, D. G., and Bush, M. D. (2004) "Top-Down Reservoir Modelling." Paper SPE 89974, presented at the SPE Annual Technical Conference and Exhibition, Houston, TX, 26–29 September, 2004.

Whyatt, M., Bowen, J.M. & Rhodes, D.N. (1992). "The Nelson Field: a successful application of a development geoseismic model in North Sea exploration." In: Hardman, R.F.P. (ed.) *Exploration Britain: Geological insights for the next decade. Geological Society*, London, Special Publications, **(67)**, pp. 283–305.

Yang, P. H. and Watson, A. T. (1988). "Automatic History Matching With Variable-Metric Methods." *SPE Reservoir Engineering* **3(3)**, pp. 995-1001.

Zhang, F., and Reynolds, A.C. (2002). "Optimization algorithms for automatic history matching of production data," Proc. 8th European Conference on the Mathematics of Oil Recovery, Freiberg, Germany, 3 – 6 Sept. 2002.

Zhang, F., Skjervheim, J. A., Reynolds, A. C. and Oliver, D. S. (2005). "Automatic History Matching in a Bayesian Framework, Example Applications." *SPE Reservoir Evaluation & Engineering* **8(3)**, pp. 214-223.